A STUDY OF CERTAIN PROPERTIES OF SUPERFLUID HELIUM-4 BASED ON MACRO-ORBITAL THEORY

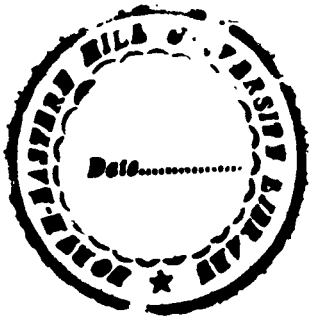

SIMANTA CHUTIA
DEPARTMENT OF PHYSICS
SCHOOL OF PHYSICAL SCIENCES

A THESIS
SUBMITTED
IN
PARTIAL FULFILMENT OF THE REQUIREMENT OF THE
DEGREE OF DOCTOR OF PHILOSOPHY

TO
NORTH EASTERN HILL UNIVERSITY
SHILLONG
INDIA
NOVEMBER 2007

A dedication to my
Parents and Teachers

CERTIFICATE

This is to certify that the research work presented in this thesis entitled "A Study of Certain Properties of Superfluid Helium-4 based on Macro-orbital Theory" is carried out by Shri Simanta Chutia under our supervision in the Department of Physics, School of Physical Sciences, North-Eastern Hill University, Shillong. The work embodied in this thesis does not form the basis for the award of any previous degree, diploma, fellowship or any other similar title and it represents entirely an independent work on the part of the candidate.

P. Nongkynrih

Prof P. Nongkynrih
Head, Dept. of Physics
NEHU

Prof. & Head
Physics Department,
N.E.H.U, Shillong-793022.

Y.S. Jain

Prof. Y.S. Jain
(Supervisor)

Dr. S.S. Pohlong
(Co-supervisor)

Place: Shillong
Date: 26-11-07.

DECLARATION

I, Simanta Chutia, hereby declare that the thesis entitled "A Study of Certain Properties of Superfluid Helium-4 based on Macro-orbital Theory" is the record of the work carried out by me under the supervision of Prof. Y.S. Jain, Department of Physics, North-Eastern Hill University, Shillong. The contents of this thesis did not form the basis for the award of any previous degree to me or to the best of my knowledge to anybody else. I also declare that the thesis has not been submitted by me for any research degree in any other University/Institute.

This is being submitted to the North-Eastern Hill University for the degree of Doctor of Philosophy in Physics.

Place: Shillong
Date: 26.11.07

Simanta Chutia
Department of Physics
North-Eastern Hill University
Shillong

ACKNOWLEDGEMENT

First and foremost, I express my hearty gratitude and immense thanks to Prof. Y.S. Jain for inspiring guidance, keen interest and never failing encouragement throughout the course of my research work. I shall ever be grateful to him for his timely suggestions and discussions with up to date ideas. I also thank him for providing me with all requisite facilities.

I am grateful to Dr SS Pohlong, co-supervisor, for his constant inspiration.

I wish to convey my cordial thanks to Prof. M.K. Parida, former Head, Department of Physics, NEHU, and the present Head Prof. P. Nongkynrih for their encouragements.

I record my sincere thanks to all faculty members of the Physics department, NEHU, for their encouragements. I extend my thanks to all the non teaching staff of the department for their cooperation.

It is my great pleasure to convey my heartfelt thanks to Mr. Dhriti Sundar Ghosh, Mr. Lalmuanawma Chhangte, Mr. Ashok Jha, Mr. Jeeban Gewali, Mr Samrat Dey and Miss N. Thoinganbi Chanu for the helpful discussion and cooperation which remain in my heart. I would like to thank all the research scholars of the department for their assistance in miscellaneous ways.

I am grateful to Fr. I. Warpakma, Principal of St. Anthony's College, Shillong, for his kind permission to pursue my research work on part time basis.

I indebted to my departmental colleagues Dr J.A. Blah, Mr. S. Bhattacharjya, Mr. R.S. Kharwanlang, Mr. S. Saikia, Mr. V. Khongwir, and Miss Meeranda Kharkongor for their co-operation and mutual understanding during my entire Ph.D. programme which cannot be repaid with thanks. I am also indebted to my colleague Anjan Das, Computer Science department, for his valuable help and suggestion in preparing my thesis.

I take this opportunity to express my gratitude and love to my parents, brothers, sisters and friends who have directly or indirectly contributed a lot in the completion of my Ph.D. thesis. Their untold moral support always encouraged me in all my endeavours.

Lastly but not the least, I acknowledge my beloved wife Vijayalaxmi for her untold moral support which always encouraged me.

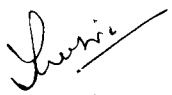

Simanta Chutia
Place: Shillong
Date:

Contents

List of Tables

List of Figures

SYNOPSIS

Helium-4, a noble element, was first liquified by Kamerlingh Onnes in 1908 [1]. Since then liquid helium-4 (LHE-4) (a system of interacting bosons) has become a subject of extensive investigation. Onnes also observed that LHE-4 exhibits a liquid to liquid transition at $\sim 2.1\,K(T_\lambda)$ [2] which transforms the liquid from its normal phase (*helium-I*) of all properties of a normal liquid to a super-fluid phase (*helium-II*) of very low viscosity and very high thermal conductivity [3, 4]. LHE-4 remains as liquid even at $0\,K$ unless a pressure of about $25\,atms$ is applied. Super-fluid phase of LHE-4 possesses some more unique properties such as: (i) it can flow against the gravity along the walls of the container, (ii) its specific heat and related thermodynamic response functions such as expansion co-efficient, pressure co-efficient *etc.* diverge logarithmically at $\lambda-$transition, (iii) it exhibits thermo-mechanical and mechanocaloric effects, (iv) below T_λ, its volume increases with decreasing temperature, (v) for certain velocity (flow/rotational) it sustains quantized circulation, (vi) it sustains four different sound modes, (vii) its dispersion curve at low Q shows anomalous nature, (viii) it remains calm and still on boiling (no bubble formation), *etc.*

The wealth of experimental and theoretical results has been reviewed by several authors [3, 5, 6]. Several attempts have been made to develop a full microscopic theory but with little success. Most of the microscopic theories so far developed [7–15] start with the basic assumption that the super-fluid phase has macroscopic occupation of $p = 0$ state. However, the existence of $p = 0$ condensate has not been confirmed experimentally even after repeated efforts [16]. Recently, in a review article Legget remarks "In the sixty years since London's original proposal, while there has been almost universal belief that the key to super-fluidity is indeed the onset of BEC at T_λ it has proved very difficult, if not impossible, to verify the existence of the latter phenomenon directly. The main evidence for it comes from high-energy neutron scattering and, very, recently, from the spectrum of atoms evaporated from the liquid surface, and while both are certainly consistent with the existence of a condensate fraction of approximately 10%, neither can be said to establish it beyond all possible doubts." Consequently, Landau's two fluid model [17, 18] supplemented by the idea of quantized circulation presented by Onsager [19] and Feynman [20] remains as the only way to understand the properties of LHE-4 despite its several shortcomings [6]. Since a wholly microscopic

theory is not available, LHE-4 continues to be a subject of great interest.

Over the last several years Jain has used a new approach to develop the microscopic understanding of the phenomenon [21–23]; this approach does not assume the existence of either Cooper type pairs in a fermionic system or BEC state (existence of $p = 0$ condensate) in a bosonic system. This theory (Macro-orbital theory) consistent with microscopic as well as macroscopic uncertainty, and excluded volume principle. It also provides microscopic foundation for the system to behave as a mixture of two fluid as envisage by Landau [17]. Basic objective of the present thesis is to show the agreement of experimentally observed thermodynamic and hydrodynamics properties of LHE-4 with those calculated by using macro-orbital theory and thereby to conclude that the theory has great potential to explain the properties of similar system and to provide a frame work that unifies the physics of bosonic and fermionic system.

This thesis contains seven chapters.

In Chapter-1 we present a brief discussion and review on experimental and theoretical studies of LHE-4.

Chapter-2 describes the salient features of macro-orbital theory. This theory reveals that:

1. Each particle in a fluid can be described by a kind of pair waveform $\chi = \psi(1,2)$ representing its wave superposition with another particle. For distinction χ is proposed to be known as macro-orbital state [22].

2. Each particle in its macro-orbital has two motion; the $q-$motion representing the relative motion of one particle with respect to the other particle decides the quantum size ($\lambda/2 = \pi/q$) of the particle (or the size of the space exclusively occupied by the particle), and the $K-$motion (not affected by the inter particle interaction) that participates in defining the quasi-particle excitations of the system. Note that this aspect successfully accounts for the two fluid behavior of a super-fluid [22].

3. All particles in the ground state of a bosonic system have $q = q_o = \pi/d$ with $K = 0$, and they represent an ordered state in the the phase space with $\Delta\phi = 2\pi$ which accounts for their phase coherence [22]. They also develop a kind of collective binding which explains critical velocities for which superfluidity vanishes [22].

4. Particles in the super-fluid state defines a closed packed arrangement of their equal size wave packets. Consequently, they cease to have relative motion rendering loss of viscosity; they can move in order of their locations on a closed path with $\Delta\phi = 2n\pi\,(n = 1, 2, 3, ..)$ which accounts for the observed quantum vortices [22].

Chapter-3 presents our theoretical results on the logarithmic divergence of the specific heat at constant pressure(C_p), expansion coefficient (α_P), isothermal compressibility(κ_T) and pressure coefficient (β) of LHE-4 which are found to have very good agreement with experimental results.

Chapter-4 gives a detailed analysis of the excitation spectrum of LHE-4 at low Q. Following the ordered arrangement of the atoms we estimate the excitation energy at different Q by assuming different atomic arrangements namely sc, bcc, fcc and hcp arrangements. We also obtain group velocity (v_g) as well as phase velocity (v_p).

In Chapter-5 we estimate energy gap (the collective binding of atoms in superfluid state) and use it to obtain superfluid density, critical velocity of linear flow and rotational motion, vortex line density, vortex energy *etc.*

In Chapter-6 we make a systematic study of transition temperature, surface tension, bulk potential energy and surface layer thickness. Our results agree closely with their experimental values.

In Chapter-7 we list the important conclusion of our investigation and future course of studies where macro-orbital theory can be used.

Bibliography

[1] H.K. Onnes. *Leiden Comm.*, 108, 1938.

[2] H.K. Onnes. *Proc. Roy. Acad., Amsterdam*, 13:1093, 1911.

[3] D.R. Tilley and J. Tilley. *Superfluidity and Superconductivity.* Adam Hisger Ltd., Bristol and Boston, 1986.

[4] Zygmunt M. Galasiewicz. *Helium-4.* Pragamon Press, Oxford, 1971.

[5] J. Wilks. *The Properties of Liquid and Solid Helium.* Clerendon Press, Oxford, 1967.

[6] S.J. Putterman. *Superfluid Hydrodynamics.* North Holland/American Elsevier, Amsterdam, 1974.

[7] N. Bogoliubov. *J. Phys. (USSR) (reprinted in Ref. 1)*, 11:23, 1947.

[8] K.A. Brueckner and K. Sawada. *Phys. Rev.*, 106:1117, 1957.

[9] K.A. Brueckner and K. Sawada. *Phys. Rev.*, 106:1128, 1957.

[10] K.K. Singh and S. Kumar. *Phys. Rev.*, 162:173, 1967.

[11] K.K. Singh and S. Kumar. *Phys. Rev. A*, 1:497, 1970.

[12] Y.A. Tserkonikov. *Sov. Phys. - DOKL*, 9:1110, 1965.

[13] T.H. Cheung and A. Griffin. *Can. J. Phys.*, 48:2135, 1970.

[14] T.H. Cheung and A. Griffin. *Phys. Rev.*, A 4:237, 1971.

[15] N.M. Hugenholtz and D. Pines. *Phys. Rev.*, 116:489, 1959.

[16] H.R. Glyde and E.C. Svensson. In D.L. Price and K. Skold, editors, *Methods of Experimental Physics*, volume 23, Part-B, page 303. Academic Press, London, 1987.

[17] L.D. Landau. *J. Phys. U.S.S.R. (reprinted in Ref. 1)*, 5:71, 1941.

[18] L.D. Landau. *J. Phys. U.S.S.R. (reprinted in Ref. 1)*, 11:91, 1947.

[19] L. Onsager. *Nuovo Cimento*, 6 (supplement-2):249, 1949.

[20] R.P. Feynman. In C.J. Gorter, editor, *Prog. Low Temp. Phys.*, volume I, page 1. North-Holland, Amsterdam, 1955.

[21] Y.S. Jain. *J. Sci. Exlor.*, 16:67, 2002.

[22] Y.S. Jain. *J. Sci. Expl.*, 16:77, 2002. More detailed version of this paper is available for ready reference as a paper entitled, *"Macro-orbitals and microscopic theory of a system of interacting bosons"* in www.arXiv.org/cond-mat/0606571.

[23] Y.S. Jain. *J. Sci. Expl.*, 16:117, 2002.

Chapter 1

Introduction

1.1 Liquid Helium-4

Helium-4 is the first element of group VIIIA of the periodic table with atomic number 2, mass $6.6455X10^{-27}$ kg and ground state electronic structure $1s^2$. Existence of helium-4 in nature was noted for the first time in the Sun's atmosphere during an eclipse in 1868 [1]. Many observers observed the yellow D3 line very close to Sodium D lines. However, this line was not observed in any laboratory flame. In 1869, Rayat declared that the gas emitting D3 line was a new element which was proposed to be known as Helium by Frankland and Lockyer [1]. Helium-4 was discovered on earth in 1895 by Ramsay who obtained it from the mineral clevite. It is also available in earth's atmosphere with a concentration of about 1 part in 2,00,000 [1].

In 1908, Kamerlingh Onnes obtained liquid helium-4 (LHE-4) with boiling point $4.21\,K$ at atmospheric pressure which exhibits a liquid to liquid phase transition at $T = T_\lambda = 2.17\,K$ [2–4]. Since the transition shows no latent heat [5] it is ought to be a *second order* phase transition, as concluded by Ehrenfest [6]. At $T > T_\lambda$, the LHE-4 exhibits all properties of a normal fluid and is referred to as *helium-I*. However, at $T < T_\lambda$, it assumes the unique property of super-fluidity (characterized by zero viscosity) [1, 4, 7, 8], and is identified as *helium-II*

Due to weak inter atomic Van der Waals forces added with zero point repulsion, LHE-4 remains liquid even at absolute zero unless a pressure of about 25 atms is applied. It may be noted that the zero point energy of a ^4He atom arising from its quantum nature assumes high magnitude and overcomes the potential energy arising from the inter-atomic forces. Consequently, *helium-II* is considered as a quantum liquid and its super-fluidity has rightly been recognized as the manifestation of quantum nature of particles at macroscopic level.

Various physical properties of LHE-4 have been studied since 1909 and surprisingly, many of these are found to be unique. For example, a jump in the specific heat curve at around $2.19\,K$ observed by Keesom and Clusius [5], very large thermal conductivity observed by Keesom and Keesom [9], vanishingly small viscosity observed by Burton [10] and Wilhem, Misener and Clark [11] and fountain effect discovered by Allen and Jones [12], *etc.*

LHE-4 has been extensively investigated over the last eight decades. A large number of research papers, review articles and books have been published

on the subject. In the following sections we attempt to summarize these works and the present understanding of the system.

1.2 Experimental Studies

1.2.1 Density

The variation of density (ρ) of LHE-4 with temperature (T) was first studied by Kamerlingh Onnes [13] who observed a density maximum at about $2.2\,K$. This was confirmed by more accurate measurements of Onnes and Boks [14]. The most important conclusion of these experiments was a sharp discontinuity in $\partial\rho/\partial T$ at $2.2\,K$ which is illustrated in figure 1.1. It is important to note that ρ, decreasing with temperature below $2.2\,K$, assumes a constant value below $1.4\,K$.

Keesom and Keesom [9] studied the pressure dependence of density for the first time in 1933. Some other density measurements were reported by Kerr in 1957 [15], Kerr and Taylor in 1964 [16], Peshkov and Borovikov in 1966 [17], Boghosian and Meyer in 1967 [18], Elwell and Meyer in 1967 [19], Roach in 1968 [20] and Hanson *et al* in 1976 [21]. More recently Neimela and Donnelly [22] calculated density from the dielectric constant using Clausius-Mossotti equation for the range 1.15 to $4.9\,K$.

In recent times, Chan and co-workers [23] performed an experiment to study the influence of quenched disorder on the critical behavior of *helium-II* by confining the liquid to pores of three different porous media: Vycor, Xerogel and Aerogel glasses. They introduced disorder in *helium-II* by forcing its flow through the structure of these media. Their results reveal a well defined power law behavior of super-fluid density near the transition temperature.

1.2.2 Expansion Coefficient

Early measurements of ρ [13, 14], indicating a negative volume expansion coefficient (α) at about $2.2\,K$, were repeated with improved accuracy by Atkins and Edwards [24], and Kerr [15]. Edwards [25] obtained α from the measurement of refractive index while Chase *et al* [26] derived it from the measurement of dielectric constant. These results are reviewed elegantly by Kerr and Taylor [16].

Ahlers [27] obtained α very close to T_λ on six different isobars. The typical nature of $\alpha(T)$ under saturated vapour pressure is shown in figure 1.2. It indicates that $\alpha(T)$ having negative values below λ-point, assumes positive values at $T \leq 1.2\,K$.

1.2.3 Dielectric Constant

Keesom and Wolfke [28] measured the dielectric constant of LHE-4 between its boiling point and $1.9\,K$. They observed that the dielectric constant shows a sudden jump in the vicinity of $2.3\,K$ which they attributed to a liquid to liquid phase transition. They called the phases *helium-I* (stable at higher temperature) and *helium-II* (stable at lower temperature). They observed that the dielectric constant of *helium-I* is higher than that of *helium-II*. Similar results were obtained by Grebenkemper and Hagen [29] at 9100 MHz by measuring the resonant frequency of helium filled microwave cavity. However, Chase *et al* [26] measuring the dielectric constant for the temperature range $1.4\,K$ to $4.2\,K$ showed that polarizability is independent of temperature. While some other measurements have been reported in [30, 31], an apparently most recent measurement has been made by Neimela and Donnelly [22].

1.2.4 Specific Heat

Specific heat of LHE-4 was first measured by Dona and Kamerlingh Onnes [32] in 1926 at constant volume between $2.16\,K$ and $4.05\,K$. It has also been studied by Keesom and Clusius [5] at saturated vapour pressure (SVP) in the range $1.4\,K$ to $4.1\,K$ who observed that it increases sharply at $1.4\,K$ until it shows a steep maximum at about $2.19\,K$ followed by a sharp fall at $T > 2.19\,K$ to a shallow minimum at $2.6\,K$, beyond which it again increases slowly. The shape of the specific heat versus temperature curve resembles the shape of the letter λ and therefore, the singular point on this curve is called λ-point as suggested by Ehrenfest [1]. Keesom and Clusius [5] observed that no latent heat is associated with this transition which, obviously, concludes it to be a 2nd order phase transition, similar to a superconducting transition. These results were confirmed by a series of more accurate measurements performed by Fairbank and coworkers [33,34] who were able to measure the specific heat within almost 10^{-6} of λ-point and also to show that the changes at this point can be described as logarithmic discontinuity

of specific heat. Some other measurements of the specific heat under SVP were reported in [35-42]. Ahlers studied the temperature dependence of the specific heat along six different isobars and isochores [27]. The typical nature of temperature dependence of the specific heat is shown in figures 1.3 and 1.4. Specific heat measurements of pure ^4He as well as $^3He -^4 He$ mixture were reported by Gasparini and Moldover [43, 44]. They observed that the specific heat of $^3He -^4 He$ mixture at constant chemical potential becomes infinite on the λ-line at all ^3He concentration. The effect of the finite size of the sample was studied by Lipa *et al* [45–47] and Gasparini *et al* [48–50]. Recently, Lipa and coworkers [51,52] have reported very carefully measured C_p, *in and out of earth's gravitational field.* To isolate the effect of gravity they made their measurements on STS-52 space craft, space shuttle Columbia.

1.2.5 Thermal Conductivity

Measurements of thermal conductivity of liquid helium was first reported in 1936 by Keesom and Keesom [9]. They observed large thermal conductivity of *helium-II* which attained a maximum value of $810\, cal\, cm^{-1} sec^{-1} K^{-1}$ below λ-point. Allen *et al* [53] observed that the mechanism of conduction in *helium-II* is different from other fluids, although they did not specify the details of the mechanism. Allen and Johnes [12] discovered the so called "fountain effect" (thermo-mechanical effect) in 1938. London [54] derived the fountain effect equation which was used by Meijdenberg *et al* [40] to determine accurate entropy and its variation with pressure and temperature. Inverse fountain effect i.e. mechanocaloric effect was discovered by Daunt and Mendelssohn [55] which was confirmed by Brewer and Edwards [56]. The co-efficient of thermal conductivity in thin and bulk ^4He as function of temperature was measured by Um *et al* [57]. Kahn and Ahlers [58] measured the thermal conductivity at SVP confined to a fine glass capillary tubes. They observed that the thermal conductivity becomes effectively infinite below T_λ when the bulk correlation length becomes smaller compared to the diameter of the confining capillaries.

1.2.6 Viscosity

Three different methods are employed to measure the viscosity of *helium-II*: (i) damping method (ii) flow method and (iii) rotational viscometer method.

Damping Method

In this method viscosity is measured by measuring the damping of the motion of a body (disc, cylinder or wire) immersed in it and was used for the first time for *helium-II* by Burton [10] and Wilhelm *et al* [11] in 1935 who studied the damping of the torsional oscillations of a cylinder. While they observed a drop in viscosity below λ-point, their results did not agree with those of Kapitza [7] who used capillary flow method. In this context Kapitza [7] pointed out a discrepancy in their method.

Later, Keesom and MacWood [59], Keesom and Keesom [60], Smith [61] and deTroyer *et al* [62] measured the viscosity using the torsional oscillation of a disc immersed in the liquid. On lowering the temperature through λ-point, they also found marked decrease in viscosity of *helium-II* which appears to take a value, at *say* $1\,K$, about twenty-five times smaller than those at $4.1\,K$. Similar results are also observed by Tough *et al* [63] by using vibrating wire method. As such these experiments showed that *helium-II* is a viscous fluid with very low viscosity.

Flow Method

In this method the rate of flow of the fluid through capillary tubes or channels between two parallel plates is measured to find the viscosity. Johns and co-workers [64] and Bowers and Mendelssohn [65, 66] used capillary tubes to measure the viscosity of *helium-I* and observed it to have a value of 30 micro-poise (practically independent of temperature in the range $2.8 - 4.2\,K$).

Viscosity of *helium-II* using this method was measured simultaneously in 1938 by Allen and Misener [12] in Cambridge and by Kapitza [7] in Moscow. In total variance with *helium-I*, they found that the flow of *helium-II* through a capillary is independent of the pressure head and the length of the capillary tube and concluded it to be non-viscous. Allen and Misener later investigated this property in considerable detail [67, 68]. Kapitza [69, 70] performed another set of experiments by allowing the *helium-II* to flow through fine slits and estimated the upper limit of the viscosity (less than 10^{-11} poise). However, these results were contradictory to those obtained from oscillatory disc method in which viscosity was found to be more than 10^{-6} poise. This contradiction was resolved by Tisza

in his two fluid model [71,72]. Some other measurements using the flow of *helium-II* through narrow channels are reported by Giauque *et al* [73,74] and Johns *et al* [64].

Rotational Viscometer Method

The rotational viscometer developed by Hollis Hallet and co-workers [75–77] consists of two hollow cylinders of different radii, one rotating inside the other which is kept stationary. Viscosity of the fluid is measured by measuring the torque transferred from the rotating inner cylinder to the outer cylinder. In contradiction to the findings of flow method, these experiments also showed the viscous nature of *helium-II* as observed in the damping method. Interestingly, though the results of rotating and damping methods showed viscous nature of *helium-II*, they too are found to differ and in no method, viscosity drops instantaneously to zero at $\lambda-$point. While in damping method it decreases gradually to zero with decreasing temperature, in rotational method it remains finite at all $T < T_\lambda$; in the latter case, it is even observed to increase when T is lowered below $1.8\,K$ and exceeds the viscosity of *helium-I* below $1\,K$.

1.2.7 Surface Tension

Surface tension of LHE-4 was first measured by van Urk *et al* in 1925 [78]. In the subsequent year, they reported extended measurements [79] showing a jump at T_λ. Many other measurements have since been made [80]. Different methods of measurement such as rise of the liquid level in capillaries [78, 79, 81–84], measurements of force required to lift a metal ring from liquid surface [85] and measurements of surface wave velocity [86,87] have been used to measure the surface tension. Edwards *et al* [88] and Eckardt *et al* [89] used a method in which changes in the capillary rise of the liquid in parallel plate capacitor is balanced by an electric field which keeps the meniscus stationary. Measurements by Allen and Misener [81], Dickson *et al* [84], and King and Wyatt [86] show good agreement with each other, while the data of Atkins *et al* [82] and Zinov'eva *et al* [83] are slightly larger. Zinov'eva *et al* reported a value $378\,mdynes/cm$ as against Atkins *et al* who found $371.9\,mdynes/cm$ at absolute zero. In a later experiment, Iino *et al* [90] used surface-wave resonance and reported $354.4 \pm 0.5\,mdynes/cm$ at $T = 0$.

Measurements of surface tension near T_λ are reported by Atkins and Narahara [82], Gasparini *et al* [91], Magerlein and Sanders [92] and Suzuki *et al* [93], while the surface and inter-facial tensions of $^3He-^4He$ mixtures were measured by Guo *et al* [94], Sato and Suzuki [95] and Sato *et al* [96] A study of the liquid-solid helium interfacial tension was reported by Gallet *et al* [97]

In recent times surface tension of LHE-4 was measured by Roche *et al* [98], Nakanishi and Suzuki [99] and Vicente *et al* [100] Roche *et al* [98] obtained surface tension of the liquid by using a slightly complex arrangement of capillaries patterned in chromium on a mono-crystalline sapphire as substrate The extrapolation of their results yields a value $375 \pm 3\, mdynes/cm$ at absolute zero which differs by 6% from Iino *et al* [90] They attributed this difference to the meniscus effects which was not considered by Iino *et al* The measurements by Nakanishi and Suzuki [99] confirmed the findings of Iino *et al* [90] while Vicente *et al* [100] found values in agreement with Roche *et al* [98] It may be mentioned that Vicente *et al* [100] employed a completely independent technique in which surface tension was obtained by using the frequency of the normal modes of vibrations of magnetically levitated helium drops

1.2.8 Sound Velocities

In *helium-II* we find four different sound modes namely *first second third* and *fourth* sound While *first* sound is the normal longitudinal sound mode corresponding to the fluctuation in total density of the system at constant T, the *second* sound corresponds to the fluctuation of temperature Existence of second sound was predicted by Tisza [71] and Landau [101] in their respective two fluids models Similarly while the *third* sound is a surface wave on a *helium-II* film, in which the super-fluid oscillates parallel to the substrate with normal fluid clamped for its finite viscosity, the *fourth* sound represents pressure wave in *helium-II* inside a super-leak where the normal component is immobilised and super-fluid is free for motion Existence of *third* and *fourth* sound was predicted by Atkins [102]

Velocity of *first* sound was determined by Findlay *et al* [103] in 1938 using an ultrasonic method for a temperature range 4 22 K to 1 76 K They used their values to calculate compressibility of liquid helium, however, their experiments did not show any discontinuity at the λ-transition Chase [104] measured the *first*

sound velocity by a radar-pulse technique and used resonant quartz-crystal oscillator as transmitter and detector. In a different method Itterbeek *et al* [105, 106] measured it at different frequenies (200, 226, 500, 523, 800, 1485 and $1500\,kHz$) and temperature (1 and $0.985\,K$).

Shalnikov and Sokolov [107] attempted to generate and measure the *second* sound velocity by using a oscillating piezo-quartz, but without success. Lifshitz [108] showed that the intensity of the *second* sound radiated by oscillating plate is million times less than the ordinary sound due to which Shalnikov and Sokolov was unable to detect it. However, Peshkov [107] detected and measured it successfully by using an electrical heater supplied with alternating current as transmitter and a resistance thermometer as detector. While Hall and Vinen [109, 110] studied the *second* sound in rotating *helium-II*, Vinen [111–113] measured its attenuation arising from the super-fluid turbulence.

Rudnick *et al* [114] reported early generation and detection of *third* sound. Most of the early experiments on *third* sound are reviewed by Atkins and Rudnick [115]. Temperature dependence of *third* sound velocity was studied by Rudnick [116] who observed that it disappears near the transition temperature for steep rise of its dissipation. Ekholm and Hallock [117] measured the *third* sound velocity on static films.

Temperature dependence of *fourth* sound velocity was studied by Shapiro and Rudnick [118] by setting up standing waves of fourth sound in an acoustic resonator.

1.2.9 Neutron Scattering Experiments

LHE-4 has been studied extensively by neutron scattering. The first neutron scattering experiment on the liquid was reported by Goldstein *et al* [119] in 1951. This was followed by a large number of transmission measurements using a wide range of neutron energies as well as by diffraction measurements (Henshaw and Hurst [120, 121]). Guided by the idea of Cohen and Feynman [122] that neutron scattering could be used to determine the dispersion relation of the elementary excitations of LHE-4, a series of inelastic scattering measurement were performed in late 1950's [123–127]. These experiments revealed a "phonon-roton" dispersion which agrees qualitatively with that as envisaged by Landau [101]. While the

neutron scattering experiments till 1970 have been reviewed elegantly by Woods and Cowley [128] and Price [129], results of additional studies performed till early 1980's are summed up by Glyde and Svensson [130].

The basic objectives of neutron scattering experiments of 1970's and onward were to find out (i) the nature (*anomalous or normal*) of the energy dispersion of thermal excitations at low Q (wave vector), (ii) the temperature dependence of static structure factor [S(Q)], and dynamic form factor [S(Q,ω)] and (iii) the relation between condensate fraction (macroscopic occupation of $p = 0$ state) and super-fluid density if Bose Einstein condensation really exists in the liquid. Similarly as mentioned by Glyde and Svensson [130], these experiments were also aimed to answer (i) why S(Q,ω) does not change abruptly at transition temperature? (ii) why the width and peak position of S(Q,ω) at large Q oscillate with Q? and (iii) why S(Q,ω) shows no evidence of a sharp central component arising from a scattering by zero-momentum atoms in the Bose condensate of LHE-4? While these experiments served their purpose for certain objectives, the findings related to condensate fraction remained inconclusive [130–132]. Moreover, these experiments reveal a set of new puzzles to be addressed by future investigators, for example an IBG single particle momentum distribution function ($n(p)$) with no condensate can provide a satisfactory explanation of the observed scattering which indicates that condensate is not necessary to explain the observed scattering. Moreover, the empirical relations that are used to show the existence of the condensate have no firm foundation in theory and the conclusion on condensate fraction derived from the neutron scattering experiments will not have much meaning if these empirical relations are found to be incorrect.

1.2.10 Basic Properties of *helium-II*

We have already mentioned about different unique properties exhibited by *helium-II*. In this section we summarise these important properties of the liquid.

1. Different values of viscosity: *helium-II* behaves as a non-viscous fluid in flow measurement methods and exhibits a non-zero viscosity in rotatory or oscillatory measurement. Even the values of viscosity from rotatory and oscillatory methods do not agree with each other.

2. It can flow against the gravity along the walls of the container.

3. It has very high thermal conductivity (1000 times that of copper).
4. The specific heat and other related thermodynamic response functions such as expansion co-efficient, pressure co-efficient *etc.* diverge logarithmically at $\lambda-$point.
5. It exhibits thermo-mechanical and mechanocaloric effects.
6. Below T_λ, volume increases with decreasing temperature.
7. Above a certain velocity (flow/rotational), circulation becomes quantized.
8. It sustains four different sound modes.
9. Its dispersion curve at low Q shows anomalous nature.
10. It remains calm and still on boiling against the bubble formation.

1.3 Theoretical Studies

Most of the remarkable properties of LHE-4 were discovered within the first three decades of its liquification in 1908. However, theoretical investigation of the system had not started for a long time. Frohlich [133] was the first to provide an explanation of λ-transition who considered it to be a special kind of order-disorder transition. However, this idea was criticised by London [134] who considered the phenomenon as a manifestation of "Bose Einstein Condensation"(BEC) of ideal Bose gas (IBG) [135, 136] distorted by inter-molecular forces. London was led to this conclusion by some similarity in specific heat curves of LHE-4 and IBG which he reproduced later [137]. Using the parameters of LHE-4, he also showed that the BEC temperature ($= 3.13\,K$) for Helium is close to its T_λ i.e. $2.19\,K$.

To explain some of the important experimental results, a phenomenological "two fluid theory" was first proposed by Tisza [71,72,138]. In his theory, *helium-II* is considered to be a degenerate ideal Bose gas where atoms in their lowest energy state do not take part in dissipative motion indicating that viscosity of the fluid is entirely due to the atoms in excited states. Tisza initially considered the *helium-II* motion to be turbulent because velocity-pressure dependence for *helium-II* is more similar to turbulent than to laminar motion. The most important success of his theory was the prediction of the existence of temperature waves (*second* sound) in *helium-II*.

In 1941, Landau [101] also developed a "two fluid theory" of LHE-4 which was based on different considerations. Landau was critical about Tisza's theory. He pointed out that liquid helium has nothing to do with ideal gas and emphasized that nothing could prevent atoms in the lowest energy state from colliding with excited atoms and they should experience friction on moving through the liquid which implies that there should be no super-fluidity at all. In his theory there exist two independent motions of atoms in *helium-II* which are assumed to have no transfer of momentum from one to another. To be more specific, Landau considered *helium-II* to be a homogeneous mixture of two fluids: *normal fluid* (N-fluid) and *super-fluid* (S-fluid) with

$$\rho = \rho_n + \rho_s \tag{1.1}$$

with ρ, ρ_n and ρ_s respectively representing its total density, and densities of its N-fluid and S-fluid components. While ρ_n represents the gas of elementary excitations (phonons and rotons) and accounts for its total viscosity and entropy, ρ_s represents a component of zero viscosity and entropy. He showed that below a particular velocity (the so called critical velocity, v_c) of the flow of the liquid, creation of phonons or rotons is energetically not favourable and the liquid can behave as "super-fluid". In case of rotational motion he proposed that only a part of the liquid (N-fluid) is carried along by the walls of the container and the other part (S-fluid) remains stationary. Landau also showed that since the super-fluid does not enter into a rotation, the curl of the velocity of S-fluid must vanish.

As such by using the definition N-fluid, the viscosity of the liquid can be calculated in the same way as that of a mixture of phonons and rotons. He proposed two independent relations for phonon and roton modes, respectively, as:

$$\epsilon = cp \tag{1.2}$$

$$\epsilon = \Delta + \frac{p^2}{2\mu} \tag{1.3}$$

where c is the velocity of the sound, p is the momentum of the excitation, Δ represents an energy gap for roton mode and μ is an "effective mass" of the roton. However, Landau [139] later combined these relations by shifting the roton minimum to p_o to form a single excitation spectrum, and we have

$$\epsilon = \Delta + \frac{(p - p_o)^2}{2\mu} \tag{1.4}$$

for roton excitations; the energy of the long wave excitation (i.e. phonon) was not changed.

Landau's 1941 paper is undoubtedly the most influential single contribution to the development of the phenomenological theory of LHE-4 for which he was awarded Nobel Prize. However, this has several shortcomings, inconsistencies and quantitative disagreements with certain experimental results *viz.* the critical velocity, *second* sound velocity, viscosity paradox etc. The shortcomings of this theory have been discussed in details by Putterman [135].

In the process of development of the microscopic theory, the first significant contribution came from Bogoliubov [140] in 1947. He analyzed a system of weakly interacting bosons and tried to overcome the basic objection to the London's idea of associating BEC to the unique behavior of *helium-II*. Considering the degeneracy of a non-perfect Bose gas, he used the method of second quantization to show that in the presence of small interactions between the atoms, the low excited states of the gas can be described as a perfect Bose gas of certain "quasi particles" (elementary excitations). He established a relation which indicates that the fraction of atoms condense into $p = 0$ state does not assume 1.0 value even at absolute zero. The atoms in this state can move without any friction with respect to the elementary excitations. Most significantly his theory reproduces Landau's "phonon-roton" spectrum for low Q.

Since the inter-atomic interactions between helium atoms to a good approximation are strong, LHE-4 cannot be considered as a weakly interacting Bose gas. Evidently, despite Bogoliubov's work, microscopic understanding of Landau's spectrum was not clear and the subject remained open for further investigation. The problem was then undertaken by Feynman [141 143]. Using the quantum path integral method, Feynman first showed that in spite of the strong inter-atomic interactions, LHE-4 should exhibit a transition analogous to the transition of an IBG [141]. He further observed that no low energy excitation other than phonon could exist in the liquid [142] which agrees with Landau. Consequently the low temperature specific heat must vary as T^3 and the flow resistance of the fluid should be small. In his third paper, Feynman used the variational approach to find the wave function that represents an excitation in the liquid and obtained

$$\epsilon(Q) = \frac{\hbar^2 Q^2}{2mS(Q)} \tag{1.5}$$

for its energy $\epsilon(Q)$; here $S(Q)$ is the structure factor of the liquid. For larger Q, $S(Q)$ has a maximum leading to a minimum in $E(Q)$. Although Feynman relation gave an energy-momentum curve having the qualitative shape as suggested by

Landau, quantitative agreement was very poor. While Feynman's relation gave $\Delta = 19.1\,K$, (equation 1.4), thermodynamic data required $\Delta = 9.6\,K$. In a subsequent paper Feynman, in collaboration with Cohen [144], used the concept of back flow to find modified form of wave function yielding $\Delta = 11.5\,K$, which has a better agreement with experiments. The new wave function suggested that the roton is a kind of quantum-mechanical analog of a microscopic vortex ring, of diameter equal to about the atomic spacing. In addition, they showed that neutron scattering experiment could be used to determine $\epsilon(Q)$ [122].

Different physical descriptions of roton came from de Boer [145], Chester [146], Miller *et al* [147] and Lee and Mohling [148]. According to de Boer the roton loses its 'vortex' or rotation character and should be considered as short-wavelength longitudinal elastic mode. Chester proposed that roton is associated with the motion of a ^4He atom with modified mass. Miller *et al* proposed that quasi-particle for Q lying between $1\mathring{A}^{-1}$ and $2\mathring{A}^{-1}$ behave like the slow-moving impurity atoms in their coupling to the long wavelength excitations. Finally, Lee and Mohling studied the experimental data for the total cross-section of the inelastic scattering of cold neutrons in *helium-II* and found that the projection of the angular momentum on the direction of momentum p of the roton is zero. In other words the roton excitation has zero angular momentum implying that it loses rotational character.

The idea of vortex line and quantization of super-fluid circulation was first introduced by Onsager (as cited in [1]) which was later developed by Feynman [149]. Feynman showed that the quantized circulation around a vortex line representing a cylindrical hole, where no atom can enter, is given by:

$$\oint v_s.ds = n\frac{2\pi\hbar}{m} \tag{1.6}$$

Feynman considered the radius of the hole to be equal to atomic spacing which he took arbitrarily as $4.0\mathring{A}$. However, Vinen [150] estimated it to be $\sim 0.5\mathring{A}$ which indicates that no real macroscopic hole exists in the super-fluid but only vortex lines.

The experimental evidence of vortex lines was first given by Hall and vinen [109]. They [110] suggested that the *second* sound attenuation [109] can be explained in the presence of vortex line. Further experimental evidence of quantized circulation are provided by experiments of [151–154]. In the above mentioned Bogoliubov [140] theory "degenerate condensate" plays an important role. This idea

was further developed by Onsager and Penrose [155] and by Bogoliubov [156,157]. Using the properties of ground-state wave function and an assumption that there is no "long-range configurational order", Onsager and Penrose showed that BEC occurs in *helium-II* at absolute zero. They found that almost 8% of the atoms condensate into zero momentum state and proved that for such a state of the system, one has $< \psi(t,r) > \neq 0$ where $\psi(t,r)$ is the Bose operator. This property allows one to derive the hydrodynamical equations (with two velocities) from the microscopic theory which was done independently by Bogoliubov [157] and Hohenberg and Martin [158]. In his field theoretical approach, Bogoliubov observed broken gause invariance and showed that if some kind of symmetry in the system is broken then in statistical mechanics "quasi-average" is preferable over "normal average". Bogoliubov as well as Hohenberg and Martin obtained Landau's hydrodynamic equations by considering an external scalar potential and sources of particles. These equations with viscous terms were derived by Galasiewicz [159, 160] and Krasnikov [161] using Bogoliubov's approach. Similar equations were also derived by Khalatnikov [162] using a different approach where the distribution function of elementary excitations in *helium-II* satisfies Boltzman equation.

Landau and Khalatnikov [163] calculated the temperature dependence of the viscosity coefficient(η) by calculating the effective differential cross-section for the scattering of quasi-particles by each other. Later, Khalatnikov [164] used the same method to calculate temperature dependence of thermal conductivity(κ) and η.

Generalised form of off-diagonal long-range order (ODLRO) of the reduced matrices in the coordinate space representation was introduced by Yang [165]. However, existence of such ODLRO in single particle density matrix was hinted by Penrose [166] and later by Penrose and Onsager [155]. Yang has shown that ODLRO leads to a new thermodynamic phase of the system and super-fluidity of *helium-II* is characterized by its existence. The smallest N for which ODLRO occurs is a set of particles that forms a basic group exhibiting the long range correlation. He also reveals that the basic group necessarily be composed of bosons or even number of fermions. Kane and Kadanoff [167] showed that such a long range correlation appears only in 3-D implying that the phase transition in 1-D or 2-D systems must differ from that in 3-D system.

In deriving the hydrodynamic equations for a system in thermodynamic equilibrium, the impact of thermal fluctuations should obviously be small. However, in the absence of the said equilibrium the state of the system would be collision dominated because local in-equilibrium leads to frequent collisions between particles. This situation brings serious mathematical complexity in developing a theory that explains important thermodynamic and hydrodynamic aspects of the system. For example a viable theory must be consistent with hydrodynamical equations as well as with thermodynamic relations which is needed to obtain the excitation spectrum of the system. Several methods were developed to overcome such difficulties [157, 158, 168, 169].

Use of field theoretical approach to develop a microscopic theory of LHE-4 type system started with Bogoliubov's [140] study of weakly interacting bosons. However, the helium atoms experience strong short range repulsion which forbids any two helium atoms from occupying same point in real space and offers serious difficulties in formulating a viable theory of LHE-4. Brueckner and Sawada [170, 171] tried to overcome these difficulties by considering the system to be a dilute one. They found that the expectation value of the interaction energy for dense system like LHE-4 diverges and the divergence is intimately connected with the large amount of energy required to remove particles from the ground state. Consequently, they first considered a dilute system of ^4He type atoms and analysed its low energy excitations; the analysis was later extended to include high energy excitation. Goble and Trainor [172] used this theory for various hard core radii to find that condensate fraction varied from 0.37 to 0.79 as the hard core radius was altered from 3.0 to 1.0 A. In a similar study Parry and ter Haar [173] found that roton minimum disappears if the depletion effect is included in such calculations; even poorer results were rendered when an attractive trail was added to the hard core. These difficulties, evidently, showed that hard sphere boson gas is not a good model for liquid helium. Liu *et al* [174, 175] showed that a qualitatively correct excitations spectrum can be obtained if two body pseudo-potential ([176] and [177]) is used.

Despite various difficulties, Brueckner and Sawada's method has been considered as an important tool for microscopic derivation of the excitations spectrum of LHE-4. The accuracy of this method has been examined by Bycking [178] who used Green's function techniques to find the depletion of $p = 0$ state and a new method of solving scattering matrix equation. He obtained numerical values for

excitation energy by using hard sphere potential with hard core radius of $2.6\mathring{A}$ as well as Lennerd-Jones (LJ) 6-8 potential with $\sigma = 2.8\mathring{A}$ and $\epsilon = 6.34\,K$. Although both potentials rendered qualitatively acceptable excitations spectrum, however, first sound velocity was larger than the measured one for hard sphere potential and smaller for LJ potential. In addition Bycking was unable to obtain self consistently correct condensate fraction; the value of condensate fraction obtained by him in both cases was larger than unity (unphysical value).

Singh and Kumar [179, 180] included a weak long-range attraction along with the short ranged repulsive interaction in their field theoretical approach. They have shown that at zero temperature, if the parameters of the attractive part of the interaction are suitably restricted, the self energy part of the Green's function leads to a phonon like excitation spectrum for small momentum. They extended the theory to non zero temperature using temperature dependent Green's function.

Depletion of the ground state also leads to several difficulties in the application of many body techniques to LHE-4. Beliaev [181], Hugenholtz and Pines [182] tried to overcome these difficulties using perturbation technique. While Beliaev developed a method to rigorously account for the depletion and found a formulation free from all kinds of divergence, Hugenholtz and Pines obtained a result eliminating the $p = 0$ state that agree with Beliaev. They found that energy gap does not exist for phonon dispersion.

Brandow [183, 184] developed a perturbation theory which is somewhat different from Beliaev [181] and Hugenholtz and Pines [182]. He emphasized the similarity between ground state and collective excitations of LHE-4 and those of a normal Fermi liquid. He extended Goldstone's [185] cluster expansion for normal fermionic systems to bosons.

Another approach approximating the self energy term has been used by Tserkovnikov [186,187], Pines [188,189], Etters [190] and Cheung and Griffin [191, 192] but without much improvement in the correct understanding of the system.

Following the success of BCS theory of superconductivity significant attempts have been made to develop analogous pairing models of ^4He. Valatin and Butler [193] were the first to develop a pair condensate theory of homogeneous boson system. Later Girardeau and Arnowitt [194] and Gross [195] combined the idea of a single particle and pair condensate. This approach was further developed

by Zubarev and Tserkovnikov [196], Girardeau [197], Wentzel [198], Luban [199], Cummings and Johnston [200], Kobe [201], Parmenter [202], Evans and Imry [203], Brown and Coopersmith [204], Coniglio *et al* [205], Evans and Rashid [206]. A phenomenological pairing model was put forward by Hastings and Halley [207,208] to propose an explanation of the anomalous dispersion of the elementary excitations at long wavelength. Ristig [209] derived pairing function which represents the fundamental component of a pairing model.

In a different approach to the microscopic understanding of LHE-4 type systems, variational techniques with presumed approximate form of the wave function have been used to find the structure factor $S(Q)$ and pair distribution fluctuation $(g(r))$ which have well defined relationships with different properties of a fluid. In this context Jastrow wave function

$$\Psi = \sum_{i<j} \exp(U(r_{ij})/2) \tag{1.7}$$

has been widely used in most of the initial theoretical formulations. Here $U(r_{ij})$ is so defined that Ψ vanishes when the inter-particle pair potential assumes infinitely large value for two particles occupying close positions. It appears that two different approaches have been used to express $U(r)$.

As used by McMillan [210] and Schiff and Verlet [211], $U(r)$ is approximated by

$$U_s(r) = -(a/r)^n \tag{1.8}$$

where a and n can be chosen to have suitable values. While McMillan [210] used Monte Carlo procedure on two different sets of 32 and 108 atoms, Schiff and Verlet [211] used techniques of molecular dynamics for a set of 864 atoms to obtain minimum energy, density, condensate fraction for certain values of a and n. In a similar related study Padmore and Chester [212] used Monte Carlo method to calculate the excitation energy using the Jastrow function.

In the alternative approach, different relations between $U(r)$ and the pair distribution function $(g(r))$ such as BBGKY (Bogoliubov, Born, Green, Kirkwood and Yvon) equation [213], the hypernated chain (HNC) equation, the Percus-Yevick equation [214], the modified Percus-Yevick equation [215] *etc.* have been employed to find $g(r)$ and the ground state energy. One finds that different equations have been used by different groups. For example, while Lee [216] used the HNC equation, Massey [217] and Massey and Woo [218] used BBGKY equation.

However, all these calculations reveal a non-zero value for $S(Q)$ for $Q = 0$ in contradiction to the exact result. Reatto and Chester [219] showed that this discrepancy arises from the inadequacy of the assumed form of $U(r)$ and can be removed by considering long range correlations in the ground state wave function due to the virtual phonons.

Correlated Basis Function (CBF) method has been developed by Feenberg and collaborators [220–225] and has reviewed elegantly by Woo [226]. This method was used by Campbell and Feenberg [227] to calculate the long range correlation in the ground state wave function. In their calculation they initially took $U(r)$ of Massey and Woo [218] and then used their formalism to obtain an improved $S(Q)$. While Jackson and Feenberg [221] calculated the second order contribution from two-phonon intermediate states, Lee and Lee [228] included the second order effects of three phonon states. Four phonon contribution has also been calculated by Lee [229] and Lai *et al* [230]. CBF calculation using two- and three-body correlations were performed by Chang and Campbell [231]. Schmidt and Pandharipande [232] included the three-body correlations in the ground state wave function and used HNC summation method to find the excitation energy. Manousakis and Pandharipande [233] generalized CBF perturbation theory to include back flow correlations and used Variational Green's-function Monte Carlo method and experimental pair distribution function to calculate the second order correction. While Iwamoto [234], Jackson [235] and Zawadowski [236] discussed the dependence of $S(Q)$ on the density of two-phonon states, temperature dependence of roton energies was discussed by Ruvalds [237], Jackle [238], Takeno [239] and Nagai [240].

Sim *et al* [241,242] have applied both the canonical transformation method [140, 170, 171] and the Jastrow function approach [243–245] to obtain the energy of the dilute Bose gas. They showed that both approaches give identical results for those terms involving the potential $(V)^m$ for m less than 4. However, Jastrow function approach fails to give higher order interaction term correctly. In a similar approach, Wong *et al* [246, 247] used a method developed by Wong and Fung [248] to establish a relationship between the two. They expressed the explicit matrix representation of the linear unitary transformation in terms of the multi-particle basis-correlation function. However, they did not propose any specific form of the Hamiltonian.

In recent time various Monte Carlo methods such as Variational Monte Carlo (VMC), Green-function Monte Carlo (GFMC), Path Integral Monte Carlo (PIMC) are used to calculate the properties of LHE-4. Whitlock and Panoff [249] has used GFMC method to find the momentum distribution of LHE-4 at zero temperature. Similar calculations are performed by Caperley and Pollock [250–252] using PIMC method and by Masserini *et al* [253] using VMC method for non zero temperature. Caperley *et al* [254, 255] and Moroni *et al* [256] have used diffusion Monte Carlo (DMC) method to calculate the properties of ground state. This method is also used by Moroni *et al* [257] to calculate one body density matrix and the momentum distribution of LHE-4 as well as of liquid ^3He. Euler Monte Carlo (EMC) method is developed by Vitiello and Schmidt [258] and Moroni *et al* [256] and used by Moroni *et al* [256, 259] to calculate the properties of LHE-4 and liquid ^3He.

1.4 Conclusion

During the last six decades untiring efforts have been made to develop either a microscopic theory or a phenomenological theory that accounts all the unique properties of LHE-4. Tisza's model [71.72,138], Landau's two fluid model [101,139] and Ginzburg-Landau $\Psi-$theory [260] are prominent among the phenomenological theories. The microscopic formalism of LHE-4 are broadly based on two different approaches: field theoretical approach and variational approach. Field theoretical approach has been started with Bogoliubov's theory of weakly interacting Bose gas [140] which was further developed by Beliaev, Hugenholtz and Pines, Brueckner and Sawawda and others. Variational approach was first used by Feynman and contributed further by Jackson and Feenberg, Jastrow, Penrose and Onsager and others. In microscopic approach there are theories which presume the existence of $p = 0$ condensate, there are theories which presume 'pair' condensation, there are theories with no condensation and there are theories which presume $p = 0$ condensate together with pair condensation and many particles condensation. Despite all these efforts there is no single theoretical framework which explains all important properties of LHE-4. One may find one theory for one property then other for other property. Moreover, the existence of $p = 0$ condensate, which plays an important role in most of the above mentioned microscopic theories, has not been established beyond doubt [130,131]. Deep inelastic neutron

scattering (DINS) experiments, which have been performed with a primary goal to observe direct evidence of $p = 0$ condensate, has not succeeded in reaching its goal. Various methods of analyzing of the DINS data lead to estimate the condensate fraction(n_o) that ranges between 2.4 and 17% [130, 132, 261]. However, the value of n_o so inferred is inconsistent and model dependent. Jackson [261] also observed that data are consistent with the absence of a condensate too. Reviewing the results of neutron scattering experiments up to 1987, Glyde and Svensson [130] remarked:

> *The equations which are used to interpret the neutron scattering data are essentially empirical relations with no firm foundation in theory. To apply these relationships it is necessary to make some assumptions. These assumptions are often major source of uncertainty in the analysis.*

In another article Sokol [132] remarked:

> *If the underlying assumptions of the expressions used in the fits (neutron scattering data) are incorrect. then the results inferred will not have much meaning. It is interesting to note that the observed scattering in liquid helium can be fit extremely well simply by using the momentum distribution (n(p)) of the ideal Bose gas. This holds true in both the normal and super-fluid phase. The best description of the scattering in the super-fluid is obtained by using an ideal Bose gas $n(p)$ with no condensate.*

Very recently, in a review article Leggett [131] remarked:

> *In the sixty years since London's original proposal, while there has been almost universal belief that the key to super-fluidity is indeed the onset of BEC at T_λ it has proved very difficult, if not impossible, to verify the existence of the latter phenomenon directly. The main evidence for it comes from high-energy neutron scattering and, very. recently, from the spectrum of atoms evaporated from the liquid surface, and while both are certainly consistent with the existence of a condensate fraction of approximately 10%, neither can be said to establish it beyond all possible doubts.*

These comments of the experts in the field reflect that still there is a doubt about the existence of $p = 0$ condensate in super-fluid helium. It is unfortunate that while there is no firm foundation for the existence of $p = 0$ condensate in super-fluid helium, most of the microscopic theories start with the basic assumption that this state ($p = 0$ condensate) really exists in the system. Reviewing the progress of theoretical work at the fifteenth Scottish University summer school Rickayzen [262] stated:

> *There is no microscopic theory of superfluid* ^4He*. There are many mathematical models which appear to provide insight into the behavior of superfluids but there is no theory which provides quantitative prediction that agree with observation. Even some of the most widely held assumptions of the theory such as the idea of condensation in a zero momentum state can not be said to be proved beyond reasonable doubt.*

Concluding a review article, Woods and Cowley [128] also observed:

> *Despite all the experimental information and numerous theoretical discussions there is still no convincing theory of the excitations which begins with the known interaction between helium atoms.*

At the same time Kleban [263] proved that theories assuming the existence of $p = 0$ condensate contradict the excluded volume principle-a direct consequence of hard core nature of particles. It is interesting to note that very recently Ettouhami [264] questions the validity of the Bogoliubov theory [140], which was the starting point of the field theoretical approach. As such, the only way to understand the properties of LHE-4 is the two fluid model of Landau [101,139] supplemented by the idea of quantized circulation presented by Onsager [265] and Feynman [149]. However, this combination has several shortcomings too. Discussing these shortcomings Putterman [135] remarked,

> *The two fluid theory plus quantization bears striking similarity to the old quantum theory. Just as the old quantum theory had to be modified in light of the wave particle duality, one must expect that our deterministic two fluid theory of* helium-II *will be modified by microscopic wave particle duality.*

The above mentioned facts motivated Jain to use an entirely new approach to develop a microscopic theory of super-fluid helium known as "Macro orbital theory" [266-268]. This theory neither assumes the existence of $p = 0$ condensate nor applies the variational method. We discuss the salient features of this theory and its significant results in Chapter 2. One may find that the theoretical results obtained by Jain's Macro-orbital theory closely agree with the experimental results which indicates that this theoretical framework has great potential in accounting for the properties of widely different system of interacting bosons. And to this effect the present thesis has succeeded in its major objective.

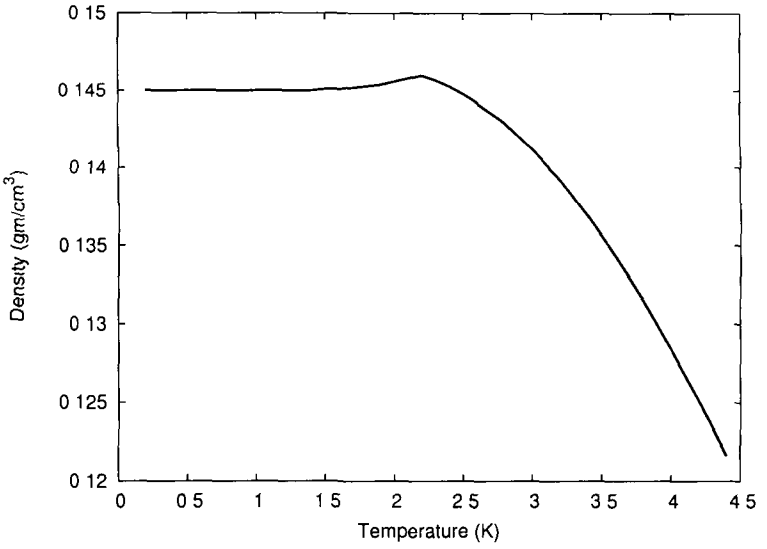

Figure 1.1: The density of LHE-4 under the saturated vapour pressure. (Source: Kerr and Taylor [16] as cited in [8])

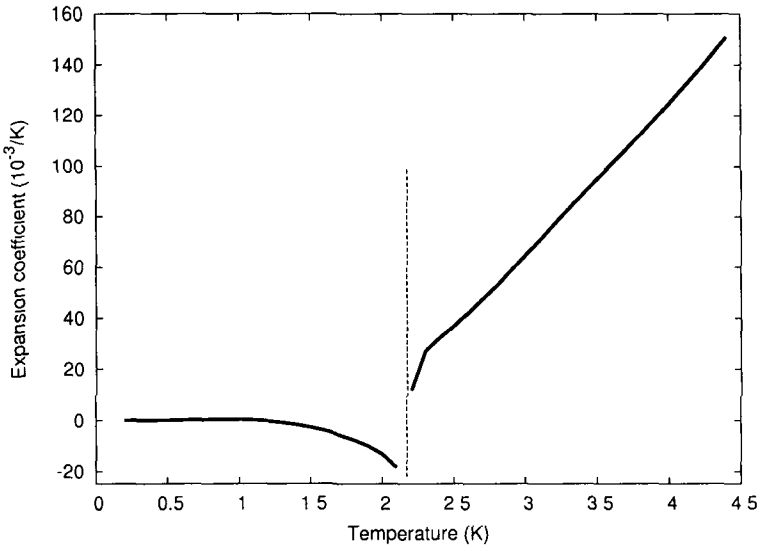

Figure 1.2: Expansion coefficient of LHE-4 under the saturated vapour pressure. (Source: Kerr and Taylor [16] as cited in [8])

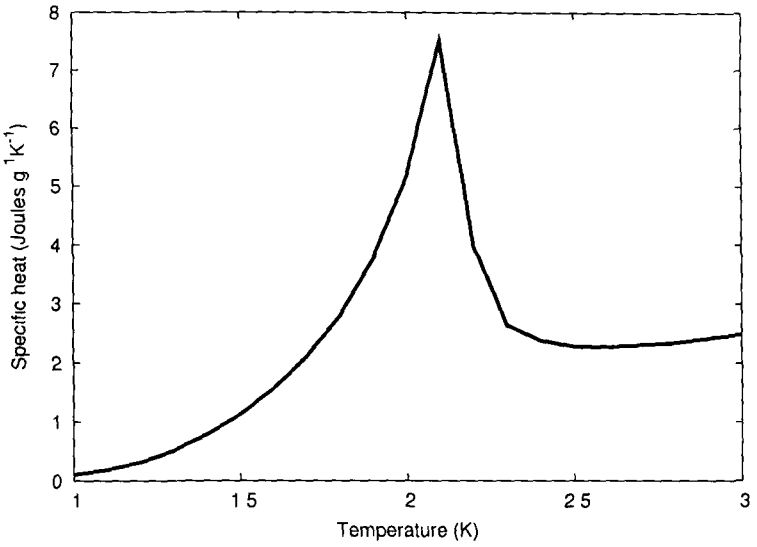

Figure 1.3: The specific heat of LHE-4 under the saturated vapour pressure (Source: Wilks [8], p-666)

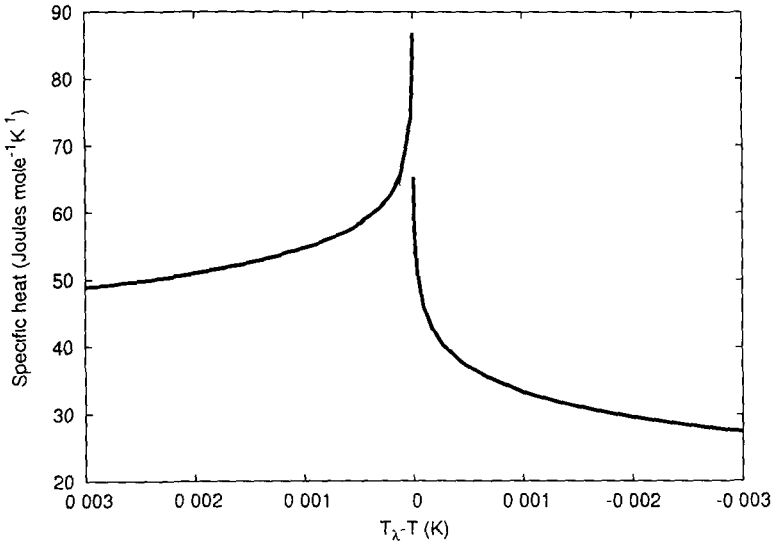

Figure 1.4: The specific heat of LHE-4 under the saturated vapour pressure (Source: G. Ahlers [42])

Bibliography

[1] Zygmunt M. Galasiewicz. *Helium-4.* Pragamon Press, Oxford, 1971.

[2] H.K. Onnes. *Leiden Comm.*, 108, 1938.

[3] H.K. Onnes. *Proc. Sect. Sci. K. ned. A kad. Wet.*, 11:16, 1908.

[4] D.R. Tilley and J. Tilley. *Superfluidity and Superconductivity.* Adam Hisger Ltd., Bristol and Boston, 1986.

[5] W.H. Keesom and K. Clusius. *Leiden Comm. (reprinted in Ref. 1)*, 219e, 1932.

[6] P. Ehrenfest. *Leiden Comm.*, Suppl. 75b:8, 1933.

[7] P. Kapitza. *Nature*, 141:74, 1938.

[8] J. Wilks. *The Properties of Liquid and Solid Helium.* Clerendon Press, Oxford, 1967.

[9] W.H. Keesom and A.P. Keesom. *Physica (reprinted in Ref. 1)*, 3:359, 1936.

[10] Burton. *Nature*, 135:265, 1935.

[11] J.O. Wilhem, A.D. Misener, and A.R. Clark. *Proc. Roy. Soc.*, A. 151:342, 1935.

[12] J.F. Allen and H. Jones. *Nature*, 141:243, 1938.

[13] H.K. Onnes. *Proc. Roy. Acad., Amsterdam*, 13:1093, 1911.

[14] H.K. Onnes and J.D.A. Boks. *Leiden Comm.*, 170b, 1924.

[15] E.C. Kerr. *J. Chem. Phys.*, 26:511, 1957.

[16] E.C. Kerr and R.D. Taylor. *Ann. Phys* , 26:292, 1964.

[17] V.P. Peshkov and A.P. Borovikov. *Sov. Phys. JETP*, 23:559, 1966.

[18] C. Boghosian and H. Meyer. *Phys. Rev.*, 163:200, 1967.

[19] D.L. Elwell and H. Meyer. *Phys. Rev.*, 164:245, 1967.

[20] P.R. Roach. *Phys. Rev.*, 170:213, 1968.

[21] H.N. Hanson, J.E. Berthold, G.M. Seidel, and H.J. Maris. *Phys. Rev. B*, 14:1911, 1976.

[22] J.J. Neimela and R.J. Donnelly. *J. Low Temp. Phys.*, 98:1, 1995.

[23] M.H.W. Chan, K.I. Blum, S.Q. Murphy, G.K.S. Wong, and J.D. Reppy. *Phys. Rev. Lett.*, 61:1950, 1988.

[24] K.R. Atkins and M.H. Edwards. *Phys. Rev.*, 97:1429, 1955.

[25] M.H. Edwards. *Can. J. Phys.*, 36:884, 1958.

[26] C.E.Chase, E. Maxwell, and W.E. Millett. *Physica*, 27:1129, 1961.

[27] G. Ahlers. *Phys. Rev.*, A 8:530, 1973.

[28] W.H. Keesom and M.Wolfke. *Leiden Comm.*, 190b, 1927.

[29] J. Grebenkemper and J.P. Hagen. *Phys.Rev.*, 80:89, 1950.

[30] H.A. Kierstead. *J. Low Temp. Phys.*, 23:791, 1976.

[31] M. Chan, M. Ryschkewitsch, and H. Meyer. *J. Low Temp. Phys.*, 26:211, 1977.

[32] L.I. Dona and H.K. Onnes. *Leiden Comm*, Suppl. 179d, 1926.

[33] W.M. Fairbank, M.J. Buckinghum, and C.F. Kellers. *Proc.* 5^{th} *Int. Conf. Low. Temp. Phys.* University of Wiscousin, 1958.

[34] M.J. Buckinghum and W.M. Fairbank. In C.J. Gorter, editor, *Progress in Low Temperature Physics*, volume VIII. North-Holland, Amsterdam, 1961.

[35] H.C. Kramers, J.D. Wasscher, and C.J. Gorter. *Physica*, 18:329, 1952.

[36] R.W. Hills and O.V. Lounasmaa. *Phil. Mag.*, 2:143, 1957.

[37] J. Wiebes, C.J. Nells Hakkenberg, and H.C. Kramers. *Physica*, 23:625, 1957.

[38] O.V. Lounasmaa and E. Kojo. *Ann. Acad. Sci. Finncae. Ser.*, A VI:No. 36, 1959.

[39] G.J.C. Bots and C.J. Gorter. *Physica*, 26:337, 1960.

[40] C.J.N. Van den Meijdenberg, K.W. Taconis, and R. de Bruyn Ouboter. *Physica*, 27:197, 1961.

[41] G. Ahlers. *Phys. Rev. Lett.*, 23:464, 1969.

[42] G. Ahlers. *Phys. Rev.*, A 3:696, 1971.

[43] F. Gasparini and M.R. Molodover. *Phys. Rev. Lett.*, 23:749, 1969.

[44] F.M. Gasparini and M.R. Molodover. *Phys. Rev.*, B 12:93, 1975.

[45] J.A. Lipa and T.C.P. Chui. *Phys. Rev. Lett.*, 51:2291, 1983.

[46] M. Coleman and J.A. Lipa. *Phys. Rev. Lett.*, 74:286, 1995.

[47] J.A. Lipa, D.R. Swansson, J.A. Nissan, Z.K. Geng, P.R. Williamson, D.A. Stricker, T.C.P. Chui, U.E. Israelsson, and M. Larson. *Phys. Rev. Lett.*, 84:4894, 2000.

[48] T. Chen and F.F. Gasparini. *Phys. Rev. Lett.*, 40:331, 1978.

[49] S. Mehta and F.M. Gasparini. *Phys. Rev. Lett.*, 78:2596, 1997.

[50] S. Mehta, M.O. Kimball, and F.M. Gasparini. *J. Low Temp. Phys.*, 113:435, 1998.

[51] J.A. Lipa, D.R. Swanson, J.A. Nissen, T.C.P. Chui, and U.E. Israelsson. *Phys. Rev. Lett.*, 76:944, 1996.

[52] J.A. Lipa, D.A. Swansson, and T.C.P. Chui. *Phys. Rev.*, B 68:174518–1, 2003.

[53] J.F. Allen, R. Peierls, and Z. Uddin. *Nature*, 62:62, 1937.

[54] F. London. *Proc. Roy. Soc.*, A 171:484, 1939.

[55] J.G. Daunt and K. Mendelssohn. *Nature*, 143:719, 1939.

[56] D.F. Brewer and D.O. Edwards. *Proc. Phys. Soc.*, 71:117, 1958.

[57] C.I. Um, S.K. Yoo, S.Y. Lee, S.T. Nam, T.F. George, and L.N. Pandey. *Physica*, B 203:151, 1994.

[58] A.M. Kahn and G. Ahlers. *Phys. Rev. Lett.*, 74:944, 1995.

[59] W.H. Keesom and G. MacWood. *Physica*, 5:737, 1938.

[60] W.H. Keesom and P.H.Keesom. *Physica*, 8:65, 1941.

[61] P.L. Smith. *Physica*, 16:16, 1950.

[62] deTroyer, van Itterbeck, and van den Berg. *Physica*, 17:50, 1951.

[63] J.T. Tough, W.D. McCormick, and J.G. Dash. *Phys. Rev.*, 132:2373, 1963.

[64] Johns, Wilhelm, and Grayson-Smith. *Can. J. Research*, A17:149, 1939.

[65] R. Bowers and K. Mendelssohn. *Proc. Phys. Soc. (London)*, A 62:394, 1949.

[66] R. Bowers and K. Mendelssohn. *Proc. Roy. Soc. (London)*, A 204:366, 1950.

[67] J.F. Allen and A.D. Misener. *Nature*, 142:643, 1939.

[68] J.F. Allen and A.D. Misener. *Proc. Roy. Soc. (London)*, A172:467, 1939.

[69] P. Kapitza. *J. Phys. U.S.S.R.*, 4:181, 1941.

[70] P. Kapitza. *J. Phys. U.S.S.R.*, 5:59, 1941.

[71] L. Tisza. *Nature*, 141:913, 1938.

[72] L. Tisza. *J. Phys. at radium (8)*, 1:164, 350, 1940.

[73] Giauque, Stout, and Barieau. *Phys. Rev.*, 54:146, 1938.

[74] Giauque, Stout, and Barieau. *J. Am. Chem. Soc.*, 61:654, 1939.

[75] A.C. Hollis Hallett. *Proc. Camb. Phil. Soc. math.phys. Sci.*, 49:717, 1953.

[76] W.J. Heikkila and A.C. Hollis Hallett. *Can. J. Phys.*, 33:420, 1955.

[77] A.D.B. Woods and A.C. Hollis Hallett. *Can. J. Phys.*, 41:596, 1963.

[78] A.T. van Urk, W.H. Keesom, and H.K. Onnes. *Proc. Roy. Acad. Sci. Amsterdam*, 28:58, 1925.

[79] A.T. van Urk, W.H. Keesom, and H.K. Onnes. *Leiden Comm.*, 179a, 1926.

[80] D.O. Edwards and W.F. Saam. In D.F. Brewer, editor, *Progress in Low Temperature Physics*, volume VIIA. North-Holland, Amsterdam, 1978.

[81] J.F. Allen and A.D. Misener. *Nature*, 141:75, 1938.

[82] K.R. Atkins and Y. Narahara. *Phys. Rev.*, 136:A437, 1965.

[83] K.N. Zinov'eva and S.T. Bolarev. *Sov. Phys. JETP*, 56:585, 1969.

[84] D.P.E. Dickson, D. Caroline, and E. Mendoza. *Phys. Lett. A*, 33A:139, 1970.

[85] N. Devraj and A.C.H. Hellett. *Can. J. Phys.*, 45:2113, 1967.

[86] I.J. King and A.F.G. Wyatt. *Proc. Roy. Soc. London*, A 322:355, 1971.

[87] S.T. Boldarev and V.P. Peshkov. *Physica (Amsterdam)*, 69:141, 1973.

[88] D.O. Edwards, P.P. Fatouros, G.G. Ihas, and P. Mrozinski an S.Y. Shen. *Phys. Rev. B*, 11:4734, 1975.

[89] J.R. Eckardt, D.O. Edwards, S.Y. Shen, and F.M. Gasparini. *Phys. Rev. B*, 16:1944, 1977.

[90] M. Iino, M. Suzuki, and A.J. Ikushima. *J. Low Temp. Phys.*, 61:155, 1985.

[91] F.M. Gasparini, J. Eckwrdt, D.O. Edwards, and S.Y. Shen. *J. Low Temp. Phys.*, 13:437, 1973.

[92] J.H. Magerlein and T.M. Sanders Jr. *Phys. Rev. Lett.*, 36:258, 1976.

[93] M. Suzuki, M. Iino, and A.J. Ikushima. *J. Low Temp. Phys.*, 63:129, 1986.

[94] H.M. Guo, D.O. Edwards, R.E. Sarwinski, and J.T. Tough. *Phys. Rev. Lett.*, 27:1259, 1971.

[95] A. Sato and M. Suzuki. *J. Low Temp. Phys.*, 99:727, 1995.

[96] A. Sato, K. Ohishi, and M. Suzuki. *J. Low Temp. Phys.*, 107:165, 1997.

[97] F. Gallet, P.E. Wolf, and S. Balibar. *Phys. Rev. Lett.*, 52:2253, 1984.

[98] P. Roche, G. Deville, N.J. Appleyard, and F.I.B. Williams. *J. Low Temp. Phys.*, 106:565, 1997.

[99] Kazuhito Nakanishi and Masaru Suzuki. *J. Low Temp. Phys.*, 113:585, 1998.

[100] C. Vicente, W. Yao, H.J. Maris, and G.M. Seidel. *Phys. Rev. B*, 66:214504, 2002.

[101] L.D. Landau. *J. Phys. U.S.S.R. (reprinted in Ref. 1)*, 5:71, 1941.

[102] K.R. Atkins. *Phys. Rev.*, 113:962, 1959.

[103] J.C. Findlay, A. Pitt, H. Grayson Smith, and J.O. Wilhelm. *Phys. Rev.*, 54:506, 1938.

[104] C.E. Chase. *Proc. Roy. Soc.*, A 220:116, 1953.

[105] A. van Itterbeek, G. Forrez, and M. Teirlinek. *Physica*, 23:63, 1957.

[106] A. van Itterbeek, G. Forrez, and M. Teirlinek. *Physica*, 23:905, 1957.

[107] V. Peshkov. *J. Phys. (U.S.S.R) (reprinted in Ref. 1)*, 10:389, 1946.

[108] Lifshitz. *J. Phys. (U.S.S.R.)(reprinted in Ref. 1)*, 8:110, 1944.

[109] H.E. Hall and W.F. Vinen. *Proc. Roy. Soc.*, A 238:204, 1956.

[110] H.E. Hall and W.F. Vinen. *Proc. Roy. Soc.*, A 238:215, 1956.

[111] W.F. Vinen. *Proc. Roy. Soc.*, A 240:114, 128, 1957.

[112] W.F. Vinen. *Proc. Roy. Soc.*, A 242:1493, 1957.

[113] W.F. Vinen. *Proc. Roy. Soc.*, A 243:400, 1957.

[114] I. Rudnick, R.S. Kagiwada, J.C. Fraser, and E. Guyon. *Phys. Rev. Lett.*, 20:430, 1968.

[115] K.R. Atkins and I. Rudnick. In C.J. Gorter, editor, *Prog. Low Temp. Phys.*, volume VI. North-Holland, Amsterdam, 1970.

[116] I. Rudnick. *Phys. Rev. Lett.*, 40:1454, 1978.

[117] D.T. Ekholm and R.B. Hallock. *J. Low Temp. Phys.*, 42:339, 1981.

[118] R.S. Shapiro and I. Rudnick. *Phys. Rev.*, 137:A 1383, 1965.

[119] L. Goldstein, H.S. Sommers Jr, L.D.P. King, and C.J. Hoffman. *Proc. Int. Conf. Low Temp. Phys. (*R. Bowers, ed.*)*. 1951.

[120] D.G. Henshaw and D.G. Hurst. *Phys. Rev.*, 91:1222, 1953.

[121] D.G. Hurst and D.G. Henshaw. *Phys. Rev.*, 100:994, 1955.

[122] M. Cohen and R.P. Feynman. *Phys. Rev.*, 107:13, 1957.

[123] H. Palevsky, K. Otnes, K.E. Larsson, R. Pauli, and R. Stedman. *Phys. Rev.*, 108:1346, 1957.

[124] H. Palevsky, K. Otnes, and K.E. Larsson. *Phys. Rev.*, 112:11, 1958.

[125] J.L. Yarnell, G.P. Arnold, P.J. Bendt, and E.C. Kerr. *Phys. Rev. Lett.*, 1:9, 1958.

[126] J.L. Yarnell, G.P. Arnold, P.J. Bendt, and E.C. Kerr. *Phys. Rev.*, 113:1379, 1959.

[127] D.G. Henshaw. *Phys. Rev. Lett.*, 1:127, 1958.

[128] A.D. Woods and R.A. Cowley. *Rep Prog. Phys.*, 36:1135, 1973.

[129] D.L. Price. In K.H. Bennemann and J.B. Ketterson, editors, *The Physics of Liquid and Solid Helium, Part-II*, page 675. Wiley, New York, 1978.

[130] H.R. Glyde and E.C. Svensson. In D.L. Price and K. Skold, editors, *Methods of Experimental Physics*, volume 23, Part-B, page 303. Academic Press, London, 1987.

[131] A.J. Leggett. *Rev. Mod. Phys.*, 71:S318, 1999.

[132] P.E. Sokol. In A. Griffin, D.W. Snoke, and S. Stringari, editors, *Bose-Einstein Condensation*. Cambridge University Press, Cambridge, 1995.

[133] H. Frohlich. *Physica*, 4:639, 1937.

[134] F. London. *Nature*, 141:644, 1938.

[135] S.J. Putterman. *Superfluid Hydrodynamics*. North Holland/American Elsevier, Amsterdam, 1974.

[136] R.K. Pathria. *Statistical Mechanics*. Pergamon, Oxford, 1979.

[137] F. London. *Phys. Rev.*, 54:947, 1938.

[138] L. Tisza. *Phys. Rev.*, 72:838, 1947.

[139] L.D. Landau. *J. Phys. U.S.S.R. (reprinted in Ref. 1)*, 11:91, 1947.

[140] N. Bogoliubov. *J. Phys. (USSR) (reprinted in Ref. 1)*, 11:23, 1947.

[141] R.P. Feynman. *Phys. Rev.*, 91:1291, 1953.

[142] R.P. Feynman. *Phys. Rev.*, 91:1301, 1953.

[143] R.P. Feynman. *Phys. Rev.*, 94:262, 1954.

[144] R.P. Feynman and M. Cohen. *Phys. Rev.*, 102:1189, 1956.

[145] de Boer. In Careri, editor, *Liquid Helium*. Academic Press, 1963.

[146] G.V. Chester. In Careri, editor, *Liquid Helium*. Academic Press, 1963.

[147] A. Miller, D. Pines, and P. Nozieres. *Phys. Rev.*, 127:1452, 1965.

[148] T.D. Lee and F. Mohling. *Phys. Rev Lett.*, 2:284, 1959.

[149] R.P. Feynman. In C.J. Gorter, editor, *Prog. Low Temp. Phys.*, volume I, page 1. North-Holland, Amsterdam, 1955.

[150] W.F. Vinen. In C.J. Gorter, editor, *Prog. Low Temp. Phys.*, volume III. North-Holland, Amsterdam, 1961.

[151] W.F. Vinen. *Proc. Roy. Soc.*, A 260:218, 1961.

[152] S.C. Whitmore and W. Zimmerman. *Phys. Rev. Lett.*, 15:389, 1965.

[153] G.W. Rayfield and F. Reif. *Phys. Rev. Lett.*, 11:305, 1963.

[154] G.W. Rayfield and F. Reif. *Phys. Rev.*, 136:A 1194, 1964.

[155] L. Onsager and O. Penrose. *Phys. Rev.*, 104:576, 1956.

[156] N.N. Bogoliubov. *The Quasi-averages in Problems of Statistical Physics.* Dubna preprint (2nd ed. 1963), 1961.

[157] N.N. Bogoliubov. *On the Hydrodynamics of a Superfluid.* Dubna preprint, 1963.

[158] P.C. Hohenberg and P.C. Martin. *Ann. Phys.*, 34:291, 1965.

[159] Z.M. Galasiewicz. *Superconductivity and Quantum Fluids.* Pergamon Press, Oxford, 1970.

[160] Z.M. Galasiewicz. *Bull. de l' Acad. de Sci. Polon.*, 15:191, 1967.

[161] W.A. Krasnikov. *Ph.D. Dissertation.* Moscow State University, 1967.

[162] I.M. Khalatnikov. *J.E.T.P. (reprinted in Ref. 1)*, 23:8, 1952.

[163] L.D. Landau and I.M. Khalatnikov. *J.E.T.P.*, 19:637, 709, 1949.

[164] I.M. Khalatnikov. *J.E.T.P*, 23:21, 1952.

[165] C.N. Yang. *Rev. Mod. Phys.*, 34:694, 1962.

[166] O. Penrose. *Phil. Mag.*, 42:1373, 1951.

[167] J.W. Kane and L.P. Kadanoff. *Phys. Rev.*, 155:80, 1967.

[168] D.N. Zubarev. *Sov. Phys. -Uspekhi*, 3:320, 1960.

[169] L.P. Kadanoff and P.C. Martin. *Ann. Phys. (N.Y.)*, 24:419, 1963.

[170] K.A. Brueckner and K. Sawada. *Phys. Rev.*, 106:1117, 1957.

[171] K.A. Brueckner and K. Sawada. *Phys. Rev.*, 106:1128, 1957.

[172] D.F. Goble and L.E.H. Trainor. *Can. J. Phys.*, 46:839, 1968.

[173] W.E. Parry and D. ter Haar. *Ann. Phys.(N.Y.)*, 19:496, 1962.

[174] L. Liu and K.W. Wong. *Phys. Rev.*, 132:1349, 1963.

[175] L. Liu, Lu Sun Liu, and K.W. Wong. *Phys. Rev.*, 135:A1166, 1964.

[176] K. Huang and C.N. Yang. *Phys. Rev.*, 105:767, 1957.

[177] T.D. Lee, K. Huang, and C.N. Yang. *Phys. Rev.*, 106:1135, 1957.

[178] E. Bycking. *Phys. Rev.*, 145:71, 1966.

[179] K.K. Singh and S. Kumar. *Phys. Rev.*, 162:173, 1967.

[180] K.K. Singh and S. Kumar. *Phys. Rev. A*, 1:497, 1970.

[181] S.T. Baliaev. *Soviet Phys. JETP*, 7:289, 1958.

[182] N.M. Hugenholtz and D. Pines. *Phys. Rev.*, 116:489, 1959.

[183] B.H. Brandow. *Phys. Rev. Lett.*, 22:173, 1969.

[184] B.H. Brandow. *Ann. Phys.*, 64:21, 1971.

[185] J. Goldstone. *Proc. Roy. Soc. (London)*, A 239:267, 1957.

[186] Y.A. Tserkonikov. *Sov. Phys. - DOKL*, 9:1110, 1965.

[187] Y.A. Tserkonikov. *Sov. Phys. - DOKL*, 11:723, 1965.

[188] D. Pines. In D.F. Brewer, editor, *Quantum Fluids*. North-Holland, Amsterdam, 1966.

[189] D. Pines. In R. Kubo, editor, *Many Body Theory*. Benjamin, New York, 1966.

[190] R.P. Etters. *Phys. Rev. Lett.*, 16:119, 1966.

[191] T.H. Cheung and A. Griffin. *Can. J. Phys.*, 48:2135, 1970.

[192] T.H. Cheung and A. Griffin. *Phys. Rev.*, A 4:237, 1971.

[193] J.G. Valatin and D. Butler. *Nuovo Cimento*, 10:37, 1958.

[194] M. Girardeau and R. Arnowitt. *Phys. Rev.*, 113:755, 1959.

[195] E.P. Gross. *Ann. Phys. (N.Y.)*, 9:292, 1960.

[196] D.N. Zubarev and Iu. A. Tserkovnikov. *Soviet Phys.-Dokolady*, 3:603, 1958.

[197] M. Girardeau. *Phys. Rev.*, 115:1090, 1959.

[198] G. Wentzel. *Phys. Rev.*, 120:1570, 1960.

[199] M. Luban. *Phys. Rev.*, 128:965, 1962.

[200] F.W. Cummings and J.R. Johnston. *Phys. Rev.*, 151:105, 1966.

[201] D.H. Kobe. *Ann. Phys. (N.Y.)*, 47:15, 1968.

[202] R.H. Parmenter. *Phys. Rev.*, 170:194, 1968.

[203] W.A.B. Evans and Y. Imry. *Nuovo Cimento*, B 63:155, 1969.

[204] G.V. Brown and M.H. Coopersmith. *Phys. Rev.*, 178:327, 1969.

[205] A. Coniglio, F. Mancini, and M. Maturi. *Nuovo Cimento*, B 63:227, 1969.

[206] W.A.B. Evans and R.J.M.A. Rashid. *J. Low Temp. Phys.*, 11:93, 1973.

[207] R. Hastings and J.W. Halley. *Phys. Rev.*, B 12:267, 1975.

[208] R. Hastings and J.W. Halley. *Phys. Rev.*, B 13:3799, 1976.

[209] M.L. Ristig. *Phys. Rev.*, B 18:1207, 1978.

[210] W.L. McMillan. *Phys. Rev.*, 138:A 442, 1965.

[211] D. Schiff and L. Verlet. *Phys. Rev.*, 160:208, 1967.

[212] T.C. Padmore and C.V. Chester. *Phys. Rev.*, A 9:1725, 1974.

[213] F.Y. Wu and E. Feenberg. *Phys. Rev.*, 128:943, 1962.

[214] E. Feenberg. *Am. J. Phys.*, 38:684, 1970.

[215] W.P. Francis, G.V. Chester, and L. Reatto. *Phys. Rev.*, A 1:86, 1970.

[216] D.K. Lee. *Physica*, 43:132, 1969.

[217] W.E. Massey. *Phys. Rev.*, 151:153, 1966.

[218] W.E. Massey and C.W. Woo. *Phys. Rev.*, 164:256, 1967.

[219] L. Reatto and G.V. Chester. *Phys. Rev.*, 155:88, 1967.

[220] H.W. Jackson and E. Feenberg. *Ann. Phys. NY*, 15:266, 1961.

[221] H.W. Jackson and E. Feenberg. *Rev. Mod. Phys.*, 34:686, 1962.

[222] E. Feenberg. *Theory of Quantum Fluids.* Academic Press, New York, 1969.

[223] F.Y. Wu. *J. Math. Phys.*, 12:1923, 1971.

[224] F.Y. Wu and M.K. Chien. *J. Math. Phys.*, 11:1912, 1970.

[225] F.Y. Wu. *J. Low Temp. Phys.*, 9:177, 1972.

[226] C.W. Woo. In K.H. Benneman and J.B. Ketterson, editors, *The Physics of Liquid and Solid Helium, Part-I*, pages 349–501. John Wiley and Sons, New York, 1976.

[227] C.E. Campbell and E. Feenberg. *Phys. Rev.*, 188:396, 1969.

[228] D.K. Lee and F.J. Lee. *Phys. Rev.*, B 11:4318, 1975.

[229] D.K. Lee. *Phys. Rev.*, 162:134, 1967.

[230] H.W. Lai, H.K. Sim, and C.W. Woo. *Phys. Rev.*, A 1:1536, 1970.

[231] C.C. Chang and C.E. Campbell. *Phys. Rev.*, B 13:3779, 1976.

[232] K.E. Schmidt and V.R. Pandharipande. *Phys. Rev.*, B 21:3945, 1980.

[233] E. Manousakis and V.R. Pandharipande. *Phys. Rev.*, B 30:5062, 1984.

[234] F. Iwamot. *Prog. Theor. Phys.*, 44:1121, 1970.

[235] H.W. Jackson. *Phys. Rev.*, A 4:2386, 1971.

[236] A. Zawadowski, J. Ruvalds, and J. Solana. *Phys. Rev.*, 5:399, 1972.

[237] J. Ruvalds. *Physical Review Letters*, 27:1769, 1971.

[238] J. Jackel. *Z. Phys.*, 27:14, 1972.

[239] S. Takeno. *Prog. Theor. Phys.*, 48:2107, 1972.

[240] K. Nagai. *Prog. Theor. Phys.*, 49:46, 1973.

[241] H.K. Sim, C.W. Woo, and J.R. Buckner. *Phys. Rev.*, A 2:2024, 1970.

[242] H.K. Sim, C.W. Woo, and J.R. Buckner. *Phys. Rev.*, A 2:2032, 1970.

[243] A. Bijl. *Physica*, 7:869, 1940.

[244] R.B. Dingle. *Phil. Mag.*, 40:573, 1949.

[245] R. Jastrow. *Phys. Rev.*, 98:1479, 1955.

[246] P.C.W. Fung, H.K. Tsang, and K.W. Wong. *Nuovo Cimento*, 28 B:313, 1975.

[247] K.W. Wong, P.C.W. Fung, and C.C. Lau. *Phys. Rev.*, A 22:1272, 1980.

[248] K.W. Wong and P.C.W. Fung. *Nuovo Cimento*, 25 B:595, 1975.

[249] P.A. Whitlock and R. Panoff. *Can. J. Phys.*, 65:1409, 1987.

[250] D.M. Caperley and E.L. Pollock. *Phys. Rev. Lett.*, 56:351, 1986.

[251] D.M. Caperley and E.L. Pollock. *Can. J. Physics*, 65:1416, 1986.

[252] E.L. Pollock and D.M. Caperley. *Phys. Rev.*, B 36:8343, 1986.

[253] G.L. Masserini, L. Reatto, and S.A. Vitiello. *Phys. Rev. Lett.*, 69:2098, 1992.

[254] P.J. Reynolds, D.M. Caperley, B.J. Alder, and W.A. Lester. *J. Chem. Phys.*, 77:5593, 1982.

[255] D.M. Caperley. *J. Stat. Phys.*, 63:1237, 1991.

[256] S. Moroni, S. Fantoni, and G. Senatore. *Phys. Rev.*, B 52:13457, 1995.

[257] S. Moroni, G. Senatore, and S. Fantoni. *Phys. Rev.*, B 55:1040, 1997.

[258] S.A. Vitiello and K.E. Schmidt. *Phys. Rev.*, B 46:5442, 1992.

[259] S. Moroni, S. Fantoni, and G. Senatore. *Euro. Phys. Lett.*, 30:93, 1995.

[260] V.L. Ginzburg and L.D. Landau. *Zh. Eksperim. i. Teor. Fiz.*, 20:1064, 1950.

[261] H.W. Jackson. *Phys. Rev. A*, 10:278, 1974.

[262] C. Rickayzen. In J.G.M. Armitage and I.E. Ferquhur, editors, *The Helium Liquids*. Academic Press, 1975.

[263] P. Kleban. *Phys. Lett.*, 49A:19, 1974.

[264] A.M. Ettouhami. *arXiv.org*, 0703498, 2007.

[265] L. Onsager. *Nuovo Cimento*, 6 (supplement-2):249, 1949.

[266] Y.S. Jain. *Microscopic Theory of Superfluidity of A System of Interacting Bosons: The Liquid ^4He*. Technical report, Physics Department, NEHU, Shillong, 1995.

[267] Y.S. Jain. *J. Sci. Expl.*, 16:77, 2002. More detailed version of this paper is available for ready reference as a paper entitled, *"Macro-orbitals and microscopic theory of a system of interacting bosons"* in www.arXiv.org/cond-mat/0606571.

[268] Y.S. Jain. in *cond-mat/0606571*, e-print, www.arXiv.org, 2006.

Chapter 2

Macro-orbital Theory

2.1 Introduction

Liquid helium-4 (LHE-4) is a system of interacting bosons (SIB). As discussed in Chapter-1 inter-atomic interactions have been posing great difficulties in formulating a viable theory of the liquid. Consequently, some of the earlier theories are related to a system of weakly interacting bosons or a dilute (low density) Bose gas. Although, later studies tried to overcome these difficulties by using different approaches (cf., Chapter-1) but with little success.

Over the last few years, Jain [1–4] used a non-conventional approach after identifying several sources of errors in the basic considerations of the conventional approaches and concluded his Macro-orbital theory. In developing his approach, he first identifies the following realities of LHE-4.

1. ^4He atoms in LHE-4 move freely within its volume on a surface of constant -ve potential $(-V_o)$ unless they collide with each other. One may find that inter-atomic interactions in the liquid can be represented by a two body central potential $V(r_{ij})$ such as Lennard Jones potential,

$$V(r_{ij}) = 4\epsilon \left[\left(\frac{\sigma}{r_{ij}} \right)^{12} - \left(\frac{\sigma}{r_{ij}} \right)^{6} \right] \tag{2.1}$$

   which could be identified as a sum of: (i) a short range strong repulsive term $V^R(r_{ij})$ and (ii) a relatively weak long range attractive term $V^A(r_{ij})$. While $V^R(r_{ij})$ can be approximated to hard-core repulsion $V_{HC}(r_{ij})$ ($V_{HC}(r_{ij} < \sigma) = \infty$ and $V_{HC}(r_{ij} \geq \sigma) = 0$ with σ being the hard core diameter of an atom), $V^A(r_{ij})$ is approximated to a constant negative potential $-V_o$. It is obvious that $V_{HC}(r_{ij})$ forbids two particle from occupying same point in real space and $-V_o$ keeps particles confined to a fixed volume.

2. Following a systematic analysis of a $3-D$ case of two HC particles of finite size, Huang [5] establishes $V_{HC}(r) \equiv A\delta(r)$. Same result has been obtained for 1-D dynamics of two HC particles by Jain by studying the possible configuration of $P1$ and $P2$ just at the instant of their collision. He finds that while $P1$ and $P2$ keep their centers of gravity at $x = \sigma$ (with $x_2 = \sigma/2$ and $x_1 = -\sigma/2$), they register their physical touch at $x = 0$. Their encounter with $V_{HC}(x)$ in this process is a result of this contact at $x = 0$ beyond which two HC particles can not be pushed in. Naturally, in this process, σ has no importance either as the size of $P1$ or $P2$ or as a distance between their

centers of gravity. The process of collision only identifies that particles are hard spheres, (whether of finite σ or of infinitely small σ) and this means $V_{HC}(x) \equiv A\delta(x)$.

3. Analysing the basic nature of the possible dynamics of two particles (say $P1$ and $P2$) in the system, Jain observes that $P1$ and $P2$ encounter $\delta-$potential only when they suffer a collision. While in a two body collision, they simply exchange their momenta, k_1 and k_2, in a many body collision, where they may collide simultaneously with other particle(s), they could be identified to jump from their state of k_1 and k_2 (or their relative momentum $k = k_2 - k_1$ and center of mass (CM) momentum $K = k_1 + k_2$) to that of new momenta k_1' and k_2' (or k' and K'). It is obvious that each of them has free particle motion between two collisions. Evidently, a state of two particles even in the presence of other particles of the system can be identified characteristically with a state of two HC particles. In other words a pair of particles forms the basic unit of the system and the wave mechanics of two HC particles serves as an important basis for understanding a many body system.

In the following section we discuss the dynamics of two HC particles in a 1-D box and its results can be extended to $2-D$ and $3-D$ systems. While the dynamics of a many body system is discussed in section-2.3, important inferences of Macro-orbital theory are discussed in section-2.4. In section-2.5 we put our observations as concluding remarks.

2.2 Wave Mechanics of Two Hard Core Quantum Particles in 1-D Box

The dynamics of $P1$ and $P2$ can be described by the Scrödinger equation expressed in the CM coordinate system as

$$\left[-\frac{\hbar^2}{4m}\frac{\partial^2}{\partial X^2} - \frac{\hbar^2}{m}\frac{\partial^2}{\partial x^2} + A\delta(x)\right]\Psi(x,X) = E\Psi(x,X) \tag{2.2}$$

with

$$\Psi(x,X) = \psi_k(x)\, exp\,[i(KX)] \tag{2.3}$$

with $\psi_k(x)$ representing their relative motion and $exp\,[i(KX)]$ -the CM motion. It is evident that their relative motion can be described by the equation

$$\left[-\frac{\hbar^2}{m}\frac{\partial^2}{\partial x^2} + A\delta(x)\right]\psi(x) = E_k\psi_k(x) \tag{2.4}$$

with $E_k = E - \hbar^2K^2/4m$. All notations in equations 2.2 and 2.3 including

$$x = \mathrm{x}_2 - \mathrm{x}_1 \quad and \quad k = \mathrm{k}_2 - \mathrm{k}_1 \tag{2.5}$$

$$X = (\mathrm{x}_1 + \mathrm{x}_2)/2 \quad and \quad K = \mathrm{k}_1 + \mathrm{k}_2 \tag{2.6}$$

have their usual meanings. Alternatively for k_1 and k_2 we also have

$$\mathrm{k}_1 = -q + K/2 \quad and \quad \mathrm{k}_2 = q + K/2 \tag{2.7}$$

Evidently in CM coordinate $P1$ and $P2$ are seen to move with equal and opposite momenta (q, -q) and maintain a center of symmetry at their CM. This renders,

$$\mathrm{k}_{CM}(1) = -\mathrm{k}_{CM}(2) = q \quad and \quad \mathrm{x}_{CM}(1) = -\mathrm{x}_{CM}(2) \tag{2.8}$$

where x_{CM} and k_{CM} represent respectively the position and momentum of a particle with respect to CM. Equations 2.8 and 2.7 define the characteristic details of $\psi_k(x)$.

2.2.1 Characteristics of Two Body Dynamics

Functional form of $\psi_k(x)$

Using the step potential nature of $A\delta(x)$ Jain finds that each particle of the system can be described by separate plane wave such as $u_{\mathbf{k}_i}(\mathbf{x}_i) = \exp(i\mathbf{k}_i\mathbf{x}_i)\,\exp[-iE_it/\hbar]$ (assumed to have unit normalization). However, for the possible superposition of the waves representing $P1$ and $P2$, a state of two particles is better expressed by

$$\Psi(\mathrm{x}_1, \mathrm{x}_2, t)^{\pm} = 1/\sqrt{2}\,[u_{\mathrm{k}_1}(\mathrm{x}_1, t)u_{\mathrm{k}_2}(\mathrm{x}_2, t) \pm u_{\mathrm{k}_2}(\mathrm{x}_1, t)u_{\mathrm{k}_1}(\mathrm{x}_2, t)] \tag{2.9}$$

which can be rearranged as

$$\Psi(x, X, t)^{\pm} = \psi_k(x, t)^{\pm}\,\exp\,(iKX)exp[-i(E_k + E_K)t/\hbar] \tag{2.10}$$

with

$$\psi_k(x, t)^{+} = \sqrt{2}\cos(kx/2)exp[-iE_kt/\hbar] \tag{2.11}$$

$$\psi_k(x, t)^{-} = \sqrt{2}\sin(kx/2)exp[-iE_kt/\hbar] \tag{2.12}$$

Both $\psi_k(x,t)^+$ and $\psi_k(x,t)^-$ represent a kind of stationary matter wave (SMW) that modulates the relative phase positions ($\phi = kx$) of $P1$ and $P2$. Although, $\psi_k(x,t)^-$ is a desired solution of equation 2.4 because it vanishes at $x = 0$, its anti symmetric nature forbids it to be a wave function of two HC bosons. However, even symmetry of $A\delta(x)$ reveals that $\phi_k(x,t)^+ = \sin(|kx/2|)exp[-iE_kt/\hbar]$, which is also a solution of equation 2.4, can represent the eigen state of two HC bosons [6]. Moreover, as $|\psi_k(x,t)^-|^2 = |\phi_k(x,t)^+|^2$, the modulation of the relative position of two HC fermions represented by $\psi_k(x,t)^-$ is exactly identical to that of two HC bosons represented by $\phi_k(x,t)^+$. This concludes that relative configuration and dynamics of two HC particles are not influenced by their fermionic or bosonic nature and these aspects can be determined by analyzing either $\psi_k(x,t)^-$ or $\phi_k(x,t)^+$. In general, the eigen function that represents the two HC particles state is expressible in the form of

$$\zeta(x,\, X,t)^{\pm} = \zeta_k(x,t)^{\pm}\, \exp\left[i(KX)\right]exp[-i(E_k + E_K)t/\hbar] \tag{2.13}$$

with

$$\zeta(x,t)^- = \psi_k(x,t)^- = \sqrt{2}\sin(kx/2)exp[-iE_kt/\hbar] \tag{2.14}$$

and

$$\zeta(x,t)^+ = \phi_k(x,t)^+ = \sqrt{2}\sin(|kx|/2)exp[-iE_kt/\hbar] \tag{2.15}$$

Expectation value of energy

Expectation value of the energy operator is given by

$$< H(2) >= \frac{\hbar^2K^2}{4m} + \frac{\hbar^2k^2}{4m} = \frac{\hbar^2\,(k_1^2 + k_2^2)}{2m} \tag{2.16}$$

which represents purely a kinetic energy. This is because $A\delta(x) = 0$ for $x \neq 0$ and $\zeta(x,t)^{\pm} = 0$ for $x = 0$ rendering $< A\delta(x) >= 0$. However, as shown in [6] this does not imply that the problem is equivalent to a non-interacting system. As shown in [6], the quantized values of q and K are expressed by

$$q_n = k_n/2 = (n + 1)\pi/d \;\; (n = 0, 1, 2, ...) \tag{2.17}$$

and

$$K_N = (N + 1)\pi/L \;\; (N = 0, 1, 2, ...) \tag{2.18}$$

As such Jain concludes that the two particles for their relative motion behave as if they are confined to different halves of the one dimensional box which agrees

with excluded volume condition envisaged by Kleban [7]. Equations 2.17 and 2.18 render the total energy $E(n, N)$ of $P1$ and $P2$ as

$$E(n, N) = \frac{h^2}{16mL^2}[16(n + 1)^2 + (N + 1)^2] \tag{2.19}$$

while the *ground state* (G-state) is characterized by

$$q_o = \pi/d \quad and \quad K_o = \pi/L \tag{2.20}$$

and

$$E_o = \frac{h^2}{8md^2}\frac{17}{8} = 2.12\epsilon_o \tag{2.21}$$

Here $\epsilon_o = h^2/8md^2$ is the G-state energy of a particle in a box of size d.

Ground state configuration

The ground state configuration of the system is represented by

$$q = \pi/d = 2\pi/\lambda, < x >= \lambda/2 \quad and \quad < \phi >= 2\pi \tag{2.22}$$

where $\lambda = L = 2d$. This indicates that in the ground state configuration $P1$ and $P2$ define a closed-packed arrangement occupying a space ($= \lambda/2$) equal to their wave packets size and their motion becomes collisionless. However, in excited state wave packets size decreases with increasing energy and the motion becomes collisional.

Macro-orbital

The particles in their quantum state either experience a repulsion (when $x \leq \lambda/2$) or no force (when $x \geq \lambda/2$). In both cases they have no binding in x-space and retain their independent particle state in spite of their inter particle phase correlation, which can keep them locked at $< \phi >= 2n\pi$ (n=1,2,3,....) in the ϕ-space. Before a collision $P1$ and $P2$ move towards each other with opposite momenta and after collision they either exchange their momenta or their respective position. The first possibility gives a kind of self-superposition (i.e. superposition of plane waves of the same particle in their respective half) and the other renders a mutual-superposition (i.e. superposition of the plane waves of the different particles). In wave mechanics there is no way to find out whether the particles have their self-superposition or mutual-superposition. However, there is no distinction

between the two because both of them arise from the superposition of the plane waves of momenta k_1 and k_2. The self-superposition identifies each particle as an independent entity in a state represented by a (q, -q) pair moving with CM momentum K. In other words, the state of each particle of the pair can be described by a separate pair wave form, *say* $\xi(x_{(i)}, X_{(i)})$. This is different from $\zeta(x, X)$ and proposed to be called a *Macro-orbital.*

For a general usage Macro-orbital is obtained by using $\xi(x_{(i)}, X_{(i)}) \equiv \zeta(x, X)$ and replacing x, X, q and K, respectively, by $x_{(i)}$, $X_{(i)}$, $q_{(i)}$, *and* $K_{(i)}$ to make a reference to i^{th} particle. This renders

$$\xi(x_{(i)}, X_{(i)}) = B\zeta_{q_{(i)}}(x_{(i)}) \exp[K_{(i)}X_{(i)}] \tag{2.23}$$

where B is a normalization constant and $\zeta_{q_{(i)}}$ is that part of a Macro-orbital which does not overlap with similar part of other Macro-orbitals. Since, the Macro-orbital represents a particle in its self superposition state, it is not a solution of equation 2.2. However, if the Hamiltonian of the system is expressed as

$$H(2) = h_1 + h_2 = h(1) + h(2) \tag{2.24}$$

where $h_i = \frac{\hbar^2}{2m}\frac{\partial^2}{\partial x_i^2}$ being the kinetic energy operator of the i^{th} particle and

$$h(i) = \frac{h_i + h_{i+1}}{2} = -\frac{\hbar^2}{8m}\frac{\partial^2}{\partial^2_{X_{(i)}}} - \frac{\hbar^2}{2m}\frac{\partial^2}{\partial^2_{x_{(i)}}} \tag{2.25}$$

then $\xi(x_{(i)}, X_{(i)})$ becomes a eigen function of the operator h(i).

2.3 Many Body Interacting Bosonic System

The Macro-orbital theory starts with

$$H(N) = -\frac{\hbar^2}{2m}\sum_{i=1}^{N}\nabla_i^2 + \sum_{i<j}^{N} V(|r_i - r_j|) = H_o + \sum_{i<j}^{N} V(|r_i - r_j|) \tag{2.26}$$

representing the microscopic quantum Hamiltonian of a system of N-interacting bosons. Here $\frac{\hbar^2}{2m}\nabla_i^2$ represents the K.E. operator of the i^{th} particle.

2.3.1 State Function

In view of what has been inferred in Sections 2.1 and 2.2, the state of each particle in the system can be represented by a Macro-orbital

$$\xi(r_{(i)}, R_{(i)}) = B_i\zeta_{q_{(i)}}(r_{(i)})\, exp\,(iK_{(i)}R_{(i)}) \tag{2.27}$$

where $\zeta_{q_{(i)}}(r_{(i)})$ stands either for $\psi_{q_{(i)}}$ or $\phi_{q_{(i)}}$. Since a Macro-orbital is an eigen function of the Hamiltonian of a pair of HC particles expressed in terms of $h(i)$, the kinetic energy part (H_o) of the Hamiltonian (equation 2.26) should be rearranged in terms of $h(i)$ [3] with which a Macro-orbital is consistent as an eigen function. Using N Macro-orbitals for N particles, the state functions of n^{th} quantum state of equal energy E_n can be expressed as

$$\psi_n = \phi_n(q)\phi_n(K) \tag{2.28}$$

with

$$\phi_n(q) = \left[\left(\frac{2}{V}\right)^{N/2} \prod_{i=1}^{N} \sin(q_i.r_i)\right] \exp[-iE_n(k)t/\hbar] \tag{2.29}$$

$$\phi_n(K) = \left[A\left(\frac{1}{V}\right)^{N/2} \sum_{pK} (\pm 1)^P \prod_{i=1}^{N} \exp[i(K_i.R_i)\right] \exp[-iE_n(K)t/\hbar] \tag{2.30}$$

with

$$E_n(k) = \sum_{i=1}^{N} \epsilon(k)_i \quad E_n(K) = \sum_{i=1}^{N} \epsilon(K)_i \ \ and \ \ A = (\frac{1}{N!})^{1/2} \tag{2.31}$$

The term $\sum_{pK}(\pm 1)^P$ in equation 2.30 refers to the sum of different permutations of K over all particles, $(+1)^p$ used for bosonic system and $(-1)^p$ is used for fermionic system. The fact that no two particles in the system are expected to occupy same r [8] is ensured by the restriction, $q_j \geq \pi/d$ or $\lambda_j/2 \leq d$. Since one has $\Sigma = N!$ different ψ_n for a given state, the general state function can be written as:

$$\phi_n = \frac{1}{\sqrt{\Sigma}} \sum_{i=1}^{\Sigma} \psi_n^{(i)} \tag{2.32}$$

2.3.2 Energy Eigenvalue

Expectation value of energy of the n^{th} state is

$$E_n = \frac{<\phi_n|H_n|\phi_n>}{<\phi_n|\phi_n>} = \frac{<\phi_n|(H_o(N) + A\delta(r_{ij}))|\phi_n>}{<\phi_n|\phi_n>} \tag{2.33}$$

Two particles dynamics reveals that each particle in the system is represented by a SMW pair of CM momentum K_i and relative momentum $k_i = 2q_i$ and $< A\delta(r_{ij}) >= 0$. This gives the energy of the n^{th} state as:

$$E_n = \frac{<\phi_n|H_o(N)|\phi_n>}{<\phi_n|\phi_n>} = \sum_{i=1}^{N} \left(\frac{\hbar^2 K^2}{8m} + \frac{\hbar^2 q_i^2}{2m}\right) \tag{2.34}$$

Where K_i can have any value between 0 to ∞, while the lowest q_i is decided by the volume v_i available to $i-$th particle. Naturally, for the ground state energy all $K_i = 0$ and q_i can be obtained by using the fact that each particle in the ground state has lowest possible energy i.e. largest possible $\lambda/2$ (obviously, equal to the size of the cavity exclusively occupied by the particle) indicating that the largest volume occupied by i^{th} particle is $v_i = (\lambda/2)^3$. In principle, this renders ground state energy of the system as

$$E_o = \sum_i^N \frac{h^2 q_i^2}{8\pi^2 m} = \sum_i^N \frac{h^2}{8m v_i^{2/3}} \tag{2.35}$$

with

$$\sum_{i=1}^N v_i = V \tag{2.36}$$

Minimizing E_o by using equation 2.36 one easily finds that

$$E_o = N\frac{h^2}{8md^2} = N\epsilon_o \tag{2.37}$$

2.4 Inferences of the Macro-orbital Theory

2.4.1 Evolution of the System with Decreasing T

For a constant particle density of the system the inter particle separation d remains constant while λ_T (thermal de Broglie wavelength) increases with decreasing temperature (T). As a result $(d - \lambda/2)$ decreases with T and at a certain $T = T_c$, $(d-\lambda/2)$ vanishes and q motion gets frozen into zero point motion of $q = q_o = \pi/d$. Evidently, the system moves from a state of $\lambda/2 \leq d$ to a new state of $\lambda/2 = d$. While the former state with $\phi(= 2qd) \geq 2\pi$ represents randomness in ϕ positions (i.e. a disorder in ϕ-space), the latter state of $\phi = 2\pi$ represents an ordered state. Thus the particles of the system move from their disordered to ordered state in ϕ-space at T_c where we obviously have all $q_i = q_o$. Consequently, at $T \leq T_c$, all $\psi_n^{(i)}$ become identical and ϕ_n attains the form of single ψ_n. As a result, all the Σ micro states merge into one state indicating a kind of oneness of the system and therefore, the system at $T \leq T_c$ is described by

$$\phi_n = \phi_n^o(q = q_o)\phi_n^e(K) \tag{2.38}$$

2.4.2 Effective Inter Particle Interaction

Macro-orbital theory replaces $V_{ij}^R(r)$ by $V_{HC}(r)$ and imposes the condition, "no two particles should share same r in configuration space". This shows that WP manifestation of particles extends the range of influence of $V_{HC}(r)$ from $r_a = \sigma$ to $r_a = \lambda/2$ when $\lambda/2 > \sigma$. This repulsion is the zero point repulsion and can be derived as the first d derivative of the ground state energy, $E_o = \frac{Nh^2}{8md^2}$. Evidently, A in $V_{HC}(r) = A\delta(r)$ should be proportional to $\frac{Nh^2}{8md^2}$. In most systems of interacting bosons (SIB) inter particle interaction falls faster than the zero point repulsion particularly for all $\sigma < r \leq \lambda/2$. Because of this zero point repulsion LHE-4 does not solidify even at $T = 0$ unless an external pressure of 25 atms is applied. This zero point repulsion also explains the negative volume expansion in LHE-4 with falling T around T_λ. As T decreases, the wave packet size of the particles increases and the wave packets of neighbouring particles get overlapped. To remove this overlapping of the wave packets, zero point repulsion increases the inter particle separation.

2.4.3 Quantum Correlation Potential

One of the main features of Macro-orbital theory is the quantum correlation potential (QCP) which has two components. The U_{ij}^s pertaining to k motion controls the $\phi = kr$ position of a particle and is given by:

$$U_{ij}^s = -k_B T_o \ln\left[2\sin^2(\phi/2)\right] \tag{2.39}$$

where T has been replaced by T_o because T equivalence of k motion energy at all $T \leq T_\lambda$ is T_o. This potential has the minimum value $-k_B T_o \ln 2$ at $\phi = (2n+1)\pi$ (with n=0,1,2,3,....) and maximum value ∞ at $\phi = 2n\pi$ (with n=0,1,2,....). U_{ij}^s always increases for any small change $\delta\phi$ in ϕ at its minimum, as

$$\frac{1}{2}\mathbf{C}(\delta\phi)^2 = \frac{1}{4}k_B T_o(\delta\phi)^2 \tag{2.40}$$

with force constant

$$\mathbf{C} = \frac{1}{2}k_B T_o. \tag{2.41}$$

Therefore, the particles experience a $force = -\mathbf{C}\delta\phi$ which tries to maintain $\delta\phi = 0$ and sustain the order of particles in ϕ-space.

The second component pertaining to K motion is expressed by

$$U_{ij} = -k_B T \ln\left[1 + \exp\left(\frac{-2\pi|R' - R''|^2}{\lambda_T'^2}\right)\right] \tag{2.42}$$

with $\lambda_T' = h/(2\pi(4m)k_BT)^{1/2}$ which is identical to the expression obtained for non interacting bosons [9]. This potential is the origin of the force that drives the particles of the system in $K-$space towards $K = 0$, (BEC state of K motion) where it has its minimum value $-k_BT \ln 2$.

2.4.4 Transition Temperature (T_λ)

What follows from Sec-2.4.1 that the lower bound of T_c is

$$T_c = T_o = \frac{h^2}{2\pi m k_B \lambda_T^2} = \frac{h^2}{8\pi m k_B d^2} \tag{2.43}$$

which is T equivalent of ground state energy where the particles have $\lambda_T = 2d$. However, to obtain real $T_c = T_\lambda$ one must note that with T moving below T_λ, particles of the system not only have $q = q_o$, but also start attaining $K = 0$. Evidently, λ transition follows two processes simultaneously: (i) ordering of particles in $\phi-$space rendering $q = q_o$ and (ii) BEC of particles (as SMW pairs) driving them towards $K = 0$, which gives a transition temperature

$$T_\lambda = T_o + \frac{1}{4}T_{BEC} = \frac{h^2}{8\pi m k_B T}\left[\frac{1}{d^2} + \left(\frac{N}{2.62V}\right)^{2/3}\right] \tag{2.44}$$

where T_{BEC} is usual BEC temperature [9]. The factor $\frac{1}{4}$ appears because the plane wave of K motion of a particle has $\frac{\hbar^2K^2}{2(4m)}$ energy and T_{BEC} varies as 1/m. The sharpness of the transition is well evident from its condition $\lambda = 2d$.

While the particles of the system can be assumed, to a good approximation, to represent HC particles moving freely on a surface of constant potential $-V_o$, the fact that two neighbouring particles do experience inter-particle interaction during their relative motion which causes a change to the inertia of the particles. To incorporate this effect, Jain introduces effective mass $m^\star$ to replace m in equation 2.44 (which was obtained from a model based on free particle picture) and obtains

$$T_\lambda = \frac{h^2}{8\pi m^* k_B}\left[\frac{1}{d^2} + \left(\frac{N}{2.61V}\right)^{2/3}\right] \tag{2.45}$$

Evidently, d, V and $m^\star$ are three pressure (P) dependent quantities which in turn explain the pressure dependence of T_λ. While T_λ is expected to increase with increasing P for the usual decrease in the values of d and V, however, T_λ may show a reverse change if $m^\star$ increases with P. In this context Jain notes that $m^\star$ of ^4He atom should increase with P for an obvious increase in the strength of inter-particle attraction with increasing P.

2.4.5 Thermal Excitation

The ground state configuration of the system is defined by

$$\Delta\phi = 2n\pi, \quad q_o = \frac{\pi}{d} \quad and \quad < r >= d \tag{2.46}$$

Evidently, the system is a closed packed arrangement of wave packets leaving no freedom for the particles to move across each other. Particles can move in the order of their locations maintaining $\Delta\phi = 2n\pi$. If $\Delta\phi = kr = 2n\pi$ configuration is disturbed by some excitation, the particles are restored to its original configuration by U^s_{ij} generating waves of ϕ oscillation. The frequency ($\omega_\phi(Q)$) of such oscillations can be obtained by considering a chain of atoms and nearest neighbour interaction as the only responsible force present in the system, and we have

$$\omega_\phi(Q) = \sqrt{\frac{4\mathbf{C}}{\beta}} |\sin(Qd/2)| \tag{2.47}$$

where Q is the wave vector and β is the measure of inertia for ϕ motion. It is clear from the relation $\delta\phi = 2q(\delta r) + 2r(\delta q)$ that ϕ oscillation can appear as the oscillations of both r and q. While $r-$oscillations could be identified as phonon modes when all particles retain $q = q_o$, the $q-$oscillation represents the phonon like waves of momentum oscillations when the particles in the chain maintain $r = d$. The quantum quasi-particle that arises from the $q-$oscillation is named as *Omon*. The system like LHE-4 exhibits no transverse mode because the shear forces between particles are negligible and only one branch of longitudinal mode because the system is isotropic. Evidently, $\omega_r(Q)$ of phonons can be represented, to a good approximation, by the dispersion of the elastic waves in a chain of identical atoms and it can be obtained from equation 2.47 by replacing β and $\mathbf{C}$ by m and C, respectively. From equation 2.41

$$C = 4\pi^2\mathbf{C}/d^2 = 2\pi^2 k_B T_o/d^2 = \pi h^2/4md^4 \tag{2.48}$$

It may be mentioned that d and C are descending and ascending function of Q because an increase in energy of the particles by an excitation reduces wave packet size of the particles which renders a decrease in d and increase in C. As such the phonon energy, $E_{ph}(Q)$, is obtained from

$$E_{ph}(Q) = \hbar\omega_r(Q) = \hbar\sqrt{\frac{4C(Q)}{m}} |\sin(Qd(Q)/2)| \tag{2.49}$$

However, since $d \not< \sigma$, $d(Q)$ and $C(Q)$ are bound to become Q independent for $Q > \pi/\sigma$ and maximum in $E_{ph}(Q)$ falls at $Q_{max} = \pi/\sigma$. $E_{ph}(Q)$ over the range

$Q > \pi/\sigma$ and $< 2\pi/d$ follows

$$E_{ph}(Q) = \hbar\omega_r(Q) = \hbar\sqrt{\frac{4C(Q_{max})}{m}}|\sin(Q\sigma/2)| \tag{2.50}$$

Since phonon like dispersion is expected only till the excitation wavelength $\Lambda > d$ (i.e. $Q < 2\pi/d$), the spectrum for $\Lambda < \sigma$ (i.e. $Q > 2\pi/\sigma$) could be identified to follow

$$E_{sp}(Q) = \frac{\hbar^2 Q^2}{2m_F} \tag{2.51}$$

a kind of single particle dispersion. Here m_F represents a kind of mass factor that measures the effect of quantum correlation in the (q,-q) pair. A transition from $E_{ph}(Q)$ to $E_{sp}(Q)$ takes place over the range $2\pi/d < Q < 2\pi/\sigma$ before $E_{ph}(Q)$ meets zero value at $Q = 2\pi/\sigma$. Macro-orbital theory predicts a minimum value of energy at

$$Q_{min} \cong [\frac{\pi}{d} + \frac{\pi}{\sigma}] \tag{2.52}$$

2.4.6 Two Fluid Behaviour

For $T < T_\lambda$, the system is described by the state function of equation 2.38 where $\phi_n^o(q_o)$ deals with q motions and $\phi_n^e(K)$ with K motions of the particles. The component $\phi_n^o(q_o)$ represents the ground state of the system in which all particles are constrained by the relation $\Delta\phi = 2n\pi$. This state has zero entropy ($S = 0$) and zero viscosity ($\eta = 0$). The excitations are the effects that can propagate from one end of the system to the other against the closely packed WPs in the background. They, obviously, form a kind of gas (as envisaged by Landau [10,11]) that accounts for total S and other thermal properties of the system. Moreover, the excitations render $\eta \neq 0$ because their effects can lead to frictional movements of the particles. As such, $\phi_n^o(q_o)$ has the basic properties of super-fluid ($S-$phase) while $\phi_n^e(K)$ has those of normal fluid ($N-$phase). As all the particles take part in both $\phi_n^o(q_o)$ and $\phi_n^e(K)$, none of them can be labeled as N or S particle. All these aspects justify the use of inertial mass density associated with excitations to obtain normal fluid density $\rho_n(T)$ and super-fluid density $\rho_s(T) = \rho(T) - \rho_n(T)$ and vindicate Landau's two fluid model.

For $T > T_\lambda$, the state of the system can not be described as the product of two independent functions, rather this state is represented by equation 2.32. As a result, the system should be like a single component fluid as observed for LHE-4.

2.4.7 Energy Gap and Its Consequences

With T moving below T_λ, the WPs of neighbouring particles having increased size ($> d$) get overlapped and pushes the particles against the inter-particle attraction. This overlapping and $V_{ij}^A(r)$ perturb the state $|K = 0, q_o >$ as well as its energy ε_o to $\varepsilon_o \pm |\nu|$ where $|\nu|$ is the expectation value of the interaction potential due to the overlapping of the wave packets. However, it is better to replace $|\nu|$ by $|\nu(T)|$ as the overlapping may depend on T. The state of lower energy, i.e. $\varepsilon_o - |\nu(T)|$ represents a kind of bonding (or paired) state while $\varepsilon_o + |\nu(T)|$ represents an anti-bonding state. Since this happens to all particles of the system, the ground state energy of the system falls below $N\varepsilon_o(T_\lambda)$. The new energy of the system is given by

$$N\varepsilon_o(T < T_\lambda) = N\varepsilon_o(T_\lambda) - N|\nu(T)| = N\varepsilon_o - E_g(T) \tag{2.53}$$

When the system moves to the lower energy state, size of the wave packets get increased depending on $\nu(T)$. This forces the system to expand against inter molecular interaction with decreasing T as exhibited by LHE-4. The expansion, however, needs energy to work against inter-particle attraction. Incidentally, there exist a small number of $N^\star(T)$ of thermally excited particles even at $T < T_\lambda$ which avoid quantum correlation with other particles. With fall in T below T_λ, the number of these particles decreases from $N^\star(T_\lambda)$ to $N^\star(T)$ and in the process they release an additional energy $\Delta\varepsilon(T) = k_B T_o \ln 2[N^\star(T_\lambda) - N^\star(T)]$ with

$$N^\star(T) = \frac{V}{4\pi^2}\left[\frac{2m}{\hbar^2}\right]^{3/2} \int_{\varepsilon_c}^{\infty} \left[\exp\left(\frac{\varepsilon - \varepsilon_o}{k_B T}\right) - 1\right]^{-1} \sqrt{\varepsilon} d\varepsilon \tag{2.54}$$

where $\varepsilon_c = \frac{\hbar^2 Q_c^2}{2m}$ represents such energy that an atom of $\varepsilon > \varepsilon_c$ has no quantum correlation with its neighbours. For LHE-4 system, $\Delta\varepsilon(T)$ and $E_g(T)$ closely satisfy the relation $\Delta\varepsilon(T) = E_g(T)$, which holds good for all $T < T_\lambda$. As such, $\Delta\varepsilon(T)$ energy released from quantum correlation becomes available for the expansion of the system and used to push the particles to a higher potential energy by an amount $\Delta V_s(t) = \Delta\varepsilon(T)$. The net loss of energy is $\Delta\varepsilon(T) + E_g(T) = 2E_g(T)$ out of which $\Delta V_s(T) = \Delta\varepsilon(T)$ is restored back as an increase in potential energy (work done against $V_{ij}^A(r)$) of the particles. This energy represents a kind of strain in the system and termed as self energy of the particle. $\Delta V_s(T)$ depends on the size of the wave packets and q, hence it serves as a source of *Omon*. Increase of $\Delta V_s(T)$ with falling T implies that *Omon* field intensity increases with decreasing phonon field intensity.

At $T < T_\lambda$, the system is in a peculiar state of equilibrium in which particles are held at higher potential than the normal state. But net energy $N\varepsilon_o(T_\lambda) - 2E_g(T) + \Delta V_s(T) = N\varepsilon_o(T_\lambda) - E_g(T)$ is lower than $N\epsilon_o$. $E_g(T)$, is identified as collective binding energy among the particles rendering the system to become a liquid of single molecule and energy gap between normal and super-fluid state. The value of $E_g(T)$ can be calculated from the relation

$$E_g(T) = N\varepsilon(T) - N\varepsilon(T_\lambda) = \frac{Nh^2}{8m}\left[\frac{1}{d_T^2} - \frac{1}{d_\lambda^2}\right] \cong \frac{Nh^2}{4md_\lambda^3}[d_\lambda - d_T] \tag{2.55}$$

High Thermal Conductivity and Low Viscosity:

If two heads X and Y in the system maintain a small T and P differences, Macro-orbital theory predicts the equation of state as $E_g(X) = E_g(Y) + S\Delta T - V\Delta P$. For equilibrium $E_g(X) = E_g(Y)$ which gives

$$S\Delta T = V\Delta P \tag{2.56}$$

This equation reveals that the system should exhibits thermo-mechanical and mechanocaloric effects. This also shows that the co-efficient of viscosity η should be zero if it is measured by capillary method under the condition $\Delta T = 0$ and thermal conductivity Θ should be infinitely high if it is measured under $\Delta P = 0$. Because of this high Θ and closed packed structure, thermal convection currents are absent in the system, therefore, S-phase does not boil like N-phase. Since the particles in S-phase can only move in the order of their location, they cease to have relative motion, particularly during their linear motion. Therefore, the system exhibits vanishingly small η for linear motion. However, in the rotating fluid, the particles moving in neighbouring concentric circular path have relative velocity producing quantized vortices as the source of natural viscous behaviour.

Critical Velocity and S-phase:

The state function of the S-phase $\phi_n(q_o)$ changes to $\phi_n^\star(q_o)$ when the system flows with velocity $\frac{\hbar}{m}\Delta q$. This new state function is represented by:

$$\phi_n^\star(q_o) = \phi_n(q_o)\exp(iK.\sum_i^N R_i)\exp[-i[N(\varepsilon_o + \varepsilon(K)) - E_g(T)]t/\hbar] \tag{2.57}$$

with $2\Delta q = K$. The S-state function remains stable against such a flow unless the flow energy $\frac{1}{2}Nmv_f^2 = N\varepsilon(K)$ overtakes the collective binding energy $E_g(T)$ of the

system. The critical velocity at which the system loses its super-fluid behaviour is given by

$$v_c(T) = \sqrt{\frac{2E_g(T)}{Nm}} \tag{2.58}$$

Even at $V < v_c(T)$ the super-fluid may show sign of viscous behavior due to creation of quantized vortices. However, the system retains its super-fluidity unless energy of all vortices produced in the system exceeds $E_g(T)$.

Super-fluid Density:

In Macro-orbital theory super-fluid density ρ_s is related to $E_g(T)$ through the relation

$$\rho_s(T) = \frac{E_g(T)}{E_g(0)}\rho(T) \tag{2.59}$$

and normal density $\rho_n(T) = \rho(T) - \rho_s(T)$. Knowing the value of $E_g(T)$ (using equation 2.55), values of $v_c(T)$ and $\rho_s(T)$ can be obtained easily. This relation also shows that at T_λ the super-fluid component vanishes (as $\rho_s(T) = 0$ for $E_g(T_\lambda) = 0$) and at $T = 0$ the normal fluid component vanishes (as $\rho_s(0) = \rho(0)$). For $0 < T < T_\lambda$, the fluid maintains its two fluid nature. Considering the time independent part of the equation 2.57 super-fluid velocity, v_s, can be expressed as

$$v_s = \frac{\hbar}{2m}\nabla_{R_j} S(r) = \frac{h\Delta q}{m} \tag{2.60}$$

with $S(R) = K.\sum_i^N R_i$. The factor $2m$ appears because of the fact that $\nabla_{R_j} S(R)$ render the momentum of the pair. This relation also shows the relationship between super-fluid velocity v_s and the phase $S(r)$ of $S-$state wave function.

2.4.8 Quantized Vortices

This theory also shows the existence of quantized vortices in *helium-II* as mentioned by Feynman [12, 13]. It also gives a satisfactory explanation to Wilks [14] reservation about Feynman model. The circulation of velocity field

$$\kappa = \sum_i v_s(i).\Delta r_i = \frac{\hbar}{m}\sum_i \Delta q_i.\Delta r_i = \frac{nh}{m} \tag{2.61}$$

with $\sum_i \Delta q_i.\Delta r_i = 2n\pi$, which presumes that the relative configuration of particles during their reshuffle on a closed path maintain phase correlation. Only the particles of $S-$phase satisfy the relation $\Delta\phi = 2n\pi$ whereas for the particles of normal phase satisfy $\Delta\phi \geq 2n\pi$. This explains why quantized vortices do not exist in normal phase.

2.4.9 Logarithmic Singularity of Specific Heat

Macro-orbital theory predicts simultaneous occurrence of two separate phenomena at T_λ: (i) BEC of SMW pairs and (ii) ordering of particles in phase space. It is predicted that when the particles move from their uncorrelated state ($\phi = 2n\pi \pm \delta\phi_\lambda$) at T_λ^+ (just above T_λ) to correlated state ($\phi = (2n+1)\pi$) at T_λ^- (just below T_λ), the system releases an excess amount of energy which makes a significant contribution to the specific heat at $\lambda-$transition. If N_λ particles move from their uncorrelated state to correlated state, the excess amount of energy is given by:

$$\Delta\varepsilon = -Nk_BT_o\left[\ln 2\sin^2\left(\frac{2n\pi \pm \delta\phi_\lambda}{2}\right) - \ln 2\right] \tag{2.62}$$

Following the theories [15] of critical phenomena one finds

$$\delta\phi_\lambda = \delta\phi_\lambda(0)|\zeta|^\nu[1 + a_2|\zeta|^2 + a_3|\zeta|^3] \tag{2.63}$$

with $\zeta = \frac{T-T_\lambda}{T_\lambda}$. To a good approximation

$$\Delta\varepsilon = -N\frac{T-T_\lambda}{T_\lambda}k_BT_o\ln\left(\frac{\delta\phi_\lambda(0)|\zeta|^2}{2}\right) \tag{2.64}$$

where

$$\delta\phi_\lambda = \delta\phi_\lambda(0)|\zeta|^\nu \ \textit{and}\ N_\lambda = \frac{N(T-T_\lambda)}{T_\lambda} \tag{2.65}$$

A choice for LHE-4 parameters and $\nu = 0.55$ and $\delta\phi_\lambda(0) = \pi$, equation 2.64 gives

$$C_p(J/mole.K) = -5.71\ln|\zeta| - 10.35 = -A\ln|\zeta| + B \tag{2.66}$$

while experimental results reveal $A = 5.355$ and $B = -7.77$ for $T > T_\lambda$ and $A = 5.1$ and $B = 15.52$ for $T < T_\lambda$ [16].

2.4.10 Thermodynamic Properties

In Macro-orbital theory, energy of a particle in SMW configuration is given by

$$E = \varepsilon(K) + \varepsilon(k) = \frac{\hbar^2K^2}{8m} + \frac{\hbar^2k^2}{8m} \tag{2.67}$$

Possible values of E ranges between its ground state energy $\varepsilon_o = h^2/8md^2 = E$ (for $K = 0$, $k = 2\pi/d$) to ∞ (for $K = \infty$) and this range is available from the relation

$$E = \frac{\hbar^2K^2}{8m} + \varepsilon_O = \varepsilon(K) + \varepsilon_0 \tag{2.68}$$

This energy expression is used in starting expression of the standard BEC theory [9], to find

$$\frac{PV}{k_BT} = -\sum_{\varepsilon(K)} \ln[1 - z\, exp(-\beta[\varepsilon(K) + \varepsilon_o])] \tag{2.69}$$

and

$$N = \sum_{\varepsilon(K)} \frac{1}{z_1 \exp(\beta[\varepsilon(K) + \varepsilon_o]) - 1} \tag{2.70}$$

with $\beta = 1/k_BT$ and fugacity $z = \exp(\beta\mu)$ (μ is chemical potential). Redefining the fugacity by

$$z' = z\, \exp(-\beta\varepsilon_o) = \exp[\beta(\mu - \varepsilon_o] \tag{2.71}$$

and following the procedure of standard BEC [9], Macro-orbital theory reveals

$$\frac{P}{k_BT} = -\frac{2\pi(8mk_BT)^{3/2}}{h^3} \int_0^\infty x^{1/2} \ln(1 - z'e^{-x})dx = \frac{1}{\lambda^3} g_{3/2}(z') \tag{2.72}$$

and

$$\frac{N - N_o}{V} = \frac{2\pi(8mk_BT)^{3/2}}{h^3} \int_0^\infty \frac{x^{1/2}dx}{z'^{-1}} = \frac{1}{\lambda} g_{3/2}(z') \tag{2.73}$$

where $x = \beta\varepsilon(K)$, $\lambda = h/(2\pi(4m)k_BT)^{1/2}$ and $g_{3/2}(z')$ has usual expression. This reduces the problem to that of non interacting bosons but with a difference. In this formulation $z' = 1$ expected for $T < T_\lambda$ which implies $\mu = \varepsilon$ and $z' < 1$ for $T > T_\lambda$ implies $\mu < \varepsilon_o$, however, for a system of non-interacting bosons $\mu = 0$ for $T \leq T_\lambda$ and $\mu < 0$ for $T > T_\lambda$.

2.5 Conclusion

Deviating from the conventional thought, Jain successfully develops the microscopic theory of a system of interacting bosons which is well equipped to explain the properties of LHE-4. His theory vindicates (i) Landau two fluid phenomenology [10], (ii) London's idea of macroscopic wave function of the S-state [17], (iii) the observation of Bogoliubov [18] that super-fluidity is the manifestation of an inter-particle interaction *etc.* Jain's theory explains different properties of LHE-4 within experimental error.

The main features of Jain's theory are : (i) the formation of (q,-q) pairs of particles (with $q = q_o$) around T_λ, (ii) the pair formation arising from the quantum correlation and inter-particle attraction which is shown to be energetically favourable, (iii) the binding of these pairs differs from the binding of two electrons

in a Cooper pair in the sense that the necessary attraction is the inherent ^4He-^4He attraction and it leads to the collective binding of all particles in the system for which the entire system behaves like a single macro-molecule. (iv) this binding serves as an energy gap between the super-fluid and normal phases of the system, (v) it has been successfully developed within the framework of the wave mechanics, (vi) it is consistent with excluded volume condition as well as microscopic and macroscopic uncertainty, (vii) while the atoms in *helium-I* are randomly distributed in normal space, momentum space and phase space, in *helium-II* they define an orderly arrangement in these spaces with a kind of crystalline arrangement in normal space, a momentum $q = \pi/d$ or its integer values, and relative phase position of $\Delta\phi = 2n\pi$; they cease to have relative motion and remain free to move in order of their positions on a closed path, (viii) its mathematical formulations are exceptionally simple and its inferences have unparalleled clarity.

Bibliography

[1] Y.S. Jain. *J. Sci. Exlor.*, 16:67, 2002.

[2] Y.S. Jain. *Cent. Euro. J. Phys.*, 2:709, 2004.

[3] Y.S. Jain. *J. Sci. Expl.*, 16:77, 2002. More detailed version of this paper is available for ready reference as a paper entitled, *"Macro-orbitals and microscopic theory of a system of interacting bosons"* in www.arXiv.org/cond-mat/0606571.

[4] Y.S. Jain. in *cond-mat/0606409*, e-print, www.arXiv.org, 2006.

[5] K. Huang. *Statistical Mechanics.* McGraw Hill, New Delhi, 1991.

[6] Y.S. Jain. in *cond-mat/0603233*, e-print, www.arXiv.org, 2006.

[7] P. Kleban. *Phys. Lett.*, 49A:19, 1974.

[8] C.W. Woo. In K.H. Benneman and J.B. Ketterson, editors, *The Physics of Liquid and Solid Helium, Part-I*, pages 349–501. John Wiley and Sons, New York, 1976.

[9] R.K. Pathria. *Statistical Mechanics.* Pergamon Press, Oxford, 1976.

[10] L.D. Landau. *J. Phys. U.S.S.R. (reprinted in Ref. 1)*, 5:71, 1941.

[11] L.D. Landau. *J. Phys. U.S.S.R (reprinted in Ref. 1)*, 11:91, 1947.

[12] R.P. Feynman. In C.J. Gorter, editor, *Prog. Low Temp. Phys.*, volume I, page 1. North-Holland, Amsterdam, 1955.

[13] R.P. Feynman. *In Statistical Mechanics, MA: W.A. Benjamin.* 1976.

[14] J. Wilks. *The Properties of Liquid and Solid Helium.* Clerendon Press, Oxford, 1967.

[15] M.E. Fisher. *Reports on the Progress of Physics*, 30:615, 1967.

[16] G Ahlers. In K.H. Benneman and J.B. Ketterson, editors, *The Physics of Liquid and Solid Helium.* Wiley, New York, 1976.

[17] F. London. *Nature*, 141:644, 1938.

[18] N. Bogoliubov. *J. Phys (USSR) (reprinted in Ref. 1)*, 11:23, 1947.

Chapter 3

Thermodynamic Response Functions and Their Logarithmic Singularities at λ-Point

Abstract *The singularity of specific heat (C_p) and related properties (viz thermal expansion coefficient, α_p isothermal compressibility, κ_T and pressure coefficient β) of liquid helium-4 at $\lambda-$point is studied and the accuracy of its logarithmic nature as concluded for the first time from a microscopic theory (Macro orbital theory) of a system of interacting bosons is examined A very good agreement between the results of this theory and experiments concludes that the singularity is intrinsically logarithmic However, as shown by other studies reportingcarefully measured C_p of liquid helium-4 around T_λ for $|t| = |(T_\lambda - T)/T_\lambda|$ ranging between 10^{-1} to 10^{-9}, in and out of earth's gravitationalfield and in finite size samples, weak effects arising from earth's gravity and small size round it off and C_p assumes asymptotic nature near $t \sim 0$*

3.1 Introduction:

One of the most significant properties of LHE-4 is the observed discontinuity in the specific heat at $\lambda-$transition. Keesom and Clusius [1, 2] were the first to measure the temperature dependence of the specific heat. They observed a jump in the specific heat in the vicinity of $2.19/, K$. Their results showed that the shape of the specific heat *versus* temperature curve resembles the shape of the letter λ and hence, the transition is called λ-transition as suggested by Ehrenfest [3]. A series of more accurate measurements [4–10] revealed that the discontinuity of the specific heat is logarithmic in nature. Data of the earlier measurements [4–6] are best fitted to the empirical relation

$$C_P = -A \log |T - T_\lambda| + B \tag{3.1}$$

with $A = 3.00$ joules/gm/deg for both $T > T_\lambda$ and $T < T_\lambda$ and $B = -0.65$ joules/gm/deg for $T > T_\lambda$ and $B = 4.55$ joules/gm/deg for $T < T_\lambda$ [11, 12]. However, a series of later measurements [7–10] reveals a deviation from the above relation. This set of data are not consistent with equal amplitudes of logarithmic term specifically when $T_\lambda - T \geq 10^{-3}K$. These measurements yield [7, 12]

$$1.04 \leq \frac{A}{A'} \leq 1.06 \tag{3.2}$$

where primed and unprimed coefficients refers to $T < T_\lambda$ and $T > T_\lambda$ respectively.

Recently, Lipa and coworkers [13,14] have reported very carefully measured C_p, *in and out of earth's gravitational field.* To isolate the effect of gravity they made their measurements on STS-52 space craft, space shuttle Columbia. While the net dependence of their C_p on $t = (T_\lambda - T)/T_\lambda$ is certainly asymptotic but their analysis indicates that once the observed C_p is corrected for the factors which round off its values near T_λ, the corrected C_p fits closely logarithmic variation. Similarly, careful investigation of the effects of finite size of the sample performed by Lipa *et al* [15–17] and Gasparini *et al* [18–20] also reveals that C_p variations are intrinsically logarithmic; they assume asymptotic dependence on t when the sample size becomes smaller than coherence length.

In addition to specific heat, the λ-transition of liquid helium-4 (LHE-4) is characterized by logarithmic singularity of: (i) expansion coefficient (α_p), (ii) isothermal compressibility (k_T) and (iii) pressure coefficient (β) [11, 12] with varying strength.

Early measurements of density of LHE-4 [21, 22] which show peak at λ-point (indicative of a divergence of α_p) were repeated with improved accuracy by Atkins and Edwards [23], Kerr [24], Edwards [25], and Chase *et al* [26] for detailed analysis. These results are reviewed elegantly by Kerr and Taylor [27]. It is evident that α_p for its linear relation with C_p should have logarithmic divergence at $\lambda-$point. Similarly, the divergence of β investigated by Ahlers [9], Lounasmaa and Kaunisto [28], Lounasmaa [29], and Kiersted [30,31] is ought to be logarithmic. We note that thermodynamic relations between various response functions, as discussed by Rice [32], Pippard [33,34], and Buckingham and Fairbank [5], indicate that K_T is an asymptotically linear function of C_p and hence of α_p. Evidently, k_T is naturally expected to show logarithmic singularity at $\lambda-$point. However, the identification of this behavior from experimental observation is obscured by large regular contribution.

Despite a long and rich history of experimental works and untiring efforts of nearly seven decades for developing a viable microscopic theory of LHE-4, the exact nature and origin of the above stated singularities has been unknown. The importance of this is reflected by a comment from Feynman in his book [35]. Recently, Jain [36] used unconventional approach to develop a long awaited microscopic theory of a system of interacting bosons such as LHE-4 based on Macro-orbital representation of a particle in a many body system and obtained a relation for the logarithmic singularity of C_p. In this chapter we have attempted to examine his relation for its agreement with experiments and used it to find similar relations for α_p, κ_T and β.

3.2 Thermodynamic Response Functions and Their Relations

Basic thermodynamic response functions are the specific heats at constant pressure and constant volume i.e. C_p and C_v, the isothermal and adiabatic compressibility, κ_T and κ_S, the isobaric expansion coefficient, α_p, and the pressure coefficient, β. These quantities are defined by

$$C_p = T\left(\frac{\partial S}{\partial T}\right)_P, \tag{3.3}$$

$$C_v = T\left(\frac{\partial S}{\partial T}\right)_V, \tag{3.4}$$

$$\kappa_T = -V^{-1}\left(\frac{\partial V}{\partial P}\right)_T, \tag{3.5}$$

$$\kappa_S = -V^{-1}\left(\frac{\partial V}{\partial P}\right)_S, \tag{3.6}$$

$$\alpha_P = V^{-1}\left(\frac{\partial V}{\partial T}\right)_P, \tag{3.7}$$

$$\beta = \left(\frac{\partial P}{\partial T}\right)_V. \tag{3.8}$$

Here V and S are the volume and entropy per mole. Basic relations between these response functions and their singular behavior at $\lambda-$transition are obtainable from the fundamental thermodynamic relations. Considering the entropy as a function of P and T, we get

$$dS = \left(\frac{\partial S}{\partial T}\right)_P dT + \left(\frac{\partial S}{\partial P}\right)_T dP \tag{3.9}$$

Using the Maxwell's relation $(\partial S/\partial P)_T = -(\partial V/\partial T)_P$ and equations 3.3 and 3.7 one can obtain

$$dS = -V\alpha_P\, dP + T^{-1}C_P\, dT \tag{3.10}$$

From this equation, the temperature derivative of S along any arbitrary thermodynamic path can be obtained as

$$\left(\frac{\partial S}{\partial T}\right)_t = -V\left(\frac{\partial P}{\partial T}\right)_t \alpha_P + \frac{C_P}{T} \tag{3.11}$$

On rearrangement this equation gives

$$C_P = T\left(\frac{\partial S}{\partial T}\right)_t + VT\left(\frac{\partial P}{\partial T}\right)_t \alpha_P \tag{3.12}$$

Equation 3.12 gives the relation between specific heat at constant pressure and isobaric expansion co-efficient. Considering the entropy as a function of V and T, one can obtain

$$dS = \left(\frac{\partial S}{\partial V}\right)_T dV + \left(\frac{\partial S}{\partial T}\right)_V dT \tag{3.13}$$

Using Maxwell relation $(\partial S/\partial V)_T = (\partial P/\partial T)_V$ and equation 3.4, the temperature derivative of S along any arbitrary thermodynamic path can be obtained as

$$\left(\frac{\partial S}{\partial T}\right)_t = \left(\frac{\partial P}{\partial T}\right)_V \left(\frac{\partial V}{\partial T}\right)_t + \frac{C_V}{T} \tag{3.14}$$

After rearrangement this equation gives

$$C_V = T\left(\frac{\partial S}{\partial T}\right)_t - T\left(\frac{\partial P}{\partial T}\right)_V \left(\frac{\partial V}{\partial T}\right)_t \tag{3.15}$$

Using equations 3.12 and 3.15, one can find

$$C_P - C_V = VT\left(\frac{\partial P}{\partial T}\right)_t \alpha_P + T\left(\frac{\partial P}{\partial T}\right)_V \left(\frac{\partial V}{\partial T}\right)_t \tag{3.16}$$

Considering the volume as a function of P and T, one can get

$$dV = \left(\frac{\partial V}{\partial P}\right)_T dP + \left(\frac{\partial V}{\partial T}\right)_P dT \tag{3.17}$$

Using equations 3.5 and 3.7 we get

$$dV = -V\kappa_T\, dP + V\alpha_P\, dT \tag{3.18}$$

From this, temperature derivative of V along any arbitrary thermodynamic path can be obtained as

$$\left(\frac{\partial V}{\partial T}\right)_t = -V\left(\frac{\partial P}{\partial T}\right)_t \kappa_T + V\alpha_P, \tag{3.19}$$

on rearrangement which yields

$$\alpha_P = V^{-1}\left(\frac{\partial V}{\partial T}\right)_t + \left(\frac{\partial P}{\partial T}\right)_t \kappa_T \tag{3.20}$$

Eliminating α_P from equation 3.12 and rearranging the terms, we get

$$\kappa_T = \left[VT\left(\frac{\partial P}{\partial T}\right)_t^2\right]^{-1} C_P - \frac{[(\partial S/\partial T)_t/(\partial P/\partial T)_t^2 + (\partial V/\partial T)_t/(\partial P/\partial T)_t]}{V} \tag{3.21}$$

Starting from Maxwell's relation $(\partial S/\partial V)_T = (\partial P/\partial T)_V$ we get

$$\beta = \left(\frac{\partial S}{\partial V}\right)_T = \left(\frac{\partial S}{\partial P}\right)_T \left(\frac{\partial P}{\partial V}\right)_T$$

$$\Rightarrow \beta = -\left(\frac{\partial V}{\partial T}\right)_P \left(\frac{\partial P}{\partial V}\right)_T$$

$$or,\ \beta = -\frac{\alpha_P}{\kappa_T} \tag{3.22}$$

To study the singularities in the response functions given by 3.3- 3.8 at $\lambda-$transition, it is advantageous to choose a thermodynamic path (along which t is constant) in some sense "parallel" to the $\lambda-$line. In that case t will represent a distance from the $\lambda-$point. The coefficients in equations 3.12, 3.15, 3.16, 3.20 and 3.22 depend upon the detailed definition of t. It follows from [12] that when t vanishes, the coefficients become independent of the choice t and equal to derivative along the $\lambda-$line. It is also shown that $(\partial S/\partial T)_\lambda$, $(\partial P/\partial T)_\lambda$ and $(\partial V/\partial T)_\lambda$ are finite along the $\lambda-$line.

3.3 Logarithmic Singularity in C_P

In what follows from chapter-2 that $\lambda-$transition is the manifestation of two separate but simultaneous phenomena: (i) BEC condensation of (q,-q) pairs at $K = 0$ state and (ii) ordering of particles in phase space. Macro-orbital theory predicts an energy [36]

$$\Delta\varepsilon = -Nk_BT_o\left[\ln 2\sin^2\left(\frac{2n\pi \pm \delta\phi_\lambda}{2}\right) - \ln 2\right], \tag{3.23}$$

to be associated with the ordering of particles in the phase space. This energy is the origin of logarithmic singularity of C_P at $\lambda-$point. For a small range of $|t| < 0.1\,K$, Macro-orbital theory concludes

$$C_P(J/mole.K) = -A\ln|t| + B \tag{3.24}$$

with

$$A = \frac{N}{T_\lambda}k_BT_o2\nu \tag{3.25}$$

and

$$B = \frac{N}{T_\lambda}k_BT_o\left[2\ln(\delta\phi_\lambda(0)) - \ln 4 + 2\nu\right] \tag{3.26}$$

In order to demonstrate the fact that equation 3.24 obtained from Macro-orbital theory can correctly account for the logarithmic divergence of C_p, Jain [36] used $T_o = 1.49K$, $\nu = 0.55$ and $\delta\phi_\lambda(0) = \pi$ to conclude $A = 5.71$ (both for $T < T_\lambda$ and $T > T_\lambda$) matching closely with: (i) similar estimates based on Widom-Kadanoff scaling laws [34,37–40] and (ii) $A = 5.1$ for $T < T_\lambda$ and 5.355 for $T > T_\lambda$ obtained from experimental C_P. While the close agreement between theoretical A and experimental A showed the accuracy of equation 3.24, but the choice of parameters rendered $B = -10.35$ which, however, differs significantly from $B = -7.77$ (for $T > T_\lambda$) and 15.52 (for $T < T_\lambda$) estimated from experimental C_p [12]. Here we examine this aspect more deeply to find that: (i) $\delta\phi_\lambda(0)$ should, in principle, be lower than π because the shift in $\phi-$positions of all particles in the process of their order-disorder in ϕ space need not be equal to π and (ii) $\delta\phi_\lambda(0)$ should not, necessarily, be equal for both sides of T_λ because particles on T_λ^+ side nearly have random positions in $\phi-$space while the same on T_λ^- side are largely locked with $\Delta\phi = 2n\pi$ which indicates that $\delta\phi_\lambda(0)$ on $+ve$ side should be slightly lower than π, while that on $-ve$ side should be fairly small. Guided by these points, we find that $\delta\phi_\lambda(0) = 0.75\pi$ for $T > T_\lambda$ and $\delta\phi = 0.084\pi$ for $T < T_\lambda$ with $\nu = 0.47$ render $A = 5.1148$ and $B = 16.9319$ for $T < T_\lambda$ and $A = 5.1148$ and $B = -6.8930$ for

$T > T_\lambda$ which agree closely with their experimental values. This agreement can be better perceived from figures 3.1-3.3 where we plot our calculated $C_P \, vs. \, T_\lambda - T$ along with the experimental values [7] for comparison. We present our calculated values of specific heat in Table-3.1. Further since A depends on ν and our choice of its equal value for both sides of T_λ renders $A^+ = A^-$ whose experimental values, however, have small difference [7,9,40]. Evidently, if ν is presumed to have slightly different values on two sides of T_λ for the same reason, the difference in A^+ and A^- is easily explained. Evidently, Macro-orbital theory accounts for the observed logarithmic singularity in all its details.

3.4 Logarithmic Singularities in α_P, κ_T and β

It is evident from equations 3.12, 3.20 and 3.21 that α_P and κ_t have linear relations with C_P. Therefore, the singularities in these response functions should be similar to that of C_P. For a divergent C_P, however, C_V and β are less singular because the leading singularities in β (equation 3.22) get cancelled and C_V is linear with β [12].

3.4.1 Expansion Coefficient (α_P)

Temperature dependence of α_P around T_λ can be obtained by using equation 3.24 in equation 3.12.

$$V_\lambda T_\lambda \left(\frac{\partial P}{\partial T}\right)_\lambda \alpha_P = -A \ln|t| + B - T_\lambda \left(\frac{\partial S}{\partial T}\right)_\lambda \tag{3.27}$$

On rearrangement this equation yields

$$\alpha_P = A_\alpha \log|T - T_\lambda| + B_\lambda \tag{3.28}$$

with

$$A_\alpha = -2.3025 \frac{A}{T_\lambda V_\lambda \left(\partial P/\partial T\right)_\lambda} \tag{3.29}$$

and

$$B_\alpha = \frac{B + A \ln T_\lambda - T_\lambda \left(\partial S/\partial T\right)_\lambda}{V_\lambda T_\lambda (\partial P/\partial T)_\lambda} \tag{3.30}$$

where A and B are the same coefficients given by equations 3.25 and 3.26 respectively. To estimate the coefficients A_α and B_α we use $\left(\partial P/\partial T\right)_\lambda = -112.5 \, bar/K$, $\left(\partial S/\partial T\right)_\lambda = 102 \, cm^3 \, bar/mole/K^2$ and $V_\lambda = 27.38 \, cm^3/mole$ [12]. These parameters give $A_\alpha = 0.0166$ and $B_\alpha = 0.0032$ for $T < T_\lambda$ and $A_\alpha = 0.0166$ and

$B_\alpha = 0.0367$ for $T > T_\lambda$, while experiments reveal $A_\alpha = 0.01680$ and $B_\alpha = 0.0025$ for $T < T_\lambda$ and $A_\alpha = 0.0169$ and $B_\alpha = 0.0379$ for $T > T_\lambda$ [11]. We depict our results in figure 3.4 along with the experimental results of [23] and [9], respectively, marked as Exp.(1) and Exp(2). Numerical values are presented in Table-3.2.

3.4.2 Isothermal Compressibility (κ_T):

Equations 3.20 and 3.21 provide linear relations between the isothermal compressibility and α_P and C_p, respectively. Substituting the C_P given by equation 3.24 in equation 3.21 we find

$$\kappa_T = A_\kappa \log|T - T_\lambda| + B_\kappa \tag{3.31}$$

with

$$A_\kappa = -2.3025 \frac{A}{V_\lambda T_\lambda (\partial P/\partial T)_\lambda^2} \tag{3.32}$$

and

$$B_\kappa = \frac{A \ln T_\lambda + B}{V_\lambda T_\lambda (\partial P/\partial T)_\lambda^2} - \frac{1}{V}\left[\frac{(\partial S/\partial T)_\lambda}{(\partial P/\partial T)_\lambda^2} + \frac{(\partial V/\partial T)_t}{(\partial P/\partial T)_\lambda}\right] \tag{3.33}$$

Using $(\partial V/\partial T)_\lambda = 43.82 cm^3/mole/K$ and other parameters as used above we find $A_\kappa = -0.0001$ and $B_\kappa = 0.0141$ for $T < T_\lambda$ and $A_\kappa = -0.0001$ and $B_\kappa = 0.0138$ for $T > T_\lambda$. Our calculated κ_T is depicted in figure 3.5 with the experimental values taken from [10]. Though, our results exhibit a logarithmic divergence, there exist a systematic difference from Ahlers findings.

3.4.3 Pressure Coefficient (β)

Values of pressure coefficient near T_λ can be obtained by using the calculated values of α_P and κ_T in equation 3.22. We have plotted our values in figure 3.6 along with the experimental points obtained from [7] and [23]. These points are marked respectively as Expt.(1) and Expt.(2). As expected, the divergence of β at $\lambda-$point undoubtedly appears to be logarithmic.

3.5 Discussion

Several experimental studies of specific heat of LHE-4, *viz.* in bulk, investigated out of earth's gravity [13, 14] and confined to different geometries [15–19], have

been performed near $\lambda-$point for various reasons discussed elegantly by these authors as well as by Bhattacharya and Bhattacherjee [41] and Schultka and Manousakis [42]. In particular, these studies aim at verifying several predictions of renormalization group theory. For the same reasons, extensive investigation of the C_p of liquid ^4He-^3He mixtures near their $\lambda-$points have also been made by Gasparini *et al* [43,44] and second sound propagation in LHE-4 has been studied by Marek *et al* [45] and Swanson *et al* [46]. One, evidently, finds that the gravity of earth and the effects of finite size sample round off the C_p of LHE-4 at the $\lambda-$point and the position of its maximum is shifted to a temperature (say T_m) below T_λ by a small amount. However, in the absence of these effects C_p divergence is logarithmic as concluded by Jain's theory [36]. In this context it may be mentioned that Jain's theory [36] does not incorporate weak effects arising from gravity of earth, finite size of the sample, *etc.* while concluding equation 3.24. Since such effects would always be present, the experimental C_p would always be rounded for one reason or the other as one tries to reach closer and closer to T_λ.

It may be noted that Jain's approach [36] to the microscopic theory of LHE-4 type systems differs from conventional approaches (see Ref [36]) for its use of a Macro-orbital (a kind of pair waveform [47]) to represent the self superposition state of a particle in a many body system where each particle assumes its self superposition when its collision with other particle(s) forces its pre-collision and post-collision states (both represented by plane waves of two different momenta) to have their superposition. This, naturally, tends to organize two particles in collision at phase positions differing by $\Delta\phi = 2n\pi$, particularly, when particles are of low energy with de Broglie wave length λ being equal to or larger than the inter-particle separation d and this is achieved for nearly all particles in the system at low temperatures with thermal de Broglie wave length $\lambda_T \approx 2d$ [36]. Since Jain's approach gives due importance to all consequences of this superposition which represents *one of the simple truths* of wave nature of a quantum particle, its results are naturally expected to agree with experiments. In addition the merits of Jain's approach also rest with the facts that: (i) it makes no assumption like conventional theories of a system of interacting bosons which assume that $p = 0$ condensate exists in super-fluid state of LHE-4 type systems or Cooper type bound pairs of ^3He atoms are the origin of super-fluidity of liquid ^3He type systems, (ii) its all inferences are based on a systematic critical analysis of the solutions of $N-$particle Schrödinger equation, (iii) as seen from [36, 48], it proposes a single

framework for all many body systems of interacting bosons (or fermions) like ^4He (or electrons in solids or ^3He) atoms, (iv) its simple mathematical framework is easy to comprehend and does not permit many adjustable parameters like conventional theories where one finds widely different theoretical predictions depending on the values of such parameters (*for example as discussed in* [49], *different papers using BCS picture predicted widely different super-fluid* T_c *for liquid* ^3He), (v) as shown in this paper it explains even those observations, *viz.* the logarithmic singularity of C_p and related properties of LHE-4, which found no basis in the framework of conventional theories, *etc.* In addition, the fact that the theoretical results, obtained by using Jain's approach, for example for super-fluid T_c of liquid ^3He and its pressure dependence [49], excitation spectrum of LHE-4 [50], and those reported here, match closely with experiments, clearly indicates that Jain's theoretical approach has great potential to explain the physics of widely different many body systems. This has been demonstrated in his recent work related to the basic foundations of superconductivity [48] and ground state of N hard core particles in 1-D box [49], unification of the physics of widely different many body systems [51] and wave mechanics of two hard core particles in 1-D system [47].

Recently, Fliessbach [52] reported a semi-phenomenological microscopic model of $\lambda-$transition of *helium-II*, proposed to be known as "*almost ideal Bose gas model*" (AIBG). To this effect, he intuitively modifies the wave function $\Psi_{IBG} = \sum \Pi_k[\phi_k]^{n_k}$ representing a state of ideal Bose gas (IBG) with $\phi_k = \exp(i\mathbf{k}.\mathbf{r}_j)$ replaced by $\phi_k = \sin(qx_j + \theta_j)$ and introduces the concept of localized phase ordering by physical (or Dirichlet) boundary conditions at the walls of macroscopic volume V. While there is considerable resemblance of these aspects of Fliessbach's single particle function $\phi_k = \sin(qx_j + \theta_j)$ with Jain's Macro-orbital $\phi_{mo} = \sin(\mathbf{q}.\mathbf{r})\exp(\mathbf{K}.\mathbf{R})$ function which identifies each atom like a particle of quantum size $\lambda/2 = \pi/q$ moving freely with momentum $\mathbf{K}$, there is great deal of difference in the allowed values of q permitted by his theory [52] (*viz.*, $q \geq \pi/L$ with L being the size of macroscopic V) and Jain's theory [36] (*viz.*, $q \geq \pi/d$ with $d = (V/N)^{1/3}$). It may be noted that Jain's theory uses purely microscopic considerations and the possibility of wave superposition to conclude a Macro-orbital as the right wave function for a particle in a system like *helium-II* [36]. Interestingly, we note that Fliessbach finds that the energy, responsible for the logarithmic singularity of the specific heat of LHE-4 at $\lambda-$point, is related to phase ordering and it depends on t as $t\ln|t|$ which agrees with Jain's result forming the basis

of equation 3.24 used in the present analysis, of course with different multiplying factors to $t \ln|t|$. It may be noted that Fliessbach does not use his relation to show the nature of agreement of his theoretical results with experiments, hence no comparative analysis of his results with our results could be possible. However, since Fliessbach's model also uses phase ordering (although introduced intuitively) to explain the logarithmic nature of the said singularity, it may be argued that the phase ordering of particles, as concluded by Jain's microscopic theory, has strong foundation and the fact that this ordering is an important characteristic of super-fluid phase of LHE-4 type systems, can not be ignored. In this context, it may be mentioned that studying the coupled low dimensional super-fluids, Mathey *et al* [53] find that super-fluids have strong tendency to phase lock which falls in line with an important inference of Jain's theory that inter-particle phase locking is an inherent aspect of a super-fluid.

3.6 Conclusion

It is evident that C_p of LHE-4, when observed in absence of the effects of earth's gravity or of finite size of the sample, exhibits logarithmic singularity at T_λ and this agrees closely with Jain's microscopic theory [36]. As per Jain's theory, the logarithmic singularity of C_p is a consequence of order-disorder of particles in phase space forced by the wave nature of particles or quantum correlation between a pair of bosons. We find that Jain's theory [36] is capable of accounting for the difference in C_p at $T < T_\lambda$ and $T > T_\lambda$ for the same value of $|T_\lambda - T|$. It is noted that α_P, κ_T and β exhibit logarithmic divergence for their relation with C_p which implies that the divergence of these quantities also originates from the ordering of the particles in the phase space. The agreement of our theoretical values obtained from Jain's theory [36] with experimental results confirms the accuracy of Jain's relation for C_p beyond doubt. In other words it may be concluded that Jain's Macro-orbital theory is equipped to explain the origin of logarithmic divergence of thermodynamic response functions and it is more advantageous for its accuracy, simplicity and clarity. As such the present work answers the long standing question related to origin of the logarithmic divergence of C_p and related properties which found no answer from conventional theories.

Table 3.1: Calculated and Experimental C_p of LHE-4 at SVP near T_λ

$10^{-4}(T_\lambda - T)$ (K)	$C_p(Theory)$ $(J.mole^{-1}K^{-1})$	$C_p(Expt.)$	$10^{-4}(T_\lambda - T)$ (K)	$C_p(Theory)$ $(J.mole^{-1}K^{-1})$	$C_p(Expt.)$
35.720	34.04	34.61	0.4865	58.34	57.99
32.020	34.94	35.21	0.4739	58.46	58.13
27.730	35.89	35.99	0.4482	58.98	58.44
24.030	36.97	36.77	0.3533	60.04	59.73
16.810	39.17	38.71	0.3348	60.31	60.02
15.890	39.48	39.02	0.3178	60.50	60.31
14.190	39.76	39.64	0.2885	61.05	60.83
10.840	41.76	41.10	0.2168	62.40	62.39
10.000	42.30	41.54	0.1850	63.29	63.25
9.159	42.76	42.02	0.1685	63.88	63.76
7.495	43.89	43.11	0.1282	65.28	65.25
6.660	44.60	43.75	0.1220	65.51	65.52
6.532	44.67	43.86	0.1215	65.37	65.54
6.199	44.92	44.14	0.0190	74.00	75.64
5.862	45.25	44.45	0.0143	77.10	77.18
5.826	45.30	44.48	0.0100	77.70	79.13
5.520	45.54	44.77	0.0098	78.00	79.24
5.169	45.93	45.13	0.0081	80.50	80.27
4.827	46.27	45.50	0.0070	81.90	81.07
4.649	46.52	45.71	0.0065	82.20	81.47
4.372	46.86	46.04	0.0050	82.80	82.90
4.155	47.07	46.32	0.0050	83.50	82.90
3.817	47.60	46.78	0.0024	86.80	86.89
3.689	47.79	46.97	-0.0032	65.30	64.10
3.478	48.06	47.29	-0.0034	63.80	63.77
3.136	48.61	47.85	-0.0063	59.00	60.42
3.033	48.86	48.03	-0.0065	58.00	60.25
2.792	49.23	48.48	-0.0096	56.80	58.13
2.627	49.61	48.81	-0.0100	57.60	57.90

Experimental values are from ref [7]

Cont.

$10^{-4}(T_\lambda - T)$ (K)	$C_p(Theory)$ $(J.mole^{-1}K^{-1})$	$C_p(Expt.)$	$10^{-4}(T_\lambda - T)$ (K)	$C_p(Theory)$ $(J.mole^{-1}K^{-1})$	$C_p(Expt.)$
2.4600	49.88	49.17	-0.0114	57.10	57.19
2.1270	50.65	49.96	-0.0168	53.70	55.08
1.9570	51.12	50.42	-0.0179	54.60	54.74
1.7560	51.71	51.01	-0.0371	51.00	50.77
1.7250	51.79	51.10	-0.0895	46.14	45.98
1.7210	51.84	51.12	-0.1728	42.75	42.40
1.5560	52.28	51.66	-0.2379	41.08	40.66
1.4820	52.60	51.93	-0.2660	40.43	40.05
1.4170	52.85	52.17	-0.4383	37.78	37.33
1.3890	52.93	52.28	-0.5097	36.98	36.51
1.2860	53.32	52.70	-0.6855	35.41	34.90
1.2220	53.58	52.98	-1.0250	3.22	32.71
1.1530	54.02	53.30	-1.1840	2.50	31.93
1.0830	54.28	53.64	-1.3780	1.63	31.10
1.0710	54.28	53.70	1.7240	0.43	29.88
1.0550	54.44	53.78	-1.7240	30.43	29.88
1.0080	54.60	54.03	-1.8780	29.99	29.42
0.8881	55.22	54.72	-2.0690	29.46	28.89
0.8392	55.56	55.02	-2.4140	28.64	28.05
0.7972	55.92	55.30	-2.7530	27.93	27.33
0.7495	56.20	55.64	-3.0140	27.48	26.84
0.7197	56.36	55.86	-3.0800	27.33	26.72
0.6708	56.72	56.24	-3.4040	26.80	26.18
0.6244	57.03	56.63	-3.9490	26.04	25.37
0.5175	57.97	57.65	-4.6310	25.20	24.50
0.5030	58.30	57.81	-5.3390	24.44	23.73
0.4973	58.32	57.87	-6.0480	23.77	23.05

Table 3.2: Calculated values of α_p, κ_T and β of LHE-4 at SVP near T_λ

$10^{-3}(T_\lambda - T)$	α_P	κ_T	β	$10^{-3}(T_\lambda - T)$	α_P	κ_T	β
K	$/K$	$/Bar$	bar/K	K	$/K$	$/Bar$	bar/K
10.00	-0.0254	0.01440	-1.7639	-0.001	-0.0660	0.01500	-4.4000
9.00	-0.0262	0.01441	-1.8187	-0.002	-0.0607	0.01494	-4.0631
8.00	-0.0271	0.01442	-1.8798	-0.003	-0.0576	0.01490	-3.8648
7.00	-0.0281	0.01443	-1.9490	-0.004	-0.0554	0.01488	-3.7235
6.00	-0.0293	0.01444	-2.0288	-0.005	-0.0537	0.01486	-3.6136
5.00	-0.0307	0.01446	-2.1229	-0.006	-0.0523	0.01484	-3.5235
4.00	-0.0324	0.01448	-2.2379	-0.007	-0.0511	0.01483	-3.4473
3.00	-0.0346	0.01450	-2.3856	-0.008	-0.0501	0.01482	-3.3811
2.00	-0.0377	0.01454	-2.5930	-0.009	-0.0492	0.01481	-3.3226
1.00	-0.0430	0.01460	-2.9452	-0.010	-0.0484	0.01480	-3.2703
0.90	-0.0438	0.01461	-2.9985	-0.020	-0.0431	0.01474	-2.9242
0.80	-0.0447	0.01462	-3.0580	-0.030	-0.0400	0.01470	-2.7204
0.70	-0.0457	0.01463	-3.1253	-0.040	-0.0378	0.01468	-2.5753
0.60	-0.0469	0.01464	-3.2029	-0.050	-0.0361	0.01466	-2.4623
0.50	-0.0483	0.01466	-3.2945	-0.060	-0.0347	0.01464	-2.3698
0.40	-0.0500	0.01468	-3.4063	-0.070	-0.0335	0.01463	-2.2915
0.40	-0.0500	0.01468	-3.4063	-0.070	-0.0335	0.01463	-2.2915
0.30	-0.0522	0.01470	-3.5501	-0.080	-0.0325	0.01462	-2.2235
0.20	-0.0553	0.01474	-3.7519	-0.090	-0.0316	0.01461	-2.1634
0.10	-0.0606	0.01480	-4.0946	-0.100	-0.0308	0.01460	-2.1096
0.09	-0.0614	0.01481	-4.1464	-0.200	-0.0255	0.01454	-1.7539
0.08	-0.0623	0.01482	-4.2043	-0.300	-0.0224	0.01450	-1.5445
0.07	-0.0633	0.01483	-4.2699	-0.400	-0.0202	0.01448	-1.3953
0.06	-0.0645	0.01484	-4.3454	-0.500	-0.0185	0.01446	-1.2792
0.05	-0.0659	0.01486	-4.4345	-0.600	-0.0171	0.01444	-1.1842
0.04	-0.0676	0.01488	-4.5434	-0.700	-0.0159	0.01443	-1.1036
0.03	-0.0698	0.01490	-4.6833	-0.800	-0.0149	0.01442	-1.0337
0.02	-0.0729	0.01494	-4.8797	-0.900	-0.0140	0.01441	-0.9720
0.01	-0.0782	0.01500	-5.2133	-1.000	-0.0132	0.01440	-0.9167

Cont.

$10^{-3}(T_\lambda - T)$ K	α_P $/K$	κ_T $/Bar$	β bar/K	$10^{-3}(T_\lambda - T)$ K	α_P $/K$	κ_T $/Bar$	β bar/K
0.009	-0.0790	0.01501	-5.2638	-2.0	-0.0079	0.01434	-0.5510
0.008	-0.0799	0.01502	-5.3202	-3.0	-0.0048	0.01430	-0.3357
0.007	-0.0809	0.01503	-5.3840	-4.0	-0.0026	0.01428	-0.1823
0.006	-0.0821	0.01504	-5.4575	-5.0	-0.0009	0.01426	-0.0630
0.005	-0.0835	0.01506	-5.5443	-6.0	0.0005	0.01424	0.0348
0.004	-0.0852	0.01508	-5.6503	-7.0	0.0017	0.01423	0.1176
0.003	-0.0874	0.01510	-5.7865	-8.0	0.0027	0.01422	0.1895
0.002	-0.0905	0.01514	-5.9777	-9.0	0.0036	0.01421	0.2530
0.001	-0.0958	0.01520	-6.3026	-10.0	0.0044	0.01420	0.3099

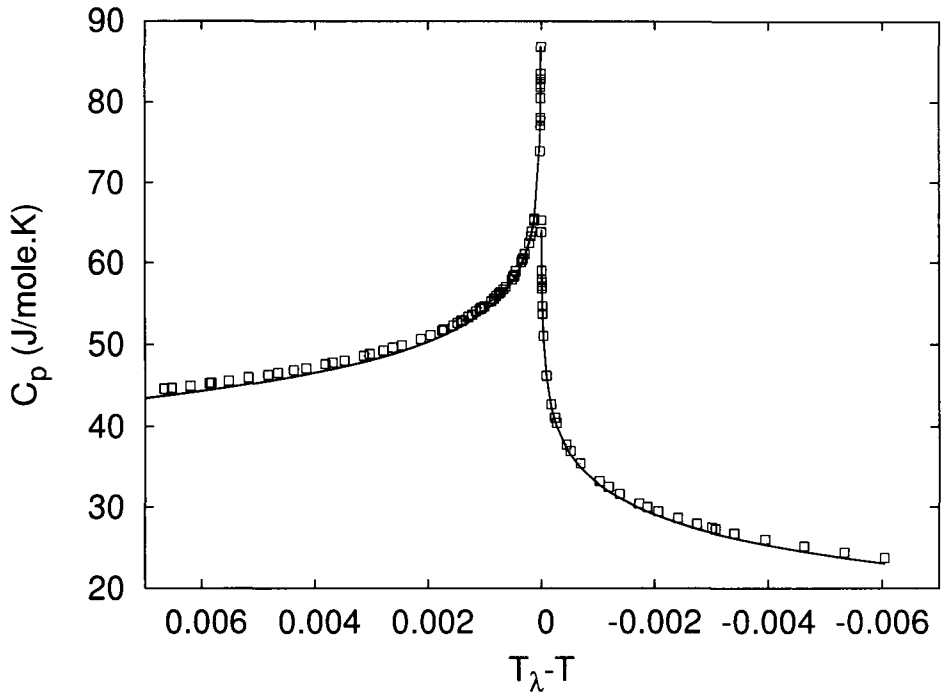

Figure 3.1: C_p of LHE-4 around $\lambda-$point with squares indicating experimental values [7] and line representing our theoretical results.

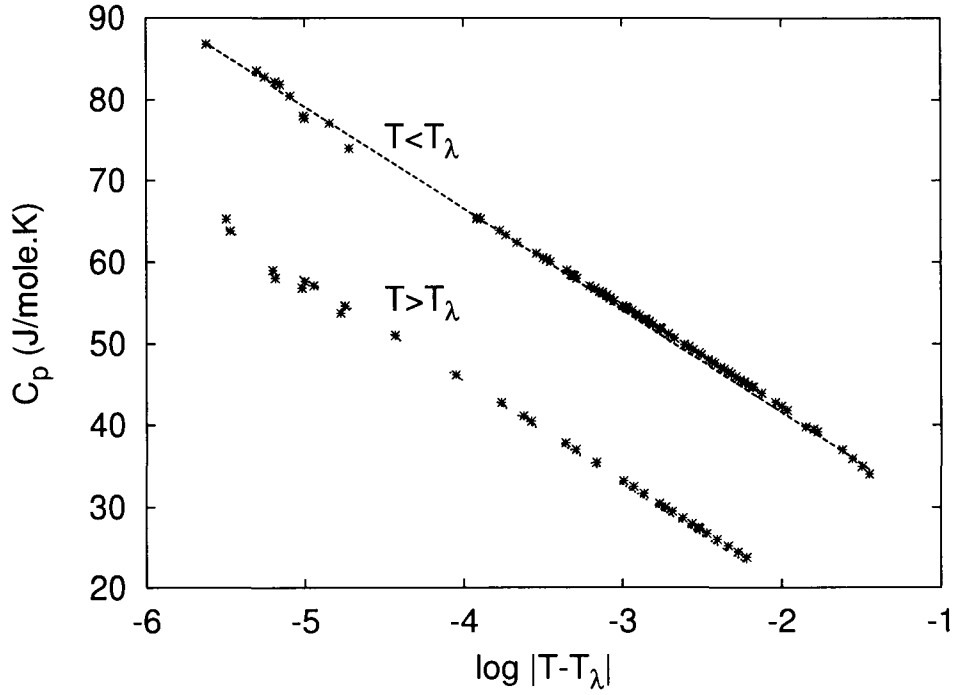

Figure 3.2: C_p *vs.* $\log|T_\lambda - T|$ curve for LHE-4 around λ-point on log scale Experimental points are taken from ref [7]

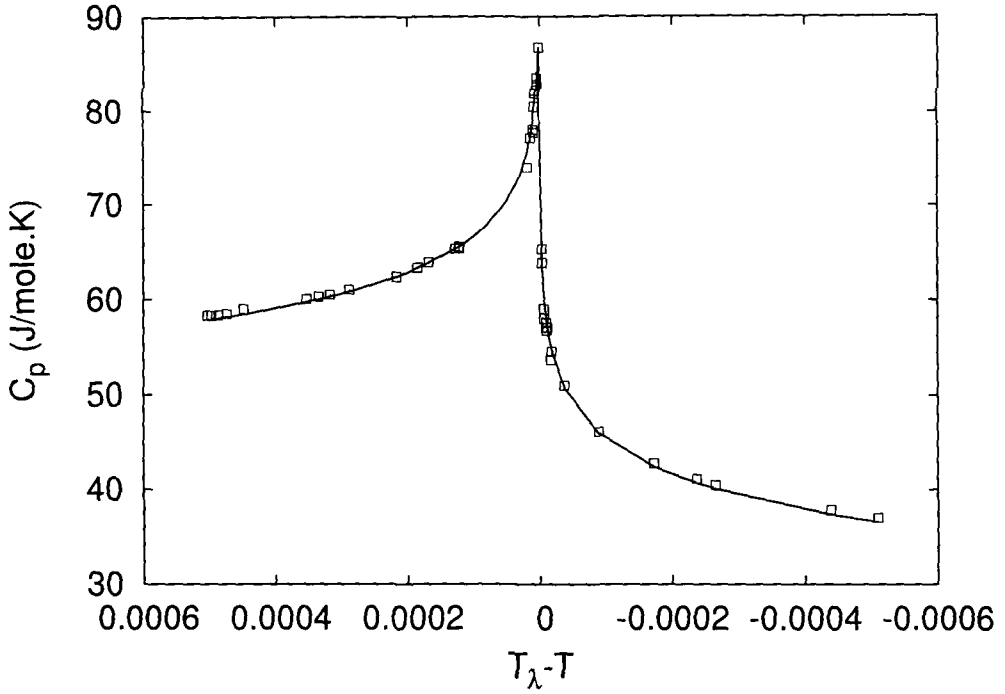

Figure 3.3: C_p *vs.* $T_\lambda - T$ curve for LHE-4 around λ-point (the points in this figure are closer to $\lambda-$point in comparison to figure 3.1). Curves on two sides of $\lambda-$point join each other (*as shown here*) when weak perturbation on logarithmic singularity round it off. Experimental points are taken from ref [7]

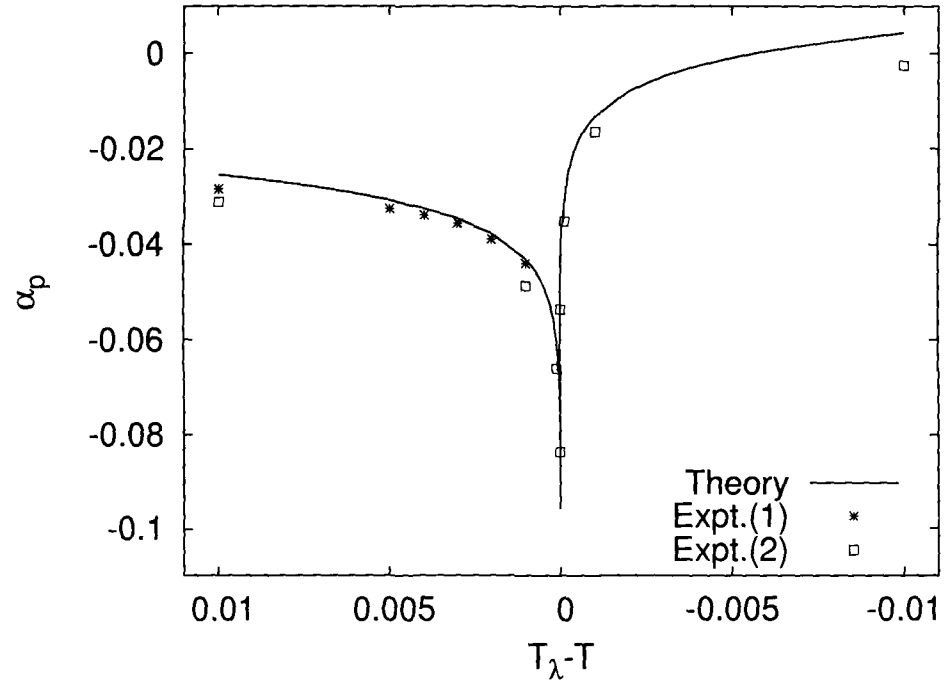

Figure 3.4: α_p *vs.* $T_\lambda - T$ curve for LHE-4 around $\lambda-$point.

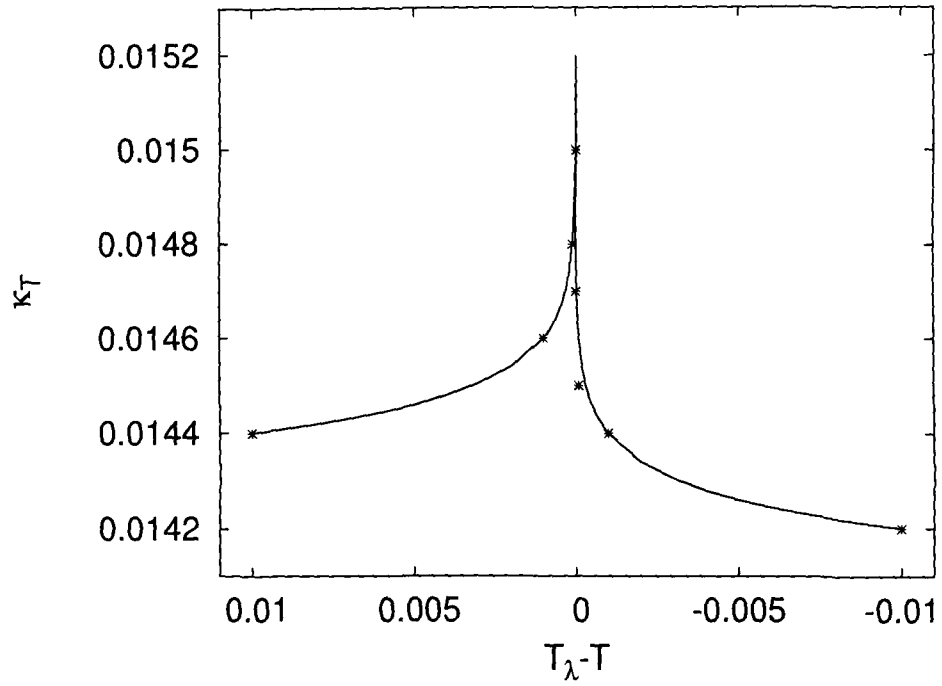

Figure 3.5: κ_T *vs.* $T_\lambda - T$ curve for LHE-4 around $\lambda-$point with stars indicating experimental points [10] and line representing our theoretical results.

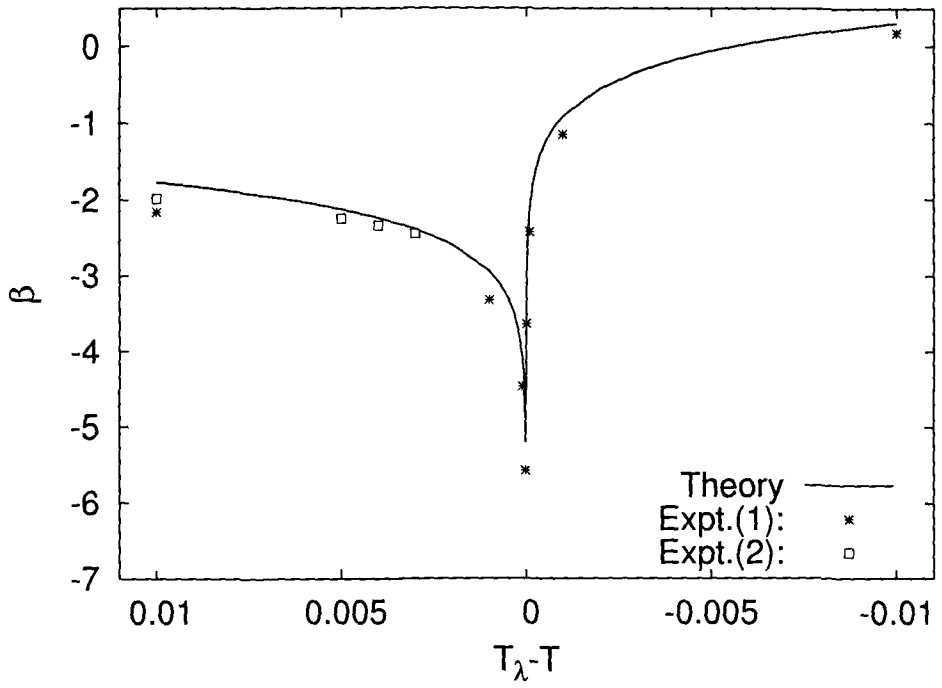

Figure 3.6: β *vs.* $T_\lambda - T$ curve for LHE-4 around $\lambda-$point.

Bibliography

[1] W.H. Keesom and K. Clusius. *Leiden Comm (reprinted in Ref. 1)*, 219e, 1932.

[2] W.H. Keesom and K. Clusius. *Proc. Sect. Sci. K. ned. Akad. Wet.*, 35:307, 1932.

[3] Zygmunt M. Galasiewicz. *Helium-4*. Pragamon Press, Oxford, 1971.

[4] W.M. Fairbank, M.J. Buckinghum, and C.F. Kellers. In J.R. Dillinger, editor, *Proceedings of the Fifth International Conference on Low Temperature Physics and Chemistry*, page 50, Madison, Wisc, 1958. University of Wisconsin Press.

[5] M.J. Buckinghum and W.M. Fairbank. In C.J. Gorter, editor, *Progress in Low Temperature Physics*, volume VIII. North-Holland, Amsterdam, 1961.

[6] W.M. Fairbank and C.F. Kellers. In M.S. Green and J.V. Sengers, editors, *Critical Phenomena, Proceedings of a Conference*, number 273, page 71, U.S. GPO, Washington D.C., 1966. Natl. Bur. Std. Misc. Pub.

[7] G. Ahlers. *Phys. Rev. Lett.*, 23:464, 1969.

[8] F. Gasparini and M.R. Molodover. *Phys. Rev. Lett.*, 23:749, 1969.

[9] G. Ahlers. *Phys. Rev.*, A 3:696, 1971.

[10] G. Ahlers. *Phys. Rev.*, A 8:530, 1973.

[11] J. Wilks. *The Properties of Liquid and Solid Helium.* Clerendon Press, Oxford, 1967.

[12] G Ahlers. In K.H. Benneman and J.B. Ketterson, editors, *The Physics of Liquid and Solid Helium.* Wiley, New York, 1976.

[13] J.A. Lipa, D.R. Swanson, J.A. Nissen, T.C.P. Chui, and U.E. Israelsson. *Phys. Rev. Lett.*, 76:944, 1996.

[14] J.A. Lipa, D.A. Swansson, and T.C.P. Chui. *Phys. Rev.*, B 68:174518–1, 2003.

[15] J.A. Lipa and T.C.P. Chui. *Phys. Rev. Lett.*, 51:2291, 1983.

[16] M. Coleman and J.A. Lipa. *Phys. Rev. Lett.*, 74:286, 1995.

[17] J.A. Lipa, D.R. Swansson, J.A. Nissan, Z.K. Geng, P.R. Williamson, D.A. Stricker, T.C.P. Chui, U.E. Israelsson, and M. Larson. *Phys. Rev. Lett.*, 84:4894, 2000.

[18] T. Chen and F.F. Gasparini. *Phys. Rev. Lett.*, 40:331, 1978.

[19] S. Mehta and F.M. Gasparini. *Phys. Rev. Lett.*, 78:2596, 1997.

[20] S. Mehta, M.O. Kimball, and F.M. Gasparini. *J. Low Temp. Phys.*, 113:435, 1998.

[21] H.K. Onnes and J.D.A. Boks. *Leiden Comm.*, 170b, 1924.

[22] E. Mathias, C.A. Crommelin, H.K. Onnes, and J.C. Swallow. *Leiden Comm.*, 172, 1925.

[23] K.R. Atkins and M.H. Edwards. *Phys. Rev.*, 97:1429, 1955.

[24] E.C. Kerr. *J. Chem. Phys.*, 26:511, 1957.

[25] M.H. Edwards. *Can. J. Phys.*, 36:884, 1958.

[26] C.E.Chase, E. Maxwell, and W.E. Millett. *Physica*, 27:1129, 1961.

[27] E.C. Kerr and R.D. Taylor. *Ann. Phys.*, 26:292, 1964.

[28] O. Lounasmaa and L. Kaunisto. *Ann. Acad. Sci. Fenn. Sev.*, A VI(59), 1960.

[29] O.V. Lounasmaa. *Phys. Rev.*, 130:847, 1963.

[30] H.A. Kiersted. *Phys. Rev.*, 138:A1594, 1965.

[31] H.A. Kiersted. *Phys. Rev.*, 153:258, 1967.

[32] O.K. Rice. *J. Chem. Phys.*, 22:1535, 1954.

[33] A.B. Pippard. *Phil. Mag.*, 1:473, 1956.

[34] A.B. Pippard. In *The Elements of Classical Thermodynamics*, chapter IX. Cambridge Univ. Press, 1957.

[35] R.P. Feynman. In *Statistical Mechanics*, page 34. W.A. Benjamin Inc, 1972.

[36] Y.S. Jain. *J. Sci. Expl.*, 16:77, 2002. More detailed version of this paper is available for ready reference as a paper entitled, *"Macro-orbitals and microscopic theory of a system of interacting bosons"* in www.arXiv.org/cond-mat/0606571.

[37] M.E. Fisher. *Reports on the Progress of Physics*, 30:615, 1967.

[38] B. Widom. *J. Chem. Phys.*, 43:3892, 1965.

[39] B. Widom. *J. Chem. Phys.*, 43:3898, 1965.

[40] L.P. Kadanoff, W. Gotze, D. Hamblen, R. Hecht, E.A.S. Lewis, V.V. Palciauskas, M. Rayl, and J. Swift. *Rev. Mod. Phys*, 39:395, 1967.

[41] S. Bhattacharya and J.K. Bhattacharjee. *Phys. Rev.*, B 59:3341, 1991.

[42] N. Schultka and E. Manousakis. *Phys. Rev. Lett.*, 75:2710, 1995.

[43] F.M. Gasparini and M.R. Molodover. *Phys. Rev.*, B 12:93, 1975.

[44] F.M. Gasparini and A.A. Gaeta. *Phys. Rev.*, B 17:1466, 1978.

[45] D. Marek, J.A. Lipa, and D. Phillips. *Phys. Rev.*, B 38:4465, 1988.

[46] D.R. Swanson, T.C.P. Chui, and J.A. Lipa. *Phys. Rev.*, B 46:9041, 1992.

[47] Y.S. Jain. *Cent. Euro. J. Phys.*, 2:709, 2004.

[48] Y.S. Jain. in *cond-mat/0606571*, e-print, www.arXiv.org, 2006.

[49] Y.S. Jain. in *cond-mat/0606409*, e-print, www.arXiv.org, 2006.

[50] Y.S. Jain. A study of elementary excitations of liquid helium-4 using macro-orbital microscopic theory. www.arXiv.org/cond-mat/0609418, 2006.

[51] Y.S. Jain. *J. Sci. Expl.*, 16:117, 2002.

[52] T. Fliessbach. in *cond-mat/0203353*, e-print, www.arXiv.org, 2002.

[53] L. Mathey, A. Polkovinikov, and A.H. Castro Neto. Phase locking transition of coupled low dimensional superfluids. www.arXiv.org/cond-mat/0612174, 2006.

Chapter 4

A Study of Elementary Excitations and Anomalous Dispersion in Liquid Helium-4

Abstract *Elementary excitations in helium-II at long wavelengths have been investigated by using Jain's Macro orbital theory We have estimated $E(Q)$, V_q and V_p using Q dependent values of d and C and considering different atomic arrangements namely for sc, bcc, fcc and hcp arrangements Estimated values for $E(Q)$, V_g and V_p agree closely with experiments Anomalous nature of V_p and V_g at low Q is well established Our results reveal that anomalous nature exists up to $Q \sim 0.43 \AA^{-1}$ which closely agrees with experiments*

4.1 Introduction:

The study of elementary excitations in liquid helium-4 (LHE-4) has a long and rich history. It started in 1941 when Landau [1] published his first paper on the subject entitled, "The Theory of Superfluidity of Helium II". He was of the opinion that in LHE-4 like systems only collective excitations involving many atoms exist and these could be known as "elementary excitations". He also argued that these excitations should follow a 'phonon' like energy spectrum, namely,

$$E(Q) = cQ \tag{4.1}$$

at low Q (excitation wave vector). Guided by the existence of critical velocity for which surperfluidity vanishes, he further argued that the spectrum at higher Q should have a form,

$$E(Q) = \Delta + Q^2/2\mu \tag{4.2}$$

where Δ represents a kind of energy gap in the spectrum of elementary excitations. He called these excitations as 'rotons'. In 1947, Bogoliubov [2] established an approximate relation for $E(Q)$ by using a microscopic theory of weakly interacting Bose gas and at the same time, Landau [3] proposed a modification in his higher energy spectrum (equation 4.2). In order to account for the observed thermodynamic properties of LHE-4, he concluded that the modified spectrum should have the form

$$E(Q) = \Delta + (Q - Q_o)^2/2\mu \tag{4.3}$$

and argued that the relations 4.1 and 4.3 are two different parts of a single excitation spectrum (*cf* figure 4.1). Here, Q_o represents minimum energy position in roton region and Δ represents roton minimum energy. Using the experimentally observed thermodynamic properties of LHE-4, he obtained $\Delta = 9.6K$, $Q_o = 1.95\mathring{A}^{-1}$, and $\mu = 0.77M$, where M is the ^4He atomic mass. Using $V(Q) = \sin Q/Q$ (Fourier transform of the inter-atomic potential) Bogoliubov showed that $E(Q)$ for weakly interacting boson gas agrees qualitatively with Landau's phonon-roton spectrum. Efforts to develop a microscopic understanding of the elementary excitations in LHE-4 started with Feynman [4] who used variational approach to establish a relationship between $E(Q)$ and $S(Q)$ (the structure factor of LHE-4). He obtained

$$E(Q) = \frac{\hbar^2 Q^2}{2MS(Q)} \tag{4.4}$$

which was found to be about twice the experimental $E(Q)$. Guided by this observation, Feynman and Cohen [5] introduced a phenomenon of back flow and used it

to obtain a relation for $E(Q)$, which showed a better agreement with experimental values at saturated vapour pressure (SVP). While similar results were obtained by Pitaevskii [6] by using quantum liquid hydrodynamics, Padmore and Chester [7] pointed out that Feynman and Cohen's $E(Q)$ does not describe the pressure dependence of roton minimum. It appears that later studies by Feenberg [8], Jackson and Feenberg [9,10] and others [11–13] have included the effects of phonon-phonon interactions more fully to obtain an improved $E(Q)$. The progress up to 1975 is reviewed by Woo [11] and Campbell [14].

The neutron scattering experiment on LHE-4 was reported for the first time in transmission geometry in 1951. It was followed by diffraction measurements by Henshaw and Hurst [15,16]. In 1957, Cohen and Feynman [17] showed that the neutron inelastic scattering (NIS) could be used to determine $E(Q)$ of LHE-4. Stimulated by this inference, a large number of NIS measurements were performed in late 1950's [18–22] and it was observed that $E(Q)$ of *helium-II* indeed agrees with "phonon-roton" spectrum envisaged by Landau. A typical nature of the excitations spectrum as obtained from NIS is shown in figure 4.1. The segment ABC of the graph represents the phonon excitations with point B representing what we call as 'maxon' (maximum energy position, Q_{max}), and the region around point C where excitations have nearly zero group velocity represents what we call as 'roton' with point C representing minimum energy position (roton minimum, Q_o). While segment CD represents nearly free particle excitations, segment DE represents the plateau region which arises due to mixing of single particle excitations with multi phonon modes.

4.2 Anomalous Dispersion

Existence of anomalous dispersion in *helium-II* was first suggested by Maris and Massey [23] in 1970. Immediately this topic has received a great deal of attention and numerous functional forms for the dispersion at low Q have been proposed [11, 24–30]. The measurements by Cowley and Woods [31] gave a hint of the anomalous dispersion for the first time, however, it was Svensson *et al* [25] who established its existence beyond doubt. The measurements by Svensson *et al* covered pressure up to 24 atms, and indicated that at SVP anomalous dispersion region extended to $Q = 0.52\mathring{A}^{-1}$. They further observed that anomalous dispersion region decreases with increasing pressure. It is because of this anomalous

dispersion that higher energy excitations decay through three phonon processes rather than less favourable four phonon processes. More accurate measurements by Stirling [29] at SVP indicated an anomalous dispersion region up to $Q = 0.55\mathring{A}^{-1}$. The measurements by Dynes and Narayanmurti [32] based on ballistic phonon propagation method indicated that anomalous dispersion disappears completely at pressures above $20\,bars$.

Pitaevskii and Levinson [33] introduced three parameters which are the characteristic of anomalous dispersion curve: the parameter $\tilde{Q}_o$ is the wave vector where the group and phase velocity coincide, second parameter $\tilde{Q}_2$ is the largest wave vector beyond which decay into two identical phonons is not possible, and third parameter $\tilde{Q}_\infty$, is the wave vector where the phase velocity coincides with the velocity of sound. For $Q > \tilde{Q}_2$, decay into two phonons is not possible, but the phonon may decay into three or more phonons. As such one may find that the anomalous nature of the dispersion has not been explained from any microscopic theory. However guided by the observation that Jain's Macro-orbital theory has closely explained the origin of the anomalous dispersion in a system of interacting bosons, we in this chapter use his theory to account for the experimentally observed anomalous dispersion of LHE-4 at quantitative level.

4.3 Dispersion in Macro-orbital Theory

Macro-orbital theory predicts that below the transition temperature LHE-4 system maintains an orderly and closed packed arrangement of wave packets representing different particles leaving no space for their random motion. Evidently, the frequency of phonons can be represented, to a good approximation, by the dispersion of the elastic waves in a chain of identical atoms which have been discussed in Chapter-2. The relation

$$E_{ph}(Q) = \hbar\omega_r(Q) = \hbar\sqrt{\frac{4C(Q)}{m}}\,|\sin(Qd(Q)/2)| \tag{4.5}$$

gives detailed information about the energy spectrum of the system.

4.3.1 Quantitative Study

Earlier, Roychoudhury [34] attempted to explain the excitation spectrum as well as the anomalous nature of the dispersion curve quantitatively using Jain's Macro-

orbital theory [35]. He used equation 4.5 to obtain the best possible values of $E_{ph}(Q)$, $V_p\,(=E_{ph}(Q)/\hbar Q)$ and $V_g\,\left(=\frac{\partial E_{ph}(Q)}{\hbar \partial Q}\right)$, at different Q by using a set of $d(Q)$ and $C(Q)$, chosen to find $E_{ph}(Q)$, $V_p(Q)$ and $V_g(Q)$ which agree closely with experimental values. To calculate the Q dependence of $C(Q)$, he used the relation

$$C(Q) = \frac{\pi h^2}{4md^4(Q)} \tag{4.6}$$

for lower values of Q while Q dependence of $d(Q)$ is calculated by using the relation

$$d(Q) = \frac{2\pi}{(\frac{2\pi}{3.709} + \frac{Q}{2})} \tag{4.7}$$

which he obtained from

$$Q = 2\Delta Q = 2\left[\frac{2\pi}{d(Q)} - \frac{2\pi}{d(0)}\right] \tag{4.8}$$

He used $d(0) = 3.709\mathring{A}$ for *helium-II*. His results showed that C and d change almost linearly with Q, having $C = 2.74\,dynes/cm$ and $d = 3.709\mathring{A}$ at $Q = 0$ and $C = 5.46\,dynes/cm$ and $d = 2.85\mathring{A}$ at $Q = 1.1\mathring{A}^{-1}$. He also showed that the variation of $C(Q)$ with the change in $d(Q)$ is nearly linear except in the small range of $d(Q)$ at high Q values.

Later, Jain [36] used the relations

$$d(Q) = d - d' \sin \pi Q/2Q_{max} = 3.5787 - 0.7484 \sin \pi Q/2Q_{max} \tag{4.9}$$

and

$$C(Q) = C + C' \sin \pi Q/2Q_{max} = 3.1619 + 2.3619 \sin \pi Q/2Q_{max} \tag{4.10}$$

to find the necessary $d(Q)$ and $C(Q)$ at different $Q < Q_{max}$. He constructed these relations intuitively to ensure smooth variation of $d(Q)$ and $C(Q)$ from their values at $Q = 0$ to $Q = Q_{max}$ without any discontinuity even in their first derivative at Q_{max} beyond which they become independent of Q. He estimated $d(Q = 0) = 3.5787\mathring{A}$ using the density of *helium-II* $(0.1452gm/cc)$ [37] and used this value in equation 4.5 to fix $C(Q = 0) = 3.1681\,dynes/cm$. He used maxon position i.e. $Q_{max} = \pi/\sigma = 1.11\mathring{A}^{-1}$ to fix $d(Q_{max}) = \sigma = 2.8293\mathring{A}$ and estimated the value of $C(Q_{max}) = 5.53\,dynes/cm$ by using $E(Q_{max}) = 13.92K$ [38]. Then he used these results to fix $d' = d - \sigma = 0.7484\mathring{A}$ and $C' = C(Q_{max}) - C(Q = 0) = 2.3619\,dynes/cm$. These parameters yield energy that closely match with the experiments and qualitatively produce the anomalous character at low $Q < \pi/\sigma$ [36]. However, at the quantitative scale it differs slightly from the experimental results.

For example these parameters yield a sound velocity $V_p = 247m/sec$ at $Q = 0$ while experiments reveal $238.21m/sec$. Despite this slight disagreement with the experiments, we feel Macro-orbital theory provides a good microscopic understanding of the excitation spectrum of LHE-4. In the following section we shall attempt to show how a close agreement with the experiments is possible using same set of relations.

4.3.2 Present Study

Macro-orbital theory reveals that anomalous nature of the dispersion originates from the Q dependence of $d(Q)$. An atomic chain of constant d ($say\, d = 3.5787\mathring{A}$ or $d = \sigma = 2.8314\mathring{A}$) does not exhibit anomalous nature. Jain has obtained the maximum value of $d\,(= 3.5787\mathring{A})$ considering the volume available per atom. However, in the ordered state it is possible for the atoms to arrange themselves in one of the atomic arrangements (namely, sc, bcc, fcc and hcp) or in a mixed state. For simplicity, if we assume the arrangement to be sc, bcc, fcc or hcp, we get four possible values of d; note that the sc arrangement has been used by Jain's whose results have been summed up in the above discussion. For all cases minimum value of inter particle separation i.e. σ remains same because it is obtained from maxon position, Q_{max} (see figure 4.1). We obtain the minimum value of C from equation 4.5 using experimental value of the first sound velocity (i.e. $238.21\, m/sec$) in $Q \rightarrow 0$ limit while maximum value of $C(Q)$ is obtained from the same relation using maxon energy $E_{max} = 13.78K$. Maxon postion $Q_{max} = 1.105\mathring{A}^{-1}$ is used to fix the value of $\sigma = 2.8442\mathring{A}$. (All experimental values are used from ref [24].) To calculate the maximum value of inter particle separation i.e. $d(Q = 0)$, we use density of LHE-4, $\rho = 0.14513\, gm/cc$ [39]. We have presented the values of these parameters for different atomic arrangements in Table-4.1. Values of $d(Q)$ and $C(Q)$ at different Q have been obtained by employing above mentioned parameters in equations 4.9 and 4.10 while $E(Q)$ has been estimated using corresponding $d(Q)$ and $C(Q)$ in equation 4.5. From these energies we have calculated the phase velocity using the relation $V_p = E_{ph}(Q)/\hbar Q$ while group velocity $(= \frac{\partial E_{ph}(Q)}{\hbar \partial Q})$ is obtained by calculating energies at $Q \pm 0.00001$. We have tabulated our estimated values of energy, phase velocity and group velocity for different atomic arrangements along with the experiments in Tables 4.2 to 4.5. We also depict our findings in figures 4.2 to 4.5.

In the above estimation it is assumed that $d(Q)$ and $C(Q)$ change smoothly up to $Q = Q_{max}$ beyond which it becomes Q independent. However, $d(Q)$ and $C(Q)$ may attain their saturation values at a lower Q resulting a change in the dispersion curve. We have studied this effect considering three such values of Q namely: 0.70, 0.90 and 1.105$\mathring{A}^{-1}$. We presents our results in Tabels 4.6 to 4.9 and in figures 4.6 to 4.9. The set of parameters used to calculate $d(Q)$ and $C(Q)$ are same as Table 4.1.

Next, we have used a different approach to calculate the Q dependence of $d(Q)$ and $C(Q)$. Short life time of the excited state indicates a strong interaction between the particles in their excited state implying decrease in inter particle separation which is evident from the fact that wave packet size of particles decreases with increasing energy and the particles can come closer to each other. Therefore, d must decrease with the population in the excited state which is proportional to $\exp(-E(Q)/k_BT)$ where k_B is the Boltzmann constant and T is the temperature. Consequently we have

$$d(Q) = d_o + d' \exp(-Q^2/a) \tag{4.11}$$

and

$$C(Q) = C_o + C' \left[1 - \exp(-Q^2/a)\right] \tag{4.12}$$

to calculate $d(Q)$ and $C(Q)$ at different Q where $a = 0.18\mathring{A}^{-2}$. This set of relations yields energy which matches closely with the experiments and we get an anomalous dispersion region extended up to $\approx 0.45\mathring{A}^{-1}$ while equations 4.9 and 4.10 reveal it to be around $0.25\mathring{A}^{-1}$. This aspect of our findings is evident from the figures 4.10 to 4.13. We have presented our results in Tables 4.10-4.13 along with the experimental values for comparison. For clarity we identify the calculations based on equations 4.9 and 4.10 as model A and those based on equations 4.11 and 4.12 as model B.

4.4 Discussion

Several theoretical and empirical relations have been proposed to fit the NIS data in low Q range and reviewed briefly by Maris [27] and Dynes and Narayanamurty [32]. However, these relations are not consistent with each other in the sense that there is no general agreement on the functional form or the magnitude of the dispersion. Moreover, the parameters of these relations are not fitted

to both the neutron scattering data and data obtained from other sources (e.g. specific heat at low temperature or sound velocity measurement *etc.*). Different values of the same parameter have been proposed from time to time to fit different sets of experimental data.

First dispersion relation, that was of Landau [1, 3], did not predict any anomalous nature of the dispersion curve. Later, Landau and Khalatnikov [40] proposed a dispersion relation for excitation in superfluid helium in the form

$$E(Q)^2 = A_1Q^2 + A_2Q^4 + A_3Q^6 + A_4Q^8 \tag{4.13}$$

They showed that this could explain the whole dispersion curve including roton region provided the values of A's are calculated by imposing suitable conditions. For phonon of small Q equation 4.13 gives

$$E(Q) = c_oQ\left(1 + \gamma Q^2 + \ldots\right) \tag{4.14}$$

with $\gamma = -0.311\mathring{A}^2$ and $c_o = 2.383 \times 10^4 cm/sec.$ However, Maris [27] has pointed out that there is no theoretical basis for the equation 4.14. Moreover, the viscosity of the normal fluid calculated by Landau and Khalatnikov using this value of γ did not agree even qualitatively with its value measured by Whitworth [41]. Later, Khaltanikov [42] proposed a different value of γ $(= -0.0017\mathring{A}^2)$ to explain the sound absorption and experimental results of Chase and Herlin [43]. However, a series of later experiments posed serious problem to this value too. These difficulties led Maris and Massey [44] to propose that γ is a positive quantity which are supported by the specific heat measurements by Phillips *et al* who found $\gamma = 0.3782\mathring{A}^2$ whereas a later analysis of Maris [45] estimated a value $\simeq 0.72\mathring{A}^2$.

Neutron scattering data of Woods and Cowley [38], which were later considered to be quite inaccurate, revealed a dispersion relation

$$E = \hbar c_oQ\left(1 + \gamma Q^2 - \delta Q^4\right) \tag{4.15}$$

with $\gamma = 0 \pm 0.02\mathring{A}^2$ and $\delta = 0.30 \pm 0.02\mathring{A}^4$, an indication of a normal dispersion. To fit the more accurate neutron scattering data, Maris [45] proposed a functional form

$$E = \hbar c_oQ\left[1 + \gamma Q^2\frac{1 - Q^2/Q_A^2}{1 + Q^2/Q_B^2}\right] \tag{4.16}$$

with $\gamma = 1.112\mathring{A}^2$, $Q_A = 0.5418\mathring{A}^{-1}$, $Q_B = 0.3322\mathring{A}^{-1}$ and $c_o = 2.383 \times 10^4\, cm/sec.$ For small Q this relation becomes

$$E = \hbar c_oQ\left(1 + \gamma Q^2\right) \tag{4.17}$$

and for Q much greater than Q_A and Q_B

$$E = \hbar c_o Q \left[\left(1 + \gamma Q_B^2\right) - \left(\gamma Q_B^2 / Q_A^2\right) Q^2 \right] \tag{4.18}$$

This provides a good fit to both the specific heat and the neutron scattering data. Brooks and Donnelly [46] proposed a relation

$$E = c_o \hbar Q \left(1 + a_3 Q^2 + a_4 Q^3 + a_5 Q^4 + a_6 Q^5 + a_7 Q^6 + a_8 Q^7\right) \tag{4.19}$$

that contains terms up to eighth power of Q except the quadratic term. This expression gives a better fit to entire dispersion relation including the roton region. Molinari and Regge [47] included the quadratic term and proposed a relation in the form of

$$E = c_o \hbar Q \left(1 + \alpha_1 Q + \alpha_2 Q + \ldots\right) \tag{4.20}$$

to get a good fit to the specific heat and neutron scattering data. While the sound velocity measurement by Anderson and Sabisky [48] on helium film confirms Molinari and Regge's findings, experiment by Roach *et al* [49] concludes that the coefficient of quadratic term is small ($|\alpha_1| \leq 0.01 \mathring{A}$) and hence, can be omitted from the dispersion relation.

Dispersion relation in Macro-orbital theory is based on different footings [36]. In the superfluid state the closed packed arrangement of the wavepackets gives a dispersion relation that is similar to the elastic wave in mono-atomic 1-D chain in crystalline solid. The only difference is the inter atomic separation which is constant for solid due to its strong attractive inter molecular forces whereas in liquid helium, where inter molecular forces are relatively weak, it varies with Q. This also explains why longitudinal mode is the lone possible mode of excitation in the system. Though the dispersion relation of Macro-orbital theory seems to be different, it reduces to familiar functional form in the low Q range. In the low Q range a choice for the equations 4.9 and 4.10 (model A) gives a functional form similar to Molinari and Regge [47] with $\alpha_1 \sim 0.302 \mathring{A}$ and $\alpha_2 \sim -0.6976 \mathring{A}^2$ while Molinari and Regge's relation yields $\alpha_1 = 0.2733 \mathring{A}$ and $\alpha_2 = -0.7138 \mathring{A}^2$ [27]. On the other hand if the equations 4.11 and 4.12 are used for Q dependence of d and C (model B), dispersion relation in the low Q range reduces closely to that obtained by Maris and Massey's [23] (equation 4.15). While we have $\gamma = 1.6956 \mathring{A}^2$, they find $\gamma = 1.112 \mathring{A}^2$.

4.5 Conclusion

Our results show that Macro-orbital theory is the lone theory of LHE-4 developed within the scope of microscopic framework which yields an excitation spectrum that closely agrees with experiments and clearly provides the origin of its anomalous nature. Our calculation starts with the orderly arrangement of the atoms in the system as proposed in Macro-orbital theory and the fact that our results agree with experiments provides strong foundation to this consideration. Further the fact that our results for fcc or hcp agree more closely with the experiments indicate that the helium atoms in LHE-4 prefer to have these arrangements in comparison to sc or bcc. Anomalous nature of the dispersion originates due to the change in inter particle distance with Q. While Macro-orbital theory shows the existence of an orderly arrangement of the atoms in the system for $T < T_\lambda$, for $T > T_\lambda$ atoms are randomly distributed. This explains why "one phonon" excitations disappear at T_λ.

Table 4.1: Different Parameters (equations 4.8 and 4.9) for sc, bcc, fcc and hcp arrangements

	sc	bcc	fcc	hcp
$d_{max}\,(\mathring{A})$	3.5776	3.9036	4.0157	4.0157
$\sigma\,(\mathring{A})$	2.8442	2.8442	2.8442	2.8442
$d_o\,(\mathring{A})$	3.5776	3.9036	4.0157	4.0157
$d'\,(\mathring{A})$	-0.7334	-1.0594	-1.1715	-1.1715
$C_{max}\,(dynes/cm)$	5.4067	5.4067	5.4067	5.4067
$C_o\,(dynes/cm)$	2.9462	2.4747	2.3384	2.3384
$C\prime\,(dynes/cm)$	2.4604	2.9320	3.0683	3.0683
$Q_{max}\,(\mathring{A}^{-1})$	1.105	1.105	1.105	1.105

Table 4.2: E(Q), V_p and V_g for sc arrangement

Q	E(Q)		V_p		V_g	
$\AA^{-1}$	K		m/sec		m/sec	
	Expt	Theory	Expt	Theory	Expt	Theory
0.00	0.00	0.00	238.21	238.21	238.21	238.21
0.05	0.91	0.92	238.78	241.29	239.79	243.85
0.10	1.84	1.86	240.51	243.37	245.44	246.62
0.15	2.79	2.80	243.28	244.49	251.64	246.49
0.20	3.76	3.74	245.80	244.73	254.60	244.11
0.25	4.73	4.66	247.59	244.15	254.31	239.41
0.30	5.69	5.56	248.46	242.84	250.79	232.71
0.35	6.64	6.44	248.35	240.85	244.02	224.68
0.40	7.55	7.28	247.21	238.27	234.01	215.15
0.45	8.42	8.08	245.04	235.16	220.77	205.12
0.50	9.24	8.84	241.82	231.58	204.28	193.59
0.55	9.98	9.56	237.56	227.59	185.69	181.55
0.60	10.65	10.23	232.47	223.23	167.34	169.01
0.65	11.26	10.85	226.76	218.54	149.32	154.97
0.70	11.80	11.42	220.60	213.55	131.62	141.93
0.75	12.26	11.93	214.08	208.29	114.23	127.39
0.80	12.67	12.39	207.31	202.76	97.16	112.34
0.85	13.01	12.79	200.33	196.98	80.42	96.79
0.90	13.28	13.13	193.21	190.95	63.99	80.24
0.95	13.50	13.40	185.99	184.65	47.88	62.19
1.00	13.65	13.60	178.69	178.07	32.09	43.13
1.05	13.74	13.73	171.34	171.19	16.62	23.07
1.10	13.78	13.78	163.96	163.99	1.47	2.01
1.15	13.75	13.75	156.57	156.54	-13.36	-16.05
1.20	13.68	13.65	149.19	148.95	-27.87	-35.11
1.25	13.54	13.49	141.82	141.24	-42.07	-53.16
1.30	13.35	13.25	134.48	133.44	-55.94	-71.22

Table 4.3: E(Q), V_p and V_g for bcc arrangement

Q	E(Q)		V_p		V_g	
$\AA^{-1}$	K		m/sec		m/sec	
	Expt	Theory	Expt	Theory	Expt	Theory
0.00	0.00	0.00	238.21	238.21	238.21	238.21
0.05	0.91	0.93	238.78	242.88	239.79	246.80
0.10	1.84	1.88	240.51	246.08	245.44	251.14
0.15	2.79	2.84	243.28	247.93	251.64	251.51
0.20	3.76	3.80	245.80	248.56	254.60	248.63
0.25	4.73	4.74	247.59	248.10	254.31	243.42
0.30	5.69	5.65	248.46	246.67	250.79	235.47
0.35	6.64	6.53	248.35	244.42	244.02	226.19
0.40	7.55	7.38	247.21	241.47	234.01	215.15
0.45	8.42	8.18	245.04	237.91	220.77	203.62
0.50	9.24	8.93	241.82	233.86	204.28	191.08
0.55	9.98	9.64	237.56	229.40	185.69	178.54
0.60	10.65	10.29	232.47	224.60	167.34	165.00
0.65	11.26	10.90	226.76	219.52	149.32	151.96
0.70	11.80	11.45	220.60	214.19	131.62	138.42
0.75	12.26	11.95	214.08	208.66	114.23	124.38
0.80	12.67	12.40	207.31	202.94	97.16	109.83
0.85	13.01	12.79	200.33	197.03	80.42	94.79
0.90	13.28	13.13	193.21	190.92	63.99	78.24
0.95	13.50	13.40	185.99	184.60	47.88	62.19
1.00	13.65	13.60	178.69	178.03	32.09	44.13
1.05	13.74	13.73	171.34	171.17	16.62	24.07
1.10	13.78	13.78	163.96	163.99	1.47	2.01
1.15	13.75	13.75	156.57	156.54	-13.36	-16.05
1.20	13.68	13.65	149.19	148.95	-27.87	-35.11
1.25	13.54	13.49	141.82	141.24	-42.07	-53.16
1.30	13.35	13.25	134.48	133.44	-55.94	-71.22

Table 4.4: E(Q), V_p and V_g for fcc arrangement

Q	E(Q)		V_p		V_g	
$\AA^{-1}$	K		m/sec		m/sec	
	Expt	Theory	Expt	Theory	Expt	Theory
0.00	0.00	0.00	238.21	238.21	238.21	238.21
0.05	0.91	0.93	238.78	243.51	239.79	247.94
0.10	1.84	1.89	240.51	247.16	245.44	252.90
0.15	2.79	2.86	243.28	249.29	251.64	253.52
0.20	3.76	3.82	245.80	250.07	254.60	250.63
0.25	4.73	4.77	247.59	249.64	254.31	244.93
0.30	5.69	5.69	248.46	248.18	250.79	236.22
0.35	6.64	6.57	248.35	245.83	244.02	226.69
0.40	7.55	7.42	247.21	242.72	234.01	215.66
0.45	8.42	8.22	245.04	239.00	220.77	203.12
0.50	9.24	8.97	241.82	234.77	204.28	190.58
0.55	9.98	9.67	237.56	230.13	185.69	177.04
0.60	10.65	10.32	232.47	225.16	167.34	164.00
0.65	11.26	10.92	226.76	219.93	149.32	149.96
0.70	11.80	11.47	220.60	214.48	131.62	136.42
0.75	12.26	11.96	214.08	208.84	114.23	123.38
0.80	12.67	12.41	207.31	203.04	97.16	108.83
0.85	13.01	12.80	200.33	197.07	80.42	94.29
0.90	13.28	13.13	193.21	190.93	63.99	78.24
0.95	13.50	13.40	185.99	184.59	47.88	62.19
1.00	13.65	13.60	178.69	178.02	32.09	43.13
1.05	13.74	13.73	171.34	171.17	16.62	24.07
1.10	13.78	13.78	163.96	163.99	1.47	2.01
1.15	13.75	13.75	156.57	156.54	-13.36	-16.05
1.20	13.68	13.65	149.19	148.95	-27.87	-35.11
1.25	13.54	13.49	141.82	141.24	-42.07	-53.16
1.30	13.35	13.25	134.48	133.44	-55.94	-71.22

Table 4.5: E(Q), V_p and V_g for hcp arrangement

Q	E(Q)		V_p		V_p	
$\AA^{-1}$	K		m/sec		m/sec	
	Expt	Theory	Expt	Theory	Expt	Theory
0.00	0.00	0.00	238.21	238.21	238.21	238.21
0.05	0.91	0.93	238.78	243.51	239.79	247.94
0.10	1.84	1.89	240.51	247.16	245.44	252.90
0.15	2.79	2.86	243.28	249.29	251.64	253.52
0.20	3.76	3.82	245.80	250.07	254.60	250.63
0.25	4.73	4.77	247.59	249.64	254.31	244.93
0.30	5.69	5.69	248.46	248.18	250.79	236.22
0.35	6.64	6.57	248.35	245.83	244.02	226.69
0.40	7.55	7.42	247.21	242.72	234.01	215.66
0.45	8.42	8.22	245.04	239.00	220.77	203.12
0.50	9.24	8.97	241.82	234.77	204.28	190.58
0.55	9.98	9.67	237.56	230.13	185.69	177.04
0.60	10.65	10.32	232.47	225.16	167.34	164.00
0.65	11.26	10.92	226.76	219.93	149.32	149.96
0.70	11.80	11.47	220.60	214.48	131.62	136.42
0.75	12.26	11.96	214.08	208.84	114.23	123.38
0.80	12.67	12.41	207.31	203.04	97.16	108.83
0.85	13.01	12.80	200.33	197.07	80.42	94.29
0.90	13.28	13.13	193.21	190.93	63.99	78.24
0.95	13.50	13.40	185.99	184.59	47.88	62.19
1.00	13.65	13.60	178.69	178.02	32.09	43.13
1.05	13.74	13.73	171.34	171.17	16.62	24.07
1.10	13.78	13.78	163.96	163.99	1.47	2.01
1.15	13.75	13.75	156.57	156.54	-13.36	-16.05
1.20	13.68	13.65	149.19	148.95	-27.87	-35.11
1.25	13.54	13.49	141.82	141.24	-42.07	-53.16
1.30	13.35	13.25	134.48	133.44	-55.94	-71.22

Table 4.6: E(Q) for sc arrangement for different Q_{max} (in $\AA^{-1}$)

Q	Expt.	$Q_{max} = 1.105$	$Q_{max} = 0.90$	$Q_{max} = 0.70$
$\AA^{-1}$	K	K	K	K
0.00	0.00	0.00	0.00	0.00
0.05	0.91	0.92	0.92	0.93
0.10	1.84	1.86	1.87	1.88
0.15	2.79	2.80	2.82	2.84
0.20	3.76	3.74	3.77	3.80
0.25	4.73	4.66	4.70	4.74
0.30	5.69	5.56	5.61	5.66
0.35	6.64	6.44	6.49	6.54
0.40	7.55	7.28	7.34	7.39
0.45	8.42	8.08	8.15	8.20
0.50	9.24	8.84	8.92	8.97
0.55	9.98	9.56	9.64	9.70
0.60	10.65	10.23	10.32	10.37
0.65	11.26	10.85	10.94	11.00
0.70	11.80	11.42	11.52	11.56
0.75	12.26	11.93	12.03	12.07
0.80	12.67	12.39	12.49	12.51
0.85	13.01	12.79	12.88	12.89
0.90	13.28	13.13	13.20	13.20
0.95	13.50	13.40	13.45	13.45
1.00	13.65	13.60	13.63	13.63
1.05	13.74	13.73	13.74	13.74
1.10	13.78	13.78	13.78	13.78
1.15	13.75	13.75	13.75	13.75
1.20	13.68	13.65	13.65	13.65
1.25	13.54	13.49	13.49	13.49
1.30	13.35	13.25	13.25	13.25

Table 4.7: V_p and V_g for sc arrangement for different Q_{max} (in $\mathring{A}^{-1}$)

	Expt.		Theory					
			$Q_{max} = 1.105$		$Q_{max} = 0.90$		$Q_{max} = 0.70$	
Q	V_p	V_g	V_p	V_g	V_p	V_g	V_p	V_g
$\mathring{A}^{-1}$	m/sec	m/sec	m/sec	m/sec	m/sec	m/sec	m/sec	m/sec
0.00	238.21	238.21	238.21	238.21	238.21	238.21	238.21	238.21
0.05	238.78	239.79	241.29	243.85	242.01	245.17	243.07	247.12
0.10	240.51	245.44	243.37	246.62	244.61	248.63	246.37	251.51
0.15	243.28	251.64	244.49	246.49	246.09	249.00	248.24	251.89
0.20	245.80	254.60	244.73	244.11	246.56	246.37	248.85	248.88
0.25	247.59	254.31	244.15	239.41	246.10	241.66	248.37	243.67
0.30	248.46	250.79	242.84	232.71	244.82	234.97	246.96	235.72
0.35	248.35	244.02	240.85	224.68	242.83	226.69	244.78	227.19
0.40	247.21	234.01	238.27	215.15	240.22	217.16	241.98	217.16
0.45	245.04	220.77	235.16	205.12	237.07	206.63	238.66	206.13
0.50	241.82	204.28	231.58	193.59	233.46	195.09	234.91	195.60
0.55	237.56	185.69	227.59	181.55	229.44	182.56	230.79	184.06
0.60	232.47	167.34	223.23	169.01	225.07	170.52	226.31	170.52
0.65	226.76	149.32	218.54	154.97	220.37	157.48	221.47	155.97
0.70	220.60	131.62	213.55	141.93	215.35	142.94	216.22	139.42
0.75	214.08	114.23	208.29	127.39	210.03	127.89	210.60	123.88
0.80	207.31	97.16	202.76	112.34	204.39	111.34	204.68	107.33
0.85	200.33	80.42	196.98	96.79	198.40	93.28	198.48	91.28
0.90	193.21	63.99	190.95	80.24	192.02	73.22	192.02	73.22
0.95	185.99	47.88	184.65	62.19	185.32	56.17	185.32	56.17
1.00	178.69	32.09	178.07	43.13	178.41	38.12	178.41	38.12
1.05	171.34	16.62	171.19	23.07	171.29	19.06	171.29	19.06
1.10	163.96	1.47	163.99	2.01	163.99	1.00	163.99	1.00
1.15	156.57	-13.36	156.54	-16.05	156.54	-16.05	156.54	-16.05
1.20	149.19	-27.87	148.95	-35.11	148.95	-35.11	148.95	-35.11
1.25	141.82	-42.07	141.24	-53.16	141.24	-53.16	141.24	-53.16
1.30	134.48	-55.94	133.44	-71.22	133.44	-71.22	133.44	-71.22

Table 4.8: E(Q) for bcc arrangement for different Q_{max} (in $\mathring{A}^{-1}$)

Q	Expt.	$Q_{max} = 1.105$	$Q_{max} = 0.90$	$Q_{max} = 0.70$
$\mathring{A}^{-1}$	K	K	K	K
0.00	0.00	0.00	0.00	0.00
0.05	0.91	0.93	0.93	0.94
0.10	1.84	1.88	1.89	1.91
0.15	2.79	2.84	2.87	2.90
0.20	3.76	3.80	3.83	3.87
0.25	4.73	4.74	4.78	4.83
0.30	5.69	5.65	5.70	5.75
0.35	6.64	6.53	6.59	6.63
0.40	7.55	7.38	7.43	7.47
0.45	8.42	8.18	8.24	8.26
0.50	9.24	8.93	8.99	9.01
0.55	9.98	9.64	9.70	9.72
0.60	10.65	10.29	10.36	10.38
0.65	11.26	10.90	10.97	11.00
0.70	11.80	11.45	11.53	11.56
0.75	12.26	11.95	12.04	12.07
0.80	12.67	12.40	12.49	12.51
0.85	13.01	12.79	12.88	12.89
0.90	13.28	13.13	13.20	13.20
0.95	13.50	13.40	13.45	13.45
1.00	13.65	13.60	13.63	13.63
1.05	13.74	13.73	13.74	13.74
1.10	13.78	13.78	13.78	13.78
1.15	13.75	13.75	13.75	13.75
1.20	13.68	13.65	13.65	13.65
1.25	13.54	13.49	13.49	13.49
1.30	13.35	13.25	13.25	13.25

Table 4.9: V_p and V_g for bcc arrangement for different Q_{max} in ($\mathring{A}^{-1}$)

	Expt.		Theory					
			$Q_{max} = 1.105$		$Q_{max} = 0.90$		$Q_{max} = 0.70$	
Q	V_p	V_g	V_p	V_g	V_p	V_g	V_p	V_g
$\mathring{A}^{-1}$	m/sec	m/sec	m/sec	m/sec	m/sec	m/sec	m/sec	m/sec
0.00	238.21	238.21	238.21	238.21	238.21	238.21	238.21	238.21
0.05	238.78	239.79	242.88	246.80	243.92	248.69	245.45	251.39
0.10	240.51	245.44	246.08	251.14	247.81	253.90	250.20	257.42
0.15	243.28	251.64	247.93	251.51	250.06	254.53	252.78	257.54
0.20	245.80	254.60	248.56	248.63	250.85	251.64	253.52	253.15
0.25	247.59	254.31	248.10	243.42	250.39	245.43	252.75	245.68
0.30	248.46	250.79	246.67	235.47	248.86	236.97	250.79	235.72
0.35	248.35	244.02	244.42	226.19	246.45	226.69	247.91	225.19
0.40	247.21	234.01	241.47	215.15	243.31	215.66	244.35	213.65
0.45	245.04	220.77	237.91	203.62	239.60	204.12	240.32	202.12
0.50	241.82	204.28	233.86	191.08	235.42	191.58	235.95	190.58
0.55	237.56	185.69	229.40	178.54	230.88	179.05	231.35	179.55
0.60	232.47	167.34	224.60	165.00	226.05	167.01	226.54	167.51
0.65	226.76	149.32	219.52	151.96	220.98	153.47	221.52	154.47
0.70	220.60	131.62	214.19	138.42	215.69	140.43	216.22	139.42
0.75	214.08	114.23	208.66	124.38	210.18	125.88	210.60	123.88
0.80	207.31	97.16	202.94	109.83	204.44	110.34	204.68	107.33
0.85	200.33	80.42	197.03	94.79	198.40	92.28	198.48	91.28
0.90	193.21	63.99	190.92	78.24	192.02	73.22	192.02	73.22
0.95	185.99	47.88	184.60	62.19	185.32	56.17	185.32	56.17
1.00	178.69	32.09	178.03	44.13	178.41	38.12	178.41	38.12
1.05	171.34	16.62	171.17	24.07	171.29	19.06	171.29	19.06
1.10	163.96	1.47	163.99	2.01	163.99	1.00	163.99	1.00
1.15	156.57	-13.36	156.54	-16.05	156.54	-16.05	156.54	-16.05
1.20	149.19	-27.87	148.95	-35.11	148.95	-35.11	148.95	-35.11
1.25	141.82	-42.07	141.24	-53.16	141.24	-53.16	141.24	-53.16
1.30	134.48	-55.94	133.44	-71.22	133.44	-71.22	133.44	-71.22

Table 4.10: E(Q) for fcc arrangement for different Q_{max} (in $\mathring{A}^{-1}$)

Q	Expt.	$Q_{max} = 1.105$	$Q_{max} = 0.90$	$Q_{max} = 0.70$
$\mathring{A}^{-1}$	K	K	K	K
0.00	0.00	0.00	0.00	0.00
0.05	0.91	0.93	0.93	0.94
0.10	1.84	1.89	1.90	1.92
0.15	2.79	2.86	2.88	2.92
0.20	3.76	3.82	3.86	3.90
0.25	4.73	4.77	4.81	4.86
0.30	5.69	5.69	5.74	5.78
0.35	6.64	6.57	6.63	6.66
0.40	7.55	7.42	7.47	7.49
0.45	8.42	8.22	8.27	8.28
0.50	9.24	8.97	9.02	9.03
0.55	9.98	9.67	9.72	9.73
0.60	10.65	10.32	10.38	10.39
0.65	11.26	10.92	10.98	11.00
0.70	11.80	11.47	11.54	11.56
0.75	12.26	11.96	12.05	12.07
0.80	12.67	12.41	12.49	12.51
0.85	13.01	12.80	12.88	12.89
0.90	13.28	13.13	13.20	13.20
0.95	13.50	13.40	13.45	13.45
1.00	13.65	13.60	13.63	13.63
1.05	13.74	13.73	13.74	13.74
1.10	13.78	13.78	13.78	13.78
1.15	13.75	13.75	13.75	13.75
1.20	13.68	13.65	13.65	13.65
1.25	13.54	13.49	13.49	13.49
1.30	13.35	13.25	13.25	13.25

Table 4.11: V_p and V_g for fcc arrangement for different Q_{max} (in $\mathring{A}^{-1}$)

	Expt.		Theory					
			$Q_{max} = 1.105$		$Q_{max} = 0.90$		$Q_{max} = 0.70$	
Q	V_p	V_g	V_p	V_g	V_p	V_g	V_p	V_g
$\mathring{A}^{-1}$	m/sec	m/sec	m/sec	m/sec	m/sec	m/sec	m/sec	m/sec
0.00	238.21	238.21	238.21	238.21	238.21	238.21	238.21	238.21
0.05	238.78	239.79	243.51	247.94	244.68	250.07	246.39	253.15
0.10	240.51	245.44	247.16	252.90	249.07	255.91	251.70	259.68
0.15	243.28	251.64	249.29	253.52	251.61	256.66	254.55	259.80
0.20	245.80	254.60	250.07	250.63	252.53	253.15	255.33	254.90
0.25	247.59	254.31	249.64	244.93	252.06	246.68	254.45	246.43
0.30	248.46	250.79	248.18	236.22	250.44	237.72	252.27	236.22
0.35	248.35	244.02	245.83	226.69	247.86	227.19	249.11	224.68
0.40	247.21	234.01	242.72	215.66	244.52	214.65	245.27	212.65
0.45	245.04	220.77	239.00	203.12	240.59	202.62	240.96	200.61
0.50	241.82	204.28	234.77	190.58	236.20	190.08	236.36	190.08
0.55	237.56	185.69	230.13	177.04	231.46	177.54	231.57	177.54
0.60	232.47	167.34	225.16	164.00	226.45	165.50	226.63	166.51
0.65	226.76	149.32	219.93	149.96	221.24	152.46	221.54	153.97
0.70	220.60	131.62	214.48	136.42	215.84	138.92	216.22	139.42
0.75	214.08	114.23	208.84	123.38	210.25	125.38	210.60	123.88
0.80	207.31	97.16	203.04	108.83	204.46	110.34	204.68	107.33
0.85	200.33	80.42	197.07	94.29	198.41	93.28	198.48	91.28
0.90	193.21	63.99	190.93	78.24	192.02	73.22	192.02	73.22
0.95	185.99	47.88	184.59	62.19	185.32	56.17	185.32	56.17
1.00	178.69	32.09	178.02	43.13	178.41	38.12	178.41	38.12
1.05	171.34	16.62	171.17	24.07	171.29	19.06	171.29	19.06
1.10	163.96	1.47	163.99	2.01	163.99	1.00	163.99	1.00
1.15	156.57	-13.36	156.54	-16.05	156.54	-16.05	156.54	-16.05
1.20	149.19	-27.87	148.95	-35.11	148.95	-35.11	148.95	-35.11
1.25	141.82	-42.07	141.24	-53.16	141.24	-53.16	141.24	-53.16
1.30	134.48	-55.94	133.44	-71.22	133.44	-71.22	133.44	-71.22

Table 4.12: E(Q) for hcp arrangement for different Q_{max} (in $\AA^{-1}$)

Q	Expt.	$Q_{max} = 1.105$	$Q_{max} = 0.90$	$Q_{max} = 0.70$
$\AA^{-1}$	K	K	K	K
0.00	0.00	0.00	0.00	0.00
0.05	0.91	0.93	0.93	0.94
0.10	1.84	1.89	1.90	1.92
0.15	2.79	2.86	2.88	2.92
0.20	3.76	3.82	3.86	3.90
0.25	4.73	4.77	4.81	4.86
0.30	5.69	5.69	5.74	5.78
0.35	6.64	6.57	6.63	6.66
0.40	7.55	7.42	7.47	7.49
0.45	8.42	8.22	8.27	8.28
0.50	9.24	8.97	9.02	9.03
0.55	9.98	9.67	9.72	9.73
0.60	10.65	10.32	10.38	10.39
0.65	11.26	10.92	10.98	11.00
0.70	11.80	11.47	11.54	11.56
0.75	12.26	11.96	12.05	12.07
0.80	12.67	12.41	12.49	12.51
0.85	13.01	12.80	12.88	12.89
0.90	13.28	13.13	13.20	13.20
0.95	13.50	13.40	13.45	13.45
1.00	13.65	13.60	13.63	13.63
1.05	13.74	13.73	13.74	13.74
1.10	13.78	13.78	13.78	13.78
1.15	13.75	13.75	13.75	13.75
1.20	13.68	13.65	13.65	13.65
1.25	13.54	13.49	13.49	13.49
1.30	13.35	13.25	13.25	13.25

Table 4.13: V_p and V_g for hcp arrangement for different Q_{max} (in $\mathring{A}^{-1}$)

	Expt.		Theory					
			$Q_{max} = 1.105$		$Q_{max} = 0.90$		$Q_{max} = 0.70$	
Q	V_p	V_g	V_p	V_g	V_p	V_g	V_p	V_g
$\mathring{A}^{-1}$	m/sec	m/sec	m/sec	m/sec	m/sec	m/sec	m/sec	m/sec
0.00	238.21	238.21	238.21	238.21	238.21	238.21	238.21	238.21
0.05	238.78	239.79	243.51	247.94	244.68	250.07	246.39	253.15
0.10	240.51	245.44	247.16	252.90	249.07	255.91	251.70	259.68
0.15	243.28	251.64	249.29	253.52	251.61	256.66	254.55	259.80
0.20	245.80	254.60	250.07	250.63	252.53	253.15	255.33	254.90
0.25	247.59	254.31	249.64	244.93	252.06	246.68	254.45	246.43
0.30	248.46	250.79	248.18	236.22	250.44	237.72	252.27	236.22
0.35	248.35	244.02	245.83	226.69	247.86	227.19	249.11	224.68
0.40	247.21	234.01	242.72	215.66	244.52	214.65	245.27	212.65
0.45	245.04	220.77	239.00	203.12	240.59	202.62	240.96	200.61
0.50	241.82	204.28	234.77	190.58	236.20	190.08	236.36	190.08
0.55	237.56	185.69	230.13	177.04	231.46	177.54	231.57	177.54
0.60	232.47	167.34	225.16	164.00	226.45	165.50	226.63	166.51
0.65	226.76	149.32	219.93	149.96	221.24	152.46	221.54	153.97
0.70	220.60	131.62	214.48	136.42	215.84	138.92	216.22	139.42
0.75	214.08	114.23	208.84	123.38	210.25	125.38	210.60	123.88
0.80	207.31	97.16	203.04	108.83	204.46	110.34	204.68	107.33
0.85	200.33	80.42	197.07	94.29	198.41	93.28	198.48	91.28
0.90	193.21	63.99	190.93	78.24	192.02	73.22	192.02	73.22
0.95	185.99	47.88	184.59	62.19	185.32	56.17	185.32	56.17
1.00	178.69	32.09	178.02	43.13	178.41	38.12	178.41	38.12
1.05	171.34	16.62	171.17	24.07	171.29	19.06	171.29	19.06
1.10	163.96	1.47	163.99	2.01	163.99	1.00	163.99	1.00
1.15	156.57	-13.36	156.54	-16.05	156.54	-16.05	156.54	-16.05
1.20	149.19	-27.87	148.95	-35.11	148.95	-35.11	148.95	-35.11
1.25	141.82	-42.07	141.24	-53.16	141.24	-53.16	141.24	-53.16
1.30	134.48	-55.94	133.44	-71.22	133.44	-71.22	133.44	-71.22

Table 4.14: Different Parameters (Equations 4.11 and 4.12) for sc, bcc, fcc and hcp arrangements

	sc	bcc	fcc	hcp
d_{max}	3.5776	3.9036	4.0157	4.0157
σ	2.8442	2.8442	2.8442	2.8442
d_o	2.8434	2.843	2.8429	2.8429
d'	0.7342	1.0606	1.1728	1.1728
C_{max}	5.4067	5.4067	5.4067	5.4067
C_o	2.9462	2.4747	2.3384	2.3384
$C\prime$	2.4632	2.9353	3.0717	3.0717
Q_{max}	1.105	1.105	1.105	1.105

Table 4.15: E(Q), V_p and V_g for sc arrangement

Q	E(Q)		V_g		V_p	
$\AA^{-1}$	K		m/sec		m/sec	
	Theory	Expt	Theory	Expt	Theory	Expt
0.00	0.00	0.00	238.21	238.21	238.21	238.21
0.05	0.91	0.91	239.33	239.79	238.58	238.78
0.10	1.83	1.84	241.85	245.44	239.58	240.51
0.15	2.76	2.79	244.48	251.64	240.84	243.28
0.20	3.70	3.76	245.61	254.60	241.95	245.80
0.25	4.63	4.73	243.67	254.31	242.53	247.59
0.30	5.55	5.69	238.23	250.79	242.32	248.46
0.35	6.45	6.64	230.70	244.02	241.23	248.35
0.40	7.31	7.55	220.67	234.01	239.29	247.21
0.45	8.13	8.42	209.64	220.77	236.59	245.04
0.50	8.91	9.24	196.60	204.28	233.25	241.82
0.55	9.64	9.98	184.06	185.69	229.38	237.56
0.60	10.31	10.65	171.02	167.34	225.06	232.47
0.65	10.94	11.26	156.48	149.32	220.35	226.76
0.70	11.51	11.80	141.93	131.62	215.28	220.60
0.75	12.02	12.26	126.38	114.23	209.88	214.08
0.80	12.48	12.67	110.34	97.16	204.14	207.31
0.85	12.86	13.01	92.78	80.42	198.10	200.33
0.90	13.18	13.28	75.23	63.99	191.77	193.21
0.95	13.44	13.50	57.17	47.88	185.17	185.99
1.00	13.62	13.65	39.12	32.09	178.32	178.69
1.05	13.74	13.74	21.06	16.62	171.25	171.34
1.10	13.78	13.78	2.01	1.47	163.99	163.96

Table 4.16: E(Q), V_p and V_g for bcc arrangement

Q	E(Q)		V_g		V_p	
$\AA^{-1}$	K		m/sec		m/sec	
	Theory	Expt	Theory	Expt	Theory	Expt
0.00	0.00	0.00	238.21	238.21	238.21	238.21
0.05	0.91	0.91	240.15	239.79	238.87	238.78
0.10	1.84	1.84	244.86	245.44	240.63	240.51
0.15	2.78	2.79	249.76	251.64	242.87	243.28
0.20	3.74	3.76	251.64	254.60	244.88	245.80
0.25	4.70	4.73	249.44	254.31	246.05	247.59
0.30	5.64	5.69	242.49	250.79	246.07	248.46
0.35	6.55	6.64	232.21	244.02	244.84	248.35
0.40	7.41	7.55	220.17	234.01	242.49	247.21
0.45	8.22	8.42	206.13	220.77	239.22	245.04
0.50	8.99	9.24	193.09	204.28	235.28	241.82
0.55	9.70	9.98	179.55	185.69	230.84	237.56
0.60	10.36	10.65	167.01	167.34	226.05	232.47
0.65	10.97	11.26	153.47	149.32	220.97	226.76
0.70	11.53	11.80	139.42	131.62	215.64	220.60
0.75	12.03	12.26	124.88	114.23	210.06	214.08
0.80	12.48	12.67	109.33	97.16	204.23	207.31
0.85	12.86	13.01	92.28	80.42	198.13	200.33
0.90	13.18	13.28	75.23	63.99	191.77	193.21
0.95	13.44	13.50	57.17	47.88	185.16	185.99
1.00	13.62	13.65	38.12	32.09	178.31	178.69
1.05	13.74	13.74	21.06	16.62	171.25	171.34
1.10	13.78	13.78	3.01	1.47	163.99	163.96

Table 4.17: E(Q), V_p and V_g for fcc arrangement

Q	E(Q)		V_g		V_p	
$\AA^{-1}$	K		m/sec		m/sec	
	Theory	Expt	Theory	Expt	Theory	Expt
0.00	0.00	0.00	238.21	238.21	238.21	238.21
0.05	0.91	0.91	240.46	239.79	238.99	238.78
0.10	1.84	1.84	245.99	245.44	241.05	240.51
0.15	2.79	2.79	251.64	251.64	243.68	243.28
0.20	3.76	3.76	253.90	254.60	246.04	245.80
0.25	4.73	4.73	251.45	254.31	247.45	247.59
0.30	5.67	5.69	243.74	250.79	247.54	248.46
0.35	6.58	6.64	232.71	244.02	246.25	248.35
0.40	7.45	7.55	219.17	234.01	243.74	247.21
0.45	8.26	8.42	205.12	220.77	240.26	245.04
0.50	9.02	9.24	191.58	204.28	236.08	241.82
0.55	9.72	9.98	177.54	185.69	231.43	237.56
0.60	10.38	10.65	165.00	167.34	226.45	232.47
0.65	10.98	11.26	151.96	149.32	221.23	226.76
0.70	11.54	11.80	138.42	131.62	215.79	220.60
0.75	12.04	12.26	123.38	114.23	210.14	214.08
0.80	12.48	12.67	108.33	97.16	204.27	207.31
0.85	12.87	13.01	91.78	80.42	198.15	200.33
0.90	13.18	13.28	75.23	63.99	191.77	193.21
0.95	13.44	13.50	57.17	47.88	185.16	185.99
1.00	13.62	13.65	39.12	32.09	178.31	178.69
1.05	13.74	13.74	21.06	16.62	171.25	171.34
1.10	13.78	13.78	2.01	1.47	163.99	163.96

Table 4.18: E(Q), V_p and V_g for hcp arrangement

Q	E(Q)		V_g		V_p	
$\AA^{-1}$	K		m/sec		m/sec	
	Theory	Expt	Theory	Expt	Theory	Expt
0.00	0.00	0.00	238.21	238.21	238.21	238.21
0.05	0.91	0.91	240.46	239.79	238.99	238.78
0.10	1.84	1.84	245.99	245.44	241.05	240.51
0.15	2.79	2.79	251.64	251.64	243.68	243.28
0.20	3.76	3.76	253.90	254.60	246.04	245.80
0.25	4.73	4.73	251.45	254.31	247.45	247.59
0.30	5.67	5.69	243.74	250.79	247.54	248.46
0.35	6.58	6.64	232.71	244.02	246.25	248.35
0.40	7.45	7.55	219.17	234.01	243.74	247.21
0.45	8.26	8.42	205.12	220.77	240.26	245.04
0.50	9.02	9.24	191.58	204.28	236.08	241.82
0.55	9.72	9.98	177.54	185.69	231.43	237.56
0.60	10.38	10.65	165.00	167.34	226.45	232.47
0.65	10.98	11.26	151.96	149.32	221.23	226.76
0.70	11.54	11.80	138.42	131.62	215.79	220.60
0.75	12.04	12.26	123.38	114.23	210.14	214.08
0.80	12.48	12.67	108.33	97.16	204.27	207.31
0.85	12.87	13.01	91.78	80.42	198.15	200.33
0.90	13.18	13.28	75.23	63.99	191.77	193.21
0.95	13.44	13.50	57.17	47.88	185.16	185.99
1.00	13.62	13.65	39.12	32.09	178.31	178.69
1.05	13.74	13.74	21.06	16.62	171.25	171.34
1.10	13.78	13.78	2.01	1.47	163.99	163.96

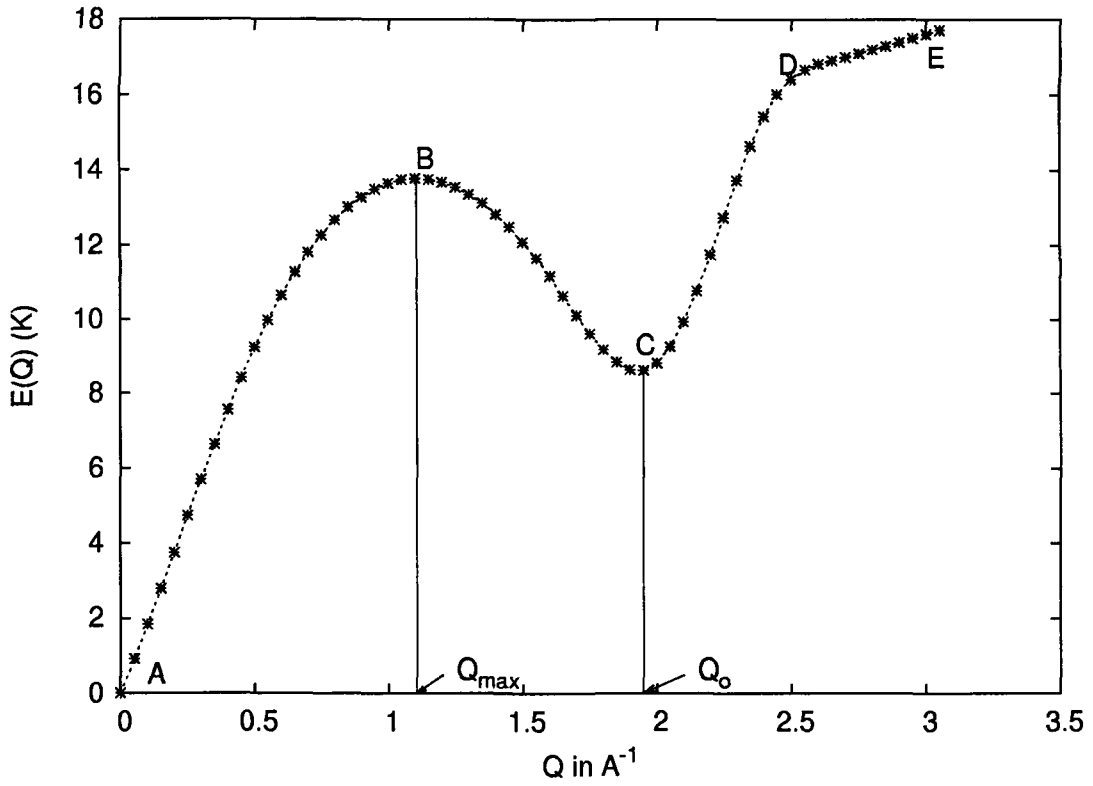

Figure 4.1: Elementary excitations spectrum of LHE-4 [24]

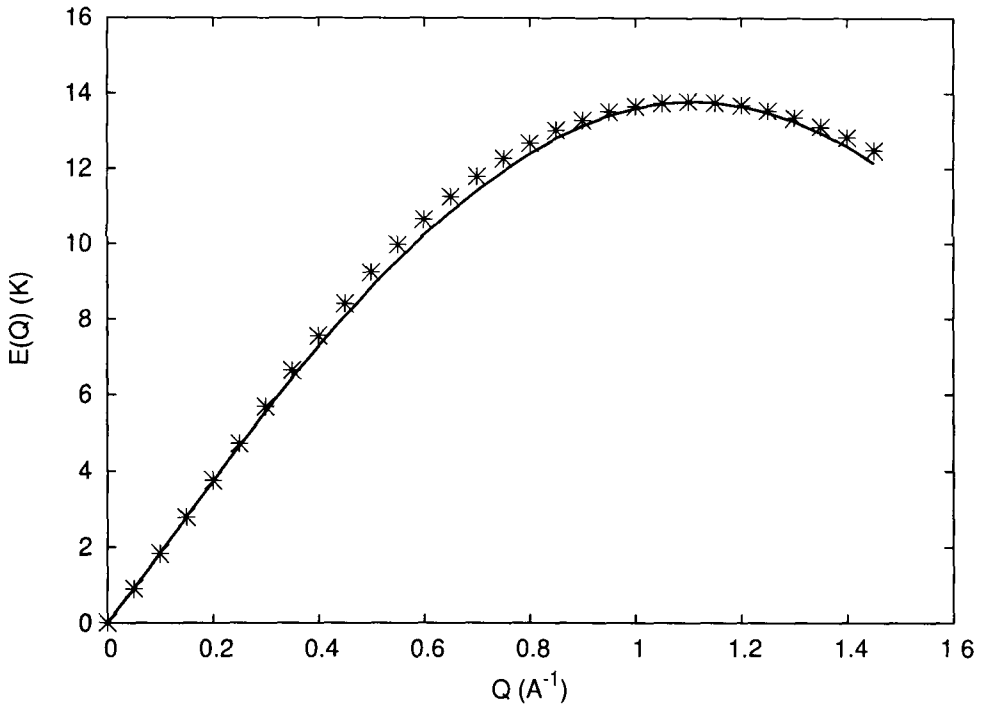

Figure 4.2· Estimated values of E(Q) (solid line) at different Q for sc arrangement (Table-4 2) along with experimental values (represented by *) [24]. $C(Q)$ and $d(Q)$ are obtained using equations 4.9 and 4.10.

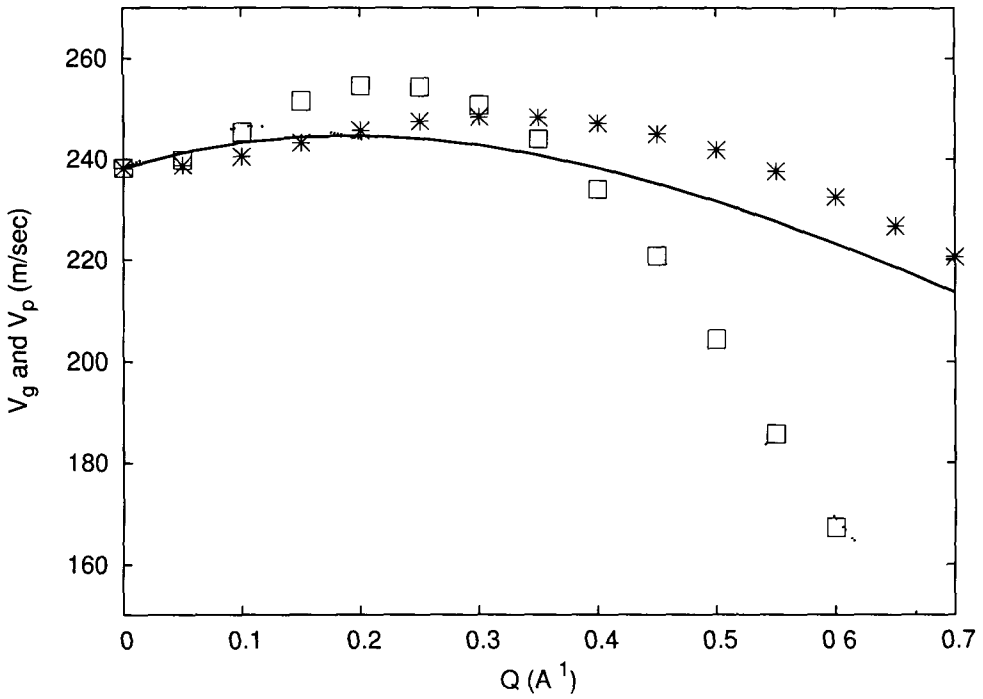

Figure 4 3: Q dependence of V_p and V_g for sc arrangement (Table-4 2) Solid line and dashed line represent theoretical values of V_p and V_g respectively. Stars and squares represent corresponding experimental values [24]

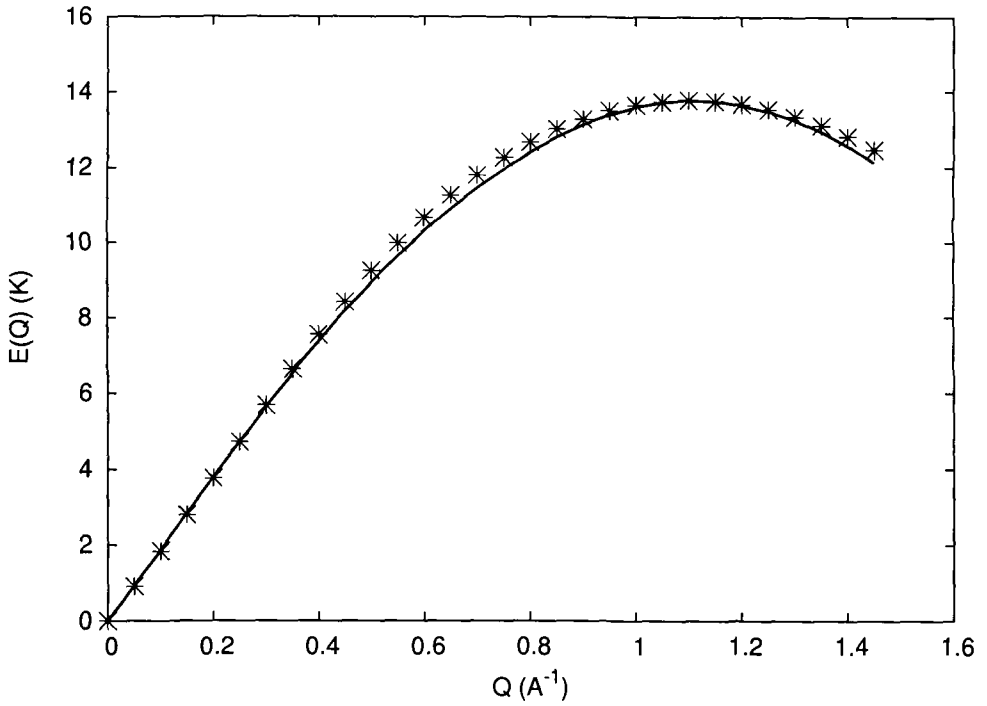

Figure 4.4: Estimated values of E(Q) (solid line) at different Q for bcc arrangement (Table-4 3) along with experimental values (represented by*) [24]. $C(Q)$ and $d(Q)$ are obtained using equations 4.9 and 4.10.

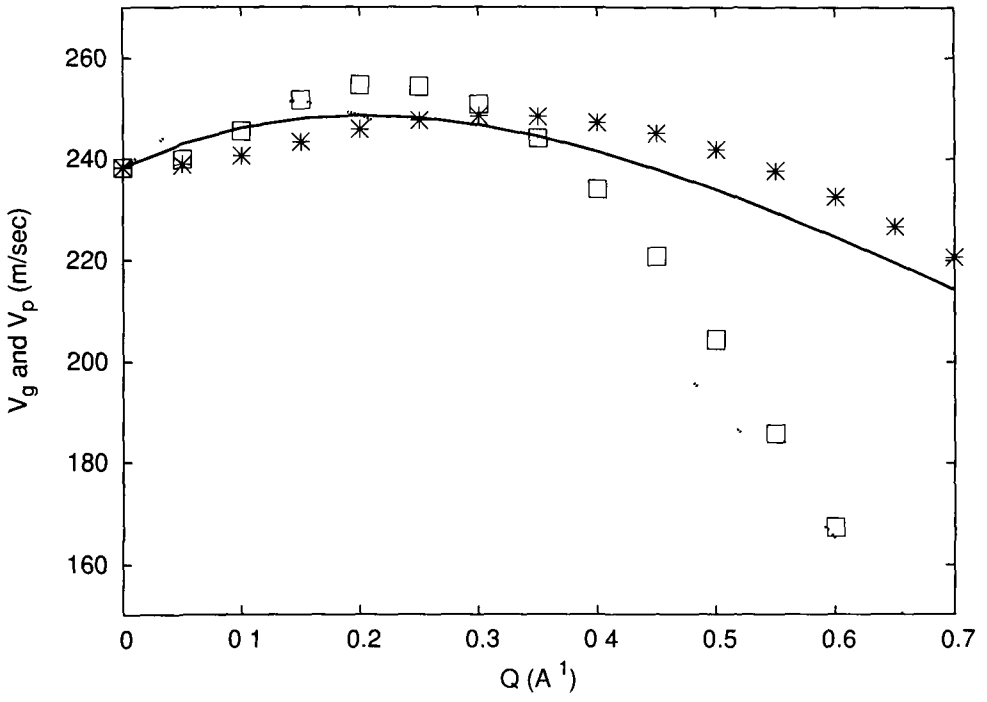

Figure 4.5: Q dependence of V_p and V_g for bcc arrangement (Table-4 3) Solid line and dashed line represent theoretical values of V_p and V_g respectively. Stars and squares represent corresponding experimental values [24]

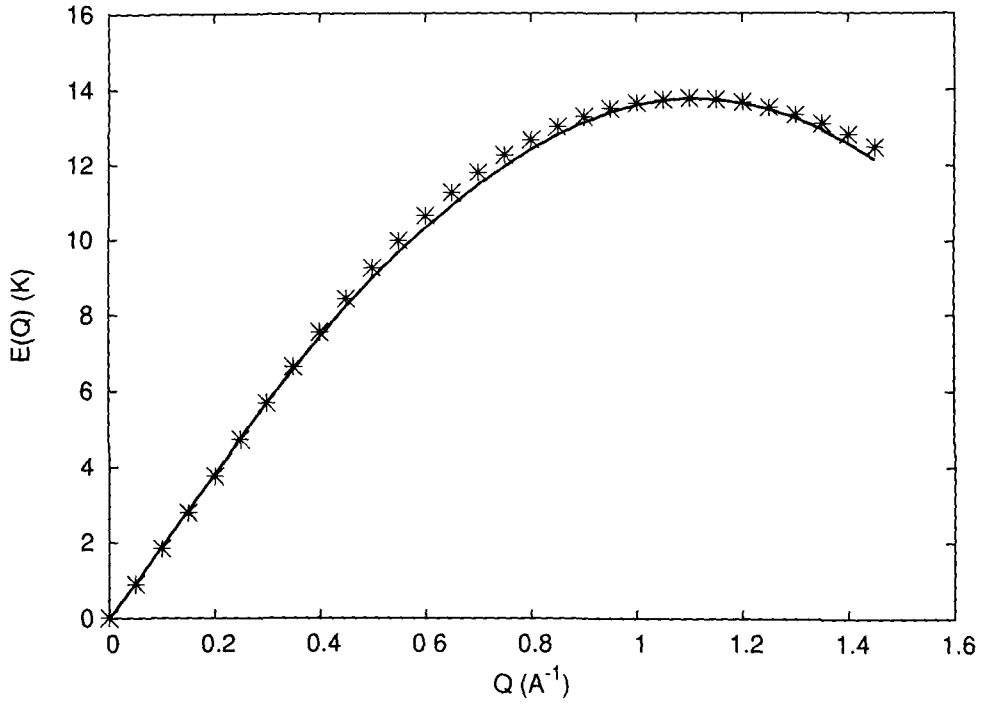

Figure 4.6: Estimated values of E(Q) (solid line) at different Q for fcc arrangement (Table-4 4) along with experimental values (represented by *) [24]. $C(Q)$ and $d(Q)$ are obtained using equations 4.9 and 4.10.

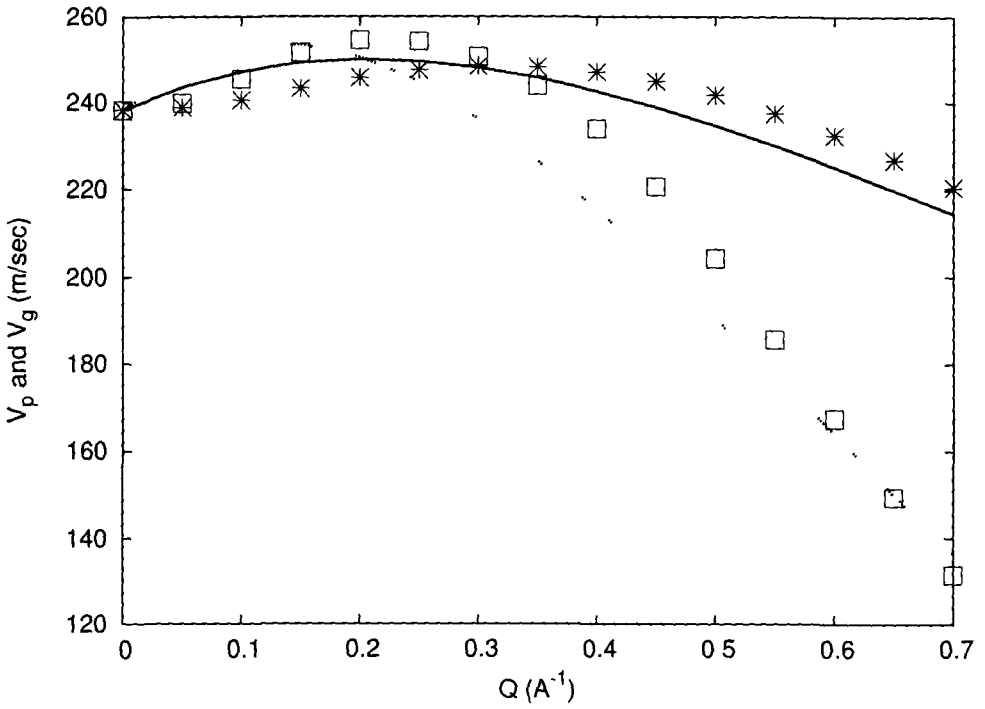

Figure 4.7. Q dependence of V_p and V_g for fcc arrangement (Table-4 4) Solid line and dashed line represents theoretical values of V_p and V_g. Stars and squares represent experimental values of V_g and V_p [24].

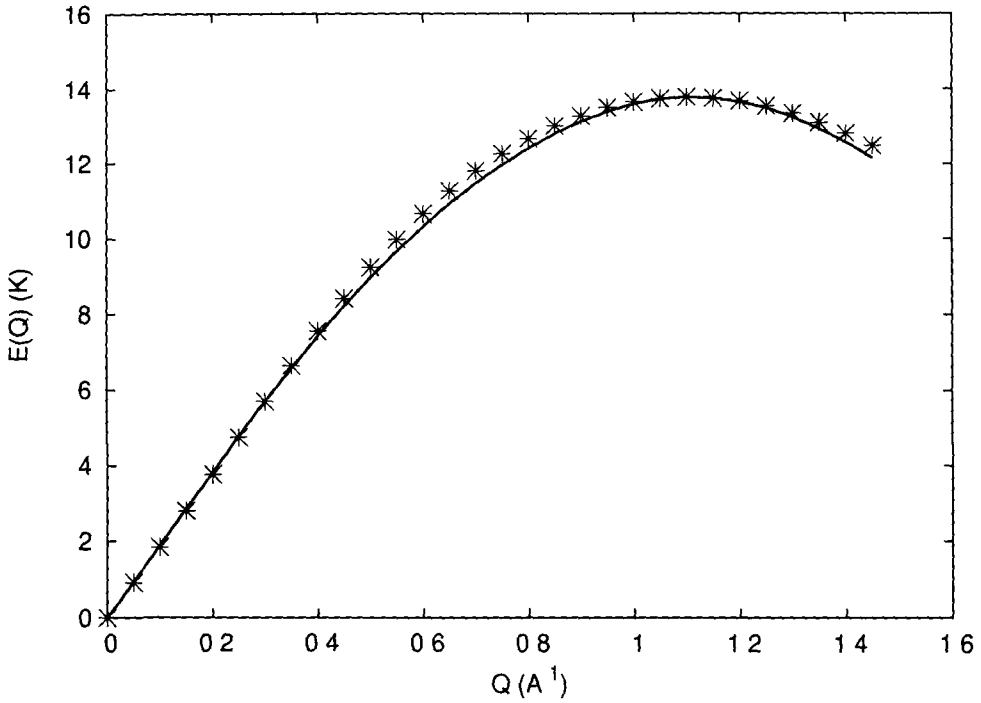

Figure 4 8 Estimated values of E(Q) (solid line) at different Q for hcp arrangement (Table-4 5) along with experimental values (represented by *) [24] $C(Q)$ and $d(Q)$ are obtained using equations 4 9 and 4 10

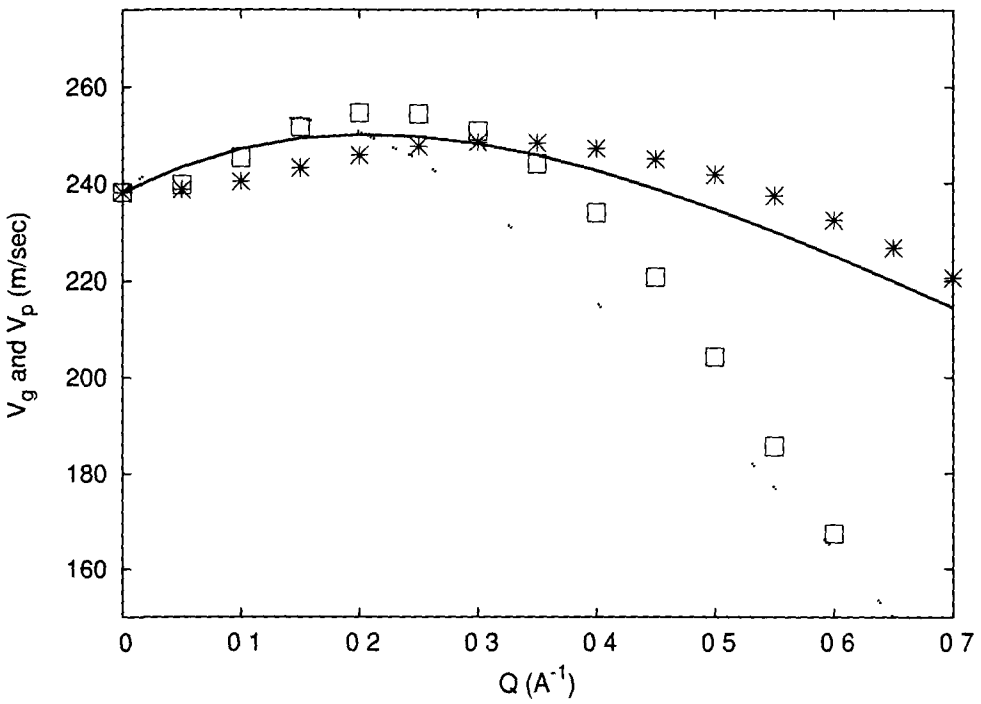

Figure 4 9 Q dependence of V_p and V_g for hcp arrangement (Table-4 5) Solid line represents theoretical values of V_p and dashed line represents theoretical values of V_g Squares and stars represent experimental values of V_g and V_p [24]

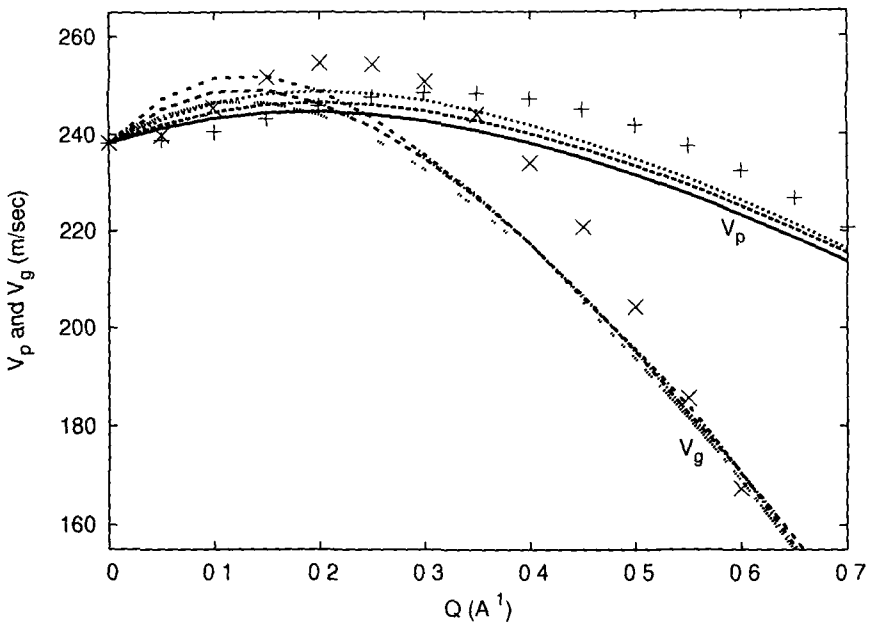

Figure 4.10: Change of V_p and V_g with Q for sc arrangement (Table-4.7). In both cases top most curve corresponds to $Q_{max} = 0.7\mathring{A}^{-1}$, middle curve corresponds to $Q_{max} = 0\,9\mathring{A}^{-1}$ and lower curve corresponds to $Q_{max} = 1.105\mathring{A}^{-1}$. The cross and plus symbols represent experimental values [24] of V_g and V_p respectively

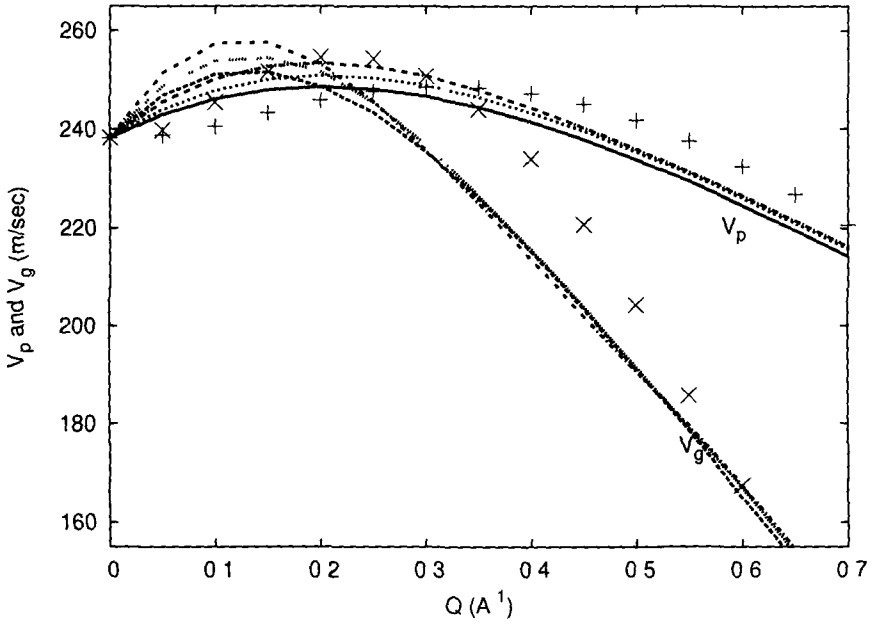

Figure 4.11. Change of V_p and V_g with Q for bcc arrangement (Table-4 9). In both cases top most curve corresponds to $Q_{max} = 0.7\mathring{A}^{-1}$, middle curve corresponds to $Q_{max} = 0\,9\mathring{A}^{-1}$ and lower curve corresponds to $Q_{max} = 1\,105\mathring{A}^{-1}$ The cross and plus symbols represent experimental values [24] of V_g and V_p respectively.

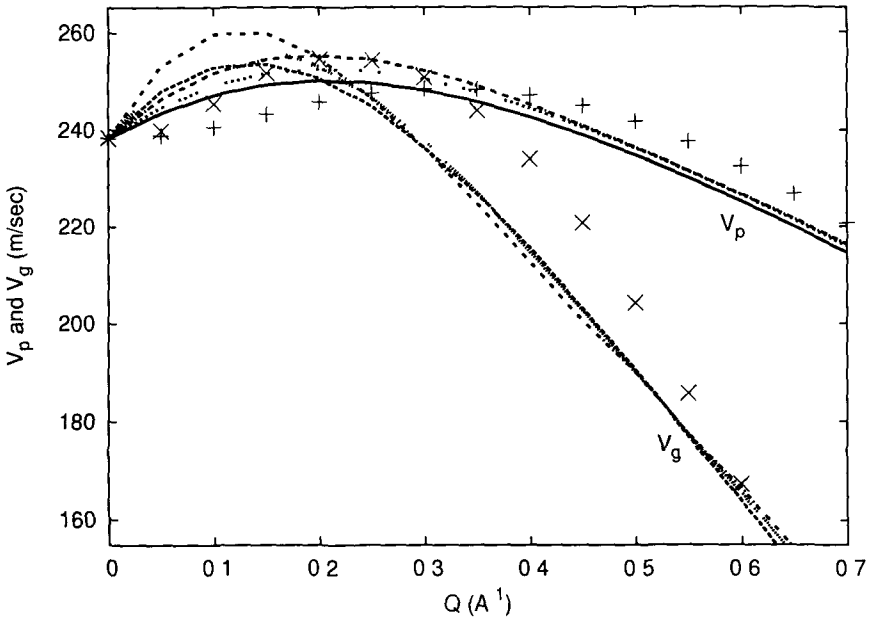

Figure 4 12 Change of V_p and V_g with Q for fcc arrangement (Table-4 11) In both cases top most curve corresponds to $Q_{max} = 0\ 7\mathring{A}^{-1}$, middle curve corresponds to $Q_{max} = 0\ 9\mathring{A}^{-1}$ and lower curve corresponds to $Q_{max} = 1\ 105\mathring{A}^{-1}$ The cross and plus symbols represent experimental values [24] of V_g and V_p respectively

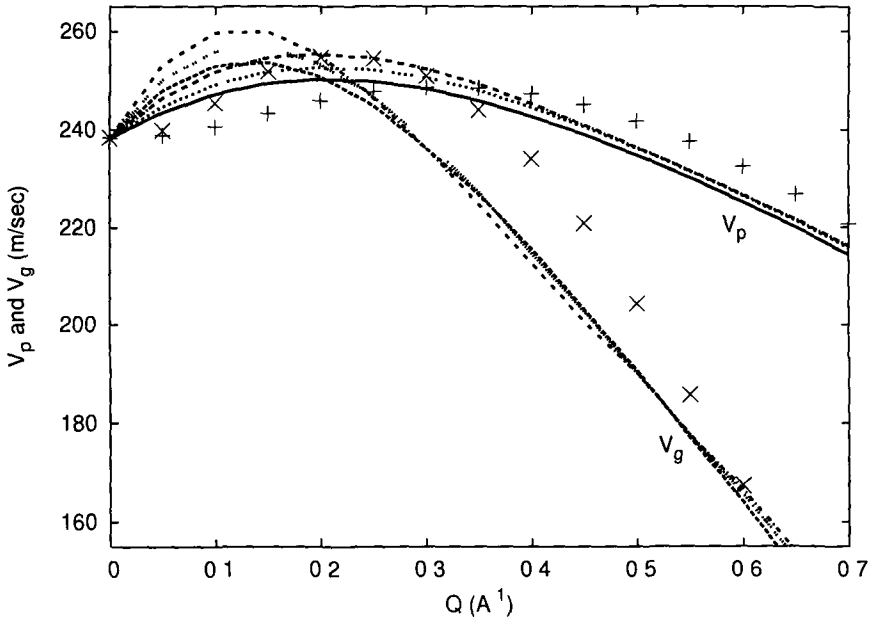

Figure 4 13 Change of V_p and V_g with Q for hcp arrangement (Table-4 13 In both cases top most curve corresponds to $Q_{max} = 0\ 7\mathring{A}^{-1}$, middle curve corresponds to $Q_{max} = 0\ 9\mathring{A}^{-1}$ and lower curve corresponds to $Q_{max} = 1\ 105\mathring{A}^{-1}$ The cross and plus symbols represent experimental values [24] of V_g and V_p respectively

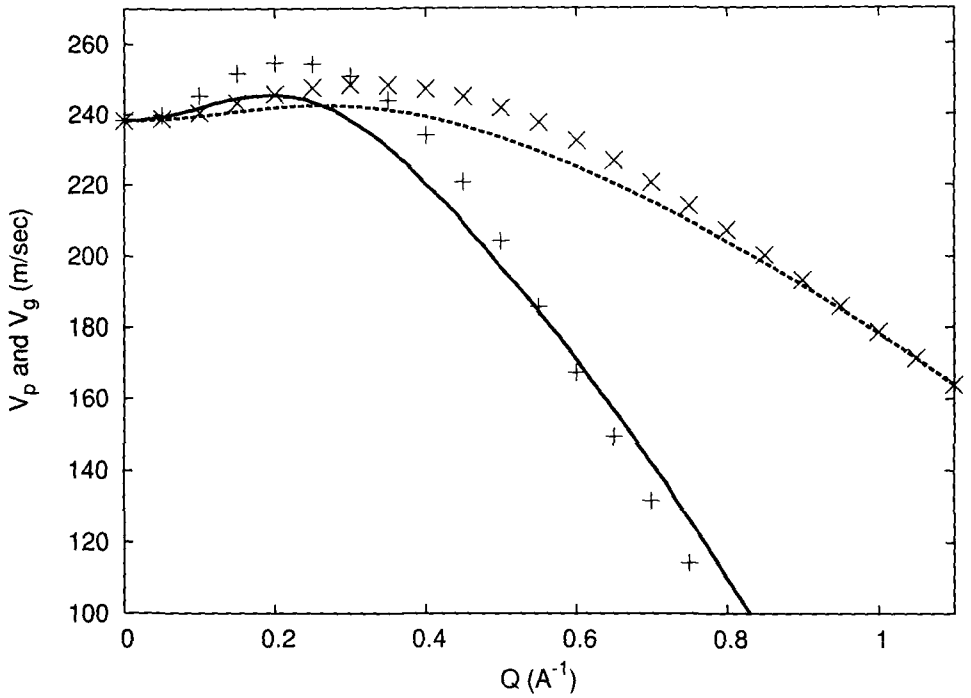

Figure 4.14: Q dependence of V_p and V_g for sc arrangement (Table-4.15). $C(Q)$ and $d(Q)$ are calculated using equations 4.11 and 4.12 Solid and dash lines represent theoretical values of V_g and V_p respectively. Plus and cross symobols represent experimental values of V_g and V_p [24].

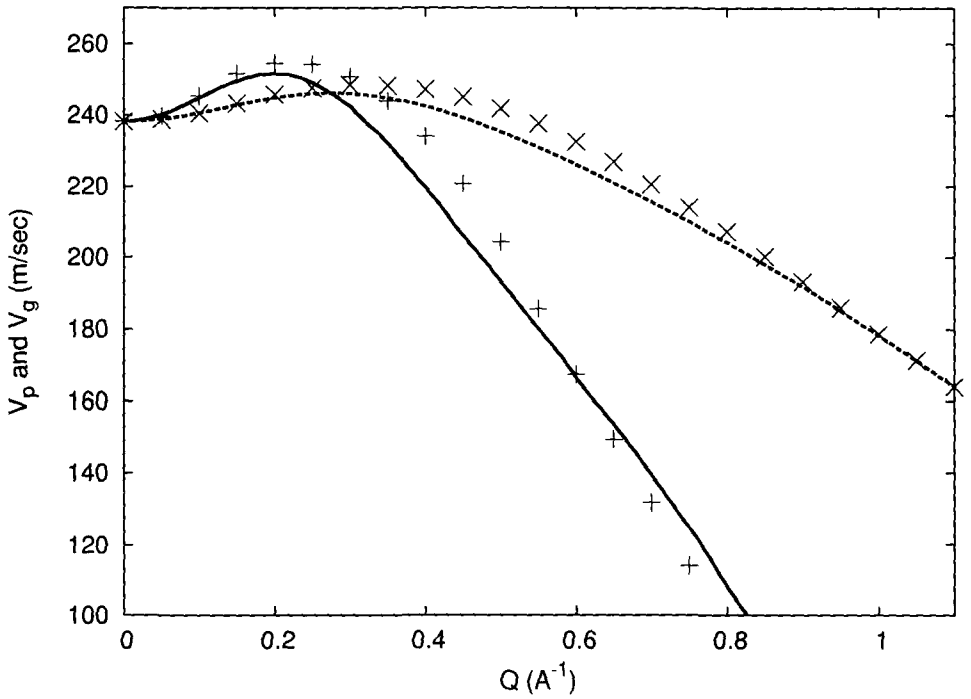

Figure 4.15: Q dependence of V_p and V_g for bcc arrangement (Table-4.16). $C(Q)$ and $d(Q)$ are calculated using equations 4.11 and 4.12. Solid and dash lines represent theoretical values of V_g and V_p. Plus and cross symbols represent experimental values of V_g and V_p [24].

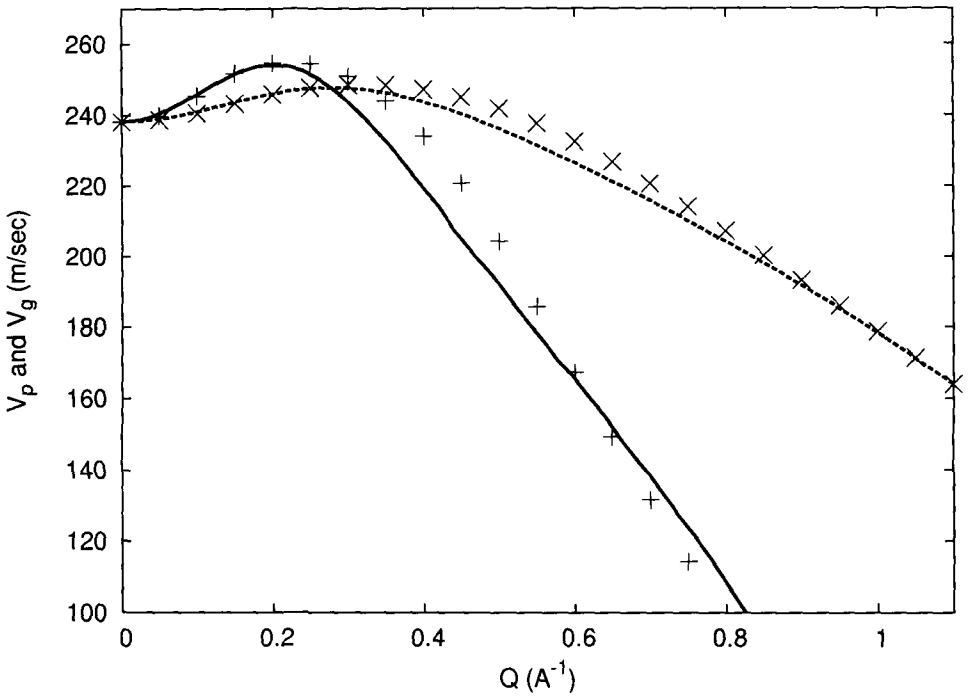

Figure 4.16: Q dependence of V_p and V_g for fcc arrangement (Table-4.17). $C(Q)$ and $d(Q)$ are calculated using equations 4.11 and 4.12. Solid and dash lines represent theoretical values of V_g and V_p. Plus and cross symbols represent experimental values of V_g and V_p [24].

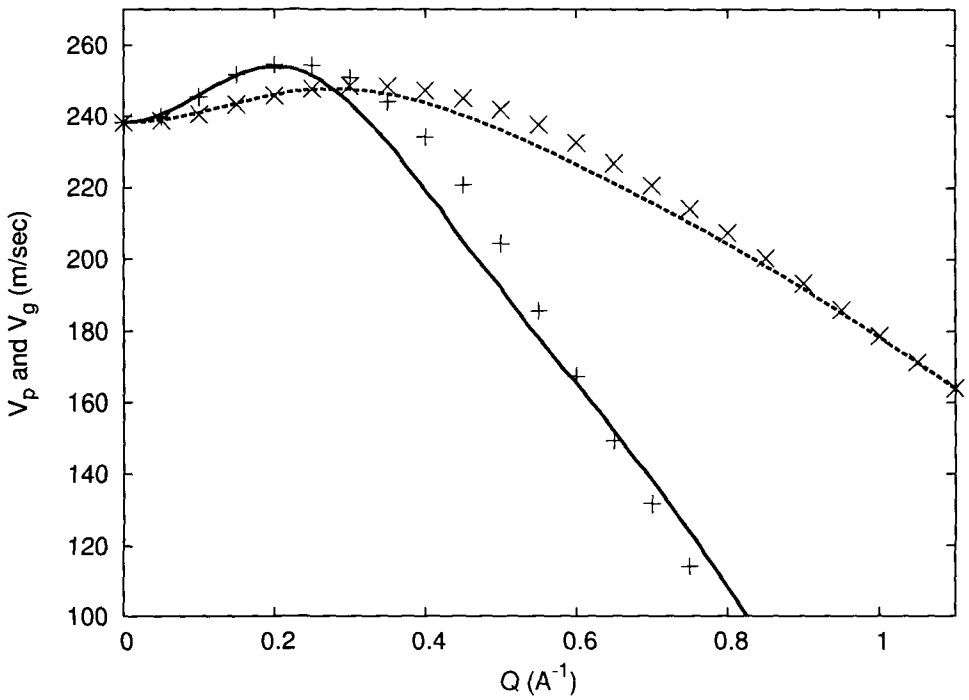

Figure 4.17: Q dependence of V_p and V_g for hcp arrangement (Table-4.18). $C(Q)$ and $d(Q)$ are calculated using equations 4.11 and 4.12. Solid and dash lines represent theoretical values of V_g and V_p. Plus and cross symbols represent experimental values of V_g and V_p [24].

Bibliography

[1] L.D. Landau. *J. Phys. U.S.S.R. (reprinted in Ref. 1)*, 5:71, 1941.

[2] N. Bogoliubov. *J. Phys. (USSR) (reprinted in Ref. 1)*, 11:23, 1947.

[3] L.D. Landau. *J. Phys. U.S.S.R. (reprinted in Ref. 1)*, 11:91, 1947.

[4] R.P. Feynman. *Phys. Rev.*, 94:262, 1954.

[5] R.P. Feynman and M. Cohen. *Phys. Rev.*, 102:1189, 1956.

[6] L.P. Pitaevskii. *Zh. Eksp. Theor. Fiz.*, 31:536, 1956.

[7] T.C. Padmore and C.V. Chester. *Phys. Rev.*, A 9:1725, 1974.

[8] E. Feenberg. *Theory of Quantum Fluids.* Academic Press, New York, 1969.

[9] H.W. Jackson and E. Feenberg. *Ann. Phys. NY*, 15:266, 1961.

[10] H.W. Jackson and E. Feenberg. *Rev. Mod. Phys.*, 34:686, 1962.

[11] C.W. Woo. *in The Physics of Liquid and Solid Helium (K.H. Bennemann and J.B. Ketterson, eds.), Part-I.* Wiley, New York, 1976.

[12] A. Bhattacharyya and C.W. Woo. *Phys. Rev. Lett.*, 28:1320, 1972.

[13] A. Bhattacharyya and C.W. Woo. *Phys. Rev.*, A 7:204, 1973.

[14] C.E. Campbell. *in Progress in Liquid Physics (Ed. C.A. Croxton)*, page 213, 1978.

[15] D.G. Henshaw and D.G. Hurst. *Phys. Rev.*, 91:1222, 1953.

[16] D.G. Hurst and D.G. Henshaw. *Phys. Rev.*, 100:994, 1955.

[17] M. Cohen and R.P. Feynman. *Phys. Rev.*, 107:13, 1957.

[18] H. Palevsky, K. Otnes, K.E. Larsson, R. Pauli, and R. Stedman. *Phys. Rev.*, 108:1346, 1957.

[19] H. Palevsky, K. Otnes, and K.E. Larsson. *Phys. Rev.*, 112:11, 1958.

[20] J.L. Yarnell, G.P. Arnold, P.J. Bendt, and E.C. Kerr. *Phys. Rev. Lett.*, 1:9, 1958.

[21] J.L. Yarnell, G.P. Arnold, P.J. Bendt, and E.C. Kerr. *Phys. Rev.*, 113:1379, 1959.

[22] D.G. Henshaw. *Phys. Rev. Lett.*, 1:127, 1958.

[23] H.J. Maris and W.E. Massey. *Phys. Rev. Lett.*, 25:220, 1970.

[24] R.J. Donnelly, J.A. Donnelly, and R.N. Hills. *J. Low Temp. Phys.*, 44:471, 1981.

[25] E.C. Svensson, P. Martel, and A.D.B. Wood. *Phys. Lett.*, 55A:151, 1975.

[26] C.H. Aldrich III, C.J. Pathick, and D. Pines. *J. Low Temp. Phys.*, 25:691, 1976.

[27] H.J. Maris. *Rev. Mod. Phys.*, 49:341, 1977.

[28] W.G. Stirlling, J.R. Copley, and P.A. Hilton. *Neutron Inelastic Scattering 1977*, volume Vol II. IAEA, Vienna, 1978.

[29] W.G. Stirlling. 75^{th} *Jubilee Conference on Helium-4 (Ed. J.G.M. Armitage)*, 1983.

[30] T.R. Kirkpatrick. *Phys. Rev B*, 29:3966, 1984.

[31] R.A. Cowley and A.D.B. Wood. *Can. J. Phys.*, 49:177, 1971.

[32] R.C. Dynes ann V. Narayanmurty. *Phys. Rev. B*, 12:1720, 1975.

[33] L.P. Pitaevskii and Y.B. Levinson. *Phys. Rev.*, B 14:263, 1976.

[34] D. Roy Choudhury. *Study of the Dynamic behavior of certain manybody system, Ph.D. Thesis, NEHU.* unpublished, 1996.

[35] Y.S. Jain. *Proc. of the International Conference INDIAS-91 on Disordered Materials, Structure and Properties*, India Feb 3-6, 1991:202, 228.

[36] Y.S. Jain. *J. Sci. Expl.*, 16:77, 2002. More detailed version of this paper is available for ready reference as a paper entitled, *"Macro-orbitals and microscopic theory of a system of interacting bosons"* in www.arXiv.org/cond-mat/0606571.

[37] J. Wilks. *The Properties of Liquid and Solid Helium.* Clerendon Press, Oxford, 1967.

[38] A.D.B. Woods and R.A. Cowley. *Phys. Rev. Lett.*, 24:646, 1970.

[39] R.J. Donnelly and C.F. Barenghi. *The Observed Properties of Liquid Helium at the Saturated Vapor Pressure.* www.darkwing.uoregon.edu, Universitas Oregonensis.

[40] L.D. Landau and I.M. Khalatnikov. *J.E.T.P.*, 19:637, 709, 1949.

[41] R.W. Whitworth. *Proc. Roy. Soc. Lon.*, A 246:390, 1958.

[42] I.M. Khalatnikov. *Sov. Phys.-JETP*, 17:519, 1963.

[43] C.E. Chase and M.A. Herlin. *Phys. Rev.*, 97:1447, 1953.

[44] H.J. Maris. *Phys. Rev. Lett.*, 28:277, 1972.

[45] H.J. Maris. *Phys. Rev.*, A 8:1980, 1973.

[46] J.S. Brooks and R.J. Donnelly. *Phys. Lett.*, A 46:111, 1973.

[47] A. Molinari and T. Regge. *Phys. Rev. Lett.*, 26:1531, 1971.

[48] C.H. Anderson and E.S. Sabisky. *Phys. Rev. Lett.*, 28:80, 1972.

[49] P.R. Roach, B.M. Abraham, J.B. Ketterson, and M. Kuchnir. *Phys. Rev. Lett.*, 29:32, 1972.

Chapter 5

Energy Gap and Related Properties

Abstract *In Macro-orbital formalism an energy gap (which is responsible for a collective binding of the atoms in superfluid phase) appears between the superfluid and normal fluid phase This energy gap is account for most of the unique properties of the superfluid helium At a certain velocity (flow/ rotational) of the superfluid, kinetic energy of the system overtakes the collective binding energy (energy gap) and the fluid becomes normal fluid This velocity is the critical velocity for which superfluidity of the system vanishes completely, however, it is different from the usual critical velocity of vortex formation In this chapter we estimate the energy gap at different temperature and use its values to estimate critical velocities for linear flow as well as rotational motion, vortex line density, radius of vortex ring* etc *We also estimate the normal and superfluid density using the energy gap A close agreement is observed between the estimated and experimental values*

5.1 Introduction

At the transition temperature, T_λ, liquid helium-4 (LHE-4) undergoes a transition from its normal phase of properties of a normal fluid (N-fluid) into super-fluid (S-fluid) phase exhibiting various properties related to the phenomenon of 'super-fluidity'. The two phases are also known as '*helium-I*' and '*helium-II*'. As concluded by Jain's theory [1], the energy of S-fluid is lower than that of N-fluid and it is also evident from the fact that only an increase in thermal energy or motional energy by definite amount destroys super-fluidity of *helium-II*. Jain's theory identifies this difference in energy by what he calls as 'Energy gap E_g'(or collective binding of the entire system) and relates it to several unique properties namely critical velocities (v_c or Ω_c), super-fluid density (ρ_s), coherence length (ξ) *etc.* In this context Jain follows standard physical reasons which are used to relate similar parameters in case of superconductors. In this chapter we analyse these relations to obtain the temperature dependent v_c, Ω_c, ρ_s, ξ *etc* and compare their values with experimental results to examine their accuracy. It may be emphasised that our theoretical results agree closely with experiments indicating the accuracy of Jain's microscopic theory.

5.2 Energy Gap

We find that energy gap between N- and S-phases of LHE-4 is responsible for its super-fluidity and related properties and is given by [1]

$$E_g(T) = \frac{N}{2}\left[\frac{h^2}{8md_\lambda^2} - \frac{h^2}{8md_T^2}\right] \tag{5.1}$$

where d_λ and d_T are the inter particle separations at T_λ and $T(< T_\lambda)$ respectively. $E_g(T)$ is also obtainable from

$$E_g(T) = \Delta\varepsilon(T) = [N^\star(T_\lambda) - N^\star(T)]k_B T_o \ln 2 \tag{5.2}$$

where $N^\star(T)$ and $N^\star(T_\lambda)$ represent the number of excited particles which are free from quantum correlation at $T(< T_\lambda)$ and T_λ respectively. The number of excited atom is given by

$$N^\star(T) = \frac{V}{4\pi^2}\left[\frac{2m}{\hbar^2}\right]^{3/2}\int_{\varepsilon_c}^{\infty}\left[\exp\left(\frac{\varepsilon-\varepsilon_o}{k_B T}\right) - 1\right]^{-1}\sqrt{\varepsilon}d\varepsilon \tag{5.3}$$

where $\varepsilon_c = \frac{\hbar^2 Q_c^2}{2m}$ (with $Q_c \sim 2\pi/\sigma$, σ being the hardcore radius) represents the lower bound of $\varepsilon > \varepsilon_c$ for which an atom has no quantum correlation with its neighbours.

Evidently, $E_g(T)$ can be calculated by using values of d_T and d_λ in equation 5.1 or by obtaining $N^\star(T)$ and $N^\star(T_\lambda)$. Since consistency of the two relations has been shown by Jain, we calculate $E_g(T)$ by using equation 5.1. We obtain required d for this calculation using temperature dependent density of *helium-II* available in ref. [2]. We present our estimated $E_g(T)$ (per particle) and d at different temperature in Table-5.1 and depict in figure 5.1.

5.3 Super-fluid and Normal Fluid Density

In Macro-orbital theory super-fluid density ($\rho_s(T)$) is considered as the order parameter of the transition and related to $E_g(T)$ through the relation

$$\rho_s(T) = [E_g(T)/E_g(0)]\,\rho(T) \tag{5.4}$$

where $\rho(T)$ is the total density. Using equation 5.2 one can also find

$$\rho_s(T) = \frac{N^\star(T_\lambda) - N^\star(T)}{N^\star(T_\lambda)}\rho(T) \tag{5.5}$$

which indicates that ρ_s can be obtained either by calculating $E_g(T)$ or the number of excited particles that avoid quantum correlation. For normal density (ρ_n) we obviously have $\rho_n(T) = \rho(T) - \rho_s(T)$.

To calculate the super-fluid density using $N^\star$ we have expressed equation 5.3 in the form

$$\frac{N^\star(T)}{N} = \frac{d^3}{4\pi^2}\left[\frac{2m}{\hbar^2}\right]^{3/2}\int_{\varepsilon_c}^{\infty}\left[\exp\left(\frac{\varepsilon-\varepsilon_o}{k_BT}\right)-1\right]^{-1}\sqrt{\varepsilon}\,d\varepsilon \tag{5.6}$$

where N is the total number of atoms in the system and d^3 is the volume available for each atom. This relation takes the form

$$\frac{N^\star(T)}{N} = \frac{2d^3}{\sqrt{\pi}}\frac{1}{\lambda_T^3}\int_{x_c}^{\infty}\frac{\sqrt{x+x_o}}{e^x-1}dx \tag{5.7}$$

with

$$x = \frac{\varepsilon-\varepsilon_o}{k_BT}, \tag{5.8}$$

$$x_o = \frac{\varepsilon_o}{k_BT} \tag{5.9}$$

and

$$\lambda_T = \frac{h}{2\pi m k_B T} \tag{5.10}$$

We solve this integration numerically by using C-programming with $\Delta x = 10^{-20}$ for every step and continue the summation until the contribution of individual step falls below 10^{-22}. It may be mentioned that the use of $\Delta x < 10^{-20}$ do not change the value of the integration.

Values of ρ_s and $\rho_n (= \rho - \rho_s)$ obtained from equation 5.4 as well as equation 5.5 are presented, respectively, in Tables 5.2 and 5.3. Although the results are slightly different, the difference is not significant. While the results obtained from equation 5.4 show $\rho_s \sim \rho$ at $T < 1.4\,K$, those obtained from equation 5.5 show $\rho_s \sim \rho$ for $T < 0.6\,K$ only. The two values at higher temperature fall smoothly and assume zero value at $T = T_\lambda$. Temperature dependence of our normalised ρ_s and ρ_n is shown in figure 5.2.

5.4 Critical Velocity

The existence of a critical velocity(v_c) in *helium-II* was put forwarded by Daunt and Mendelssohn [3] in order to explain the observations of the helium film flow out of beakers. In such films super-fluid moves due to gravitational potential difference and should possess infinite velocity due to its non-frictional motion. However, its observed finite value led Daunt and Mendelssohn to propose that there is a certain v_c for *helium-II* beyond which it loses its super-fluid nature. By measuring the film thickness, they estimated the upper limit of v_c to be about $70\,cm/sec$.

Existence of v_c was also predicted by Landau in his two fluid phenomenological theory [4] of super-fluid *helium-II*. He attributed the friction between liquid and walls of capillary through which liquid flow to a phonon or roton excitations and proved that below a certain velocity v_c creation of phonons and rotons is energetically impossible. His predicted v_c for phonon excitation found to be about $25000\,cm/sec$ and for the roton about $8000\,cm/sec$ which is much higher than the experimentally observed $v_c = 70\,cm/sec$ [5]. The disagreement between theory and experiments was addressed by Feynman [6] by introducing the idea of quantized super-fluid circulation. He suggested that the resistance to flow at higher velocities is not due to direct creation of rotons, instead it is due to the formation

of vortex rings. He showed that v_c for which flow energy is just sufficient to form vortices is

$$v_c = \frac{\hbar}{md} \ln(d/a) \tag{5.11}$$

where d is the slit width and a is the core radius of vortex ring which he assumed to be of the order of atomic spacing. For a slit width $d = 10^{-6}\,cm$ and $\ln(d/a) = 6$, his relation gives a v_c about $100\,cm/sec$ [2] which is somewhat higher than the observed critical velocities. He attributed this difference to various complications that exist in the system. For example vortex lines may be created inside the tube due to irregularities on the surface of the wall. Another widely used expression of v_c for the formation of quantized vortex ring is [2, 7]

$$v_{s,c} = (\hbar/md)\left[\ln\left(\frac{4d}{a}\right) - \frac{1}{4}\right] \tag{5.12}$$

where d is the diameter of the capillary and a is the core radius of the vortex ring. A similar expression was derived by Glaberson and Donnelly [8] considering the presence of metastable vortex lines. These relations give a v_c of the observed magnitude in relatively wide channels. However, Wilks [2] mentioned that these relations fail to give a fair account of the v_c if the channel width falls below 1μ. Even for the wide channels results do not match exactly. Moreover, these equations yield a v_c which is temperature independent while some experiments [9–11] show a strong temperature dependent v_c. A more fundamental difficulty has been pointed out by Vinen [12], who, considering the size of the channels (which is enormous in atomic scale) argued that the formation of a vortex ring as large as the diameter of the channels is almost impossible. A reasonable figure for the greatest diameter of a vortex ring which could be created instantaneously inside the liquid is probably of the order of $10^{-6}\,cm$ and this corresponds to a v_c of about $100\,cm/sec$. He further suggested that such high velocities are only required to create vortices and a few vortex line may already be present in *helium-II* at the start of an experiment possibly in metastable state. In presence of these vortex lines, turbulence sets in at much lower velocity.

Since then a large number of experimental and theoretical articles have been published proposing different explanation and interpretation for the phenomenon. For example Anderson [13] introduced the idea of quantum phase slips which was observed in the experiments of 1980's and 1990's [14–23]. This set of experiments observed a local super-flow velocity which reaches a value $22\,m/sec$ at the vortex nucleation site. Reppy *et al* [24–26] studied the properties of persistent current in

helium-II. Hess [27] and Hulin *et al* [28] measured the critical velocities in a small hole by filtering it near the hole with porous medium. This set of experiments reveals a strong temperature dependence of the critical velocity with a value about $500\,cm/sec$ at $1.4\,K$. Critical velocities of helium film are also studied by different authors [29–38].

In rotational motion vortices appear in the form of concentric circular streamlines of atoms, lying in planes perpendicular to the axis of vortex and surrounding the central core. It is believed that two different critical velocities exist for rotational motion. First critical velocity (Ω_{c1}), which is relatively small, represents the minimum angular velocity for which first vortex of macroscopic size (of the order of the cylinder) appears in the liquid and the second critical velocity (Ω_{c2}), which is very high, represents the angular velocity for which density of vortex lines becomes maximum [7]. Linear velocity of circulation in streamline of radius r is obtained using the relation [7]

$$\kappa = \oint v_s.dl = 2\pi r v_s(r) = n\frac{h}{m} \tag{5.13}$$

which gives

$$v_s(r) = \kappa/2\pi r \tag{5.14}$$

Energy associated with a single vortex line is mainly the kinetic energy of circulation and this energy per unit length is given by [7]

$$\varepsilon_v = \int_{a_o}^{b} \frac{1}{2}\rho_s v_s^2 (2\pi r) dr \tag{5.15}$$

where a_o is the core radius and b is the radius of the vortex ring. Using equation 5.14 for a particular value of κ one can find

$$\varepsilon_v = \frac{\rho_s \kappa^2}{4\pi} \ln\left(\frac{b}{a_o}\right) \tag{5.16}$$

When the first vortex appears in the rotating fluid it's associated flow pattern fills the entire container. Minimum angular velocity to create such vortex (i.e. Ω_{c1}) is given by [7]

$$\Omega_{c1} = \frac{h}{2\pi m R_o^2} \ln\left(\frac{R_o}{a_o}\right) \tag{5.17}$$

with R_o is radius of the cylinder. For example, if $R_o = 1\,cm$, Ω_{c1} takes the value $\sim 10^{-3}\,rad/sec$. Energy of vortices reveals that, an array of more lines with circulation of small κ (i.e. lower value of n) is more favourable than a single circulation with large κ (i.e. higher n). As a result more and more vortex lines

with smaller κ are developed with increasing Ω. For a particular value of the angular velocity ($> \Omega_{c1}$), density of such lines is given by [7]

$$n_v = 2\Omega/\kappa \tag{5.18}$$

However, this process can not be continued indefinitely and a theoretical limit is set on the proximity of vortex lines by the overlapping of their cores. It would happen if Ω were to reach the higher critical velocity [7]

$$\Omega_{c2} = \frac{h}{2\pi m a_o^2} \tag{5.19}$$

which is of the order of $10^{12}\, rad/sec.$

Despite these untiring and numerous efforts, no proper explanation is found for the critical velocities and it remains as one of the least understood aspects of *helium-II.* However, general belief is that it is the critical velocity for quantized vortex formation which leads to quantum turbulence and dissipation in the flow and rotational motion.

In Macro-orbital theory v_c carries a different significance. Above this flow velocity, flow energy overtakes the collective binding energy E_g of S-phase. This velocity is obtained from the condition $N\epsilon(K) = N(mv_c^2/2) = NE_g$ which gives

$$v_c(T) = \sqrt{[2E_g(T)/m]} \tag{5.20}$$

For a flow velocity $v_f < v_c$, the super-fluid phase is stable against the flow. As velocity of the flow crosses the critical limit, the super-fluidity of the system vanishes completely. This critical velocity is large and different from the critical velocity of vortex formation. However, presence of quantized vortices that causes viscous behaviour is expected even if $v_f < v_c$.

We have calculated temperature dependence of critical velocity using equation 5.20 and presented our values in Table-5.1. Our results show a strong temperature dependence of v_c from $\lambda-$point to $1.4\,K$ below which it remains constant. We depict our findings in figure 5.3.

In case of rotational motion Macro-orbital theory predicts Ω_{c2} rather than Ω_{c1}. A numerical value of Ω_{c2} can be obtained as follows:

With increasing Ω size of vortices decreases while n_v increases. When Ω reaches Ω_{c2}, n_v and radii of vortices become such that rotational kinetic energy overtakes the collective binding energy of the system and super-fluidity of the

system vanishes. If ε_v is the energy of such vortices with radius r_o, n_v can be obtained from the condition

$$\pi R^2 l n_v \varepsilon_v = E_g(T) \tag{5.21}$$

where R and l are radius and length of the cylinder respectively. This equation gives

$$n_v = \frac{E_g(T)}{\pi R^2 l \varepsilon_v} \tag{5.22}$$

In Macro-orbital theory all atoms participate in both normal and super-fluid phases indicating that all atoms serve as constituent of vortices present in the system. Hence, we can replace ρ_s by ρ in equation 5.16 and using this we find

$$n_v = \frac{4m^2 E_g(T)}{l R^2 h^2 \rho \ln r_o/a_o} \tag{5.23}$$

Substituting the value of E_g from equation 5.1 we find

$$n_v = \frac{2\pi m^2}{h^2 l R^2 \rho(T) \ln r_o/a_o} N \left[\frac{h^2}{8md_\lambda^2} - \frac{h^2}{8md_T^2}\right] \tag{5.24}$$

When N is replaced by $(\pi R^2 l \rho(T))/m$, above equation becomes

$$n_v = \frac{2\pi m}{h^2 \ln r_o/a_o} \left[\frac{h^2}{8md_\lambda^2} - \frac{h^2}{8md_T^2}\right] \tag{5.25}$$

However, n_v should simultaneously satisfy the condition,

$$n_v < \frac{1}{\pi r_o^2} \tag{5.26}$$

because this is the maximum number of vortex lines that can exist in the system for a given r_o. Therefore, rotational energy may possibly overtake the collective binding energy when

$$\frac{1}{\pi r_o^2} = \frac{2\pi m}{h^2 \ln r_o/a_o} \left[\frac{h^2}{8md_\lambda^2} - \frac{h^2}{8md_T^2}\right] \tag{5.27}$$

From this relation we obtain

$$\frac{\ln r_o/a_o}{r_o^2} = \frac{2\pi^2 m}{h^2} \left[\frac{h^2}{8md_\lambda^2} - \frac{h^2}{8md_T^2}\right] \tag{5.28}$$

This equation shows the temperature dependence of r_o as well as indicates the temperature dependence of n_v, ε_v and Ω_{c2}. Choosing a value of a_o (in our case $a_o = 1.7893 \times 10^{-8}\, cm$ which is half of the average atomic spacing) one can solve this equation analytically to find the values of r_o at different temperature. Using these values in equation 5.25 we estimate the values of n_v using which we obtain the corresponding values of Ω_{c2} at different temperature from equation 5.19. We

present our estimated values in Table:5.5. We also depict the variation of r_o, ε_v, n_v and Ω_{c2} with temperature in figures 5.4, 5.5, 5.6 and 5.7. These graphs show a strong temperature dependence of these quantities. While n_v and Ω_{c2} decrease with temperature from $1.4\,K$ to T_λ where they vanish, vortex size, r_o and its energy, ε_o increase with temperature.

5.5 Coherence Length

Below T_λ, the particles of the system get locked in phase space ($\Delta\phi = 2n\pi$) and the quantum correlation potential offers a collective binding energy, E_g, to the system [1]. As a result there exists a coherence in super-fluid state which is characterised by coherence length [1]

$$\xi(T) = \frac{h}{mv_c} = h\sqrt{\frac{N}{2mE_g(T)}} \tag{5.29}$$

We have obtained the coherence length at different temperature from the energy gap corresponding to that temperature and shown in Table-5.1 and figure 5.8. Above $1.4\,K$, result exhibits a temperature dependence.

5.6 Discussion

Concept of energy gap is an old idea in physics which is widely used to explain the properties like electrical conductivity, superconductivity *etc.* However, no phenomenological or microscopic model other than Jain's Macro-orbital theory uses this idea to explain the unique properties of *helium-II.* In Macro-orbital formalism an energy gap between S- and N-phases appears spontaneously and it explains why LHE-4 is a super-fluid below T_λ with a definite stability against weak perturbation of certain energy value. As inferred by Jain [1], wave packets of the neighbouring particles below T_λ have their overlap which perturbs the ground state energy of the system and renders anti-bonding state of energy $(\varepsilon_o + \nu(T))$ and bonding or paired state of energy $(\varepsilon_o - \nu(T))$. The latter is more favourable than the former and this becomes the source of an energy gap between the normal and super-fluid phases. As the size of the wave packets depend on temperature, strength of the perturbation as well as energy gap are also temperature dependent. Temperature dependence of energy gap is well evident from figure 5.1. Energy gap between the

two phases remains constant from $0K$ to $1.4K$ and it decreases with temperature up to T_λ where it has zero value.

We use equations 5.4 and 5.5 to estimate ρ_s and ρ_n. We depict our findings in figure 5.2 with experimental values. A close agreement between our values and experiments is well evident from this figure.

Our estimated values of v_c are higher than those obtained from the capillary or film flow measurements (Tables 5.1 and 5.6 and Ref [2]). As we have already mentioned that our v_c corresponds to that velocity above which superfluity of the system vanishes completely. The measured v_c usually represents velocity required for vortex formation and does not account for the loss of total super-fluidity. However, we note that our v_c is very close to the measured value by Hess [27] and Hulin *et al* [28]. Hess [27] found a v_c around $500\,cm/sec$ at $1.4\,K$ by placing compressed-rouge super-fluid filters in the flow path on each side of the orifice. Hulin *et al* [28] who studied the flow of the superfluid helium between two bath through a small hole (6-10 $\mu-$diameter) by filtering the liquid near the hole using either a circular porous bronze plug or jeweller's rouge compressed between two bronze plugs, observed a dependence of v_c on flow direction (inward and outward from the inner bath) for porous bronze plug which was not observed in compressed-rouge filter. While they observed maximum v_c about $1000\,cm/sec$ and $800\,cm/sec$ respectively for inward and outward flow through porous bronze filter, it was about $350\,cm/sec$ for compressed-rouge filter. Both Hess and Hulin *et al* observed strong temperature dependence of the critical velocity which agrees with our findings.

Film thickness(d), flow rate(R) and v_c in helium films are also studied in a large number of experiments. Henshaw and Jackson [39, 40] and Atkins [29] measured the thickness and flow rate simultaneously during the transfer process of the liquid from a beaker. Using these data Daunt and Smith [30] calculated v_c for the film flow. While the data of Jackson and Henshaw reveals v_c between 105 and $118\,cm/sec$ for a temperature range from $1.1\,K$ to $1.9\,K$, Atkin's data at $1.47\,K$ gives v_c between 35 to $39\,cm/sec$. In a similar experiment with improved measurement technique Jackson and Grimes [35] obtained a transfer rate $13.4 \times 10^{-5}\,cm^3/sec$ and Ham and Jackson [34] obtained a film thickness $3.02 \times 10^{-6} cm$ at $1\,cm$ height at $1.60\,K$ This gives a revised $v_c = 54.1\,cm/sec$ at $1.60\,K$. Knudsen and Dillinger [31,32] studied the spreading of *helium-II* film on a dry surface of copper or stainless steel. By measuring the velocity of advance-

ment of the front of the spreading film they obtained a $v_c = 37\,cm/sec$. As cited in [35], Dillinger recorded a value $17.7\,cm/sec$ for the average velocity in similar experiments. Pickar and Atkins [37] obtained a value $25-40\,cm/sec$ by measuring the third sound velocities in the film. Telschow *et al* [38] measured the critical velocities in unsaturated films and observed a variation of v_c with temperature as well as with d of the film. They found a maximum value around $200\,cm/sec$ for a $d \sim 11$ *atomic layers*. However, they mentioned that this value may be as high as $520\,cm/sec$ for a film of 4 *atomic layers* thickness. In Table 5.6 we have presented some of the measured values of v_c in films. This shows that v_c may take a wide range of values depending upon the experimental situations.

In rotational motion our $\Omega_{c2}(\approx 10^8 rad\,sec^{-1}$ for $T < 1.4\,K)$ corresponds to a n_v (Table:5.1) which is just allowed by the geometrical structure. Our estimated value of Ω_{c2} represents that value of Ω below which a complete transformation of super-fluid to normal fluid is not possible. However, there is a possibility that actual transformation takes place at a higher value of n_v which yields a higher Ω_{c2}. Another estimation [7] used a vortex core size$\sim 0.5\mathring{A}$ that gives a value of the order of $10^{12}\,rad\,sec^{-1}$. This value of the core radius seems to be unrealistic because every particle of the system on an average shares a volume d^3, $d(\sim 3.5776\mathring{A})$ being the inter particle separation. In this estimation vortices of core size is assumed to be formed which we find unrealistic. Value of a_o used by us is well inside the two extreme values proposed by Feynman [6] ($\sim 4.0\mathring{A}$) and Vinen [41] ($0.5\mathring{A}$) and very close to the value ($1.3\mathring{A}$) used by Rayfield and Reif [42].

Our estimated value of ξ using are shown in figure 5.8. Interestingly these values are close to the thickness of the films of flowing superfluid out of a beaker under saturated vapour pressure. We also find that the maximum radial size of a vortex line has value close to ξ.

5.7 Conclusion

Energy gap between super-fluid and normal fluid phases is one of the main inferences of Macro-orbital theory. Jain successfully uses this aspect to explain certain properties of the superfluid such as temperature dependence of ρ_s and v_c, mechano-caloric and thermo-mechanical effects *etc.* Our calculations on ρ_n, v_c and ξ are based on their relations with energy gap. A close agreement of our values with

experiments establishes the accuracy of these relations and the foundation of the Macro-orbital theory. Our results also establish that Jain's Macro-orbital theory is the most successful microscopic theory in explaining v_c and related properties.

Table 5.1: Energy Gap, Coherence length and Critical Velocity

Temp.	ρ	d	$E_g/atom$	ξ	v_c
K	gm/cc	cm	K	cm	cm/sec
0.2	0.14513	3.5776e-08	1.0405e-02	2.1450e-06	657.36
0.3	0.14513	3.5776e-08	1.0405e-02	2.1450e-06	657.36
0.4	0.14513	3.5776e-08	1.0405e-02	2.1450e-06	657.36
0.5	0.14513	3.5776e-08	1.0405e-02	2.1450e-06	657.36
0.6	0.14513	3.5776e-08	1.0405e-02	2.1450e-06	657.36
0.7	0.14513	3.5776e-08	1.0405e-02	2.1450e-06	657.36
0.8	0.14513	3.5776e-08	1.0405e-02	2.1450e-06	657.36
0.9	0.14512	3.5777e-08	1.0512e-02	2.1341e-06	660.74
1.0	0.14512	3.5777e-08	1.0512e-02	2.1341e-06	660.74
1.1	0.14511	3.5778e-08	1.0620e-02	2.1232e-06	664.12
1.2	0.14511	3.5778e-08	1.0620e-02	2.1232e-06	664.12
1.3	0.14512	3.5777e-08	1.0512e-02	2.1341e-06	660.74
1.4	0.14513	3.5776e-08	1.0405e-02	2.1450e-06	657.36
1.5	0.14516	3.5773e-08	1.0082e-02	2.1790e-06	647.10
1.6	0.14521	3.5769e-08	9.5455e-03	2.2395e-06	629.64
1.7	0.14526	3.5765e-08	9.0088e-03	2.3052e-06	611.68
1.8	0.14535	3.5758e-08	8.0429e-03	2.4397e-06	577.96
1.9	0.14546	3.5749e-08	6.8622e-03	2.6413e-06	533.86
2.0	0.14562	3.5736e-08	5.1455e-03	3.0502e-06	462.28
2.1	0.14583	3.5719e-08	2.8938e-03	4.0674e-06	346.68

Table 5.2: Calculated Values of ρ_n and ρ_s using Energy Gap

Temp.	ρ	$E_g/atom$	ρ_n	ρ_s
(K)	gm/cc	K	gm/cc	gm/cc
0.2	0.14513	1.0405e-02	0.00000	0.14513
0.3	0.14513	1.0405e-02	0.00000	0.14513
0.4	0.14513	1.0405e-02	0.00000	0.14513
0.5	0.14513	1.0405e-02	0.00000	0.14513
0.6	0.14513	1.0405e-02	0.00000	0.14513
0.7	0.14513	1.0405e-02	0.00000	0.14513
0.8	0.14513	1.0405e-02	0.00000	0.14513
0.9	0.14512	1.0512e-02	0.00000	0.14512
1.0	0.14512	1.0512e-02	0.00000	0.14512
1.1	0.14511	1.0620e-02	0.00000	0.14511
1.2	0.14511	1.0620e-02	0.00000	0.14511
1.3	0.14512	1.0512e-02	0.00000	0.14512
1.4	0.14513	1.0405e-02	0.00000	0.14513
1.5	0.14516	1.0082e-02	0.00450	0.14066
1.6	0.14521	9.5455e-03	0.01199	0.13322
1.7	0.14526	9.0088e-03	0.01949	0.12577
1.8	0.14535	8.0429e-03	0.03299	0.11236
1.9	0.14546	6.8622e-03	0.04952	0.09594
2.0	0.14562	5.1455e-03	0.07360	0.07202
2.1	0.14583	2.8938e-03	0.10527	0.04056

Table 5.3: Calculated Values of ρ_n and ρ_s from the Excited Number of Particles

Temp.	ρ	λ_T	ρ_n	ρ_s
(K)	gm/cc	cm	gm/cc	gm/cc
0.2	0.14513	1.9523e-07	0.00000	0.14513
0.3	0.14513	1.5941e-07	0.00000	0.14513
0.4	0.14513	1.3805e-07	0.00000	0.14513
0.5	0.14513	1.2348e-07	0.00001	0.14512
0.6	0.14513	1.1272e-07	0.00004	0.14509
0.7	0.14513	1.0436e-07	0.00019	0.14494
0.8	0.14513	9.7617e-08	0.00059	0.14454
0.9	0.14512	9.2034e-08	0.00145	0.14367
1.0	0.14512	8.7311e-08	0.00299	0.14213
1.1	0.14511	8.3248e-08	0.00547	0.13964
1.2	0.14511	7.9704e-08	0.00912	0.13599
1.3	0.14512	7.6577e-08	0.01416	0.13096
1.4	0.14513	7.3791e-08	0.02080	0.12433
1.5	0.14516	7.1289e-08	0.02919	0.11597
1.6	0.14521	6.9025e-08	0.03949	0.10572
1.7	0.14526	6.6964e-08	0.05180	0.09346
1.8	0.14535	6.5078e-08	0.06620	0.07915
1.9	0.14546	6.3342e-08	0.08280	0.06266
2.0	0.14562	6.1738e-08	0.10164	0.04398
2.1	0.14583	6.0250e-08	0.12268	0.02315

Table 5.4: Normal and Super-fluid Density Ratio

Temp. (K)	$\rho_n^\star/\rho$	$\rho_s^\star/\rho$	$\rho_n^{\star\star}/\rho$	$\rho_s^{\star\star}/\rho$	$\rho_n^{\star\star\star}/\rho$	$\rho_s^{\star\star\star}/\rho$
0.0	0.0000	1.0000	0.0000	1.0000	0.0000	1.0000
0.1	0.0000	1.0000	0.0000	1.0000	0.0000	1.0000
0.2	0.0000	1.0000	0.0000	1.0000	0.0000	1.0000
0.3	0.0000	1.0000	0.0000	1.0000	0.0000	1.0000
0.4	0.0000	1.0000	0.0000	1.0000	0.0000	1.0000
0.5	0.0000	1.0000	0.0000	0.9999	0.0000	1.0000
0.6	0.0000	1.0000	0.0003	0.9997	0.0000	1.0000
0.7	0.0000	1.0000	0.0013	0.9987	0.0002	0.9998
0.8	0.0000	1.0000	0.0041	0.9959	0.0008	0.9992
0.9	0.0000	1.0000	0.0100	0.9900	0.0026	0.9974
1.0	0.0000	1.0000	0.0206	0.9794	0.0066	0.9934
1.1	0.0000	1.0000	0.0377	0.9623	0.0145	0.9855
1.2	0.0000	1.0000	0.0628	0.9372	0.0279	0.9722
1.3	0.0000	1.0000	0.0976	0.9023	0.0479	0.9521
1.4	0.0000	1.0000	0.1434	0.8566	0.0765	0.9235
1.5	0.1001	0.8999	0.2010	0.7990	0.1177	0.8824
1.6	0.1001	0.8999	0.2720	0.7281	0.1674	0.8326
1.7	0.2002	0.7998	0.3565	0.6435	0.2345	0.7655
1.8	0.3003	0.6997	0.4553	0.5447	0.3244	0.6756
1.9	0.4003	0.5997	0.5691	0.4309	0.4362	0.5638
2.0	0.6003	0.3997	0.6976	0.3024	0.5816	0.4184
2.1	0.8002	0.1998	0.8409	0.1591	0.7697	0.2303
2.2	1.0000	0.0000	1.0000	0.0000	1.0000	0.0000

$\star$ data are from table-5.2

$\star\star$ data are from table-5.3

$\star\star\star$ data are from ref. [43]

Table 5.5: Critical Angular Velocity and Other Quantities

T	ρ	ρ_s	E_g	r_o	ε_v	n_v	Ω_{c2}
(K)	(gm/cc)	(gm/cc)	(K)	(cm)	(ergs)	(cm^{-2})	$(rad\,sec^{-1})$
0.20	0.14513	0.14513	1.0405e-02	5.6762e-07	3.1753e-08	9.8754e+11	4.9232e+08
0.30	0.14513	0.14513	1.0405e-02	5.6762e-07	3.1753e-08	9.8754e+11	4.9232e+08
0.40	0.14513	0.14513	1.0405e-02	5.6762e-07	3.1753e-08	9.8754e+11	4.9232e+08
0.50	0.14513	0.14513	1.0405e-02	5.6762e-07	3.1753e-08	9.8754e+11	4.9232e+08
0.60	0.14513	0.14513	1.0405e-02	5.6762e-07	3.1753e-08	9.8754e+11	4.9232e+08
0.70	0.14513	0.14513	1.0405e-02	5.6762e-07	3.1753e-08	9.8754e+11	4.9232e+08
0.80	0.14513	0.14513	1.0405e-02	5.6762e-07	3.1753e-08	9.8754e+11	4.9232e+08
0.90	0.14512	0.14662	1.0512e-02	5.6407e-07	3.1679e-08	9.9999e+11	4.9853e+08
1.00	0.14512	0.14662	1.0512e-02	5.6407e-07	3.1679e-08	9.9999e+11	4.9853e+08
1.10	0.14511	0.14811	1.0620e-02	5.6057e-07	3.1605e-08	1.0125e+12	5.0477e+08
1.20	0.14511	0.14811	1.0620e-02	5.6057e-07	3.1605e-08	1.0125e+12	5.0477e+08
1.30	0.14512	0.14662	1.0512e-02	5.6407e-07	3.1679e-08	9.9999e+11	4.9853e+08
1.40	0.14513	0.14513	1.0405e-02	5.6762e-07	3.1753e-08	9.8754e+11	4.9232e+08
1.50	0.14516	0.14066	1.0082e-02	5.7862e-07	3.1980e-08	9.5036e+11	4.7378e+08
1.60	0.14521	0.13322	9.5455e-03	5.9822e-07	3.2374e-08	8.8911e+11	4.4325e+08
1.70	0.14526	0.12577	9.0088e-03	6.1960e-07	3.2789e-08	8.2878e+11	4.1318e+08
1.80	0.14535	0.11236	8.0429e-03	6.6360e-07	3.3598e-08	7.2254e+11	3.6021e+08
1.90	0.14546	0.09594	6.8622e-03	7.3006e-07	3.4723e-08	5.9696e+11	2.9761e+08
2.00	0.14562	0.07202	5.1455e-03	8.6675e-07	3.6739e-08	4.2352e+11	2.1114e+08
2.10	0.14583	0.04056	2.8938e-03	1.2156e-06	4.0696e-08	2.1534e+11	1.0735e+08

Table 5.6: Critical Velocities in Helium Film

	T	Flow rate	d	$v_c(average)$	v_c
	K	$cm^3/sec.cm$	cm	cm/sec	cm/sec
1	1.10	$16.9\,X10^{-5}$	$1.63\,X10^{-6}$	104	105
	1.30	16.9	1.63	104	110
	1.50	16.8	1.66	101	114
	1.70	16.1	1.82	88.5	118
	1.90	12.8	1.94	66	118
2	1.60	13.4	3.02	- -	54.1
3	1.3	-	2.0	-	37
4	1.47	7.4	1.9	-	39
		7.8	2.1	-	37
		8.15	2.3	-	35
4	1.25	-	-	-	25-40
5	1.50	-	6 layer	-	200
	1.60	-	8 layer	-	180
	1.80	-	11 layer	-	100

sets 1 and 2 from Ref [44]

set 3 from Ref [31]

set 4 from Ref [37]

set 5 from Ref [38]

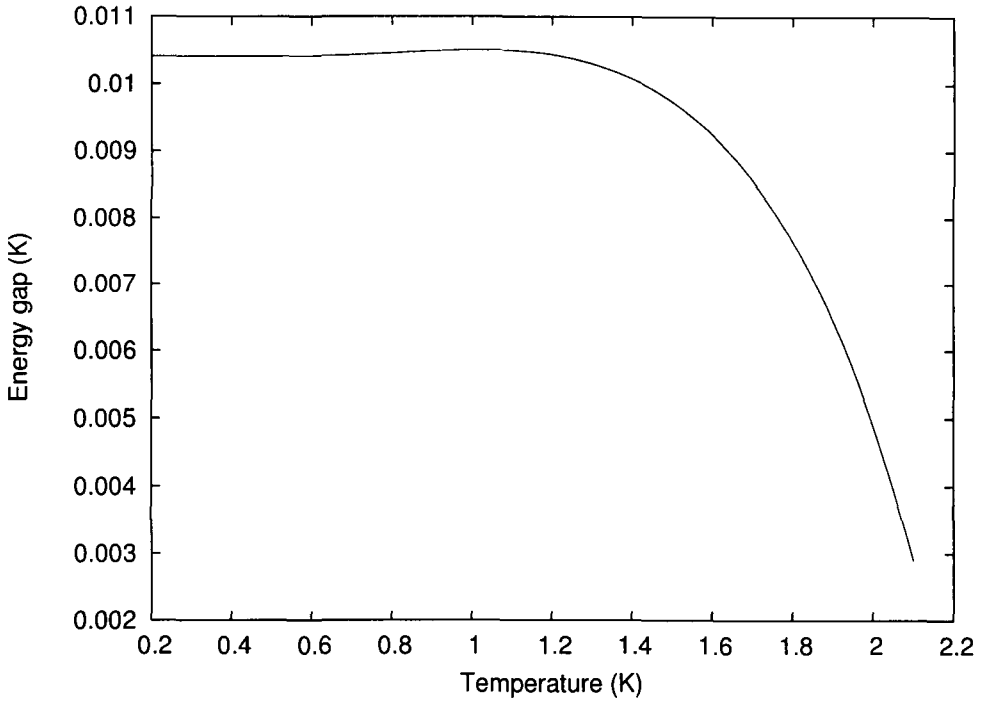

Figure 5.1: Energy gap of *helium-II* under saturated vapour pressure

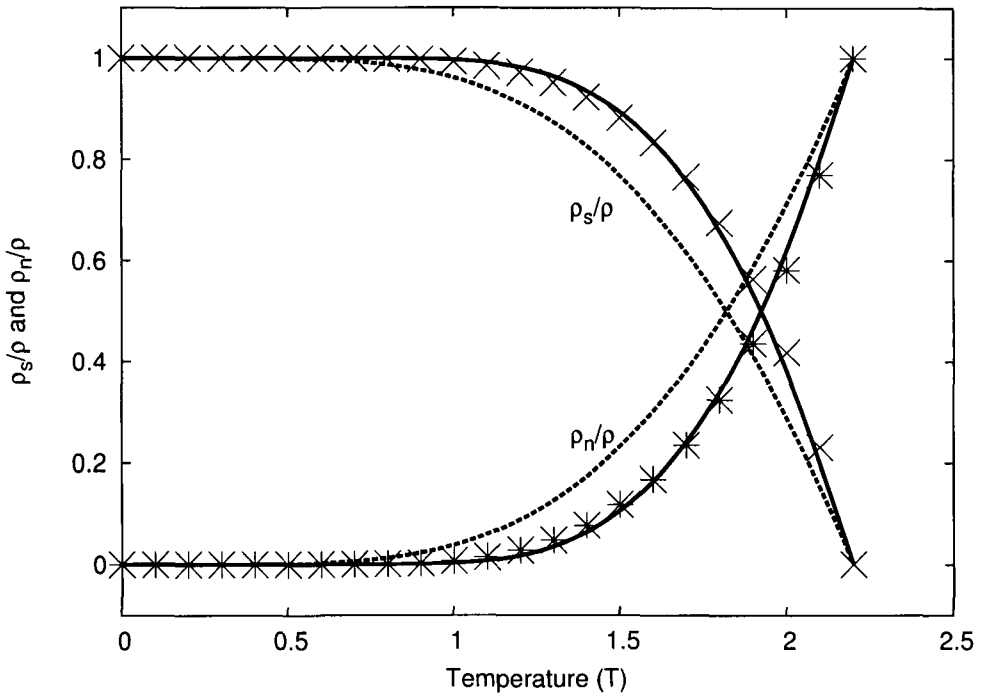

Figure 5.2: Normal and Super-fluid density ratio at saturated vapour pressure. Dotted and solid lines represent our calculated results (equations 5.4 and 5.5 respectively) and while the crosses and asteroids represent experimental points [43]

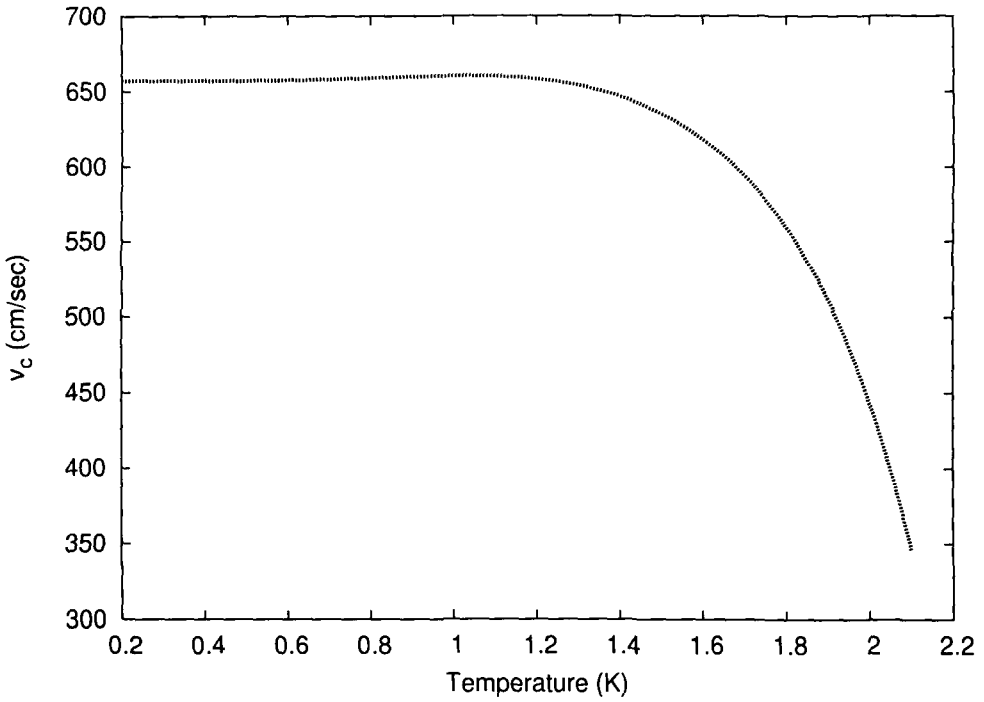

Figure 5.3: Temperature dependence of Critical Velocity of *helium-II*

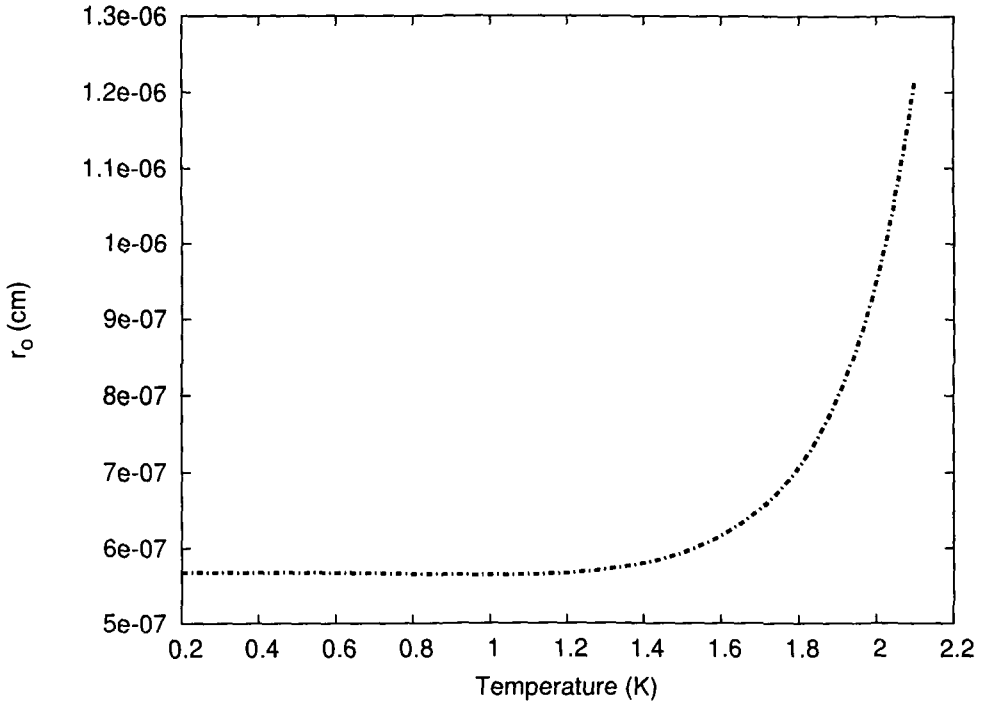

Figure 5.4: Radius of the vortex ring obtained from equation 5.28 for which rotational energy crosses the collective binding energy.

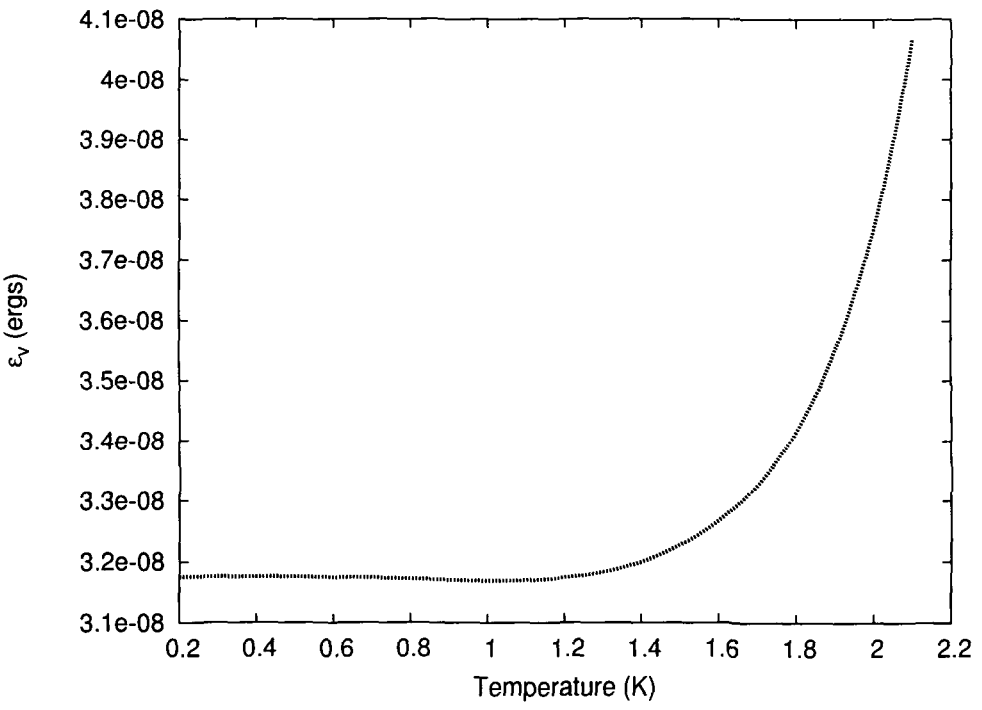

Figure 5.5: Temperature dependence of vortex energy as obtained replacing ρ_s by ρ and b by r_o in equation 5.16.

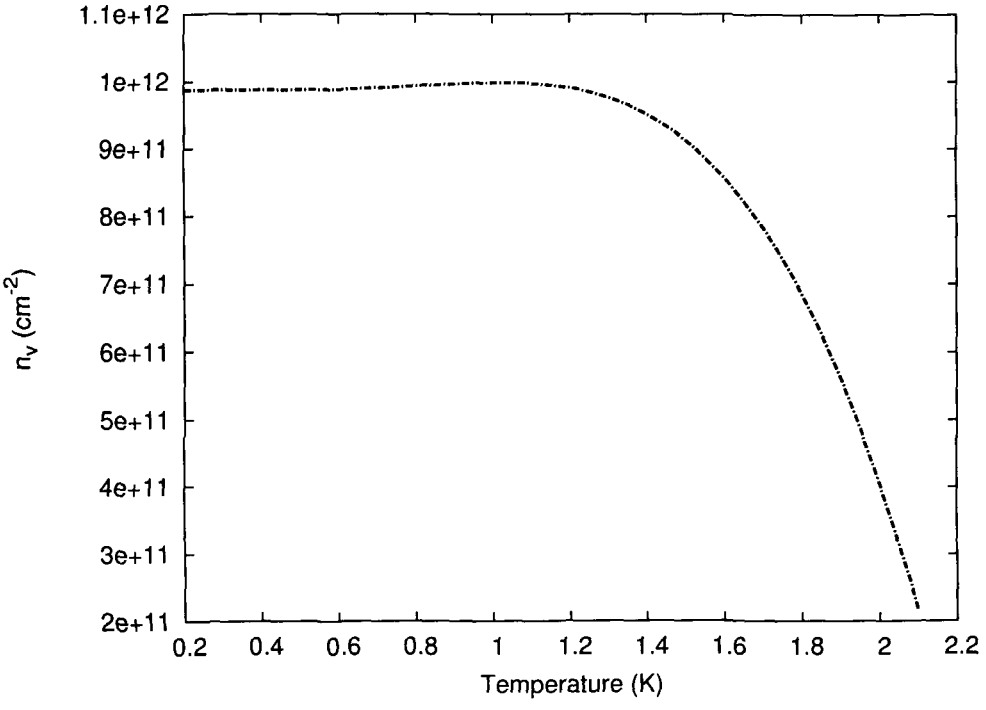

Figure 5.6: Density of vortex line as estimated from equation 5.25. For this value of n_v, superfluidity of the system loss completely.

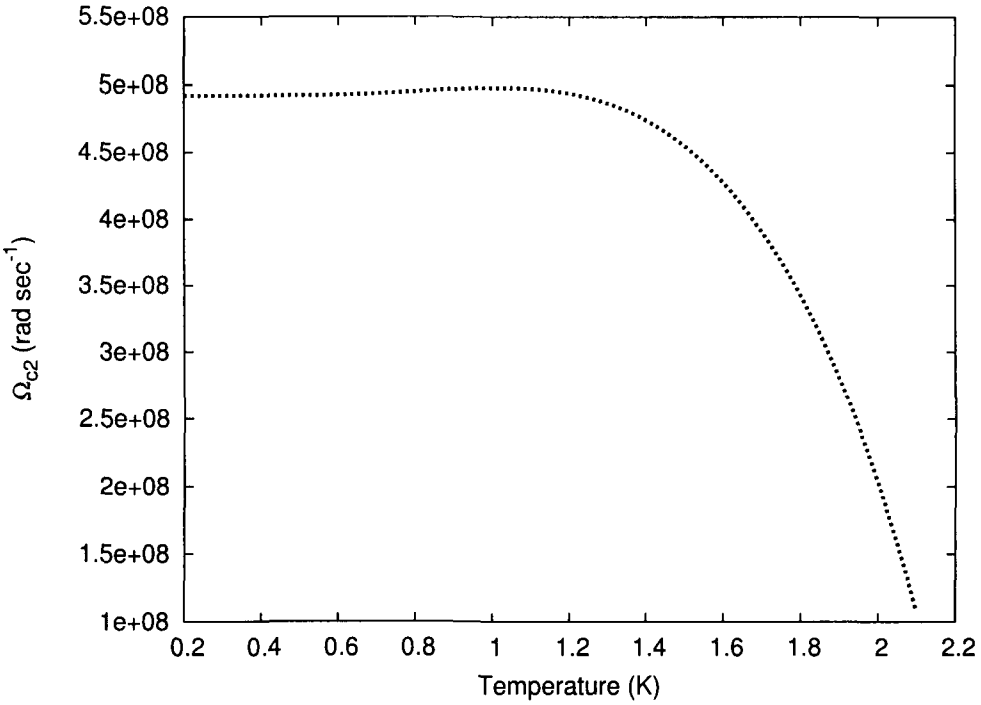

Figure 5.7: Values of higher critical angular velocity as obtained using n_v in equation 5.19. Beyond this critical angular velocity density of vortex line does not increase and the super-fluid get transformed into normal fluid.

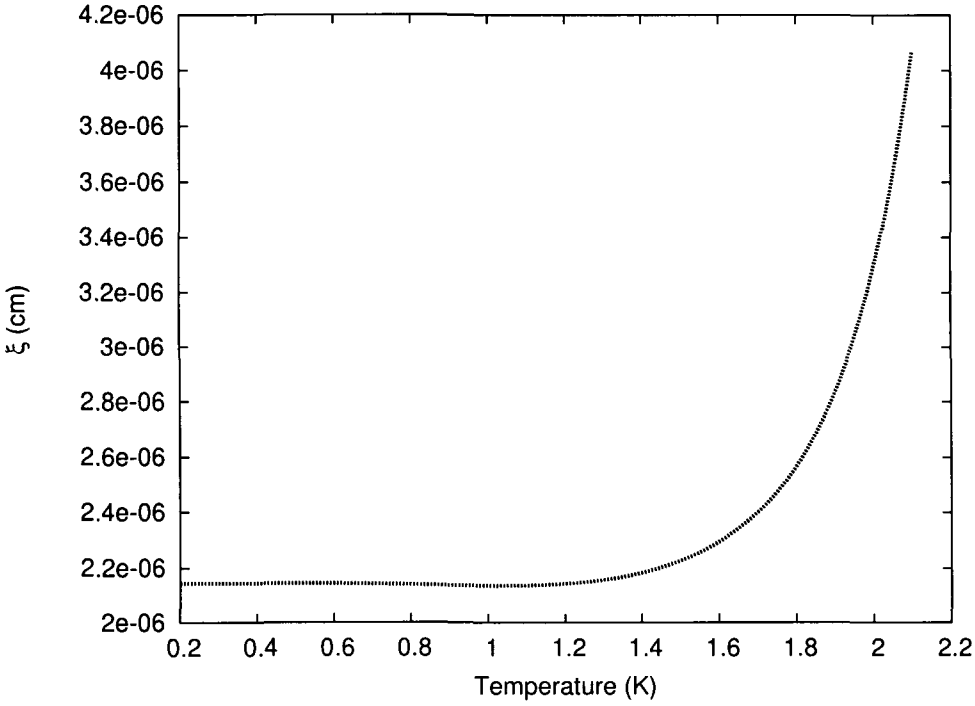

Figure 5.8: Temperature dependence of the coherence length of *helium-II*

Bibliography

[1] Y.S. Jain. *J. Sci. Expl.*, 16:77, 2002. More detailed version of this paper is available for ready reference as a paper entitled, *"Macro-orbitals and microscopic theory of a system of interacting bosons"* in www.arXiv.org/cond-mat/0606571.

[2] J. Wilks. *The Properties of Liquid and Solid Helium.* Clerendon Press, Oxford, 1967.

[3] J.G. Daunt and K. Mendelssohn. *Proc. Roy. Soc. London*, A 170:423,439, 1939.

[4] L.D. Landau. *J. Phys. U.S.S.R. (reprinted in Ref. 1)*, 5:71, 1941.

[5] Zygmunt M. Galasiewicz. *Helium-4.* Pragamon Press, Oxford, 1971.

[6] R.P. Feynman. In C.J. Gorter, editor, *Prog. Low Temp. Phys.*, volume I, page 1. North-Holland, Amsterdam, 1955.

[7] D.R. Tilley and J. Tilley. *Superfluidity and Superconductivity.* Adam Hisger Ltd., Bristol and Boston, 1986.

[8] W.I. Glaberson and R.J. Donnelly. *Phys. Rev.*, 141:208, 1966.

[9] D.F. Brewer and D.O. Edwards. *Phil. Mag.*, 6:775, 1961.

[10] P. Winkel, A.M.G. Delsing, and J.D. Poll. *Physica*, 21:331, 1955.

[11] F.A. Staas and K.W. Taconis. *Physica*, 27:924, 1961.

[12] W.F. Vinen. In Careri, editor, *Liquid Helium*, page 336. Academic Press, 1963.

[13] P.W. Anderson. *Rev. Mod. Phys.*, 38:298, 1966.

[14] O. Avenel and E. Varoquaux. *Phys. Rev. Lett.*, 55:2704, 1985.

[15] E. Varoquaux, M.W. Meisel, and O. Avenel. *Phys. Rev. Lett.*, 57:2291, 1986.

[16] B.P. Beecken and W. Zimmermann Jr. *Phys. Rev.*, B 35:74, 1987.

[17] B.P. Beecken and W. Zimmermann Jr. *Phys. Rev.*, B 35:1630, 1987.

[18] A. Amar, Y. Sasaki, R. Lozes, J.C. Davis, and R.E. Packard. *Phys. Rev. Lett.*, 68:2624, 1992.

[19] G.G. Ihas, O. Avenel, R. Aarts, R. Salmlin, and E. Varoquaux. *Phys. Rev. Lett.*, 69:327, 1992.

[20] J.C. Davis, J. Steinhauer, K. Schwab, Y. Mukharsky, A. Amar, Y. Sasaki, and R.E. Packard. *Phys. Rev. Lett.*, 69:323, 1992.

[21] W. Zimmermann Jr., O. Avenel, and E. Varoquaux. *Physica (Amsterdam)*, 165-166 B:749, 1990.

[22] E. Varoquaux, G.G. Ihas, O. Avenel, and R. Aarts. *Phys. Rev. Lett.*, 70:2114, 1993.

[23] S. Burkhart, M. Bernard, O. Avenel, and E. Varoquaux. *Phys. Rev. Lett.*, 72:380, 1994.

[24] J.D. Reppy and D.A. Depatie. *Phys. Rev. Lett.*, 12:187, 1964.

[25] J.D. Reppy. *Phys. Rev. Lett.*, 14:733, 1965.

[26] J.S. Langer and J.D. Reppy. In C.J. Gorter, editor, *Progress in Low Temperature Physics*, volume VI. North-Holland, Amsterdam, 1970.

[27] G.B. Hess. *Phys. Rev. Lett.*, 27:977, 1971.

[28] J.P. Hulin, D. D'Humieres, B. Perrin, and A. Libchaber. *Phys. Rev.*, A 9:885, 1974.

[29] K.R. Atkins. *Proc. Roy. Soc. London*, A 203:240, 1950.

[30] J.G. Daunt and R.S. Smith. *Rev. Mod. Phys.*, 25:172, 1954.

[31] W.C. Knudsen and J.R. Dillinger. *Phys. Rev.*, 91:489, 1953.

[32] W.C. Knudsen and J.R. Dillinger. *Phys. Rev.*, 95:279, 1954.

[33] B.S. Chandrasekhar and K. Mendelssohn. *Proc. Phys. Soc. London*, A 68:857, 1955.

[34] A.C. Ham and L.C. Jackson. *Proc. Roy. Soc. London*, A 240:243, 1957.

[35] L.C. Jackson and L.G. Grimes. *Advances in Physics*, 1:435, 1958.

[36] K.R. Atkins. *Liquid Helium.* Cambridge University Press, Cambridge, England, 1959.

[37] K.A. Pickar and K.R. Atkins. *Phys. Rev.*, 178:389, 1969.

[38] K. Telschow, I. Rudnick, and T.G. Wang. *Phys. Rev. Lett.*, 32:1292, 1974.

[39] L.C. Jackson and D.G. Henshaw. *Phil. Mag.*, 41:1078, 1950.

[40] L.C. Jackson and D.G. Henshaw. *Phil. Mag.*, 44:14, 1953.

[41] W.F. Vinen. In C.J. Gorter, editor, *Prog. Low Temp. Phys.*, volume III. North-Holland, Amsterdam, 1961.

[42] G.W. Rayfield and F. Reif. *Phys. Rev.*, 136:A 1194, 1964.

[43] R.J. Donnelly and C.F. Barenghi. *The Observed Properties of Liquid Helium at the Saturated Vapor Pressure.* www.darkwing.uoregon.edu, Universitas Oregonensis.

[44] J.G. Daunt and K. Mendelssohn. *Nature*, 143:719, 1939.

Chapter 6

Transition Temperature and Some Other Aspects of Liquid Helium-4

Abstract *In this chapter we estimate (i) transition temperature, (ii) absolute value of surface tension of LHE-4 and (iii) thickness of the surface layer by using Macro-orbital theory and emphasizing on the orderly arrangement of the atoms (sc, bcc, fcc and hcp arrangements) We estimate the potential energy using Leanard Jones potential Our estimated values closely agree with experiments*

6.1 Introduction

Liquid Helium-4 (LHE-4) have been studied extensively for its unique properties since its first liquification in 1908. Despite having a long and rich history of investigation, some of the key features of the system have remained unexplained. Transition temperature, surface tension at $T = 0$, surface layer thickness are few such features. In this chapter we shall try to address these aspects using Macro-orbital theory.

6.2 Transition Temperature

It was London [1,2] who initially proposed that the peculiar phase transition ("λ-transition"), that LHE-4 undergoes at $2.19\,K$ (value of T_λ estimated at that time), probably has to be regarded as the Bose-Einstein Condensation (BEC) of helium atoms, distorted, of course, by the presence of inter molecular forces and by the fact that it manifests itself in the liquid not in the gaseous state. To calculate T_λ he used the relation for critical temperature of the BEC in an ideal Bose gas i.e

$$T_{BEC} = \frac{h^2}{2\pi m k_B}\left(\frac{N}{V\zeta(3/2)}\right)^{2/3} \tag{6.1}$$

where m is the boson mass, N is the total number of atoms and V is the total volume. Using the liquid helium parameters and $\zeta(3/2) = 2.612$ he obtained $T_{BEC} = 3.13K$ which is about 44% higher than the observed value. This discrepency was attributed to the interactions of the helium atoms, effect of which was not included in London's calculation. However, it proved difficult to consider the interactions between atoms in analytical calculation of the BEC.

To develop a microscopic theory of LHE-4, the field theoretical approach starts with considering the system as weakly interacting Bose gas. Leading order effect of a weak two-body interaction on critical temperature (T_c) of a homogeneous weakly interacting Bose gas has been studied for long time and have been reviewed extensively by Haque [3] and Andersen [4]. Despite these efforts, no microscopic calculation renders the experimental value of T_c for LHE-4. Quite contrary to its observed $T_c = 2.17K$, the above mentioned calculations predict an increase in T_c compared to that of an ideal Bose gas. Lee and Yang [5] were the first to predict such an increase proportional to $\sqrt{a}$ (a being the scattering length). However,

they later predicted a shift linear with a [6] but without any definite sign (+/-) and magnitude of the shift. While Glassgold *et al* [7] predicted an increase in T_c similar to Lee and Yang [5], Huang [8] predicted an increase proportional to $a^{3/2}$. Huang's approach was used by Schakel [9] and Wilkens *et al* [10] who predicted a negative shift. Although all these calculations use perturbation theory, they render results which differ from each other significantly.

Using a different approach (normalized group calculation) Toyoda [11] predicted a shift in agreement with experimental value for LHE-4 (i.e. a negative shift in T_c) but in contradiction with the earlier findings [5, 7, 8]. However, using the same approach Bijlsma and Stoof [12] and Ledowski *et al* [13] found a positive shift. While Bijlsma and Stoof predicted a shift proportional to $alna$, calculation of Ledowski *et al* showed that leading behavior is proportional to a.

Fetter [14] used of Hartree-Fock theory and found a negative shift which, however, does not agree with the findings of Huang [15] who also used the same approach but obtained a positive shift proportional to $a^{1/2}$. Huang's conclusion was later criticized by Baym [16, 17] who included more terms in the expression to show that the result was an artifact of an approximation. Another treatment on these lines has been reported by Pethick and Smith [18].

More recently, Baym, Laloe and collaborators [16, 19–29] using effective-field theory showed that the parametric dependence of T_c is indeed linear in a i.e.

$$\frac{\Delta T_c}{T_{BEC}} = cn^{1/3}a \tag{6.2}$$

where ΔT_c is the shift in T_c from T_{BEC}. We note that the estimated values of the constant c in above equation fall in a wide range from 0.7 to 3.8 [4]. This fluctuation in c prompted Baym and his group to predict a logarithmic contribution at the next higher order [17].

Numerical calculations of T_c have been performed using the above effective-field theory with lattice gas model and Monte Carlo methods. Such calculations have been carried out by several groups [19, 21, 26–29].

Despite London's early work and voluminous work on weakly interacting dilute Bose gas, the question on the effect of the repulsive interactions on T_c (i.e. T_λ) of liquid helium remains unresolved. Only possible way to explain the observed $-ve$ shift in T_c for liquid helium was the use of effective mass of the

atoms in the liquid. Chapline [30] calculated a T_c which is quite close to actual $\lambda-$point of helium using a partition function calculated by Feynman [31] that takes into account the effective mass enhancement. After Chapline's work, this problem remained untouched until it is revisited by Jain [32] and Harada [33] very recently. Jain [32] explains the observed T_λ in his Macro-orbital theory (Chapter-2) while the idea of spontaneous symmetry breaking in a hard-core interacting Bose system is used by Harada; it may be noted that Jain's theory also attributes the $\lambda-$transition to spontaneous symmetry breaking.

6.2.1 Calculation of T_c using Macro-orbital Theory

Macro-orbital theory predicts a transition temperature (detailed discussion is presented in Chapter 2)

$$T_\lambda = T_o + \frac{1}{4}T_{BEC} = \frac{h^2}{8\pi m k_B}\left[\frac{1}{d^2} + \left(\frac{N}{2.16V}\right)^{2/3}\right] \tag{6.3}$$

where T_o is the temperature equivalent of ground state energy. We note that T_λ can be estimated simply by using d, which is the only unknown parameter in the above relation. We have calculated d for different possible atomic arrangements (i.e. sc, bcc, fcc and hcp) using the observed density $.14513\,gm/cc$ [34]. Macro-orbital theory explains the pressure dependence of the transition temperature replacing m by effective mass $m^\star$ which is expected to increase with pressure which increase inter-particle attraction.

6.2.2 Results and Discussions

Our calculation reveals $d = 3.5776\,, 3.9036\,, 4.0157$ and $4.0157\mathring{A}$, respectively, for sc, bcc, fcc and hcp atomic arrangements and corresponding values of T_λ as 2.271, 2.033, 1.964 and $1.964\,K$. Our estimated values deviate $4-12\%$ from the observed value $(2.172K)$ as against 40% deviation of London's estimation. Our results can be shown to agree exactly with the observed value if we replace real mass of the atom by its effective mass as used by Chapline [30]. We have found that the required effective mass is higher than the real mass of helium in case of sc arrangement (1.0511 times of the real mass) while it is lower in all other arrangements (it is $0.9410\,, 0.9092\,, and\, 0.9092$ times of real mass for bcc, fcc and

hcp arrangements respectively). Apparently our findings for bcc, fcc and hcp arrangements contradict with the idea of effective mass which is believed to increase inside the liquid due to the inertia of the system. However, the fact that particles of the system experience a repulsive force as soon as the system is cooled through T_λ may be responsible for the decrease of effective mass. Moreover, near T_λ the question regarding the specific arrangement of the atoms is unimportant because at this temperature the size of the atomic wave packet just crosses the inter-particle separation and the particles of the system have large fluctuations in their positions in normal, momentum and phase spaces. As the temperature of the system falls through T_λ the wave packets have mutual overlap and due to the repulsive nature of the inter-particle interaction the system assumes an orderly atomic arrangements. Near T_λ, what is more important is the average volume available to each atom, the T_c corresponding to sc arrangement assumes more relevance.

Although as mentioned above effective mass of an atom is expected to increase with pressure (P) due to increase in inter particle attraction, however, an exact relationship $m^\star$ and P is not known. The nature of the P dependence of $m^\star$ can therefore be determined by using the pressure dependent values of T_λ in equation 6.3. We estimated $m^\star$ for different atomic arrangements and presented our findings in Table-6.1 and figure 6.1. We observed a variation which is almost linear with pressure. In conclusion we find that Macro-orbital theory not only renders T_λ that agrees with experiments but also concludes that the shift in T_c has negative value. In addition it provides the microscopic origin for the pressure dependence of T_λ.

6.3 Surface Tension

Surface tension (σ) of *helium-II* has been extensively studied by experiment and theory since its first measurement by Urk *et al* [35] in 1925. This experimental study was followed by a large number of measurements, primarily with a goal of investigating the unusual temperature dependence of σ and its absolute value, $\sigma(0)$. These measurements used various techniques, *e.g.* the capillary rise method (Allen and Misener [36], Atkins and Narahara [37], Zinov'eva and Bolarev [38], Dickson *et al* [39]), the surface-wave method (King and Wyatt [40], Boldarev and Peshkov [41]) *etc.* While σ values obtained by Allen and Misener, Dickson

et al and King and Wyatt agree with each other and rendered an extrapolated $\sigma(0) \sim 0.350\, dynes/cm$ at 0 K, the data of Atkins *et al* and Zinov'eva *et al* yielded $\sigma(0) \sim 0.375\, dynes/cm$; the origin of this difference ($\sim 0.025\, dynes/cm$) is not well understood.

Similar difference is also observed in recent experiments. In 1985, Iino *et al* [42] measured σ of *helium-II* by the surface-wave resonance method and reported a $\sigma(0) = 0.354\, dynes/cm$ which is in good agreement with Allen and Misener, Dickson *et al* and King and Wyatt. Roche *et al* [43] obtained a value $0.375\, dynes/cm$ from the dispersion relation of a capillary wave at a micron wavelength. Roche *et al* explained that the difference with Iino *et al* arises due to the mass effect, i.e. the mass of the meniscus modifies the dispersion relation of the surface waves in the cavity. However, this explanation was negated by Nakanishi and Suzuki [44] who obtained the surface tension by eliminating the meniscus effect and found a value in agreement with Iino *et al.* Vicente *et al* [45] measured σ over a temperature range 0.6 to 1.6 K and from the extrapolation estimated $\sigma(o) = 0.375 \pm 4\, dynes/cm$.

The most successful theory that could give the temperature dependence of the surface tension of *helium-II* is the one due to Atkins [46], who, suggested that major contribution to the surface tension comes from the quantized surface modes of vibration (also referred to as "ripplons"). Atkins assumed that these surface modes should be similar in nature to the macroscopic capillary waves which have a frequency dependent phase velocity as given by

$$u = (2\pi\sigma\nu/\rho)^{1/3} \tag{6.4}$$

where ν is the frequency of the wave. Atkins chose a cutoff frequency ν_c such that the total number of normal modes of vibrations in the surface was equal to the total number of atoms in a monomolecular layer (of thickness δ) at the surface. According to Atkins theory, a part of the observed $\sigma(T)$ arises from the presence of quantized surface modes and accounts for the unusual temperature dependence. Considering these points for $T = 0$, Atkins obtained a relation

$$\sigma(0) = \sigma_i(0) + \frac{h}{7\pi^{1/4}} \left(\frac{8\sigma_i(0)}{\rho\delta^7} \right)^{1/2} \tag{6.5}$$

The second term on the right hand side represents the zero-point contribution to the surface modes. Using the experimental values of $\delta = d$ and $\sigma(0) = 0.370\, dynes/cm$, they obtained $\sigma_i(0) = 0.140\, dynes/cm$, which leaves about

$0.230\,dynes/cm$ as the contribution of the surface modes. At the nonzero temperature Atkins also found an added contribution of the surface modes expressed by

$$-0.0069\,T^{7/3}\,dynes/cm \tag{6.6}$$

An alternative explanation of the temperature dependence of the surface tension has been proposed by Singh [47], who used the ideal gas model for this liquid and enumerated the eigenfunctions in a bounded continuum so as to take into account the surface term. He obtained the temperature dependent part of the surface tension as

$$-0.0075\,T^{2}\,dynes/cm \tag{6.7}$$

$\sigma(0)$ has been calculated by different authors [48–59] using various methods such as Variational calculation, Variational Monte Carlo calculation etc. Using Gross and Pitaevski's imperfect-gas model, Brouwer and Pathria [48] obtained $\sigma(0)$ and surface layer thickness (t) after taking into account the contribution of quantized surface modes of vibration. Bowley [50] used modified Bijl-Jastrow wave function and performed a variational calculation to obtain the minimum surface energy and hence $\sigma(0)$. Shih and Woo [51] performed a fully microscopic calculation to determine the surface structure of *helium-II* and $\sigma(0)$. Chang and Cohen [52] calculated the surface energy and $\sigma(0)$ by taking into account the variation of the two particle-correlation function in the surface energy and minimizing it by a density profile. A Similar calculation was performed by Mackie and Woo [57]. Pandharipande *et al* [59] performed a Variational Monte Carlo (VMC) calculation of the ground states of *helium-II* drops containing $8 - 728$ atoms. More recently, Biben and Frenkel [60] used the density fluctuation theory of quantum fluids and Marin *et al* [61] applied Diffusion Monte Carlo method (DMC) to study the structure and energetics of the helium surface and hence σ.

6.3.1 Calculation of Potential Energy Using Macro-orbital Theory

Macro-orbital theory provides a simple way to calculate surface energy, surface tension and surface layer thickness. Macro-orbital theory shows that below the transition temperature the size of the wave packets associated with the atoms of the system exceeds the inter particle separation (d) (d^3 gives the volume available per atom which can be obtained from the density of the liquid) and as a result the particles get locked in the phase space and ordered in the real space. In the ordered

state, arrangement of the wave packets may be similar to the atomic arrangement sc, bcc, fcc, hcp or a mix state of these arrangements. Evidently, potential energy of an atom that arises from the inter molecular forces can be obtained using a standard potential available in the literature. In this regard we have used the Lennard-Jones potential

$$V(r_{ij}) = 4\epsilon \left[\left(\frac{\sigma}{r_{ij}} \right)^{12} - \left(\frac{\sigma}{r_{ij}} \right)^{6} \right] \tag{6.8}$$

with $\epsilon = 10.22K$ and $\sigma = 2.556\mathring{A}$ [62]. The parameters ϵ and σ depend on the polarizability and average dipole moment of an atom as well as on the core overlap. The potential energy of the system is obtained by summing up the potential of equation 6.8 over all i and j i.e. total potential

$$V = \frac{1}{2} \sum_{ij} V(r_{ij}) \tag{6.9}$$

The factor $\frac{1}{2}$ takes care of the repetition of i and j. If we express inter-particle distance r_{ij} in terms of nearest neighbour distance d as

$$r_{ij} = P_{ij} d \tag{6.10}$$

where P_{ij} is a multiplication factor and use equation 6.8 in equation 6.9, we find

$$V = 2\epsilon \left[\sum_{i,j \neq i} \left(\frac{\sigma}{P_{ij} d} \right)^{12} - \sum_{i,j \neq i} \left(\frac{\sigma}{P_{ij} d} \right)^{6} \right] \tag{6.11}$$

As in the orderly arrangement every atomic location is symmetric we find

$$V = 2N\epsilon \left[\left(\frac{\sigma}{d} \right)^{12} \sum_{j} \frac{1}{P_{ij}^{12}} - \left(\frac{\sigma}{d} \right)^{6} \sum_{j} \frac{1}{P_{ij}^{6}} \right] \tag{6.12}$$

which gives potential energy per particle V_o. However, for a particular value of P_{ij} there is a group of atoms and the expression for V_o can be simplified by combining the contribution from these atoms. If n_{ij} is the number atoms at distance $P_{ij}d$, contribution of these atoms to the potential of i^{th} particle is

$$V_o(P_{ij}) = 2\epsilon \left[\left(\frac{\sigma}{d} \right)^{12} \frac{n_{ij}}{P_{ij}^{12}} - \left(\frac{\sigma}{d} \right)^{12} \frac{n_{ij}}{P_{ij}^{6}} \right] \tag{6.13}$$

Total potential energy per particle can be estimated by considering the contribution from the atoms situated at all possible P_{ij}.

6.3.2 Calculation of Surface Energy

Equation 6.13 gives the potential energy when the atom is well within the liquid. However, potential energy per particle reduces on the surface because for every

P_{ij} there is lack of contribution from $(n_{ij} - n_p)/2$ atoms where n_p is the number of atoms at $P_{ij}d$ on the surface plane. Therefore, potential energy at an atomic location on the surface layer due to the atoms having same P_{ij} is

$$V_s(P_{ij}) = \frac{1}{2}(n_{ij} + n_p)V(P_{ij}) \tag{6.14}$$

Total potential energy is obtained by considering the contribution of all possible P_{ij}.

6.3.3 Calculation of Surface Tension

A conclusion from equation 6.13 and 6.14 is that an atom on the liquid surface is at higher potential in comparison to its counterpart well within the liquid. Excess energy on the liquid surface is

$$V_e(P_{ij}) = -\frac{n_{ij} - n_p}{2}V(P_{ij}) \tag{6.15}$$

and surface tension is the consequence of this excess energy. Surface tension, which is equal to the excess energy per unit area, can be estimated from the total excess energy associated with each particle (taking into the account the contribution from all possible P_{ij}) and surface area available for each atom on the surface.

6.3.4 Results and Discussions

Possible values of P_{ij} for different atomic arrangements are shown in Table-6.1 along with the total number of atoms n_{ij} at that neighbourhood. For a particular neighbourhood we have also tabulated the number of atoms (n_p) located in the same horizontal plane along with the number of atoms in the first, second and third horizontal plane (n_{p1}, n_{p2} and n_{p3}) respectively. Most of the atoms up to 10^{th} neighbourhood are located on these planes only.

The inter-atomic distance d depends on temperature and hence on density of the liquid. First we have calculated the lattice constant (a) for different atomic arrangement using the density (Ref [34]) in standard relations [63] and then used these values to obtain d. Temperature dependent values of d are shown in Table-6.3.

We have presented our calculated values of bulk potential, surface potential, and excess energy on the surface for sc, bcc, fcc and hcp arrangements in

Tables 6.4-6.15. Our calculation reveals that significant contribution towards the bulk potential comes only from the nearest neighbour atoms which is about 70% for sc, 65% for bcc, 83% for fcc and 84% for hcp arrangement. This contribution decreases rapidly with the distance and at 10^{th} atomic neighbourhood it reduces to 0.2%, 0.38%,0.16% and 0.55% of total potential for sc, bcc, fcc and hcp arrangements respectively. This indicates that contribution is less significant for higher neighbourhood distances. This justifies our results which include the contribution up to 10^{th} neighbourhood only.

Our potential energies are comparable to the results obtained from sophisticated computer calculations such as Green Function Monte Carlo (GFMC) method, Variational method *etc.* Table 6.16 shows a comparison of our findings with the results of few such calculation. We have observed about 12% increase in the magnitude of the potential energies for an increase in temperature from $T = 0$ to $T = 2.2\,K$. This change is associated with the change in density with temperature. Despite the fact that our estimated value of potential energy is slightly lower than the other estimations, physical picture of the system and calculation of the potential energies are much more simpler and clearer in our approach than the others.

In our model the system is considered to be free from thermal excitations and other kind of fluctuations. As a result the calculated surface tension is almost independent of temperature and the slight variation observed is due to the change of density with temperature. Our computed values represent $\sigma(0)$ (intrinsic surface tension which depends on the inter particle interaction, hence on inter particle separation) rather than $\sigma(T)$. We can include usual ripplon contribution (Equation 6.6) in our scheme to obtain the temperature dependent values of the surface tension. Our predicted σ at $T = 0$ (= 0.494, 0.518, 0.529 and 0.491 $dynes/cm$ for sc, bcc, fcc and hcp arrangements respectively) is higher than the two experimental values, $\sigma = 0.354\,dynes/cm$ [42] and $\sigma = 0.375\,dynes/cm$ [43, 45]. However, our estimation is comparable to other theoretical estimation which varies from 0.23 to 0.51 $dynes/cm$ (Table 6.19).

Another result which is comparable to experiment is the surface width t. Referring to Table 6.18 we find that for sc and hcp arrangements excess energy per particle in 2^{nd} atomic layer (from the surface layer) respectively becomes 0.44% and 0.12% of the excess energy per atom on the liquid surface. Corresponding

to bcc and fcc arrangements this energy becomes 0.26% and 0.48% in 3^{rd} layer. From these findings we predict a surface width twice of the atomic layer separation if the system follows sc or hcp arrangement and three times if the system follows bcc or fcc arrangement. Our estimated values for sc, bcc, fcc and hcp arrangements, respectively, are 7.16, 6.76, 8.52 and 6.56 $\mathring{A}$. Our estimated values for bcc and hcp arrangements are in good agreement with a recent experimental measure at $T = 0.44K$ for a 125 $\mathring{A}$ film, $t = 6.5 \pm 0.5\,\mathring{A}$ [64]. However, in an early experiment Osborne observed $t = 8.5 \pm 1.5\,\mathring{A}$ [65]. A comparison with other theoretical estimation is shown in Table 6.19.

6.4 Conclusion

Our investigation indicates that the effective mass of helium atom plays an important role on the pressure dependence of T_λ. While, as indicated from figure 6.1, this dependence is expected to be linear, its theoretical foundation may form a subject of a future investigation.

We have presented a simple calculation of $\sigma(0)$ based on Macro-orbital theory. Our $\sigma(0)$ estimates do not include the effects of parameters such as density variation and the change of atomic layer separation near the free surface of the liquid. Although we consider a static structure of the liquid, however, to a good approximation it seems to be valid for the liquid near the surface as indicated by a good agreement of our $\sigma(0)$ value with experiments. Noting the fact that our value ($\approx 495\,mdynes/cm$) is about 30% higher than experimental values $375\,mdynes/cm$ it may be stated that smaller density of helium atoms near the free surface could account for the difference. In this context it may be mentioned that this density falls from bulk value to its vapour density (relatively a very small value) over the three top atomic layers near the free surface. One may also relate the difference of our results with experiments to thermal fluctuations in density and the difference in zero point motions of atoms near the surface and in the bulk. However, the so called sophisticated theories also render $\sigma(0)$ values (Table 6.19) varying from 230 to $510\,mdynes/cm$. This not only indicates the inability of these theories in accurately accounting for the said fluctuations but also shows that our calculations are reasonably accurate. We hope that a future course of study which incorporates the said fluctuations with our model may help us in improving our results.

Table 6.1: Ratio of the estimated effective mass to real mass of the helium atom at different pressures. Effective mass is obtained using the observed transition temperature in equation 6.3

Pressure	T_c	ρ	Molar volume	m^*/m			
(in bar)	(K)	(gm/cc)	(cc/mole)	sc	bcc	fcc	hcp
0.050	2.172	0.14615	27.38	1.0511	0.9410	0.9092	0.9092
1.646	2.157	0.14927	26.81	1.0734	0.9610	0.9285	0.9285
7.328	2.095	0.15812	25.31	1.1485	1.0281	0.9934	0.9934
15.031	1.998	0.16710	23.95	1.2494	1.1185	1.0807	1.0807
18.180	1.954	0.17023	23.51	1.2935	1.1579	1.1188	1.1188
22.533	1.889	0.17423	22.97	1.3588	1.2165	1.1753	1.1753
25.868	1.836	0.17708	22.60	1.4133	1.2652	1.2224	1.2224
30.115	1.763	0.18044	22.18	1.4903	1.3342	1.2891	1.2891

Table 6.2: Values of P_{ij} and corresponding numbers of atoms

		Number of atoms			
	Total	0^{th}plane	1^{st}plane	2^{th}plane	3^{rd}plane
P_{ij}	n_{ij}	n_p	n_{p_1}	n_{p_2}	n_{p_3}
Simple Cubic					
1.000	6	4	2	0	0
1.414	12	4	8	0	0
1.732	8	0	8	0	0
2.000	6	4	0	2	0
2.236	24	8	8	8	0
2.449	24	0	16	8	0
2.824	12	4	0	8	0
3.000	30	4	8	16	2
3.162	24	8	8	0	8
3.317	24	0	16	0	8
Body Centred Cubic					
1.000	8	0	8	0	0
1.155	6	4	2	0	0
1.633	12	4	8	0	0
1.915	24	0	16	8	0
2.000	8	0	8	0	0
2.309	6	4	0	2	0
2.516	24	0	8	0	16
2.582	24	8	8	8	0
2.828	24	0	16	0	8
3.000	32	0	0	8	0

Contd.

	Number of atoms				
	Total	0^{th}plane	1^{st}plane	2^{th}plane	3^{rd}plane
P_{ij}	n_{ij}	n_p	n_{p_1}	n_{p_2}	n_{p_3}
Face Centred Cubic					
1.000	12	4	8	0	0
1.414	6	4	0	2	0
1.733	24	0	16	8	0
2.000	12	4	0	8	0
2.236	24	8	8	0	8
2.450	8	0	0	8	0
2.646	48	0	16	16	16
2.829	6	4	0	0	0
3.000	36	4	16	0	0
3.163	24	8	0	8	0
Hexagonal Closed Packed					
1.000	12	6	6	0	0
1.414	6	0	6	0	0
1.633	2	0	0	2	0
1.732	18	6	12	0	0
1.915	12	0	0	12	0
2.000	6	6	12	0	0
2.236	12	0	6	0	0
2.449	6	0	0	0	0
2.517	6	0	12	0	6
2.646	24	12	6	0	0

Table 6.3: Nearest neighbour distance for different atomic arrangements

Temp	ρ	Nearest Neighbour Distance (Å)			
(K)	gm/cc	sc	bcc	fcc	hcp
0.2	0.1451	3.5776	3.9036	4.0157	4.0157
0.3	0.1451	3.5776	3.9036	4.0157	4.0157
0.4	0.1451	3.5776	3.9036	4.0157	4.0157
0.5	0.1451	3.5776	3.9036	4.0157	4.0157
0.6	0.1451	3.5776	3.9036	4.0157	4.0157
0.7	0.1451	3.5776	3.9036	4.0157	4.0157
0.8	0.1451	3.5776	3.9036	4.0157	4.0157
0.9	0.1451	3.5777	3.9037	4.0158	4.0158
1.0	0.1451	3.5777	3.9037	4.0158	4.0158
1.1	0.1451	3.5778	3.9038	4.0159	4.0159
1.2	0.1451	3.5778	3.9038	4.0159	4.0159
1.3	0.1451	3.5777	3.9037	4.0158	4.0158
1.4	0.1451	3.5776	3.9036	4.0157	4.0157
1.5	0.1452	3.5773	3.9033	4.0154	4.0154
1.6	0.1452	3.5770	3.9030	4.0151	4.0151
1.7	0.1453	3.5764	3.9023	4.0144	4.0144
1.8	0.1453	3.5758	3.9016	4.0137	4.0137
1.9	0.1455	3.5748	3.9005	4.0126	4.0126
2.0	0.1456	3.5736	3.8992	4.0112	4.0112
2.1	0.1458	3.5719	3.8973	4.0093	4.0093
2.2	0.1461	3.5697	3.8949	4.0068	4.0068

Table 6.4: Potential energy for sc arrangement

T(K)	Potential energy per particle (K)									
	V_1	V_2	V_3	V_4	V_5	V_6	V_7	V_8	V_9	V_{10}
0.2	-14.14	-18.15	-18.96	-19.21	-19.73	-20.03	-20.10	-20.21	-20.28	-20.32
0.3	-14.14	-18.15	-18.96	-19.21	-19.73	-20.03	-20.10	-20.21	-20.28	-20.32
0.4	-14.14	-18.15	-18.96	-19.21	-19.73	-20.03	-20.10	-20.21	-20.28	-20.32
0.5	-14.14	-18.15	-18.96	-19.21	-19.73	-20.03	-20.10	-20.21	-20.28	-20.32
0.6	-14.14	-18.15	-18.96	-19.21	-19.73	-20.03	-20.10	-20.21	-20.28	-20.32
0.7	-14.14	-18.15	-18.96	-19.21	-19.73	-20.03	-20.10	-20.21	-20.28	-20.32
0.8	-14.14	-18.15	-18.96	-19.21	-19.73	-20.03	-20.10	-20.21	-20.28	-20.32
0.9	-14.14	-18.15	-18.95	-19.21	-19.73	-20.03	-20.10	-20.21	-20.27	-20.32
1.0	-14.14	-18.15	-18.95	-19.21	-19.73	-20.03	-20.10	-20.21	-20.27	-20.32
1.1	-14.14	-18.15	-18.95	-19.21	-19.73	-20.03	-20.09	-20.21	-20.27	-20.32
1.2	-14.14	-18.15	-18.95	-19.21	-19.73	-20.03	-20.09	-20.21	-20.27	-20.32
1.3	-14.14	-18.15	-18.95	-19.21	-19.73	-20.03	-20.10	-20.21	-20.27	-20.32
1.4	-14.14	-18.15	-18.96	-19.21	-19.73	-20.03	-20.10	-20.21	-20.28	-20.32
1.5	-14.15	-18.16	-18.96	-19.22	-19.74	-20.04	-20.11	-20.22	-20.28	-20.33
1.6	-14.15	-18.17	-18.97	-19.23	-19.75	-20.05	-20.12	-20.23	-20.29	-20.34
1.7	-14.16	-18.19	-18.99	-19.24	-19.77	-20.07	-20.13	-20.24	-20.31	-20.36
1.8	-14.18	-18.20	-19.01	-19.26	-19.78	-20.09	-20.15	-20.26	-20.33	-20.38
1.9	-14.20	-18.23	-19.03	-19.29	-19.81	-20.12	-20.18	-20.29	-20.36	-20.41
2.0	-14.22	-18.26	-19.07	-19.32	-19.85	-20.15	-20.22	-20.33	-20.40	-20.45
2.1	-14.26	-18.31	-19.12	-19.37	-19.90	-20.21	-20.27	-20.38	-20.45	-20.50
2.2	-14.30	-18.37	-19.18	-19.44	-19.97	-20.27	-20.34	-20.45	-20.52	-20.57

V_1, V_2, V_3 *etc.* are potential up to 1st, 2nd, 3rd neighbourhood respectively.

Table 6.5: Potential energy on the surface for sc arrangement

T(K)	Surface P.E. per Particle (K)									
	Vs_1	Vs_2	Vs_3	Vs_4	Vs_5	Vs_6	Vs_7	Vs_8	Vs_9	Vs_{10}
0.2	-11.78	-14.46	-14.86	-15.07	-15.42	-15.57	-15.61	-15.68	-15.72	-15.75
0.3	-11.78	-14.46	-14.86	-15.07	-15.42	-15.57	-15.61	-15.68	-15.72	-15.75
0.4	-11.78	-14.46	-14.86	-15.07	-15.42	-15.57	-15.61	-15.68	-15.72	-15.75
0.5	-11.78	-14.46	-14.86	-15.07	-15.42	-15.57	-15.61	-15.68	-15.72	-15.75
0.6	-11.78	-14.46	-14.86	-15.07	-15.42	-15.57	-15.61	-15.68	-15.72	-15.75
0.7	-11.78	-14.46	-14.86	-15.07	-15.42	-15.57	-15.61	-15.68	-15.72	-15.75
0.8	-11.78	-14.46	-14.86	-15.07	-15.42	-15.57	-15.61	-15.68	-15.72	-15.75
0.9	-11.78	-14.46	-14.86	-15.07	-15.42	-15.57	-15.61	-15.68	-15.72	-15.74
1.0	-11.78	-14.46	-14.86	-15.07	-15.42	-15.57	-15.61	-15.68	-15.72	-15.74
1.1	-11.78	-14.46	-14.86	-15.07	-15.42	-15.57	-15.61	-15.67	-15.72	-15.74
1.2	-11.78	-14.46	-14.86	-15.07	-15.42	-15.57	-15.61	-15.67	-15.72	-15.74
1.3	-11.78	-14.46	-14.86	-15.07	-15.42	-15.57	-15.61	-15.68	-15.72	-15.74
1.4	-11.78	-14.46	-14.86	-15.07	-15.42	-15.57	-15.61	-15.68	-15.72	-15.75
1.5	-11.79	-14.46	-14.87	-15.08	-15.43	-15.58	-15.62	-15.68	-15.73	-15.75
1.6	-11.79	-14.47	-14.87	-15.09	-15.43	-15.58	-15.63	-15.69	-15.73	-15.76
1.7	-11.80	-14.48	-14.89	-15.10	-15.45	-15.60	-15.64	-15.70	-15.75	-15.77
1.8	-11.81	-14.50	-14.90	-15.11	-15.46	-15.61	-15.66	-15.72	-15.76	-15.79
1.9	-11.83	-14.52	-14.92	-15.13	-15.48	-15.64	-15.68	-15.74	-15.79	-15.81
2.0	-11.85	-14.54	-14.95	-15.16	-15.51	-15.66	-15.71	-15.77	-15.81	-15.84
2.1	-11.88	-14.58	-14.99	-15.20	-15.55	-15.70	-15.75	-15.81	-15.85	-15.88
2.2	-11.92	-14.63	-15.03	-15.25	-15.60	-15.75	-15.80	-15.86	-15.91	-15.93

Table 6.6: Excess surface energy for sc arrangement

T(K)	Excess energy per particle (K)									
	Ve_1	Ve_2	Ve_3	Ve_4	Ve_5	Ve_6	Ve_7	Ve_8	Ve_9	Ve_{10}
0.2	2.36	3.69	4.10	4.14	4.31	4.46	4.48	4.53	4.55	4.58
0.3	2.36	3.69	4.10	4.14	4.31	4.46	4.48	4.53	4.55	4.58
0.4	2.36	3.69	4.10	4.14	4.31	4.46	4.48	4.53	4.55	4.58
0.5	2.36	3.69	4.10	4.14	4.31	4.46	4.48	4.53	4.55	4.58
0.6	2.36	3.69	4.10	4.14	4.31	4.46	4.48	4.53	4.55	4.58
0.7	2.36	3.69	4.10	4.14	4.31	4.46	4.48	4.53	4.55	4.58
0.8	2.36	3.69	4.10	4.14	4.31	4.46	4.48	4.53	4.55	4.58
0.9	2.36	3.69	4.09	4.14	4.31	4.46	4.48	4.53	4.55	4.58
1.0	2.36	3.69	4.09	4.14	4.31	4.46	4.48	4.53	4.55	4.58
1.1	2.36	3.69	4.09	4.14	4.31	4.46	4.48	4.53	4.55	4.58
1.2	2.36	3.69	4.09	4.14	4.31	4.46	4.48	4.53	4.55	4.58
1.3	2.36	3.69	4.09	4.14	4.31	4.46	4.48	4.53	4.55	4.58
1.4	2.36	3.69	4.10	4.14	4.31	4.46	4.48	4.53	4.55	4.58
1.5	2.36	3.70	4.10	4.14	4.31	4.46	4.49	4.53	4.56	4.58
1.6	2.36	3.70	4.10	4.14	4.32	4.47	4.49	4.54	4.56	4.58
1.7	2.36	3.70	4.10	4.15	4.32	4.47	4.49	4.54	4.56	4.59
1.8	2.36	3.70	4.11	4.15	4.32	4.48	4.50	4.55	4.57	4.59
1.9	2.37	3.71	4.11	4.16	4.33	4.48	4.50	4.55	4.57	4.60
2.0	2.37	3.72	4.12	4.16	4.34	4.49	4.51	4.56	4.58	4.61
2.1	2.38	3.73	4.13	4.17	4.35	4.50	4.52	4.57	4.59	4.62
2.2	2.38	3.74	4.15	4.19	4.36	4.52	4.54	4.59	4.61	4.64

Table 6.7: Potential energy for bcc arrangement

T(K)	Potential Energy per Particle (K)									
	V_1	V_2	V_3	V_4	V_5	V_6	V_7	V_8	V_9	V_{10}
0.2	-11.87	-15.82	-16.83	-17.62	-17.82	-17.88	-18.03	-18.16	-18.24	-18.31
0.3	-11.87	-15.82	-16.83	-17.62	-17.82	-17.88	-18.03	-18.16	-18.24	-18.31
0.4	-11.87	-15.82	-16.83	-17.62	-17.82	-17.88	-18.03	-18.16	-18.24	-18.31
0.5	-11.87	-15.82	-16.83	-17.62	-17.82	-17.88	-18.03	-18.16	-18.24	-18.31
0.6	-11.87	-15.82	-16.83	-17.62	-17.82	-17.88	-18.03	-18.16	-18.24	-18.31
0.7	-11.87	-15.82	-16.83	-17.62	-17.82	-17.88	-18.03	-18.16	-18.24	-18.31
0.8	-11.87	-15.82	-16.83	-17.62	-17.82	-17.88	-18.03	-18.16	-18.24	-18.31
0.9	-11.87	-15.81	-16.83	-17.61	-17.81	-17.88	-18.03	-18.16	-18.24	-18.31
1.0	-11.87	-15.81	-16.83	-17.61	-17.81	-17.88	-18.03	-18.16	-18.24	-18.31
1.1	-11.87	-15.81	-16.83	-17.61	-17.81	-17.88	-18.03	-18.16	-18.23	-18.30
1.2	-11.87	-15.81	-16.83	-17.61	-17.81	-17.88	-18.03	-18.16	-18.23	-18.30
1.3	-11.87	-15.81	-16.83	-17.61	-17.81	-17.88	-18.03	-18.16	-18.24	-18.31
1.4	-11.87	-15.82	-16.83	-17.62	-17.82	-17.88	-18.03	-18.16	-18.24	-18.31
1.5	-11.88	-15.82	-16.84	-17.62	-17.82	-17.89	-18.04	-18.17	-18.25	-18.32
1.6	-11.88	-15.83	-16.85	-17.63	-17.83	-17.90	-18.05	-18.18	-18.25	-18.33
1.7	-11.89	-15.84	-16.86	-17.65	-17.85	-17.91	-18.06	-18.20	-18.27	-18.34
1.8	-11.91	-15.86	-16.88	-17.67	-17.87	-17.93	-18.08	-18.21	-18.29	-18.36
1.9	-11.92	-15.88	-16.90	-17.69	-17.89	-17.96	-18.11	-18.24	-18.32	-18.39
2.0	-11.95	-15.91	-16.94	-17.73	-17.93	-17.99	-18.15	-18.28	-18.35	-18.43
2.1	-11.98	-15.96	-16.98	-17.77	-17.98	-18.04	-18.20	-18.33	-18.40	-18.47
2.2	-12.02	-16.01	-17.04	-17.84	-18.04	-18.10	-18.26	-18.39	-18.47	-18.54

Table 6.8: Potential energy on the surface for bcc arrangement

T(K)	Surface P.E. per particle (K)									
	Vs_1	Vs_2	Vs_3	Vs_4	Vs_5	Vs_6	Vs_7	Vs_8	Vs_9	Vs_{10}
0.2	-5.94	-9.22	-9.90	-10.29	-10.39	-10.44	-10.52	-10.61	-10.65	-10.68
0.3	-5.94	-9.22	-9.90	-10.29	-10.39	-10.44	-10.52	-10.61	-10.65	-10.68
0.4	-5.94	-9.22	-9.90	-10.29	-10.39	-10.44	-10.52	-10.61	-10.65	-10.68
0.5	-5.94	-9.22	-9.90	-10.29	-10.39	-10.44	-10.52	-10.61	-10.65	-10.68
0.6	-5.94	-9.22	-9.90	-10.29	-10.39	-10.44	-10.52	-10.61	-10.65	-10.68
0.7	-5.94	-9.22	-9.90	-10.29	-10.39	-10.44	-10.52	-10.61	-10.65	-10.68
0.8	-5.94	-9.22	-9.90	-10.29	-10.39	-10.44	-10.52	-10.61	-10.65	-10.68
0.9	-5.94	-9.22	-9.90	-10.29	-10.39	-10.44	-10.52	-10.61	-10.64	-10.68
1.0	-5.94	-9.22	-9.90	-10.29	-10.39	-10.44	-10.52	-10.61	-10.64	-10.68
1.1	-5.94	-9.22	-9.90	-10.29	-10.39	-10.44	-10.52	-10.60	-10.64	-10.68
1.2	-5.94	-9.22	-9.90	-10.29	-10.39	-10.44	-10.52	-10.60	-10.64	-10.68
1.3	-5.94	-9.22	-9.90	-10.29	-10.39	-10.44	-10.52	-10.61	-10.64	-10.68
1.4	-5.94	-9.22	-9.90	-10.29	-10.39	-10.44	-10.52	-10.61	-10.65	-10.68
1.5	-5.94	-9.23	-9.90	-10.29	-10.40	-10.45	-10.52	-10.61	-10.65	-10.69
1.6	-5.94	-9.23	-9.91	-10.30	-10.40	-10.45	-10.53	-10.62	-10.66	-10.69
1.7	-5.95	-9.24	-9.92	-10.31	-10.41	-10.46	-10.54	-10.63	-10.66	-10.70
1.8	-5.95	-9.25	-9.93	-10.32	-10.42	-10.47	-10.55	-10.64	-10.68	-10.71
1.9	-5.96	-9.26	-9.94	-10.34	-10.44	-10.49	-10.57	-10.65	-10.69	-10.73
2.0	-5.97	-9.28	-9.96	-10.36	-10.46	-10.51	-10.59	-10.68	-10.71	-10.75
2.1	-5.99	-9.30	-9.99	-10.38	-10.49	-10.54	-10.62	-10.70	-10.74	-10.78
2.2	-6.01	-9.34	-10.02	-10.42	-10.52	-10.58	-10.65	-10.74	-10.78	-10.82

Table 6.9: Excess surface energy for bcc arrangement

T(K)	Excess energy per particle (K)									
	Ve_1	Ve_2	Ve_3	Ve_4	Ve_5	Ve_6	Ve_7	Ve_8	Ve_9	Ve_{10}
0.2	5.94	6.59	6.93	7.32	7.42	7.44	7.51	7.56	7.59	7.63
0.3	5.94	6.59	6.93	7.32	7.42	7.44	7.51	7.56	7.59	7.63
0.4	5.94	6.59	6.93	7.32	7.42	7.44	7.51	7.56	7.59	7.63
0.5	5.94	6.59	6.93	7.32	7.42	7.44	7.51	7.56	7.59	7.63
0.6	5.94	6.59	6.93	7.32	7.42	7.44	7.51	7.56	7.59	7.63
0.7	5.94	6.59	6.93	7.32	7.42	7.44	7.51	7.56	7.59	7.63
0.8	5.94	6.59	6.93	7.32	7.42	7.44	7.51	7.56	7.59	7.63
0.9	5.94	6.59	6.93	7.32	7.42	7.43	7.51	7.55	7.59	7.63
1.0	5.94	6.59	6.93	7.32	7.42	7.43	7.51	7.55	7.59	7.63
1.1	5.94	6.59	6.93	7.32	7.42	7.43	7.51	7.55	7.59	7.63
1.2	5.94	6.59	6.93	7.32	7.42	7.43	7.51	7.55	7.59	7.63
1.3	5.94	6.59	6.93	7.32	7.42	7.43	7.51	7.55	7.59	7.63
1.4	5.94	6.59	6.93	7.32	7.42	7.44	7.51	7.56	7.59	7.63
1.5	5.94	6.60	6.93	7.33	7.43	7.44	7.51	7.56	7.60	7.63
1.6	5.94	6.60	6.94	7.33	7.43	7.44	7.52	7.56	7.60	7.64
1.7	5.95	6.61	6.94	7.34	7.44	7.45	7.53	7.57	7.61	7.64
1.8	5.95	6.61	6.95	7.34	7.45	7.46	7.53	7.58	7.61	7.65
1.9	5.96	6.62	6.96	7.36	7.46	7.47	7.54	7.59	7.63	7.66
2.0	5.97	6.63	6.98	7.37	7.47	7.48	7.56	7.60	7.64	7.68
2.1	5.99	6.65	6.99	7.39	7.49	7.50	7.58	7.62	7.66	7.70
2.2	6.01	6.67	7.02	7.42	7.52	7.53	7.61	7.65	7.69	7.72

Table 6.10: Potential energy for fcc arrangement

T(K)	Potential Energy per Particle (K)									
	V_1	V_2	V_3	V_4	V_5	V_6	V_7	V_8	V_9	V_{10}
0.2	-15.24	-16.25	-17.45	-17.71	-17.97	-18.02	-18.21	-18.23	-18.29	-18.32
0.3	-15.24	-16.25	-17.45	-17.71	-17.97	-18.02	-18.21	-18.23	-18.29	-18.32
0.4	-15.24	-16.25	-17.45	-17.71	-17.97	-18.02	-18.21	-18.23	-18.29	-18.32
0.5	-15.24	-16.25	-17.45	-17.71	-17.97	-18.02	-18.21	-18.23	-18.29	-18.32
0.6	-15.24	-16.25	-17.45	-17.71	-17.97	-18.02	-18.21	-18.23	-18.29	-18.32
0.7	-15.24	-16.25	-17.45	-17.71	-17.97	-18.02	-18.21	-18.23	-18.29	-18.32
0.8	-15.24	-16.25	-17.45	-17.71	-17.97	-18.02	-18.21	-18.23	-18.29	-18.32
0.9	-15.24	-16.25	-17.45	-17.71	-17.97	-18.02	-18.21	-18.22	-18.29	-18.32
1.0	-15.24	-16.25	-17.45	-17.71	-17.97	-18.02	-18.21	-18.22	-18.29	-18.32
1.1	-15.23	-16.25	-17.45	-17.70	-17.96	-18.01	-18.20	-18.22	-18.29	-18.32
1.2	-15.23	-16.25	-17.45	-17.70	-17.96	-18.01	-18.20	-18.22	-18.29	-18.32
1.3	-15.24	-16.25	-17.45	-17.71	-17.97	-18.02	-18.21	-18.22	-18.29	-18.32
1.4	-15.24	-16.25	-17.45	-17.71	-17.97	-18.02	-18.21	-18.23	-18.29	-18.32
1.5	-15.24	-16.26	-17.46	-17.71	-17.98	-18.03	-18.22	-18.23	-18.30	-18.33
1.6	-15.25	-16.26	-17.47	-17.72	-17.98	-18.04	-18.23	-18.24	-18.31	-18.34
1.7	-15.27	-16.28	-17.48	-17.74	-18.00	-18.05	-18.24	-18.26	-18.33	-18.36
1.8	-15.28	-16.30	-17.50	-17.76	-18.02	-18.07	-18.26	-18.28	-18.34	-18.38
1.9	-15.30	-16.32	-17.53	-17.79	-18.05	-18.10	-18.29	-18.31	-18.37	-18.41
2.0	-15.33	-16.35	-17.56	-17.82	-18.08	-18.13	-18.32	-18.34	-18.41	-18.44
2.1	-15.38	-16.40	-17.61	-17.87	-18.13	-18.18	-18.37	-18.39	-18.46	-18.49
2.2	-15.43	-16.45	-17.67	-17.93	-18.19	-18.25	-18.44	-18.45	-18.52	-18.56

Table 6.11: Potential energy on the surface for fcc arrangement

T(K)	Surface P.E. per Particle (K)									
	Vs_1	Vs_2	Vs_3	Vs_4	Vs_5	Vs_6	Vs_7	Vs_8	Vs_9	Vs_{10}
0.2	-10.16	-11.00	-11.60	-11.77	-11.95	-11.97	-12.07	-12.08	-12.12	-12.14
0.3	-10.16	-11.00	-11.60	-11.77	-11.95	-11.97	-12.07	-12.08	-12.12	-12.14
0.4	-10.16	-11.00	-11.60	-11.77	-11.95	-11.97	-12.07	-12.08	-12.12	-12.14
0.5	-10.16	-11.00	-11.60	-11.77	-11.95	-11.97	-12.07	-12.08	-12.12	-12.14
0.6	-10.16	-11.00	-11.60	-11.77	-11.95	-11.97	-12.07	-12.08	-12.12	-12.14
0.7	-10.16	-11.00	-11.60	-11.77	-11.95	-11.97	-12.07	-12.08	-12.12	-12.14
0.8	-10.16	-11.00	-11.60	-11.77	-11.95	-11.97	-12.07	-12.08	-12.12	-12.14
0.9	-10.16	-11.00	-11.60	-11.77	-11.95	-11.97	-12.07	-12.08	-12.12	-12.14
1.0	-10.16	-11.00	-11.60	-11.77	-11.95	-11.97	-12.07	-12.08	-12.12	-12.14
1.1	-10.16	-11.00	-11.60	-11.77	-11.94	-11.97	-12.06	-12.08	-12.11	-12.14
1.2	-10.16	-11.00	-11.60	-11.77	-11.94	-11.97	-12.06	-12.08	-12.11	-12.14
1.3	-10.16	-11.00	-11.60	-11.77	-11.95	-11.97	-12.07	-12.08	-12.12	-12.14
1.4	-10.16	-11.00	-11.60	-11.77	-11.95	-11.97	-12.07	-12.08	-12.12	-12.14
1.5	-10.16	-11.01	-11.61	-11.78	-11.95	-11.98	-12.07	-12.09	-12.12	-12.14
1.6	-10.17	-11.01	-11.61	-11.78	-11.96	-11.98	-12.08	-12.09	-12.13	-12.15
1.7	-10.18	-11.02	-11.62	-11.79	-11.97	-11.99	-12.09	-12.10	-12.14	-12.16
1.8	-10.19	-11.03	-11.64	-11.81	-11.98	-12.01	-12.10	-12.11	-12.15	-12.17
1.9	-10.20	-11.05	-11.65	-11.82	-12.00	-12.02	-12.12	-12.13	-12.17	-12.19
2.0	-10.22	-11.07	-11.68	-11.85	-12.02	-12.05	-12.14	-12.16	-12.19	-12.22
2.1	-10.25	-11.10	-11.71	-11.88	-12.06	-12.08	-12.18	-12.19	-12.23	-12.25
2.2	-10.29	-11.14	-11.75	-11.92	-12.10	-12.12	-12.22	-12.23	-12.27	-12.29

Table 6.12: Excess surface energy for fcc arrangement

T(K)	Excess energy per particle (K)									
	Ve_1	Ve_2	Ve_3	Ve_4	Ve_5	Ve_6	Ve_7	Ve_8	Ve_9	Ve_{10}
0.2	5.08	5.25	5.85	5.93	6.02	6.05	6.14	6.14	6.17	6.19
0.3	5.08	5.25	5.85	5.93	6.02	6.05	6.14	6.14	6.17	6.19
0.4	5.08	5.25	5.85	5.93	6.02	6.05	6.14	6.14	6.17	6.19
0.5	5.08	5.25	5.85	5.93	6.02	6.05	6.14	6.14	6.17	6.19
0.6	5.08	5.25	5.85	5.93	6.02	6.05	6.14	6.14	6.17	6.19
0.7	5.08	5.25	5.85	5.93	6.02	6.05	6.14	6.14	6.17	6.19
0.8	5.08	5.25	5.85	5.93	6.02	6.05	6.14	6.14	6.17	6.19
0.9	5.08	5.25	5.85	5.93	6.02	6.05	6.14	6.14	6.17	6.18
1.0	5.08	5.25	5.85	5.93	6.02	6.05	6.14	6.14	6.17	6.18
1.1	5.08	5.25	5.85	5.93	6.02	6.05	6.14	6.14	6.17	6.18
1.2	5.08	5.25	5.85	5.93	6.02	6.05	6.14	6.14	6.17	6.18
1.3	5.08	5.25	5.85	5.93	6.02	6.05	6.14	6.14	6.17	6.18
1.4	5.08	5.25	5.85	5.93	6.02	6.05	6.14	6.14	6.17	6.19
1.5	5.08	5.25	5.85	5.94	6.02	6.05	6.14	6.15	6.18	6.19
1.6	5.08	5.25	5.86	5.94	6.03	6.05	6.15	6.15	6.18	6.19
1.7	5.09	5.26	5.86	5.95	6.03	6.06	6.15	6.16	6.19	6.20
1.8	5.09	5.26	5.87	5.95	6.04	6.06	6.16	6.16	6.19	6.20
1.9	5.10	5.27	5.88	5.96	6.05	6.07	6.17	6.17	6.20	6.21
2.0	5.11	5.28	5.89	5.97	6.06	6.09	6.18	6.18	6.21	6.22
2.1	5.13	5.30	5.90	5.99	6.08	6.10	6.20	6.20	6.23	6.24
2.2	5.14	5.31	5.92	6.01	6.10	6.12	6.22	6.22	6.25	6.26

Table 6.13: Potential energy for hcp arrangement

T(K)	Potential Energy per Particle (K)									
	V_1	V_2	V_3	V_4	V_5	V_6	V_7	V_8	V_9	V_{10}
0.2	-15.23	-16.24	-16.38	-17.28	-17.61	-17.74	-17.87	-17.91	-17.94	-18.04
0.3	-15.23	-16.24	-16.38	-17.28	-17.61	-17.74	-17.87	-17.91	-17.94	-18.04
0.4	-15.23	-16.24	-16.38	-17.28	-17.61	-17.74	-17.87	-17.91	-17.94	-18.04
0.5	-15.23	-16.24	-16.38	-17.28	-17.61	-17.74	-17.87	-17.91	-17.94	-18.04
0.6	-15.23	-16.24	-16.38	-17.28	-17.61	-17.74	-17.87	-17.91	-17.94	-18.04
0.7	-15.23	-16.24	-16.38	-17.28	-17.61	-17.74	-17.87	-17.91	-17.94	-18.04
0.8	-15.23	-16.24	-16.38	-17.28	-17.61	-17.74	-17.87	-17.91	-17.94	-18.04
0.9	-15.22	-16.24	-16.38	-17.28	-17.61	-17.74	-17.87	-17.91	-17.94	-18.03
1.0	-15.22	-16.24	-16.38	-17.28	-17.61	-17.74	-17.87	-17.91	-17.94	-18.03
1.1	-15.22	-16.23	-16.38	-17.28	-17.61	-17.74	-17.87	-17.91	-17.94	-18.03
1.2	-15.22	-16.23	-16.38	-17.28	-17.61	-17.74	-17.87	-17.91	-17.94	-18.03
1.3	-15.22	-16.24	-16.38	-17.28	-17.61	-17.74	-17.87	-17.91	-17.94	-18.03
1.4	-15.23	-16.24	-16.38	-17.28	-17.61	-17.74	-17.87	-17.91	-17.94	-18.04
1.5	-15.23	-16.24	-16.39	-17.29	-17.62	-17.75	-17.88	-17.92	-17.95	-18.04
1.6	-15.24	-16.25	-16.39	-17.30	-17.63	-17.76	-17.89	-17.93	-17.96	-18.05
1.7	-15.25	-16.27	-16.41	-17.32	-17.65	-17.77	-17.90	-17.94	-17.97	-18.07
1.8	-15.27	-16.28	-16.43	-17.33	-17.66	-17.79	-17.92	-17.96	-17.99	-18.09
1.9	-15.29	-16.31	-16.45	-17.36	-17.69	-17.82	-17.95	-17.99	-18.02	-18.12
2.0	-15.32	-16.34	-16.48	-17.39	-17.73	-17.85	-17.99	-18.02	-18.06	-18.15
2.1	-15.36	-16.38	-16.53	-17.44	-17.77	-17.90	-18.03	-18.07	-18.10	-18.20
2.2	-15.41	-16.44	-16.59	-17.50	-17.84	-17.96	-18.10	-18.14	-18.17	-18.26

Table 6.14: Potential energy on the surface for hcp arrangement

T(K)	Surface P.E. per particle (K)									
	Vs_1	Vs_2	Vs_3	Vs_4	Vs_5	Vs_6	Vs_7	Vs_8	Vs_9	Vs_{10}
0.2	-11.42	-11.93	-12.00	-12.60	-12.76	-12.89	-12.96	-12.98	-12.99	-13.06
0.3	-11.42	-11.93	-12.00	-12.60	-12.76	-12.89	-12.96	-12.98	-12.99	-13.06
0.4	-11.42	-11.93	-12.00	-12.60	-12.76	-12.89	-12.96	-12.98	-12.99	-13.06
0.5	-11.42	-11.93	-12.00	-12.60	-12.76	-12.89	-12.96	-12.98	-12.99	-13.06
0.6	-11.42	-11.93	-12.00	-12.60	-12.76	-12.89	-12.96	-12.98	-12.99	-13.06
0.7	-11.42	-11.93	-12.00	-12.60	-12.76	-12.89	-12.96	-12.98	-12.99	-13.06
0.8	-11.42	-11.93	-12.00	-12.60	-12.76	-12.89	-12.96	-12.98	-12.99	-13.06
0.9	-11.42	-11.92	-11.99	-12.60	-12.76	-12.89	-12.96	-12.97	-12.99	-13.06
1.0	-11.42	-11.92	-11.99	-12.60	-12.76	-12.89	-12.96	-12.97	-12.99	-13.06
1.1	-11.42	-11.92	-11.99	-12.60	-12.76	-12.89	-12.95	-12.97	-12.99	-13.06
1.2	-11.42	-11.92	-11.99	-12.60	-12.76	-12.89	-12.95	-12.97	-12.99	-13.06
1.3	-11.42	-11.92	-11.99	-12.60	-12.76	-12.89	-12.96	-12.97	-12.99	-13.06
1.4	-11.42	-11.93	-12.00	-12.60	-12.76	-12.89	-12.96	-12.98	-12.99	-13.06
1.5	-11.42	-11.93	-12.00	-12.60	-12.77	-12.90	-12.96	-12.98	-13.00	-13.07
1.6	-11.43	-11.94	-12.01	-12.61	-12.78	-12.90	-12.97	-12.99	-13.00	-13.07
1.7	-11.44	-11.95	-12.02	-12.62	-12.79	-12.91	-12.98	-13.00	-13.02	-13.09
1.8	-11.45	-11.96	-12.03	-12.63	-12.80	-12.93	-12.99	-13.01	-13.03	-13.10
1.9	-11.47	-11.98	-12.05	-12.65	-12.82	-12.95	-13.01	-13.03	-13.05	-13.12
2.0	-11.49	-12.00	-12.07	-12.68	-12.85	-12.97	-13.04	-13.06	-13.07	-13.15
2.1	-11.52	-12.03	-12.10	-12.71	-12.88	-13.01	-13.07	-13.09	-13.11	-13.18
2.2	-11.56	-12.07	-12.15	-12.76	-12.92	-13.05	-13.12	-13.14	-13.15	-13.23

Table 6.15: Excess surface energy for hcp arrangement

T(K)	Excess Energy per Particle (K)									
	Ve_1	Ve_2	Ve_3	Ve_4	Ve_5	Ve_6	Ve_7	Ve_8	Ve_9	Ve_{10}
0.2	3.81	4.31	4.38	4.69	4.85	4.85	4.92	4.93	4.95	4.97
0.3	3.81	4.31	4.38	4.69	4.85	4.85	4.92	4.93	4.95	4.97
0.4	3.81	4.31	4.38	4.69	4.85	4.85	4.92	4.93	4.95	4.97
0.5	3.81	4.31	4.38	4.69	4.85	4.85	4.92	4.93	4.95	4.97
0.6	3.81	4.31	4.38	4.69	4.85	4.85	4.92	4.93	4.95	4.97
0.7	3.81	4.31	4.38	4.69	4.85	4.85	4.92	4.93	4.95	4.97
0.8	3.81	4.31	4.38	4.69	4.85	4.85	4.92	4.93	4.95	4.97
0.9	3.81	4.31	4.38	4.68	4.85	4.85	4.91	4.93	4.95	4.97
1.0	3.81	4.31	4.38	4.68	4.85	4.85	4.91	4.93	4.95	4.97
1.1	3.81	4.31	4.38	4.68	4.85	4.85	4.91	4.93	4.95	4.97
1.2	3.81	4.31	4.38	4.68	4.85	4.85	4.91	4.93	4.95	4.97
1.3	3.81	4.31	4.38	4.68	4.85	4.85	4.91	4.93	4.95	4.97
1.4	3.81	4.31	4.38	4.69	4.85	4.85	4.92	4.93	4.95	4.97
1.5	3.81	4.31	4.39	4.69	4.85	4.85	4.92	4.94	4.95	4.98
1.6	3.81	4.32	4.39	4.69	4.85	4.85	4.92	4.94	4.95	4.98
1.7	3.81	4.32	4.39	4.69	4.86	4.86	4.92	4.94	4.96	4.98
1.8	3.82	4.32	4.40	4.70	4.86	4.86	4.93	4.95	4.96	4.99
1.9	3.82	4.33	4.40	4.71	4.87	4.87	4.94	4.96	4.97	5.00
2.0	3.83	4.34	4.41	4.71	4.88	4.88	4.95	4.97	4.98	5.01
2.1	3.84	4.35	4.42	4.73	4.89	4.89	4.96	4.98	5.00	5.02
2.2	3.85	4.37	4.44	4.74	4.91	4.91	4.98	5.00	5.01	5.04

Table 6.16: Comparison of our computed potential energies of *helium-II* (in units of K/atom) at T=0 with some other theoretical as well as experimental results.

Authors(year)	Reference	Potential	Method	Potential Energy
McMillan (1965)	[66]	Lennard-Jones	Variational	-19.82
Schiff and Verlet (1967)	[67]	Lennard-Jones	Variational	-19.46
Massey and Woo(1967)	[68]	Lennard-Jones	Variational	-20.32
Whitlock *et al* (1979)	[69]	Lennard-Jones	GFMC	-20.47
Gaglione *et al*(1980)	[70]	Lennard-Jones	Variational	-20.06
Kalos *et al* (1981)	[62]	Lennard-Jones	GFMC	-20.47
Kalos *et al* (1981)	[62]	HFDHE2	GFMC	-21.59
Usmani *et al* (1982)	[71]	HFDHE2	Variational	-21.73
Sears (1983)($T = 1.00$ K)	[72]	HFDHE2	Experimental	-21.29
This work		Lennard-Jones		-20.32 (sc)
				-18.31 (bcc)
				-18.32 (fcc)
				-18.04 (hcp)

Table 6.17: Calculated values of the surface tension of *helium-II* at different temperatures. These values do not include the contribution of ripplon or thermal disturbance present in the system

Temp (K)	Surface tension (dynes/cm)			
	sc	bcc	fcc	hcp
0.20	0.4937	0.5181	0.5293	0.4915
0.30	0.4937	0.5181	0.5293	0.4915
0.40	0.4937	0.5181	0.5293	0.4915
0.50	0.4937	0.5181	0.5293	0.4915
0.60	0.4937	0.5181	0.5293	0.4915
0.70	0.4937	0.5181	0.5293	0.4915
0.80	0.4937	0.5181	0.5293	0.4915
0.90	0.4936	0.5180	0.5292	0.4914
1.00	0.4936	0.5180	0.5292	0.4914
1.10	0.4935	0.5179	0.5291	0.4914
1.20	0.4935	0.5179	0.5291	0.4914
1.30	0.4936	0.5180	0.5292	0.4914
1.40	0.4937	0.5181	0.5293	0.4915
1.50	0.4939	0.5184	0.5296	0.4918
1.60	0.4943	0.5188	0.5300	0.4921
1.70	0.4949	0.5194	0.5306	0.4927
1.80	0.4956	0.5201	0.5314	0.4934
1.90	0.4966	0.5212	0.5325	0.4945
2.00	0.4979	0.5226	0.5339	0.4958
2.10	0.4997	0.5245	0.5358	0.4976

Table 6.18: Excess energy (in units of $K/atom$) at different atomic layers

	for simple cubic				for body centred cubic			
T(K)	surface	below surface layer			surface	below surface layer		
	layer	1^{st}	2^{nd}	3^{rd}	layer	1^{st}	2^{nd}	3^{rd}
0.2	4.58	0.25	0.02	0.00	7.63	0.28	0.08	0.02
0.3	4.58	0.25	0.02	0.00	7.63	0.28	0.08	0.02
0.4	4.58	0.25	0.02	0.00	7.63	0.28	0.08	0.02
0.5	4.58	0.25	0.02	0.00	7.63	0.28	0.08	0.02
0.6	4.58	0.25	0.02	0.00	7.63	0.28	0.08	0.02
0.7	4.58	0.25	0.02	0.00	7.63	0.28	0.08	0.02
0.8	4.58	0.25	0.02	0.00	7.63	0.28	0.08	0.02
0.9	4.58	0.25	0.02	0.00	7.63	0.28	0.08	0.02
1.0	4.58	0.25	0.02	0.00	7.63	0.28	0.08	0.02
1.1	4.58	0.25	0.02	0.00	7.63	0.28	0.08	0.02
1.2	4.58	0.25	0.02	0.00	7.63	0.28	0.08	0.02
1.3	4.58	0.25	0.02	0.00	7.63	0.28	0.08	0.02
1.4	4.58	0.25	0.02	0.00	7.63	0.28	0.08	0.02
1.5	4.58	0.25	0.02	0.00	7.63	0.28	0.08	0.02
1.6	4.58	0.25	0.02	0.00	7.64	0.28	0.08	0.02
1.7	4.59	0.25	0.02	0.00	7.64	0.28	0.08	0.02
1.8	4.59	0.25	0.02	0.00	7.65	0.28	0.08	0.02
1.9	4.60	0.25	0.02	0.00	7.66	0.28	0.08	0.02
2.0	4.61	0.26	0.02	0.00	7.68	0.29	0.08	0.02
2.1	4.62	0.26	0.02	0.00	7.70	0.29	0.08	0.02
2.2	4.64	0.26	0.02	0.00	7.72	0.29	0.08	0.02

Contd.

	for face centred cubic				for hexagonal closed packed			
T(K)	surface	below surface layer			surface	below surface layer		
	layer	1^{st}	2^{nd}	3^{rd}	layer	1^{st}	2^{nd}	3^{rd}
0.2	6.19	1.17	0.16	0.03	8.62	0.24	0.01	0.00
0.3	6.19	1.17	0.16	0.03	8.62	0.24	0.01	0.00
0.4	6.19	1.17	0.16	0.03	8.62	0.24	0.01	0.00
0.5	6.19	1.17	0.16	0.03	8.62	0.24	0.01	0.00
0.6	6.19	1.17	0.16	0.03	8.62	0.24	0.01	0.00
0.7	6.19	1.17	0.16	0.03	8.62	0.24	0.01	0.00
0.8	6.19	1.17	0.16	0.03	8.62	0.24	0.01	0.00
0.9	6.18	1.17	0.16	0.03	8.62	0.24	0.01	0.00
1.0	6.18	1.17	0.16	0.03	8.62	0.24	0.01	0.00
1.1	6.18	1.17	0.16	0.03	8.62	0.24	0.01	0.00
1.2	6.18	1.17	0.16	0.03	8.62	0.24	0.01	0.00
1.3	6.18	1.17	0.16	0.03	8.62	0.24	0.01	0.00
1.4	6.19	1.17	0.16	0.03	8.62	0.24	0.01	0.00
1.5	6.19	1.17	0.16	0.03	8.63	0.24	0.01	0.00
1.6	6.19	1.17	0.16	0.03	8.63	0.24	0.01	0.00
1.7	6.20	1.17	0.16	0.03	8.64	0.24	0.01	0.00
1.8	6.20	1.17	0.16	0.03	8.65	0.24	0.01	0.00
1.9	6.21	1.18	0.16	0.03	8.66	0.24	0.01	0.00
2.0	6.22	1.18	0.16	0.03	8.67	0.24	0.01	0.00
2.1	6.24	1.18	0.17	0.03	8.70	0.24	0.01	0.00
2.2	6.26	1.19	0.17	0.03	8.72	0.24	0.01	0.00

Table 6.19: Comparison of our calculated surface tension and surface thickness at $T = 0$ with some other theoretical calculation and experimental observations

Authors	Reference	Surface thickness (t) ($\AA$)	Surface tension ($dynes/cm$)
Theoretical estimations			
Brouwer and Pathria (1967)	[48]	2.0	0.28
Fitts (1969)	[49]	11.5	-
Bowley (1970)	[50]	2.0	0.51
Shih and Woo (1973)	[51]	2.4	0.36
Chang and Cohen (1973)	[52]	4.5	0.40
Padmore and Cole (1974)	[73]	6.9	-
Liu *et al* (1975)	[53]	5.0	0.29
Ebner and Saam (1975)	[54]	7.8	0.38
Lekner and Henderson (1978)	[56]	3.9	0.43
Mackie and Woo (1978)	[57]	-	0.33
Saarela *et al* (1983)	[58]	6.0	0.23
Pandharipande *et al* (1986)	[59]	7	0.43
Krotschek *et al* (1987)	[74]	About 6	-
Valles and Schmidt (1988)	[75]	4	0.366
Galli and Reatto (2000) (for slabs)	[76]	4.8	.429
(for drops)		7.8	-
Biben and Frankel (2002)	[60]	6.0	0.382
Experimental Values			
Atkins and Narahara (1965)	[37]	-	0.3729
Edwards *et al* (1975)	[77]	-	0.378
Iino *et al* (1985)	[42]	-	0.354
Osborne (1989)	[65]	8.5±1.5	-
Roche *et al* (1997)	[43]	-	0.375
Nakanishi and Suzuki (1998)	[44]	-	0.354
Penanen *et al* (2000)	[64]	6.5±0.5	-
Vicente *et al* (2002)	[45]	-	0.375
This work			
simple cubic		~7.16	0.494
body centred		~6.76	0.518
face centred		~8.52	0.529
hexagonal closed packed		~6.56	0.491

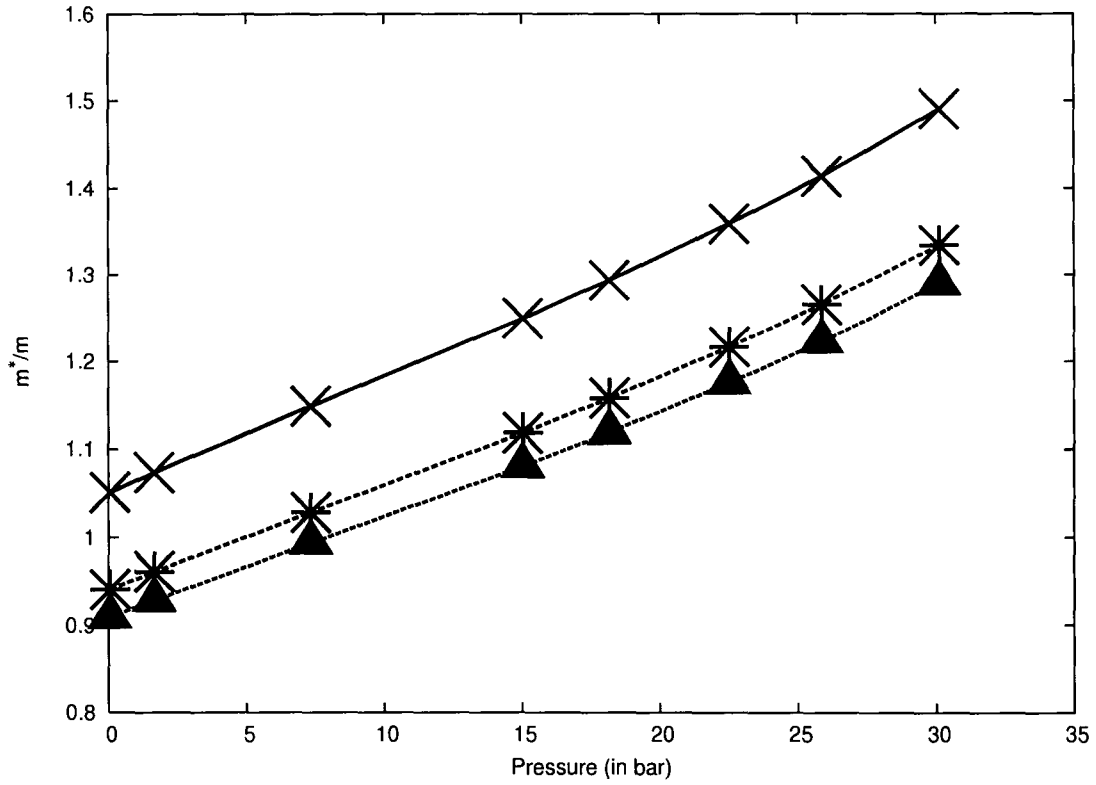

Figure 6.1: Figure represents the variation of effective mass with pressure. Effective mass are obtained using experimental values of T_c at different pressure [78]. Solid line with crosses represents the variation for sc arrangement while broken line with asteroids represents the same for bcc arrangement. Broken line with solid triangles represents the variation for fcc as well as hcp arrangement.

Bibliography

[1] F. London. *Nature*, 141:643, 1938.

[2] F. London. *Phys. Rev.*, 54:947, 1938.

[3] M. Haque. *arXiv:cond-mat.*, page 0302076, 2003.

[4] J.O. Andersen. *Rev. Mod. Phys.*, 76:599, 2004.

[5] T.D. Lee and C.N. Yang. *Phys. Rev.*, 105:1119, 1957.

[6] T.D. Lee and C.N. Yang. *Phys. Rev.*, 112:1419, 1958.

[7] A.E. Glassgold, A.N. Kaufmann, and K.M. Watson. *Phys. Rev.*, 120:660, 1960.

[8] K. Huang. In J. de Boer and G.E. Uhlenbeck, editors, *Studies in Statistical Mechanics*, volume 2, page 3. North-Holland, Amsterdam, 1964.

[9] A.M.J. Schakel. *Int. J. Mod. Phys.*, B 8:2021, 1994.

[10] M. Wilkens, F. Illuminati, and M. Kraṁer. *J. Phys.*, B 33:L779, 2000.

[11] T. Toyoda. *Ann. Phys. (N.Y.)*, 141:154, 1982.

[12] M. Bijlsma and H.T.C. Stoof. *Phys. Rev.*, A 54:5085, 1996.

[13] S. Ledowski, N. Hasselmann, and P. Kopietz. *arXiv:cond-mat*, 0311043, 2003.

[14] A. Fetter and J.D. Walecka. *Quantum Theory of Many particle Systems.* McGrow-Hill, New York, 1971.

[15] K. Huang. *Phys. Rev. Lett.*, 83:3770, 1999.

[16] G. Baym, J.P. Blaizot, M. Holzmann, F. Laloë, and D. Vautherin. *Phys. Rev. Lett.*, 83:1703, 1999.

[17] G. Baym, J.P. Blaizot, M. Holzmann, F. Laloë, and D. Vautherin. *Euro. Phys. J.*, B 24:107, 2001; also in cond-mat./0107129.

[18] C.J. Pethick and H. Smith. *Bose-Einstein Condensation in Dilute Gases.* Cambridge University Press, England, 2002.

[19] P. Grüter, D. Caperley, and F. Laloë. *Phys. Rev. Lett.*, 79:3549, 1997.

[20] M. Holzmann, P. Grüter, and F. Laloë. *Eur. Phys. J.*, B 10:739, 1999.

[21] M. Holzmann and W. Krauth. *Phys. Rev. Lett.*, 83:2687, 1999.

[22] G. Baym, J.P. Blaizot, and J. Zinn-Justin. *Europhys. Lett.*, 49:150, 2000.

[23] M. Holzmann, G. Baym, J.P. Blaizot, and F. Laloë. *Phys. Rev. Lett.*, 87:120403, 2001.

[24] E. Muller, G. Baym, and M. Holzmann. *J. Phys.*, B 34:4561, 2001 ; also in cond-mat./0105359.

[25] P. Arnold and B. Tomásik. *Phys. Rev.*, A 62:063604, 2000.

[26] P. Arnold and G. Moore. *Phys. Rev. Lett.*, 87:120401, 2001.

[27] V. A. Kashurnikov, N.V. Prokof'ev, and B.V. Svistunov. *Phys. Rev. Lett.*, 87:120402, 2001.

[28] P. Arnold and G. Moore. *Phys. Rev.*, E 64:066113, 2001.

[29] P. Arnold, G. Moore, and B. Tomásik. *Phys. Rev.*, A 65:013606, 2002.

[30] G. Chapline Jr. *Phys. Rev.*, A 3:1671, 1971.

[31] R.P. Feynman. *Phys. Rev.*, 91:1291, 1953.

[32] Y.S. Jain. *J. Sci. Expl.*, 16:77, 2002. More detailed version of this paper is available for ready reference as a paper entitled, *"Macro-orbitals and microscopic theory of a system of interacting bosons"* in www.arXiv.org/cond-mat/0606571.

[33] J. Harada. *arXiv:cond-mat.*, page 0701365, 2007.

[34] R.J. Donnelly and C.F. Barenghi. *The Observed Properties of Liquid Helium at the Saturated Vapor Pressure.* www.darkwing.uoregon.edu, Universitas Oregonensis.

[35] A.T. van Urk, W.H. Keesom, and H.K. Onnes. *Proc. Roy. Acad. Sci. Amsterdam*, 28:58, 1925.

[36] J.F. Allen and A.D. Misener. *Proc. Cambridge Philos. Soc. math.phys.Sci.*, 34:299, 1938.

[37] K.R. Atkins and Y. Narahara. *Phys. Rev.*, 136:A437, 1965.

[38] K.N. Zinov'eva and S.T. Bolarev. *Sov. Phys. JETP*, 56:585, 1969.

[39] D.P.E. Dickson, D. Caroline, and E. Mendoza. *Phys. Lett. A*, 33A:139, 1970.

[40] I.J. King and A.F.G. Wyatt. *Proc. Roy. Soc. London*, A 322:355, 1971.

[41] S.T. Boldarev and V.P. Peshkov. *Physica (Amsterdam)*, 69:141, 1973.

[42] M. Iino, M. Suzuki, and A.J. Ikushima. *J. Low Temp. Phys.*, 61:155, 1985.

[43] P. Roche, G. Deville, N.J. Appleyard, and F.I.B. Williams. *J. Low Temp. Phys.*, 106:565, 1997.

[44] Kazuhito Nakanishi and Masaru Suzuki. *J. Low Temp. Phys.*, 113:585, 1998.

[45] C. Vicente, W. Yao, H.J. Maris, and G.M. Seidel. *Phys. Rev. B*, 66:214504, 2002.

[46] K.R. Atkins. *Can. J. Phys.*, 31:1165, 1953.

[47] A.D. Singh. *Phys. Rev.*, 125:802, 1962.

[48] W. Brouwer and R.K. Pathria. *Phys. Rev.*, 163:200, 1967.

[49] D.D. Fitts. *Physica*, 42:205, 1969.

[50] R.M. Bowley. *J. Phys, C: Solid State Phys.*, 3:2012, 1970.

[51] Y.M. Shih and C.W. Woo. *Phys. Rev. Lett.*, 30:478, 1973.

[52] C.C. Chang and M. Cohen. *Phys. Rev.*, A 8:1930, 1973.

[53] K.S. Liu, M.H. Kalos, and G.V. Chester. *Phys. Rev.*, B 12:1715, 1975.

[54] C. Ebner and W.F. Saam. *Phys. Rev.*, B 12:923, 1975.

[55] J. Lekner and J.R. Henderson. *Physica*, A 94:545, 1978.

[56] J. Lekner and J.R. Henderson. *J. Low Temp. Phys.*, 31:763, 1978.

[57] F.D. Mackie and C.W. Woo. *Phys. Rev.*, B 18:529, 1978.

[58] M. Saarela, P. Pietiläinen, and A. Kallio. *Phys. Rev.*, B 27:231, 1983.

[59] V.R. Pandharipande, S.C. Piper, and R.B. Wiringa. *Phys. Rev.*, B 34:4571, 1986.

[60] T. Biben and D. Frenkel. *J. Phys.: Condense Matter*, 14:9077, 2002.

[61] J.M. Marin, J. Boronat, and J. Casulleras. *Phys. Rev.*, B 71:144518, 2005.

[62] M.H. Kalos, M.A. Lee, P.A. Whitlock, and G.V. Chester. *Phys. Rev.*, B 24:115, 1981.

[63] C. Kittel. *Introduction to Solid State Physics.* Wiley Estern, New Delhi, 1983.

[64] K. Penanen, M. Fukuto, R.K. Heilmann, I.F. Silvera, and P.S. Pershan. *Phys. Rev.*, B 62:9621, 2000.

[65] D.V. Osborne. *J. Phys.: Condens Matter*, 1:289, 1989.

[66] W.L. McMillan. *Phys. Rev.*, 138:A 442, 1965.

[67] D. Schiff and L. Verlet. *Phys. Rev.*, 160:208, 1967.

[68] W.E. Massey and C.W. Woo. *Phys. Rev.*, 164:256, 1967.

[69] P.A. Whitlock, D.M. Caperley, G.V. Chester, and M.H. Kalos. *Phys. Rev.*, B 19:5598, 1979.

[70] G. Gaglione, G.L. Masserini, and L. Reatto. *Phys. Rev.*, B 22:1237, 1980.

[71] Q.N. Usmani, S. Fantoni, and V.R. Pandharipande. *Phys. Rev.*, B 26:6123, 1982.

[72] V.F. Sears. *Phys. Rev.*, B 28:5109, 1983.

[73] T.C. Padmore and M.W. Cole. *Phys. Rev.*, A 9:807, 1974.

[74] E. Krotschek, S. Stringari, and J. Treiner. *Phys. Rev.*, B 35:4754, 1987.

[75] J.L. Valles and K.E. Schmidt. *Phys. Rev.*, B 45:2879, 1988.

[76] D.E. Galli and L. Reatto. *J. Phys.: Condens Matter.* 12:6009, 2000.

[77] D.O. Edwards, P.P. Fatouros, G.G. Ihas, and P. Mrozinski an S.Y. Shen. *Phys. Rev. B*, 11:4734, 1975.

[78] G. Ahlers. *Phys. Rev.*, A 8:530, 1973.

Chapter 7

Summary and Conclusion

7.1 Summary and Conclusion

Liquid helium-4 (LHE-4) undergoes a liquid to liquid phase transition which transforms it from its normal (N) liquid phase (*helium-I*) to superfluid (S) phase (*helium-II*) at $T = T_\lambda$ $(= 2.17\,K)$. Helium-II exhibits several fascinating physical properties such as zero resistance to linear flow, zero entropy, very high thermal conductivity, thermomechanical and mechano-caloric effects *etc.* London proposed that this transition is a manifestation of Bose-Einstein condensation of $^4He-$atoms in $p = 0$ state which is commonly called as $p = 0$ condensate representing a well known state of a many body system where quantum effects dominates the macroscopic behaviour of the system. Numerous efforts have been made to investigate LHE-4 both by theoretical and experimental physicists, however, the microscopic origin of its unique properties has not been clearly understood.

Two microscopic approaches based on pseudo-potential and variational principle have been basically used to develop a viable theory of the system but none of these efforts has concluded the desired theory even though several hundreds of research articles have been published over the last eight decades. Microscopic theories based on widely different assumptions such as: (i) the existence of $p = 0$ condensate, (ii) (q,-q) pair formation, (iii) pair condensation, and (iv) many particle condensation but none of these theories fully explains experimental properties of the liquid to an acceptable degree of accuracy. In fact no single theoretical framework has helped in explaining different aspects of *helium-II*. Similarly, hundreds of papers based on variation principle have been reported on the calculation of the amount of $p = 0$ condensate and the excitation spectrum but without satisfactory results. While excitation spectrum has not been found with desired agreement with experiments, amount of $p = 0$ condensate obtained by using sophisticated Monte Carlo methods is found to vary between $0 - 13\%$. Results of the neutron scattering experiments which have been performed with the basic objective of observing $p = 0$ condensate in LHE-4 are not conclusive on its existence. Reviewing the results of neutron scattering experiments and theoretical works on the estimation of $p = 0$ condensate, Sokol [1] remarked,

> *If the underlying assumptions of the expressions used in the fits (neutron scattering data) are incorrect, then the results inferred will not have much meaning. It is interesting to note that the observed scattering in liquid helium can be fit extremely well simply by using the momentum*

distribution (n(p)) of the ideal Bose gas. This holds true in both the normal and super-fluid phase. The best description of the scattering in the super-fluid is obtained by using an ideal Bose gas n(p) with no condensate.

In a recent review article Leggett [2] also remarked,

In the sixty years since London's original proposal, while there has been almost universal belief that the key to super-fluidity is indeed the onset of BEC at T_λ it has proved very difficult, if not impossible, to verify the existence of the latter phenomenon directly. The main evidence for it comes from high-energy neutron scattering and, very, recently, from the spectrum of atoms evaporated from the liquid surface, and while both are certainly consistent with the existence of a condensate fraction of approximately 10%*, neither can be said to establish it beyond all possible doubts.*

Similar views have been expressed by different authors from time to time [3–5]. While these comments of the experts in the field reflect that the existence of $p = 0$ condensate in super-fluid helium is still doubted, most of the microscopic theories start with the basic assumption of the existence of $p = 0$ condensate. Consequently, it is not surprising that such theories fail to give a complete description of the system. Various shortcomings of these theories are also pointed out by Woods and Cowley [3], Rickayzen [6], Kleban [7] and, very recently, by Ettouhami [8] who questions the validity of the Bogoliubov theory [9] of weakly interacting bosons which is used as starting point of the field theoretical approach clubbed with the assumption of the existence of $p = 0$ condensate. As such Landau's two fluid phenomenological theory [10, 11] supplemented by the idea of quantized circulation presented by Onsager [12] and Feynman [13] remains the only way to understand the properties of LHE-4 despite its several shortcomings.

Absence of a proper microscopic theory of LHE-4 has been felt for a long time [3,6]. Only recently, Jain has successfully developed a microscopic theory of a system of interacting bosons which is well equipped to explain the properties of LHE-4. His theory vindicates (i) Landau two fluid phenomenology [10], (ii) London's idea of macroscopic wave function of the S-state [14], (iii) the observation of Bogoliubov [9] that super-fluidity is the manifestation of an inter-particle

interaction, (iv) Ginzburg-Landau $\psi-$theory [15], *etc.* Jain's theory explains different properties of LHE-4 within experimental errors. Consequently, it could be regarded as the long awaited theory of LHE-4. Important features of the theory can be summarised as follows:

1. The theory makes no assumption such as the existence of $p = 0$ condensate. Its all inferences are derived from the solutions of the Scrödinger equation of $N-$interacting bosons.

2. The theory successfully incorporates both components of the inter-particle interaction (repulsive and attractive components).

3. The (q,-q) pairs with q and K motion form the basic unit of the system.

4. The (q,-q) bound pairs of atoms (with $q = q_o$) around T_λ arises from the quantum correlation potential and inter-particle attraction. This pair formation is energetically favourable and the binding of these pairs differs from the binding of two electrons in a Cooper pair in the sense that the necessary attraction is the inherent ^4He-^4He attraction.

5. Pair formation leads to the collective binding of all particles in the system for which the entire system behaves like a single macro-molecule. This binding serves as an energy gap between the super-fluid and normal phases of the system.

6. The theory shows that $p = 0$ condensate is not necessary for the superfluidity of the system.

7. The transition at T_λ is characterised by two separate phenomena: (i) ordering of the particles in phase space with relative phase point separation of $\Delta\phi = 2n\pi$ (n = integer number), and (ii) BEC of particles in $K = 0$ state of their $K-$motion.

8. The atoms in *helium-I* are randomly distributed in normal space, momentum space and phase space, while in *helium-II* they define an orderly arrangement in these spaces with a kind of crystalline arrangement in normal space, a momentum $q = \pi/d$ or its integral multiple, and relative phase position of $\Delta\phi = 2n\pi$; they cease to have relative motion and remain free to move in order of their positions on a closed path.

9. It has been successfully developed within the framework of the wave mechanics.

10. It is consistent with excluded volume condition as well as microscopic and macroscopic uncertainty.

11. Its mathematical formulations are exceptionally simple and its inferences have unparalleled clarity.

All these points motivated us to testify this theory by estimating numerical values of certain physical properties of superfluid helium-4 and examine their agreement with experiments. In this context we have studied logarithmic divergence of specific heat at constant pressure and related thermodynamic properties, excitations spectrum at low Q and its anomalous nature, energy gap and related properties such as superfluid density and critical velocities, transition temperature, surface tension and surface layer thickness which are presented in different chapters of this thesis. The fact that our results match closely with experiments indicates its accuracy and its great potential in explaining the behavior of LHE-4 type different systems of interacting bosons. Evidently, this fulfills one of the basic objectives of this thesis.

Macro-orbital theory estimates the energy associated with the $\lambda-$transition and concludes that this energy is responsible for the logarithmic divergence of specific heat (at constant pressure, C_p) at T_λ. In this thesis, we have used this energy to estimate the numerical values of C_p as well as expansion coefficient (α_P), isothermal compressibility (κ_T) and pressure coefficient (β) and compared them with the experimental values (cf. chapter 3). A close agreement of the estimated values with the experiments establishes the accuracy of the relations of Macro-orbital theory. We note that for the first time a microscopic theory (Jain's Macro-orbital theory) provides a proper account of the origin of logarithmic divergence of specific heat and related thermodynamic properties.

Using the dispersion relations available in Macro-orbital theory, we have estimated excitation energy $E(Q)$, group and phase velocities at different Q for different atomic arrangements (sc, bcc, fcc and hcp). Our results for $E(Q)$ closely agree with experiments and we observe an anomalous dispersion region extended up to $0.43\mathring{A}^{-1}$. Our results for fcc/hcp arrangements agree more closely with experiments (cf. chapter 4).

In Macro-orbital theory, the energy gap that exists between the normal and superfluid phase accounts for the various unique properties of the system *e.g.* critical velocity (v_c), thermomechanical and mechanocaloric effect, *etc.* We used this energy gap to estimate superfluid and normal fluid density, critical velocity for linear and rotational flow, vortex line density, vortex size *etc.* Our results for superfluid and normal fluid density agrees closely with experiments (figure 5.2). Our results for critical velocity are higher than the measured one and this difference is expected because the measured v_c usually represents the velocity required for vortex formation and does not account for the loss of total super-fluidity, while critical velocity predicted by Macro-orbital theory accounts for the total loss of superfluidity of the system. Our results are very close to the measured values of Hess [16] and Hulin *et al* [17] who measured v_c in a small hole by filtering it near the hole with porous medium. The strong temperature dependence of the critical velocity observed by Hess and Hulin *et al* agrees with our findings.

Using the expression available from Macro-orbital theory we estimated $T_\lambda =$ 2.271, 2.033, 1.964 and 1.964 K for sc, bcc, fcc and hcp arrangements respectively (cf. chapter 6). Our estimated values deviate $4 - 12\%$ from the observed value ($2.172K$) as against 40% deviation of London's estimation. Our investigation further indicates that the effective mass of helium atom plays an important role on the pressure dependence of T_λ. While, as indicated from figure 6.1, this dependence is expected to be linear, its theoretical foundation may form a subject of a future investigation.

Our simple calculations for surface tension at $T = 0$ ($\sigma(0)$) based on Macro-orbital theory do not include the effects of parameters such as density variation and the change of atomic layer separation near the free surface of the liquid. Our estimated value ($\approx 495\, mdynes/cm$) is about 30% higher than experimental values $375\, mdynes/cm$. It may be stated that smaller density of helium atoms near the free surface could account for the difference. However, the so called sophisticates theories also render $\sigma(0)$ values (Table 6.19) varying from 230 to $510\, mdynes/cm$. We hope that a future course of study which incorporates the said fluctuations with Macro-orbital theory may help us in improving our results.

The estimated results of various physical properties of LHE-4 that are presented in chapters 3, 4, 5, and 6, closely agree with experiments and thus establish that Macro-orbital theory successfully explains these properties of the

system. In addition, the theory can be used to study entropy, thermal conductivity, specific heat, pressure dependent dispersion relation, static structure factor $S(Q)$ and dynamic form factor $S(Q,\omega)$ *etc.* in the quantitative level. Formalism of this theory can be extended to different systems like $Helium-3$, superconductor, 2-D bosonic system *etc.*. Our group plans to investigate these aspects and hopes to open new frontier for future studies.

Bibliography

[1] P.E. Sokol. In A. Griffin, D.W. Snoke, and S. Stringari, editors, *Bose-Einstein Condensation.* Cambridge University Press, Cambridge, 1995.

[2] A.J. Leggett. *Rev. Mod. Phys.*, 71:S318, 1999.

[3] A.D. Woods and R.A. Cowley. *Rep. Prog. Phys.*, 36:1135, 1973.

[4] H.W. Jackson. *Phys. Rev. A*, 10:278, 1974.

[5] H.R. Glyde and E.C. Svensson. In D.L. Price and K. Skold, editors, *Methods of Experimental Physics*, volume 23, Part-B, page 303. Academic Press, London, 1987.

[6] C. Rickayzen. In J.G.M. Armitage and I.E. Ferquhur, editors, *The Helium Liquids.* Academic Press, 1975.

[7] P. Kleban. *Phys. Lett.*, 49A:19, 1974.

[8] A.M. Ettouhami. *arXiv.org*, 0703498, 2007.

[9] N. Bogoliubov. *J. Phys. (USSR) (reprinted in Ref. 1)*, 11:23, 1947.

[10] L.D. Landau. *J. Phys. U.S.S.R. (reprinted in Ref. 1)*, 5:71, 1941.

[11] L.D. Landau. *J. Phys. U.S.S.R. (reprinted in Ref. 1)*, 11:91, 1947.

[12] L. Onsager. *Nuovo Cimento*, 6 (supplement-2):249, 1949.

[13] R.P. Feynman. In C.J. Gorter, editor, *Prog. Low Temp. Phys.*, volume I, page 1. North-Holland, Amsterdam, 1955.

[14] F. London. *Nature*, 141:644, 1938.

[15] V.L. Ginzburg and L.D. Landau. *Zh. Eksperim. i. Teor. Fiz.*, 20:1064, 1950.

[16] G.B. Hess. *Phys. Rev. Lett.*, 27:977, 1971.

BIODATA

Name	: Shri Simanta Chutia
Degree	: Ph. D.
Department	: Department of Physics, NEHU
Title of the Dissertation	: A Study of Certain Properties of Superfluid Helium-4 Using Macro-orbital Theory.
Date of Admission	: 04.04.2005

Approval of Research Proposal:

1. BPGS(Physics) 19.04.2005
2. School Board: 24.05.2005

Registration No and Date : 912 of 24.05.2005

P. Nongkynrih 26.11.07.

Head,
Department of Physics
North Easter Hill University

Physics Department,
N.E.H.U, Shillong-793022.